Recruitment variability of chokka squid (*Loligo reynaudii*) — the role of the cold ridge, currents and retention on the Agulhas Bank, South Africa

MICHAEL J. ROBERTS

B. Sc. (Natal), B. Sc. Hons. (UCT), M. Sc. (UPE)

Marine and Coastal Management, Private Bag X2, Roggebaai, 8012
South Africa

Supervisor: Prof. F.A. Shillington

Thesis presented for the degree of DOCTOR OF PHILOSOPHY

in the Department of Oceanography

UNIVERSITY OF CAPE TOWN

August 2009

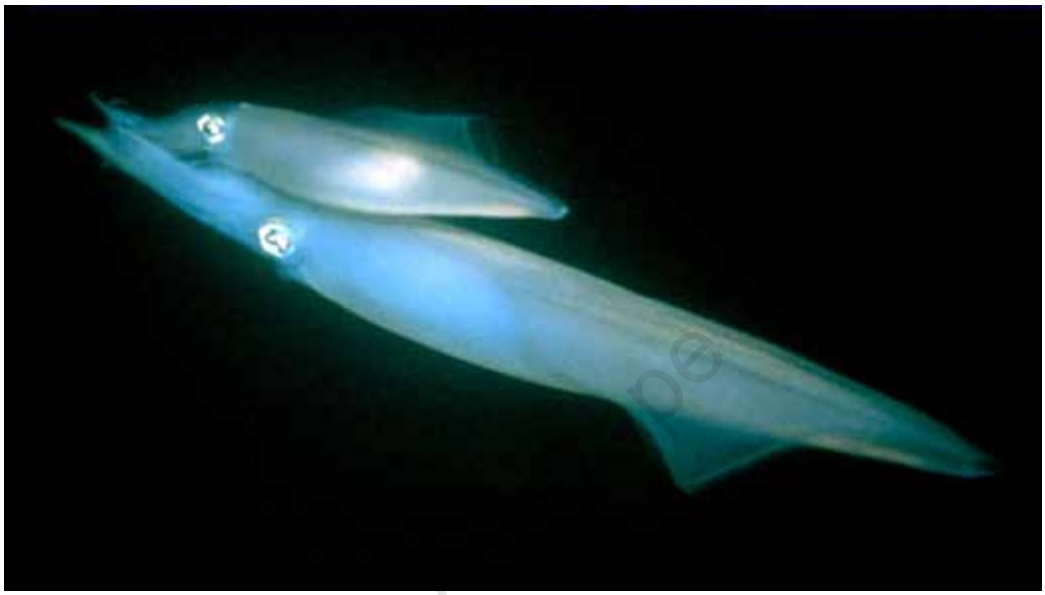

Chokka squid (*Loligo reynaudii*). Copulation — the starting point of recruitment variability!

Dearest Lynne — hope this ticks off one more thing on the "to do list" and brings a smile!

TABLE OF CONTENTS

Acknowledgements

This work forms part of the South African Climate Change and Squid Programme, a programme funded by Marine and Coastal Management (MCM), the South African Squid Management and Industrial Association (SASMIA), and the National Research Foundation (THRIP). Bay World Centre for Research and Education (Port Elizabeth Museum) provided institutional and administrative support.

Firstly, I would like thank Prof Frank Shillington for his supervision, encouragement and for staying alive long enough to witness my thesis submission. I thank Cathy Boucher for her help with artwork in chapters 2 and 3, Marcel van den Berg for working up, verifying, and loading the physical and chemical cruise data onto the MCM Oceanographic Data Base used in chapter 1 as well as for diving and instrument assistance in Chapter 2. I thank Geoff Bailey (formerly MCM), who collected and supervised early analysis of the west coast temperature and oxygen data used in Chapter 2.

I further thank John Allen of the Tsitsikamma National Marine Park for boat and diving support, Neil Needham (formerly MCM), Pieter-Jan Schön and Steve Brouwer (both Rhodes University) for their assistance in diving retrievals and deployments of instruments. I am indebted to Grev Nelson (formerly MCM) for the use of his current data analysis software, which has now been rewritten in *Delphi* and is used by many students. Jurgens Els from Star Track is thanked for his technical input on drifter electronics.

Finally, thanks Lynne for just being the most amazing life partner imaginable and giving the support I need to pursue my career as an oceanographer and explorer of the oceans.

List of Figures

Declaration

This thesis is the result of original research that I carried out in the Department of Oceanography, UCT, and at Marine and Coastal Management (MCM), my place of employment. The concepts and experiments presented in this manuscript are my own, stimulated by real resource management and fishery problems, and the science being undertaken by many of my colleagues around the world. Assistance was provided by some of my technical staff (notably Marcel van den Berg) in the deployment of a bottom-mounted ADCP current meter and thermistor array used in Chapter 3 and satellite-tracked drifter buoys in Chapter 6. In particular, the Individual-based Model (IBM) used in Chapter 5 was developed by Christian Mullon of the Institut de Recherde pour le Développement (IRD), France. Data fields to run the IBM simulations were provided by Pierrick Penven and Bruno Blanke (IRD) using the Regional Ocean Modelling System (ROMS) hydrodynamic applied to the southern Benguela region. The acquisition of oceanographic data and use of published data in Chapters 2 and 4 have been duly acknowledged. Each significant contribution and citation of other people's work has been attributed and referenced.

Note that Chapters 2, 3 and 4 are based on the following publications:

Chapter 2

Roberts MJ. 2005. Chokka squid (*Loligo vulgaris reynaudii*) abundance maybe linked to changes in the Agulhas Bank (South Africa) ecosystem during spawning and the early life cycle. *ICES Journal of Marine Science* 62(1): 33–55.

Chapter 3

Roberts MJ, van den Berg M. 2005. ADCP measured currents along the Tsitsikamma Coast (South Africa) and potential transport of squid paralarvae. *African Journal of marine Science* 27(2): 375–388.

Chapter 4

Roberts MJ, van den Berg M. 2002. Recruitment variability of chokka squid — role of currents on the Agulhas Bank (South Africa) in paralarvae distribution and food abundance. Part II. Boyle PR, Collins MA, Pierce G (eds), *Bulletin of Marine Science* 71(2): 691–710.

Chapters 5 and 6 have been submitted for publication.

This work has not been submitted for any other degree at any other university.

Michael John Roberts

August 2009

Abstract

It is well documented that biomass (and catches) for many squid species varies considerably, and moreover, that recruitment strength is strongly related to the environment. The ramifications of catch fluctuations are significant and create uncertainty for resource managers and the fishing industry with the net result of increased risk levels of stock collapse, economic instability, long term investment; and for the semi-artisanal fisheries, socio-economic hardship for the many fishers. Recruitment–environment mechanisms which underpin biomass are region specific, and in the case of the chokka squid *Loligo reynaudii*, are unknown. This thesis addresses this knowledge gap and is fundamentally based on Bakun's (1996)[1] generalised triad of requirements for successful recruitment — enrichment, concentration and retention in the ecosystem. For chokka squid this implies that recruitment depends on the survival of paralarvae in terms of food availability–feeding success (i.e. copepods biomass, density distribution and patchiness) and retention in the ecosystem. The nature of this investigation demanded a multidisciplinary approach comprising physical oceanography and biology, as well as a variety of scientific techniques.

First a synthesis of basic ecosystem components for the domain in which chokka squid live (i.e. South Africa's west coast and Agulhas Bank) was prepared using published and new data. It included bottom temperature, bottom dissolved oxygen, chlorophyll, and copepod abundance. Alongshore gradients of these indicated that the main spawning grounds on the eastern Agulhas Bank are positioned where bottom temperature and bottom dissolved oxygen are optimal for embryonic development. This location, however, appears suboptimal for hatchlings because the copepod maximum (food for paralarvae) is typically on the central Agulhas Bank some 200 km to the west. Data on currents suggest that this constraint may be overcome by the existence of a net west-flowing shelf current on the eastern Agulhas Bank, improving survivorship of paralarvae by transporting them passively towards the copepod maximum — a concept referred to as the **western transport hypothesis** or WTH (hypothesis 1). CTD (Conductivity, Temperature, Depth) data and a temporal analysis of AVHRR (Advanced Very High Resolution Radiometry) satellite imagery reveal the copepod maximum to be supported by a ''cold ridge'', a mesoscale upwelling filament present during summer when squid spawning peaks. In situ sea surface temperature (SST) data used as a proxy for cold ridge activity demonstrate considerable inter-annual variability of the feature, especially during El Niño-Southern Oscillation events. Negative linear correlations between maximum summer SST (monthly average) and squid biomass the following autumn (r^2=0.94), and annual catch (r^2=0.69), support the link between the ''cold ridge–copepod maximum'' and the early life cycle of chokka squid, and holds promise for prediction.

[1] Bakun A. 1996. *Patterns in the Ocean. Ocean processes and marine population dynamics*. California Sea Grant, National Oceanic and Atmospheric Administration and Centro de Investigaciones biológicas del Noroeste, La Paz, BCS México: 323 pp.

Transport of squid paralarvae hatched on the inshore spawning grounds (<60 m) was also investigated using a bottom-mounted Acoustic Doppler Current Profiler deployed at 36 m on the Tsitsikamma coast (in the Tsitsikamma National Park). Analysis of 12 months of data showed that surface flow was mainly eastward (alongshore), with a maximum velocity of 115 cm s^{-1} and an average of 24 cm s^{-1}. Generally, velocity decreased with depth, with a maximum bottom velocity of 65 cm s^{-1} and an average of 10 cm s^{-1}. Data from a nearby thermistor array show that the water column was usually isothermal during winter (July–September), with bottom flow in the same direction as the surface layer. In summer (December–March), vertical stratification was most intense and surface and bottom flows differed in velocity and direction. Potential net monthly displacements calculated for three depths (5 m, 23 m and 31 m) indicate that passive, neutrally buoyant biological material (e.g. squid paralarvae) would likely be transported eastwards in the surface layer for eight of the 12 months, and would generally exceed distances of 220 km $month^{-1}$. Displacement in the bottom layer was more evenly distributed between east and west, with net monthly (potential) transport typically 70–100 km, but reaching a maximum of 200 km. Wind-driven coastal upwelling prevalent during the summer, was observed to cause offshore flow for several days the surface layer of the coastal current resulting in potential displacement distances of 40 km from the coast. This mitigates eastward transport and potentially moves squid paralarvae in the Tsitsikamma current offshore and into the westward mid shelf current which flows towards the cold ridge.

Realization that currents may not always be westward led to re-examination of the dependency of squid paralarvae on the cold ridge as the only rich feeding area on the Agulhas Bank. A synthesis of existing data and materials found that chlorophyll and copepods also exist at elevated levels on the thermocline in areas other than the cold ridge, and that currents therefore may not necessarily be so critical to connect hatching position with food. Moreover, varied current data suggested that **currents may remove squid paralarvae from the Agulhas Bank ecosystem** (hypothesis 2) through the leakage of shelf water into the Indian and Atlantic Oceans. Magnitude and timing of such a phenomenon will impair recruitment, cause biomass fluctuations, and ultimately affect catches. Leakage has been cited as the root cause of the sudden drop in annual squid catches experienced in 2001.

To investigate the leakage hypothesis, a Lagrangian IBM (Individually-Based Model) coupled to a ROMS (Regional Ocean Model System) model was setup covering the west coast and Agulhas Bank to 24° E (St Francis Bay). Three simulations were performed for 12 model months using neutrally buoyant particles released from the seabed every second day on the mid shelf of the eastern, central and western parts of the Agulhas Bank. Boundary effects and resolution precluded the release of virtual particles on the inshore spawning grounds. Particles were given life spans of 40 days. Results demonstrated large particle losses from the eastern Agulhas Bank (76%) and the western Agulhas Bank (64%). In contrast few particles were lost from the central Agulhas Bank (2%) making this, in terms of the model, the most suitable place on the Agulhas Bank for spawning. Visualization of the

ROMS outputs revealed that leakage on the eastern Agulhas Bank was caused by a cyclonic eddy resident in the Agulhas Bight. Similarly leakage from the western Agulhas Bank was caused by deep water cyclonic eddies in the adjacent Atlantic Ocean.

A parallel study was also undertaken using four satellite tracked drifters released on the eastern Agulhas Bank to validate the ROMS-IBM experiments. Two drifters with drogues to 8 m were released on the inshore spawning grounds off the Tsitsikamma coast at the ADCP site. The other two drifters were released on the mid shelf where squid eggs had previously been found and "virtual paralarvae" released in the IBM. One of the mid shelf drifters was tethered to a drogue at 70 m to measure advection in the bottom layer. Both inshore drifters were transported 70 km eastwards in the Tsitsikamma coastal current to Tsitsikamma Point. Here one beached while the other moved offshore onto the mid shelf and then southwards to leave the shelf 20 days after release. The surface drifter on the mid shelf was transported westward across the central and western Agulhas Bank (550 km) to leave the shelf after 58 days south of the Cape Peninsula. The deeper drifter also travelled westward, but remained on the shelf in the vicinity of the cold ridge and was recovered after 40 days and 100 km of the release position. Satellite SST and ocean colour images indicated frequent offshore flows of shelf water near the southern tip of the Agulhas Bank, as well as an intrusion of oceanic water onto the western Bank during this experiment. The latter caused an anti-cyclonic circulation which led to further leakage of shelf water from the inner central Agulhas Bank. The combination of drifters and satellite imagery in this experiment demonstrated that retention of chokka squid paralarvae in the Agulhas Bank ecosystem is not certain, even for the inshore spawning grounds, and that the risk would be less if paralarvae were found near the bottom. So far *in situ* sampling indicates they occupy the surface layer.

Overall, this work has identified (1) environmental niches on the Agulhas Bank which the chokka squid life cycle has evolved to use (e.g. spawning grounds), (2) that the cold ridge–copepod maxima is a rich feeding ground on the Agulhas Bank and plays a role in chokka squid recruitment strength (biomass), and (3) that there is potential for chokka squid paralarvae to be advected off the shelf and removed from the Agulhas Bank ecosystem on the eastern and central Agulhas Bank — possibly resulting in biomass crashes for the following year. Importantly, the cold ridge–copepod biomass–squid biomass relationship has been quantified, and holds promise for prediction. Prediction will be further strengthened if, in the future, advective paralarval loss can be linked to early retroflection of the Agulhas Current.

CHAPTER 1

Introduction

Big Currents and big squid fisheries

There are five major western boundary currents (WBCs) on the planet. Four of these support ommastrephid squid fisheries — the Gulf Stream (*Illex illecebrosus*), the Brazil Current (*Illex argentinus*), the Kurioshio Current (*Todarodes pacificus*) and the East Australian Current (*Nototodarus sloani sloani* and *Nototodarus sloani gouldi*). Ommastrephid fisheries tend to be much larger in terms of biomass and catch than those of neritic squid (e.g. the Loliginid fisheries) but also tend to experience large fluctuations in biomass and catch (Hatanaka *et al.* 1985; Roberts *et al.* 1998a). For example, the *Illex illecebrosus* fishery peaked at 162 000 t in 1979 in Canadian waters (Rodhouse *et al.* 1998), *Todarodes pacificus* peaked at 680 000 t in 1968 (FAO, Fisheries Global Information System (FIGIS); www.fao.org/figis/), *Illex argentinus* peaked at 1 100 000 t in 1999 (FIGIS; www.fao.org/figis/) and *Nototodaras sloani sloani* ranges between 60 000–80 000 t y^{-1} (Hatanaka *et al.* 1985). Together, the WBC ommastrephid fisheries are worth some US$ 3.6 x 10^9 (based on US$ 4/kg).

By comparison the largest loliginid fishery, *Loligo gahi,* located around the Falkland Islands peaked at 119 000 t in 1998 but averages around 56 000 t y^{-1} (Falklands Island Government, 1997; FIGIS, www.fao.org/figis/). The Californian squid *Loligo opalescence* although very erratic can at times also reach an annual catch of these proportions. Most of the other *Loligo* fisheries, however, such as *L. bleekeri*, *L. edulis*, *Sepiotheuthis lessoniana* have annual catches between 10 000 and 20 000 t.

Squid life cycle and WBCs

While the fluctuations in biomass and catch of the ommastrephid fisheries can be caused by intense fishing mortality (e.g. the collapse of *Illex illecebrosus* and subsequent recruitment failure; Dawe and Warren 1993), they are also believed to be linked to the dynamics of the associated WBCs (Ceolho 1985; O'Dor 1992). This is because ommastrephids tend to use the warm subtropical WBC source waters to facilitate egg development and are reliant on the poleward transport of eggs and larvae to the nursery grounds in temperate shelf waters at higher latitudes where food is much more abundant (Hatanaka *et al.* 1985). *Illex illecebrosus* for example spawns in the source of the Gulf Stream between Cape Hatteras and Florida where water temperatures are warm. Eggs are contained in characteristic balloon type masses which appear to sink to depths of ~ 300 m where equal density to the egg mass is found. The egg balloons are then passively transported northwards in the warm Gulf Stream water to facilitate quicker development but at the same time moving the hatching place towards the Georges Bank and Scotian shelf where food biomass on the shelf is much higher

and the young squid can readily find food to sustain their rapid growth and high metabolic rates. Such an early life cycle is clearly dependent on WBCs having consistent characteristics i.e. narrow well defined trajectories of considerable length which flow closely along the continental slope with constant velocity. But this is not always true as they also have unique traits that can be devastating for life cycles reliant on consistency. For example, an early break-away of the WBC trajectory from the shelf would result in the egg balloons and larvae being displaced from the nursery grounds where food is more plentiful than the open ocean.

South African squid fishery

Interestingly, the Agulhas Current on the south east coast of Africa does not support an ommastrephid squid fishery. This is possibly due to the presence of the land mass of Madagascar, which not only shortens the length of this WBC, but also is responsible for creating mesoscale cyclonic and anticyclonic eddies in its northern reaches. These can cause the current to retroflect higher upstream, further limiting the travel time and distance in the warm current.

However, a small loliginid fishery based on the species *Loligo reynaudii* (re-named *Loligo reynaudii* in 2008: Vecchione 2008) exists on the Agulhas Bank at the southern tip of the continent (see Figure 1.1; Augustyn *et al.*1994). Locally this loliginid is called “chokka squid” and hence the “chokka fishery”. Bi-annual demersal surveys estimate an average biomass of around 25 000 t. The fleet of about 300 small (10–15 m) vessels, which target the spawning grounds on the eastern Agulhas Bank using hand-held jigs, catch on average some 7 000 t y^{-1}. The chokka fishery employs some 2 500 fishers and about 570 factory staff. In terms of catch by fishery and product value, the chokka squid fishery is ranked 4th most important fishery in South Africa. The entire product is sold to overseas markets mainly Italy and Spain and is the highest valued of all squid worldwide at times fetching $7 per kilogram. This brings much needed foreign revenue (~$35–60 million annually) to the impoverished Eastern Cape Province. A small by-catch (6% of the annual jig catch) is made by the trawl fishery and the product sold locally for fishing bait.

Catch fluctuations (the problem!)

As with all squid fisheries, chokka squid biomass and catch vary considerably (Figure 1.2). In the case of biomass the trend varies on an annual basis no doubt a consequence of the near-annual life span and spawning and recruitment success from the previous summer. Recruitment success is strongly dependent on favourable environmental conditions (Bakun 1996). Catch on the other hand varies on daily, monthly and annual time scales. Daily variability has been investigated by Roberts (1998b) who suggested that factors such as diurnal behaviour, feeding, predators and short term environmental events such as coastal upwelling (temperature), benthic nepheloid layers (turbidity) and excessive wave surge influence spawning aggregation. Monthly and annual catch not only reflect the dominance of these events but also reflect underlying biomass trends. Roberts (1998a) noted an

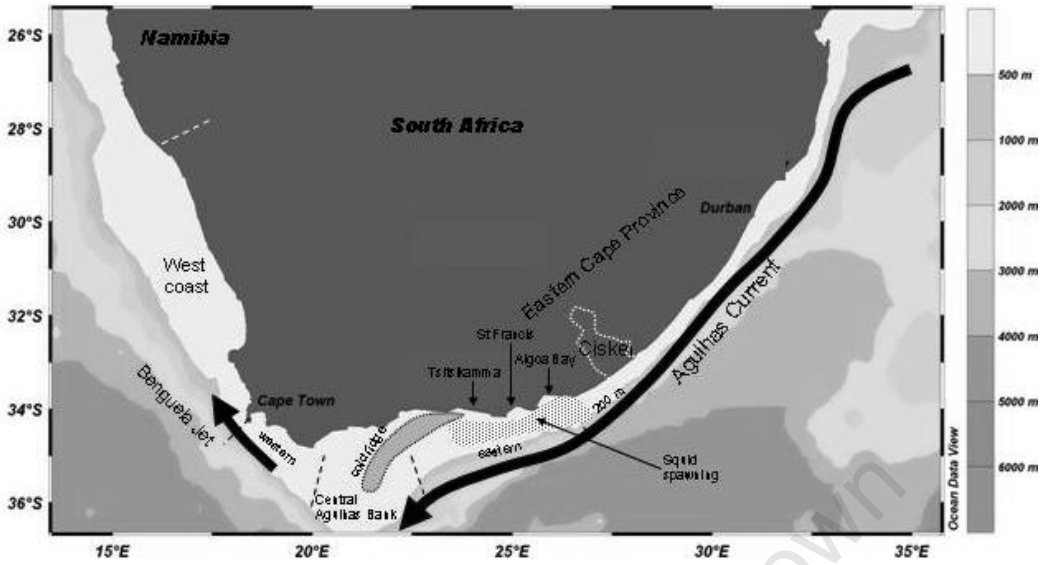

Figure 1.1: Map showing place names in the text, the cold ridge and the chokka squid spawning grounds.

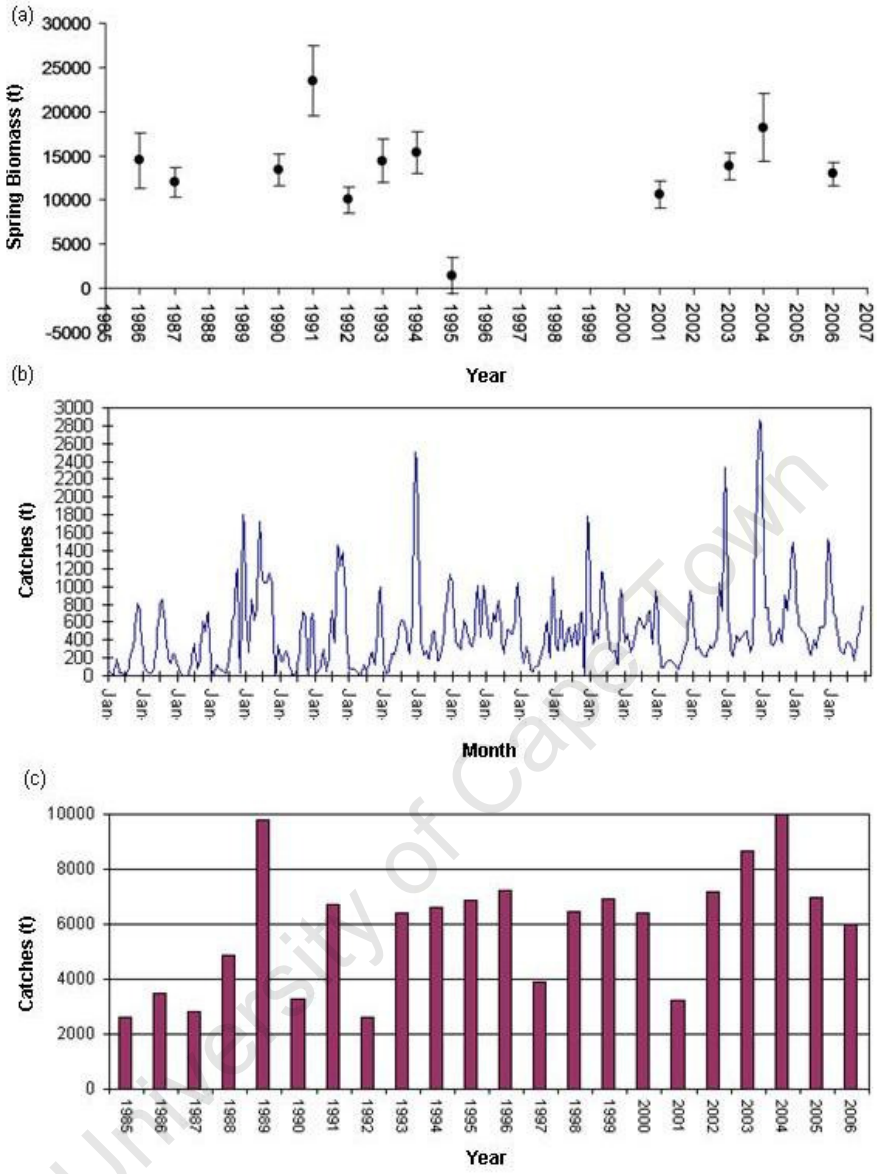

Figure 1.2: (a) Chokka squid spring biomass estimates from demersal trawl surveys, (b) total monthly hand-jig catches, and (c) annual hand-jig catches

association between El Niño Southern Oscillation (ENSO) events and catch fluctuations during the early years of the chokka fishery, and suggested that the excellent catches in 1988–9 were caused in some way by prolonged coastal upwelling on the south coast which was coincident with a strong La Niña phase in the Pacific Ocean, and that the poor catches in 1990 and 1992 were related to prolonged El Niño conditions which purportedly reduced coastal upwelling. However, over time it has become clear that this association does not always hold and that there are other factors at play which influence biomass and catch.

The ramifications of catch fluctuations of such magnitude are significant and create uncertainty for resource managers and the fishing industry with the net result of increased risk levels of stock collapse, economic instability and long term investment. Moreover, with the chokka fishery being semi-artisnal, catch fluctuations directly impact the livelihoods of the fishers and their families causing socio-economic hardship as wages are based on squid catch per fisher.

The more recent crash of the fishery in 2001 had a devastating effect and serves as a good illustration of the value of knowledge. Below is an excerpt from a front page headline report in the Eastern Province Herald newspaper on 18th July 2001:

> *'Chokka crisis hits black business — demoralizing spates of poor catches threatens livelihood of 1000s*. Once again it would seem that this fishery is going through a period of low catches with all the familiar signs of economic hardship at the fishermen and boat owner levels. Crime levels have increased recently in St Francis Bay according to a police spokesman, an indication apparently that fishing crews are making little money from catching chokka. Financial institutions report that credit has begun to be restructured as boat owners struggle to make repayments and require finance to maintain livelihood and vessel operations. Harbour masters report that payment for fuel accounts is falling behind. Generally, there is consensus amongst chokka squid fishermen that 2001 will be the worst year for catches in the fishery's 15-year history. Interestingly, best catches appear to be off the Ciskei, a restricted access region usually considered to be fringe to the main fishing grounds. Moreover, for the first time reports have been received that chokka squid is being hand-jigged off Namibia. This is thought to be beyond the normal range of this species.'

Industry and politicians at the time demanded answers from scientists and resource managers, but neither could provide an unambiguous explanation for the low catches. There was no way of telling whether effort had crossed the critical sustainable yield threshold through over zealous permit allocations in the new political dispensation, or if the low catches were caused by an environmental perturbation. Clearly there was a need to understand the factors that influence biomass and catch. Ideally, the ability to forecast fluctuations was

required, as has been pointed out by Kawahara *et al.* (1993), Sakurai (1997), Pauly (1985) and others also working in squid fisheries. With squid fisheries replacing declining traditional fisheries in many parts of the world and the global market value of squid being significantly higher than finfish, understanding the squid life cycle–environment relationship has become ever more important and relevant.

Research approach and thesis structure

In the case of the ommastrephid fisheries, particularly those tied to WBCs, a good understanding of the life cycle and its links to the environment and ecosystem has been achieved through research. This is partly because the WBC is the main ecosystem component and the characteristics and dynamics of these currents are well understood. This is highlighted by the number of papers published between 1988 and 1993 — a total 1074 papers on the Gulf Stream, 965 on the Kuroshio, 141 on the Agulhas Current, 71 on the Brazil Current and 69 on the East Australian Current (Lutjeharms 2006). But in the case of neritic squids such as *Loligo* species, very little is known about the life cycle and in particular how this is influenced by the ecosystem. Moreover, shelf ecosystems are complex, ill-defined and often the main features, components and driving forces unknown.

Fortunately the chokka squid *Loligo reynaudii* is arguably the best studied neritic squid in the world with over 100 research papers having been published to date. Nonetheless, the challenge remained on how to proceed with an investigation into the species fluctuations in biomass. It was decided to base the research approach on Bakun's (1996) triad of requirements for successful recruitment — enrichment, concentration and retention in the ecosystem. For chokka squid this implies that recruitment depends on the survival of paralarvae in terms of food availability, feeding success (copepods biomass, density distribution and patchiness) and retention in the ecosystem.

This thesis therefore provides the first step in understanding the factors which influence the biomass of the South African chokka squid *Loligo reynaudii*. The nature of this investigation demanded a multidisciplinary approach comprising physical oceanography and biology as well as a variety of scientific techniques. Each chapter is a separate investigation and has been presented in stand-alone research manuscript format including abstract and references. Chapters 2 to 4 have been published in peer-review journals while chapters 5 and 6 have been submitted for publication (see Declaration for co-authorship and contributions). Consequently some repetition exists in the introduction sections of each chapter.

Chapter 2 begins with the reasons for chokka squid using the eastern Agulhas Bank for spawning. This required an understanding of the Agulhas Bank ecosystem and identification of critical components which ensure successful recruitment (i.e. an upwelling feature called the cold ridge (see Figure 2.1a) and westward shelf currents). A combination of archived *in situ* data, published data and remote sensing data highlighted a mismatch between the place of hatching and the best place for paralarvae feeding on the Agulhas Bank. It is proposed that this mismatch is overcome by shelf currents which transport passive paralarvae to the cold

ridge area — a concept referred to as the ***westward transport hypothesis*** or ***WTH*** (hypothesis 1). The WTH was then tested by comparing the summer strength of the cold ridge (using SST at the base of this feature as a proxy) with chokka squid annual biomass and catch in the following year. The result is encouraging with 90% of the annual variation in chokka squid biomass explained by the strength of the cold ridge (r^2=0.9), but it is acknowledged that at times, e.g. during episodic phenomenon such El Nino years, this linear relationship does not hold. The WTH, however, is based on mid shelf current data and therefore mainly relevant to the deep spawning grounds.

Chapter 3 examines the circulation on the inshore spawning grounds along the Tsitsikamma coast which is east and closest to the cold ridge (Figure 2.10a Chapter 2). This coast line represents about 40% of the total inshore spawning ground and is straight. The remainder of the spawning grounds comprise large embayments St Francis Bay and Algoa Bay where circulation will be complex and more difficult to resolve. Results from an ADCP current meter deployed for 12 months midway on the Tsitsikamma coast, surprisingly indicated that flow is predominantly (70%) eastward indicating inshore transport of paralarvae away from the cold ridge. This however appears to be mitigated by coastal upwelling and a semi-permanent eddy at the end of the current which return the paralarvae to the westward mid shelf current. Consequently, the WTH is refined to accommodate these results.

While the WTH remains useful to focus studies on this species, e.g. Vidal *et al.* (2005) and Martins *et al.* (2010), Chapter 4 re-examines the dependency of squid paralarvae on the cold ridge as the only rich feeding area on the Agulhas Bank as well as the role of currents in the early squid life cycle. Existing data and materials were used to indicate that chlorophyll and copepods are also found at elevated levels on the thermocline in areas other than the cold ridge, and that currents may not necessarily be so critical to connect hatching position with food. Importantly, it is postulated that ***currents may remove squid paralarvae from the Agulhas Bank ecosystem and hence impair recruitment and ultimately catches*** (hypothesis 2).

Chapter 5 is an investigation into the possibility of advective losses of squid paralarvae. An Individual-based Model (IBM) coupled to the output of an ocean model (ROMS) is used to test this. Given some limitations of the models and the lack of knowledge regarding squid paralarvae characteristics, results indeed demonstrate that squid paralarvae can be removed from the Agulhas Bank ecosystem mainly on the eastern and western Agulhas Bank and that advective losses may well account for sudden drops in biomass and annual catches.

Chapter 6 presents an attempt to validate the results of the ROMS-IBM experiment using satellite-tracked drifters as well as investigate Lagrangian transport on the inshore spawning grounds. The latter could not be covered in the ROMS–IBM due to possible boundary effects. Two drifters were deployed on the inshore spawning grounds in the Tsitsikamma coastal current (Chapter 3) in the same position as the bottom-mounted ADCP mooring. The other two drifters were deployed at the virtual particle release position in the ROMS–IBM experiment for the eastern Agulhas Current. Results not only confirm retention

on the central Agulhas Bank but also that shelf leakage occurs on the western and eastern Agulhas Banks, even from the inshore Tsitsikamma spawning grounds.

Chapter 7 presents a synthesis of the aims, hypotheses, main findings and conclusions of these studies collectively.

References

Augustyn CJ, Lipinski MR, Sauer WHH, Roberts MJ, Mitchell-Innes BA. 1994. Chokka squid on the Agulhas Bank: life history and ecology. *South African Journal of Science* 90: 143–154.

Bakun A. 1996. *Patterns in the Ocean. Ocean processes and marine population dynamics*. California Sea Grant, National Oceanic and Atmospheric Administration and Centro de Investigaciones biológicas del Noroeste, La Paz, BCS México: 323 pp.

Ceolho ML. 1985. Review of the influence of oceanographic factors on cephalopod distribution and life cycles. *NAFO Science Council Studies* 9: 47-57.

Dawe EG, Warren WG. 1993. Recruitment of short-finned squid in the Northwest Atlantic Ocean and some environmental relationships. *Journal of Cephalopod Biology* 2(2): 1-16.

Falklands Island Government. 1997. *Falkland islands Government Fisheries Statistics*. Volume 1. Falkland Islands Government printing office, Stanely, Falkland Islands: 75 pp.

Hatanaka H, Kawahara S, Uozumi Y, Kasahara S. 1985. Comparison of life cycles of five ommastrephid squids fished by Japan: *Todarodes pacificus*, *Illex illecebrosus*, *Illex argentinus*, *Nototodarus sloani sloani* and *Nototodarus sloani gouldi*. *NAFO Science Council Studies* 9: 59–68.

Kawahara S, Uozumi Y, Hatanaka H. 1993. Is it possible to predict ommastrephid squid abundance in advance of the fishing season? *In* Recent Advances in Cephalopod Fisheries Biology. Okutani T, O'Dor RK, Kubodera T (eds). Tokai University Press, Tokyo: 728-734 pp.

Lutjeharms JRE. 2006. The Agulhas Current. Springer, Berlin: 329 pp.

Martins RS, Roberts M, Vidal EAG, Moloney CL. 2010. Effects of temperature on yolk utilization by chokka squid (*Loligo reynaudii* d"Orbigny, 1839) paralarvae. *Journal of Experimental Marine Biology and Ecology* 386(1–2): 19–26.

Roberts MJ, Rodhouse P, O'Dor RK, Sakurai Y. 1998. A global perspective of environmental research on squid. *ICES Document* CM1998/M: 27.

Roberts MJ. 1998a. What happened to the South Coast El Niño 1997-98, squid catches? *In*: Fishing Handbook: South Africa, Namibia, Moçambique 1998. 26th Edition. Stutterford M (ed): 233-238.

Roberts MJ. 1998b. The influence of the environment on chokka squid *Loligo vulgaris reynaudii* spawning aggregations: steps towards a quantified model. *South African Journal of Marine Science* 20: 134–149.

Rodhouse PG, Dawe EG O'Dor RK. 1998. Squid recruitment dynamics. The genus *Illex* as a model. The commercial *Illex* species. Influences on variability. *FAO Fisheries Technical Paper*. No 376. Rome, FAO. 273 pp.

O'Dor RK. 1992. Big squid in big currents. *South African Journal of Marine Science* 12: 225–235.

Vecchione M. 2008. *Loligo* Lamarck, 1798. Inshore squid. Version 04 March 2008 (under construction). http://tolweb.org/Loligo/19858/2008.03.04 in The Tree of Life Web Project, http://tolweb.org/

Vidal E, Martins, R, Roberts M. 2005. Yolk utilization, metabolism and growth in reared *Loligo vulgaris reynaudii* paralarvae. *Aquatic Living Resources* 18: 385–393.

CHAPTER 2

Chokka squid (*Loligo reynaudii*) abundance linked to changes in the Agulhas Bank ecosystem during spawning and the early life cycle

Chokka squid biomass and catch are highly variable, likely owing to their links to changes in the ecosystem, which impact spawning and recruitment. A synthesis of basic ecosystem components for the domain in which chokka squid live (i.e. South Africa's west coast and Agulhas Bank), was prepared using published and new data. It included substratum, bottom temperature, bottom dissolved oxygen, chlorophyll, and copepod abundance. Alongshore gradients of these indicated that the main spawning grounds on the eastern Agulhas Bank are positioned where bottom temperature and bottom dissolved oxygen are optimal for embryonic development. This location, however, appears suboptimal for hatchlings because the copepod maximum (food for paralarvae) is typically on the central Agulhas Bank some 200 km to the west. Data on currents suggest that this constraint may be overcome by the existence of a net west-flowing shelf current on the eastern Agulhas Bank, improving survivorship of paralarvae by transporting them passively towards the copepod maximum. CTD data and a temporal analysis of AVHRR satellite imagery reveal the copepod maximum to be supported by a "cold ridge", a mesoscale upwelling filament present during summer when squid spawning peaks. *In situ* sea surface temperature (SST) data used as a proxy for cold ridge activity demonstrate considerable interannual variability of the feature, especially during *El Niño*–Southern Oscillation events. Negative linear correlations between maximum summer SST (monthly average) and squid biomass the following autumn (r^2 = 0.94), and annual catch (r^2 = 0.69), support the link between the "cold ridge–copepod maximum" and the early life cycle of chokka squid, and holds promise for prediction.

Keywords: biomass, catch, chokka squid, cold ridge, currents, ecosystem, gradients, spawning, upwelling filament.

Introduction

The marine environment around southern Africa is one of the most diverse, complex, and highly variable anywhere in the world (Figure 2.1; Lutjeharms *et al*. 2001). The oceanography of South Africa's east coast and outer Agulhas Bank (south coast) is strongly influenced by the warm, fast-flowing (~ 2 m s^{-1}) Agulhas Current. This is a well-defined western boundary current with origins in the Moçambique Channel (Lutjeharms 2001), and it transports some 70–135 Sv. At the southern tip of the Agulhas Bank, the Agulhas Current undergoes a number of configurations, which include retroflection eastwards along the Subtropical Convergence into the South Indian Ocean, the formation of anticyclonic rings shed into the South Atlantic (Duncombe–Rae 1991), or continuous flow along the shelf edge of the western Bank (Lutjeharms and Cooper 1996). On the outer Agulhas Bank the oceanography is dominated by associated shear boundary processes, such as meanders, eddies, and break-

away filaments (Lutjeharms *et al.* 1989). Large-scale upwelling is common east of Port Elizabeth, as a result of the divergence between the shelf edge (and Agulhas Current) and the coast (Lutjeharms *et al.* 1999). Intense thermoclines induced by shelf-edge upwelling and insolation are characteristic of the eastern and central Bank (Largier and Swart 1987). The inner shelf is influenced by wind-driven coastal upwelling, particularly during summer (Schumann *et al.* 1982). Upward doming of the thermocline in an elongated formation is often found on the central Agulhas Bank. This feature, referred to as a "cold ridge" (Figure 2.1b), is commonly associated with high levels of primary and secondary production (Boyd and Shillington 1994). Large, solitary, transient, meanders in the Agulhas Current, referred to sometimes as a "Natal Pulse", are at times found on South Africa's east coast (De Ruijter *et al.* 1999). These have profound influences on the shelf oceanography there, as well as on the trajectory of the Agulhas Current (Roberts *et al.* Unpublished). Ring formation has been associated with the Natal Pulse (Van Leeuwen *et al.* 2000).

The west coast is completely different, dominated by the cold Benguela upwelling system (Shannon and Nelson 1996), one of the largest eastern boundary upwelling systems in the world and primarily driven by the South Atlantic High Pressure (anticyclone) and associated south-easterly winds (Figure 2.1a). Consequently, the region has abundant primary and secondary production, frequently leading to low levels of dissolved oxygen in the bottom layer, and at times almost anoxic conditions (Chapman and Shannon 1987). There, the outer shelf is influenced by the north-flowing, cooler, slower (0.25–0.50 m s^{-1}) Benguela Current (Boyd *et al.* 1992). This eastern boundary current is less defined than the Agulhas Current, and essentially is the eastern component of the South Atlantic gyre. A narrow frontal jet, referred to as the Benguela jet, is common along the shelf edge between the Cape Peninsula and Cape Columbine (Figure 2.1b). Compared with the Agulhas Current, the Benguela jet is small, with maximum velocities of ~ 0.75 m s^{-1} and a flow of 1–7 Sv. North of Cape Columbine the jet undergoes bifurcation, moving onto the wider shelf and into the South Atlantic towards the Walvis Ridge. The northern boundary of the Benguela is where the continental margin narrows at 16°S, and is marked by the permanent warm Angola–Benguela Front (Boyd 1987). Agulhas rings (Duncombe-Rae *et al.* 1992), other eddy features (Lutjeharms and Matthysen 1995), and filaments (Nelson *et al.* 1998) interact with the west coast shelf, causing water to be drawn offshore. A poleward undercurrent on the shelf and slope vary in strength and seasonal dependence (Nelson 1989).

Much of the variability on the shelf around South Africa is consequently caused by the dynamics of the Agulhas Current, Benguela Current (and jet), and north–south seasonal migration of atmospheric high-pressure cells situated over the SE Atlantic and SW Indian Oceans (Figure 2.1a; Tyson and Preston-White 2000). In winter, the westerly belt expands to the latitudes of southern Africa, causing strong westerly winds to dominate, with large swells. In summer, the westerly belt contracts south, and the wind field is then largely driven by the two anticyclones, causing coastal upwelling on the west coast and Agulhas Bank.

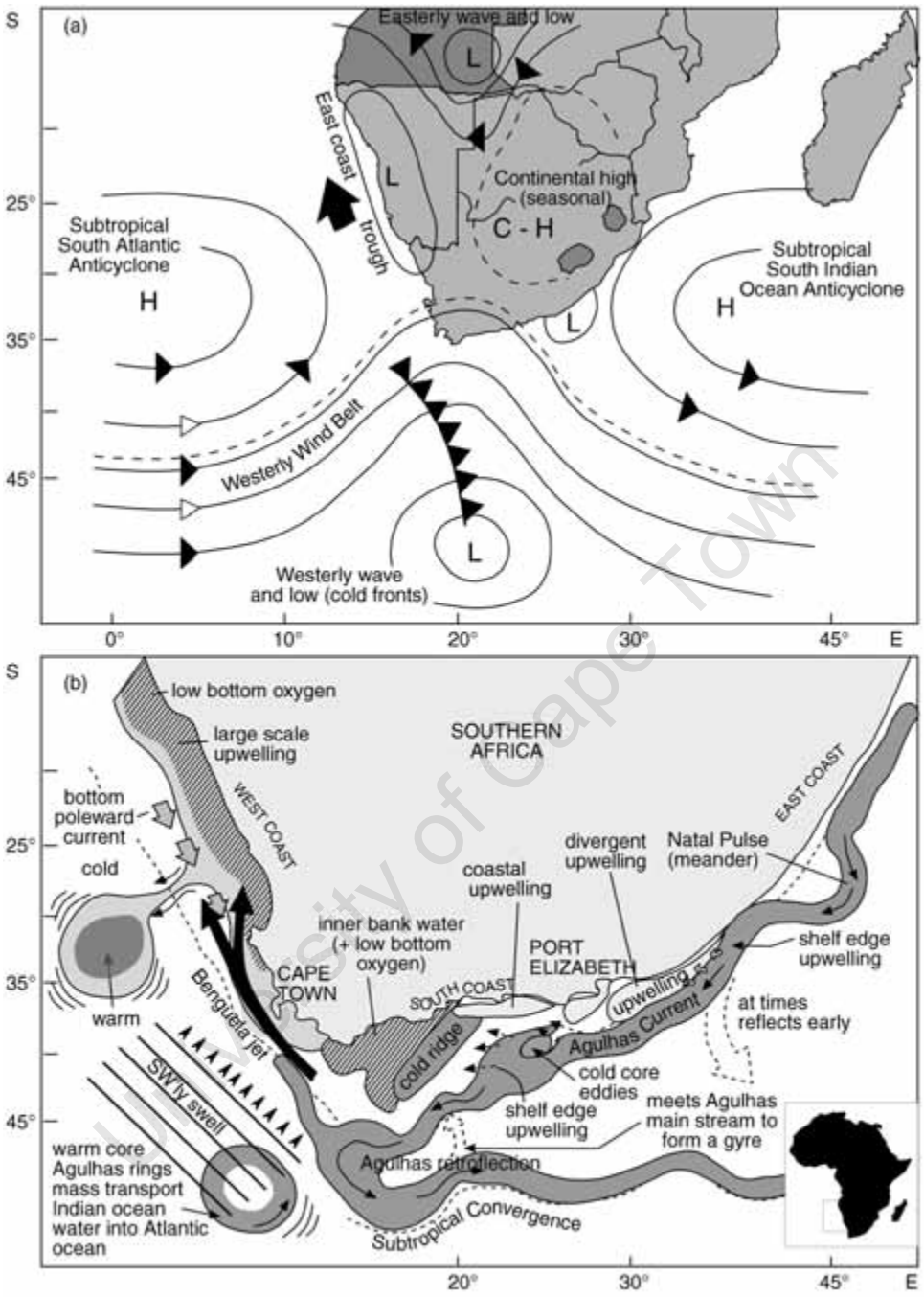

Figure 2.1: (a) The complexity and variability of the marine environment around southern Africa is partly due to the latitude and associated weather. In summer, the oceanic high pressure cells either side of southern Africa dominate the wind field, causing southeasterly winds on the west coast and northeasterly winds on the eastern Agulhas Bank and east coast. In winter, the westerly wind belt migrates north, moving cold fronts and strong westerly winds to southern Africa. (b) The oceanography is also dominated by the warm Agulhas and cold Benguela Currents. These drive many of the physical processes and key features on the shelf.

Chokka squid (*Loligo reynaudii*) live within this diverse environment on the shelf and are commonly found between the Orange River and the Great Fish River (Figure 2.2). Seldom are squid found deeper than 200 m, and most of the biomass is over the Agulhas Bank. Egg masses recovered from fishing jigs and trawlers, as well as diver observations, indicate that spawning takes place on the narrower eastern Agulhas Bank in a distinct area between Plettenberg Bay and Port Alfred (Augustyn 1990; Sauer *et al.* 1992; Sauer and Smale 1993; Sauer 1995a, Sauer 1995b; Roberts 1998a). Such a discrete geographical location for spawning suggests an environmental niche there that suits either egg development or paralarvae survival, or both. Should this be the case, then variability and uncharacteristic changes in this niche (ecosystem) could either weaken or strengthen the inherent biological advantages, and ultimately impact recruitment. This could explain, at least in part, the fluctuations in biomass and catch that impact the fishery (Figure 2.3).

To investigate this hypothesis, the approach taken was first to define the ecosystem in which chokka squid live, as quantitatively as possible. Using longshore gradients to synthesize this information, environmental advantages of the spawning grounds on the eastern Agulhas Bank were then identified. The cold ridge to the west supports the copepod maximum in the ecosystem (abundant food for squid paralarvae), and was investigated in detail to establish variability and uncharacteristic behaviour with implications for survival and recruitment of paralarvae.

Readers are referred variously to Figure 2.2, 2.4, 2.6, 2.7, 2.8 and 2.9 to identify the location of places mentioned throughout the text.

Data and methods

The study used both published and new data.

Squid biomass and catch

Estimates of chokka squid biomass and the jig catches of squid were taken from Roel (1998), and the Marine & Coastal Management (MCM) database respectively. Biomass estimates were calculated from demersal trawl surveys undertaken annually in the austral autumn (for survey detail, see Roel 1998). There were no biomass surveys in 1998, 1999, or 2000. Jig catch statistics were derived from mandatory monthly catch return forms submitted by fishers (comments on the accuracy of these data are made by Roel (1998), and Schön (2000)).

Productivity

The mean horizontal distribution of chlorophyll was obtained from Brown and Cochrane (1991), and is augmented using composite Coastal Zone Colour Scanner (CZCS) data (see below). Copepod distribution data are limited, and are currently not available in suitable format for statistical analysis and mapping, so an impression of copepod biomass distribution was derived from a west coast (May 1991) and an Agulhas Bank (November 1989) survey,

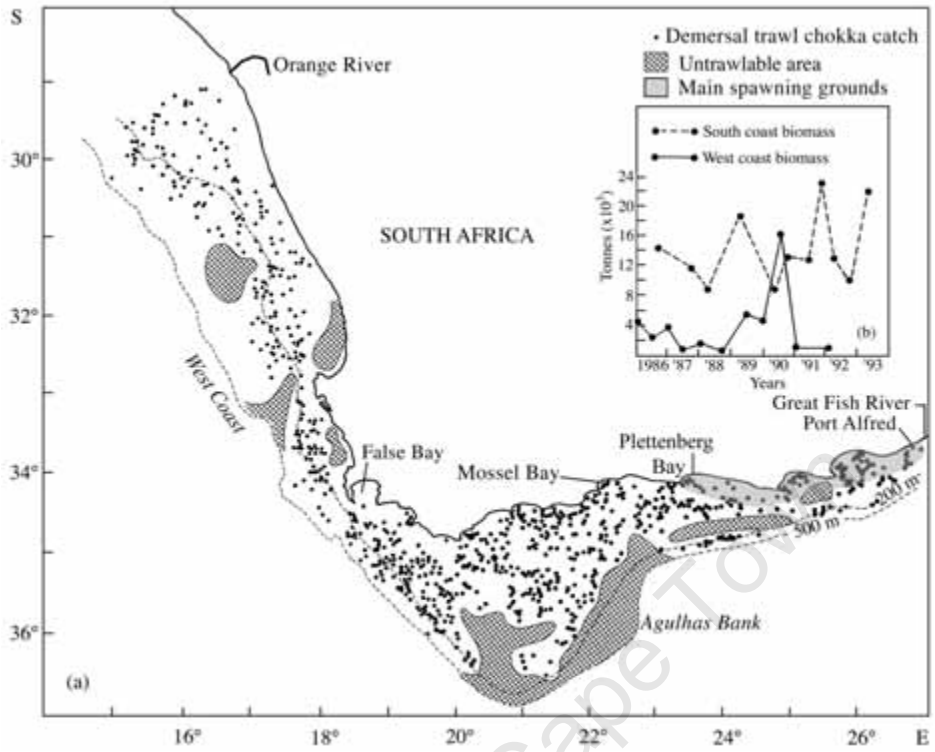

Figure 2.2: Demersal trawl catches indicate that chokka squid (*Loligo reynaudii*) are found on the west coast and Agulhas Bank to a depth of about 300 m. Most of the biomass is on the Agulhas Bank (insert b). The main spawning grounds are between Plettenberg Bay and Port Alfred.

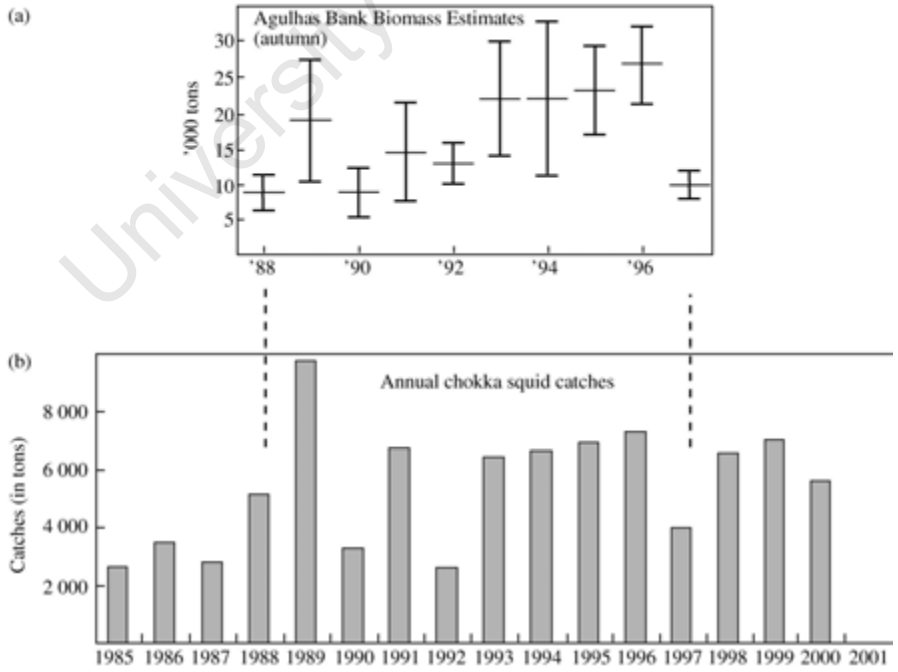

Figure 2.3: (a) The (autumn) chokka squid biomass on the Agulhas Bank is conservatively estimated to range between 8 000 and 28 000 t (no surveys were carried out for 1998–2000). (b) Annual catches appear to follow a similar trend to that in (a).

which overlapped at Cape Agulhas. In both, copepod biomass was considered unusually high (J. A. Huggett, MCM, pers. comm.).

Oceanography

The most comprehensive published record of currents in the upper mixed layer for South Africa's west coast and Agulhas Bank are those of Boyd *et al.* (1992) and Boyd and Oberholster (1994). That work was based on ADCP (150 kHz) data collected by the FRS "Africana" and "Algoa" during May, September, and November of the years 1989–1994. The data are presented as average current vectors over 15'×15' blocks of longitude and latitude, and one specific set of data used for exemplification was collected during an anchovy (*Engraulis encrasicolus*) biomass survey in November 1992.

CTD and dissolved oxygen (DO) data for 86 surveys were extracted from the MCM oceanographic database. Since 1983, routine demersal biomass surveys have been undertaken in May and September on the Agulhas Bank (20–27°E), and in January and July on the west coast (29°S–20°E). Pelagic acoustic biomass surveys undertaken in November each year cover both coasts. Measurements were made with Neil Brown Mk 3 and 5 CTDs, with water samples taken at standard depths. DO was determined from water samples taken immediately after CTD retrieval using the Winkler titration method (Strickland and Parsons 1972). Bottom CTD measurements were collected 3–10 m from the sea floor, depending on sea conditions, but ship size precluded stations in depths <30 m.

Data were statistically treated in 15'×15' blocks of longitude and latitude, though blocks with <3 stations were excluded from the analysis. Maps of bottom temperature and dissolved oxygen were produced depicting minima, means, and maxima.

SST data were collected at the entrance to the Knysna Lagoon. Until June 1994, they were collected daily using a bucket and mercury thermometer. Then, in April 1995, an electronic mini Hugrun underwater temperature recorder (UTR) was installed at the same site in a depth of 6 m. This instrument records the average hourly temperature (accuracy ± 0.01˚C). Inter-calibration between these methods showed <0.4˚C difference in the average data, and the same trends. Another SST data set was collected by a UTR located at Tsitsikamma, which yielded essentially the same monthly trends as at Knysna. All time-series of SST are ongoing (see www.oceanafrica.com).

Satellite imagery

The ocean colour image used here is a composite of Nimbus–7 Coastal Zone Colour Scanner (CZCS) data collected between 1978 and 1986, sourced from www.seawifs.gsfc.nasa.gov/SEAWIFS/CSCZ_DATA. For the temporal analysis of the cold ridge, daily NOAA AVHRR images from 1985 to 1993 were used. In all, 420 cloud-free images were scanned visually for cold-water incursions onto the Agulhas Bank between 21 and 25˚E.

West coast and Agulhas Bank ecosystem

Bottom temperature

The influence of temperature on egg development has been determined for a number of ommastrephid and loliginid squid species (e.g. Boletzky *et al.* 1973; O'Dor *et al.* 1982; Barón 2002; Oosthuizen *et al.* 2002). All showed that the rate of embryonic development increases at higher temperatures, until a threshold is reached and mortality occurs. Initial work on chokka squid by Augustyn *et al.* (1992) suggested egg mortality at temperatures <10˚C and >24˚C. More recently, however, Oosthuizen *et al.* (2002) demonstrated in laboratory trials that optimal temperatures for chokka squid egg development ranges between 12 and 17˚C, and that outside of this, the proportion of embryonic abnormalities rapidly increase, resulting in mortality.

The colour maps in Figure 2.4 depict minimum, mean, and maximum bottom temperature (BT) for the west coast and the Agulhas Bank. The benthic environment on the west coast is dominated by low temperature. If all data between 30 and 500 m are included, then the range is 3.2–16.4˚C. The average of the minimum BTs shown in Figure 2.4a is 7.7˚C. The low temperatures reflect both quasi-permanent large-scale upwelling, and a deep shelf break at 400 m. In fact, almost half the west coast shelf is between 200 and 400 m, and BTs at such depths there range between 5 and 7˚C (Figure 2.4a, c). At times, cold water (<7˚C) can almost reach the coast (Figure 2.4a). Deeper than 100 m, BTs are higher, with an average around 10˚C, but seldom exceed 11˚C. The maximum BTs on the west coast are near Cape Columbine and St Helena Bay, between 14 and 15°C (Figure 2.4c).

In contrast, the Agulhas Bank benthic environment is warmer, with an overall average BT about 2.5°C higher (11.2 vs. 8.7˚C). There too, the range of BTs between 30 and 500 m deep is greater, i.e. 3.3–22.1°C, a reflection of a shallower shelf break (200 m), the presence of the Agulhas Current, a wider shelf, and less intense coastal upwelling. BTs on the outer shelf are 2–3˚C warmer on the Bank than over the west coast outer shelf, typically 9–10˚C, and are maintained by shelf-edge upwelling induced by the dynamics of the fast flowing Agulhas Current (Lutjeharms *et al.* 1989; Roberts *et al.* Unpublished). Predictably, mean BT is highest (Figure 2.4b) adjacent to the coast, but also on the extensive shallow inner central Agulhas Bank, where the 100 m contour is >100 km offshore. Maximum BTs (Figure 2.4c) there can exceed 16˚C, and data presented by Eagle and Orren (1985) show that BT is high mainly during winter, when storms and wave action erode the intense thermocline, resulting in isothermal mixing of the water column.

The distribution of BTs on the western Agulhas Bank reflect characteristics of both the west coast and the Agulhas Bank proper. The temperature range of the inner shelf is 9–16˚C (Figure 2.4a, c), and the mean 10–11˚C (Figure 2.4b). On the outer and mid-shelf, temperatures drop to 7˚C, with maxima of about 10˚C. There is a slight warming trend from west to east. BTs at depths of 100 m are also high on the extreme eastern Agulhas Bank, east of 26˚E. There, mean BT is 14˚C, and the range 10–19˚C. BTs are higher because of the

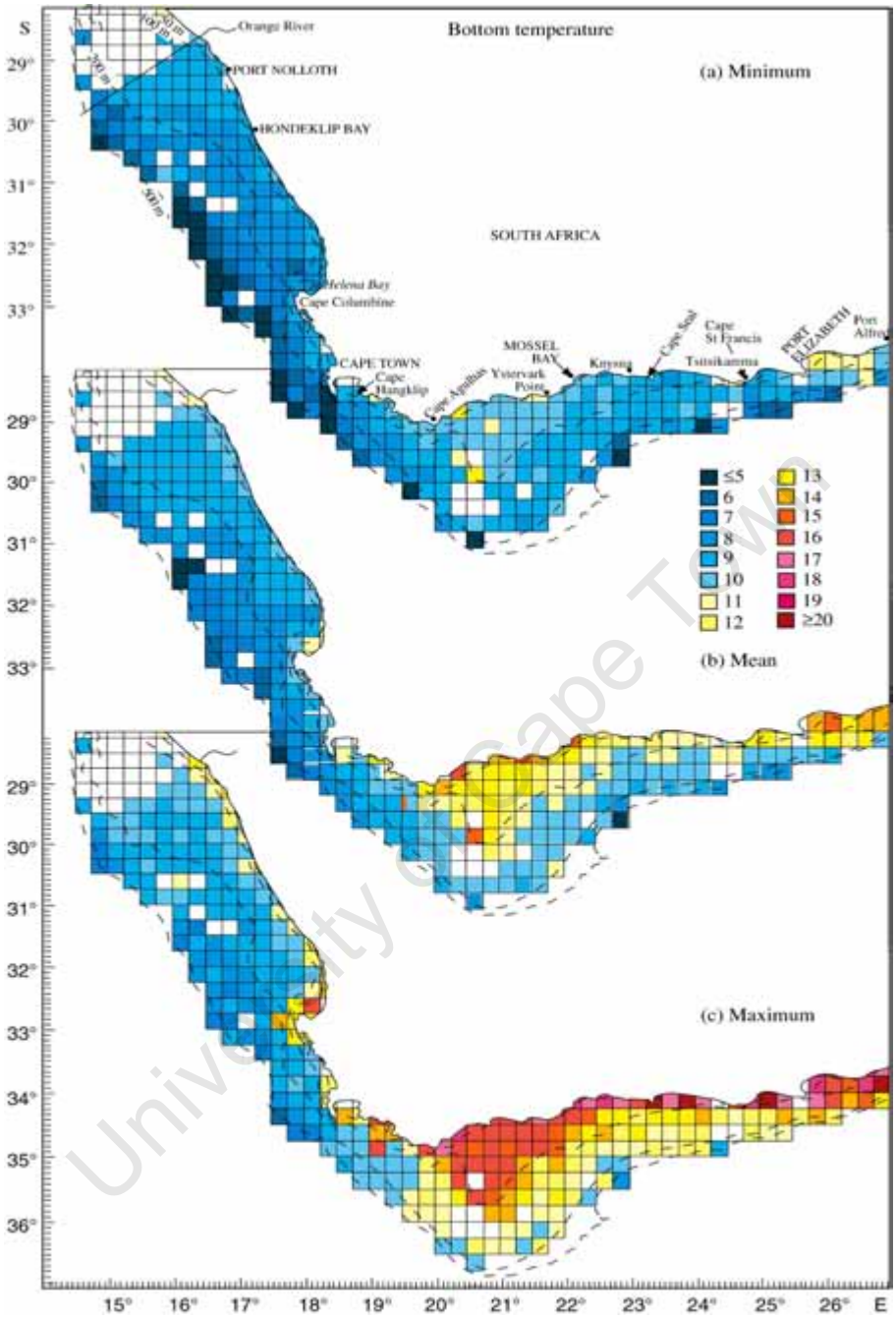

Figure 2.4: Bottom temperatures (˚C) on the shelf between the Orange River and Port Alfred. (a) Minimum, (b) mean, and (c) maximum values are shown for each 15'×15' block.

shallower shelf (the 100 m contour moves to the shelf edge between Port Elizabeth and Port Alfred), and the influence of the warm Agulhas Current. Regions of high BT (i.e. <100 m deep) account for some 32% of the Agulhas Bank shelf, compared with just 5% of the west coast.

East of Port Alfred the shelf is narrow (<20 km) and strongly influenced by the Agulhas Current. Few oceanographic data have been collected there, but of those, Beckley and Van Ballegooyen (1992) showed that shelf BT increases in an eastward direction. There is a significant subsurface front on the inner shelf near the Mbashe River, east of which the BT ranges between 19 and 24˚C. At 100 m, BTs are >18˚C.

The benthic environment on the west coast, including inshore, is clearly too cold for successful development of chokka squid eggs, which require a range of 12–17˚C. Such a temperature range is however, found on the central and eastern Agulhas Bank in the extensive area shallower than 100 m. In terms of BT, the shelf between Port Alfred and the Mbashe River also appears to be suitable for spawning, but temperatures approach the upper threshold for successful egg hatching. East of the Mbashe River, the BT is too high for hatching.

Bottom dissolved oxygen

De Mont and O'Dor (1984), O'Dor *et al.* (1994), and Pörtner and Zeillinski (1998) have demonstrated that the rate of metabolism of adult squid is high, perhaps 7× that of fish, demanding a good supply of dissolved oxygen. Howell and Simpson (1994), working in Long Island Sound, showed that squid (*Loligo pealeii*) were not found where the bottom dissolved oxygen (BDO) was <2.1 ml l^{-1}. Roberts and Sauer (1994) stated that adult chokka squid are not found inshore on the west coast where BDO is low, suggesting a threshold of 3 ml l^{-1}.

The results of a spatio-statistical analysis of BDO on the west coast and Agulhas Bank are given on Figure 2.5. As with temperature, there is a stark difference in BDO between the west coast and particularly the eastern Agulhas Bank, with the inner central and western Bank forming a transition zone of high variability. BDO on the West Coast is about 1 ml l^{-1} less than on the Agulhas Bank (3.39 vs. 4.24 ml l^{-1}).

The mean data in Figure 2.5b show BDO on the west coast to be commonly <3 ml l^{-1} on both the inner and mid-shelf, especially north of Cape Columbine. Maxima (Figure 2.5a) in many blocks do not exceed 3 ml l^{-1} at all on the inner shelf. In contrast, the bottom layer on the outer shelf is well oxygenated much of the time (Figure 2.5b) but, as indicated in Figure 2.5c, low BDO can at times almost extend to the shelf edge. Though not visible in Figure 2.5c, BDO can drop to almost zero on the inner and mid-shelf. In contrast, BDO in St Helena Bay ranges between 0.02 and 6 ml l^{-1} (Figure 2.5a, c), the largest range along the South African coastline.

Bottom water on the Agulhas Bank is well oxygenated (mean values in Figure 2.5b), especially on the eastern and outer central Bank, where minima are always >4 ml l^{-1} (Figure 2.5c). This is likely due to the active shelf-edge upwelling along the inner boundary of the

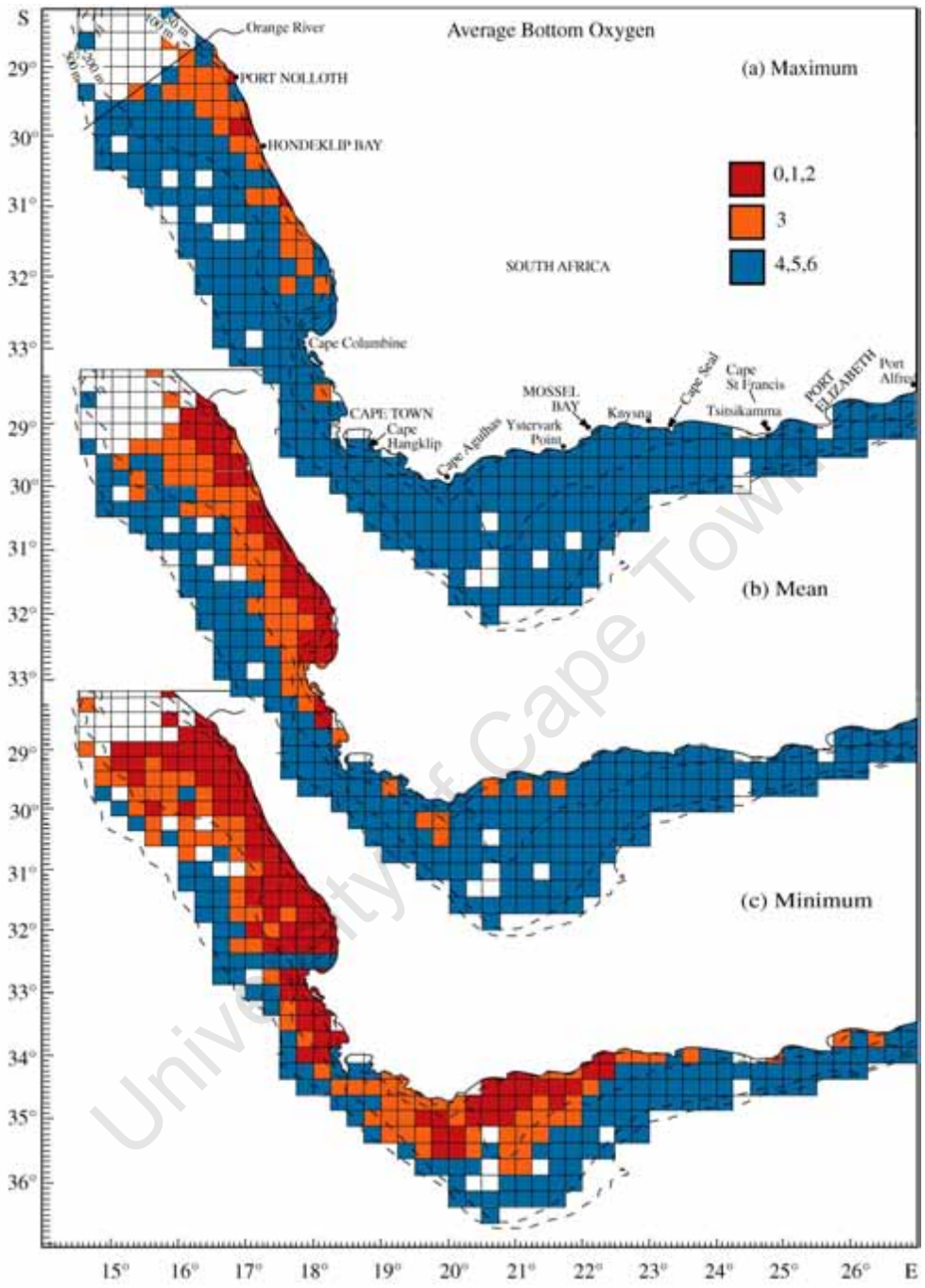

Figure 2.5: Bottom dissolved oxygen (ml l^{-1}) on the shelf between the Orange River and Port Alfred. (a) Maximum, (b) mean, and (c) minimum values are shown for each 15'×15' block.

Agulhas Current (Chapman and Largier 1989; Lutjeharms *et al.* 1999; Roberts *et al.* Unpublished). As a result, the bottom mixed layer on the eastern and outer central Bank contains Indian Ocean Central Water, with a BDO >4 ml l^{-1}.

As already mentioned, the western and inner central Bank have characteristics of both west coast and eastern Agulhas Bank. In the data set analysed here, the minimum BDO for the region east of 20˚E is 1.36 ml l^{-1}, substantially higher than on the west coast. If the western Bank (Cape Point to Cape Agulhas) is included, then the lowest BDO is 0.22 ml l^{-1}. The transient (seasonal) nature of low BDO on the western and inner central Bank is evidenced by comparing minima (Figure 2.5c) and maxima (Figure 2.5a). This data set also shows that BDO on the inner central Bank is highest of all parts of the Agulhas Bank, >6 ml l^{-1}. Only St Francis and Algoa Bays have similar high levels. Work by Chapman and Largier (1989) and Eagle and Orren (1985) showed low BDO usually on the inner central Bank during late summer and autumn, when the thermocline is most pronounced.

These data, allied to the requirements for egg development, show why chokka squid do not use the west coast or western Bank for spawning. BDO (and BT) is optimal for chokka squid spawning over the eastern Bank throughout the year, or over the inner central Agulhas Bank in early summer before BDO drops. The latter area would then be considered fringe spawning.

Phytoplankton (chlorophyll) distribution

Chokka squid recruitment is dependent on survival of their paralarvae. Once hatched, paralarvae are at risk from starvation, predation, and advective loss, the last of these significant in the context of chokka squid because the spawning grounds are close to the fast-flowing Agulhas Current. Little is known about predation levels on squid paralarvae, but starvation may be a very important control. Chokka squid paralarvae are thought to feed mainly on copepods (Venter *et al.* 1999), whose spatial distribution and abundance is driven by the oceanography and concomitant primary production.

Numerous studies of primary production have been undertaken on the west coast, but fewer on the Agulhas Bank (e.g. De Jager 1957; Shannon *et al.* 1984; Shannon and Field 1985; Mitchell-Innes 1988; Brown and Cochrane 1991; Brown 1992; McMurray *et al.* 1993; Probyn *et al.* 1994). Collectively, these studies demonstrate that the west coast, with its large-scale upwelling, is the most productive region around southern Africa. This fact is illustrated in the ocean colour image of chl–*a* shown in Figure 2.6a, a 9–year composite of Nimbus–7 CZCS satellite imagery. The orange and red colours indicate high levels of chlorophyll (2–10 mg m^{-3}) at the surface. Blue indicates very little chlorophyll (~0.15 mg m^{-3}). High levels of chlorophyll on the west coast extend along the entire coast and well onto the wide shelf (the shelf break is at 400 m), the highest predictably inshore, yielding a distinct cross-shelf gradient. By comparison, chlorophyll distribution on the Agulhas Bank is limited. Levels are highest on the eastern Bank adjacent to the coast between Algoa and Mossel Bays,

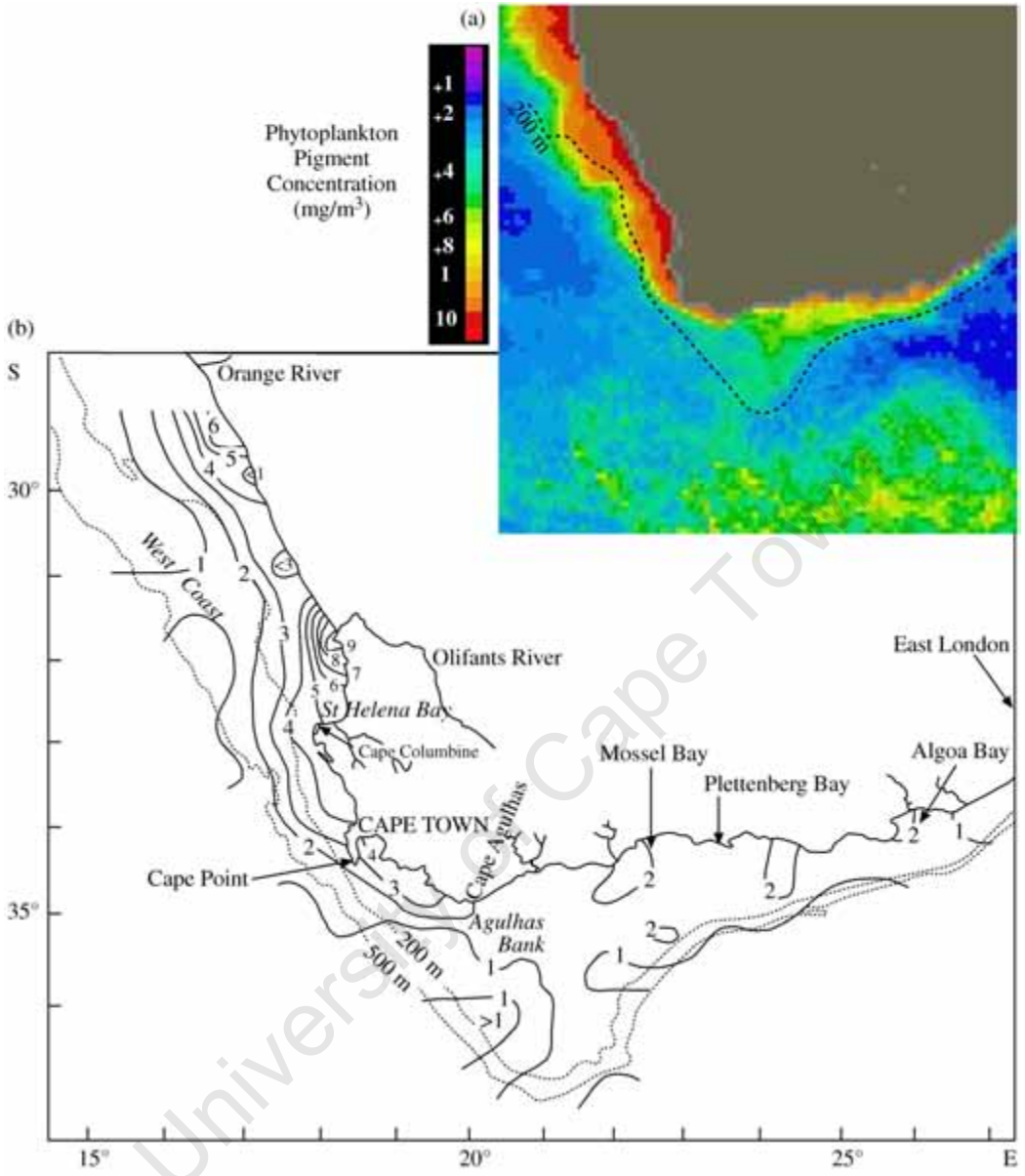

Figure 2.6: (a) Composite (1978–1986) of CZCS ocean colour satellite data, illustrating extensive high levels of chlorophyll on the west coast relative to those on the Agulhas Bank. (b) Mean distribution of chl–*a* in the upper 30 m, reproduced with modification from Brown and Cochrane (1991).

noticeably low west of Mossel Bay, and at intermediate level (green, ~0.5 mg m^{-3}) offshore over the central Bank.

The same observation was made by Brown and Cochrane (1991), who published a large-scale (Orange River–Port Alfred) perspective on mean chl–*a* in the upper 30 m (Figure 2.6b). They used a data set covering the years 1971–1989, including data used earlier by Shannon *et al.* (1984). The map in Figure 2.6b is constructed from mean concentrations of chl–*a* measured *in vitro*, either spectrophotometrically or fluorometrically, for half-degree blocks of latitude and longitude. For the west coast and western Bank, the chlorophyll distribution shown in Figure 2.6b is consistent with that depicted in Figure 2.6a, correlating with known local upwelling patterns (Shannon 1985). The cross-shelf gradient is strong, with levels ≤1 mg m^{-3} near the shelf edge, and ≥4 mg m^{-3} adjacent to the coast. Chlorophyll is also high near the mouth of the Olifants River, likely influenced by agricultural run-off, which is not seen in the satellite composite. Chlorophyll concentration over the central and eastern Bank is considerably lower than on the west coast, mainly between 1 and 2 mg m^{-3}. There are a few areas >2 mg m^{-3} inshore, notably near Mossel Bay, Tsitsikamma, and Algoa Bay, all within the coastal upwelling regions along the coast, and corresponding with the relatively high chlorophyll seen in Figure 2.6a. The intermediate chlorophyll levels observed in the satellite composite over the central Bank are also clear on Figure 2.6a, but the *in situ* mean values are 2–3 times greater. Although in general chlorophyll biomass levels on the Agulhas Bank are less extensive than on the West Coast, chlorophyll concentrations of 6–12 mg m^{-3} were found between Plettenberg Bay and Algoa Bay (Figures 14 and 15 of Shannon *et al.* 1984).

Zooplankton

Chokka squid paralarvae seemingly prey mainly on copepods (Venter *et al.* 1999), of which two large species are abundant around southern Africa — *Calanoides carinatus*, which dominates the cold Benguela upwelling system of the west coast, and *Calanus agulhensis*, which inhabits the warmer and relatively more stable waters of the Agulhas Bank (Huggett and Richardson 2000). Irrespective of species, copepod biomass is generally greatest on the west coast.

Huggett (2003) produced large-scale distribution maps of copepod biomass. For the purposes of this study, however, a more appropriate impression of copepod abundance is gained from the map shown in Figure 2.7, which combines two different surveys: to the west coast in May 1991, and to the Agulhas Bank in November 1989. These were selected from a number of unpublished surveys for their abundance of copepods, which highlights several characteristics. For instance, copepod biomass is extensive on the west coast, with large areas in the range 3–5 gC m^{-2}, and not just inshore, where upwelling and primary production are most intense. Similarly on the Agulhas Bank, copepod biomass is greatest over the mid- and outer shelf, though more restricted than on the west coast. This distribution is aligned with the main upwelling region high in chlorophyll on the south coast between Knysna and

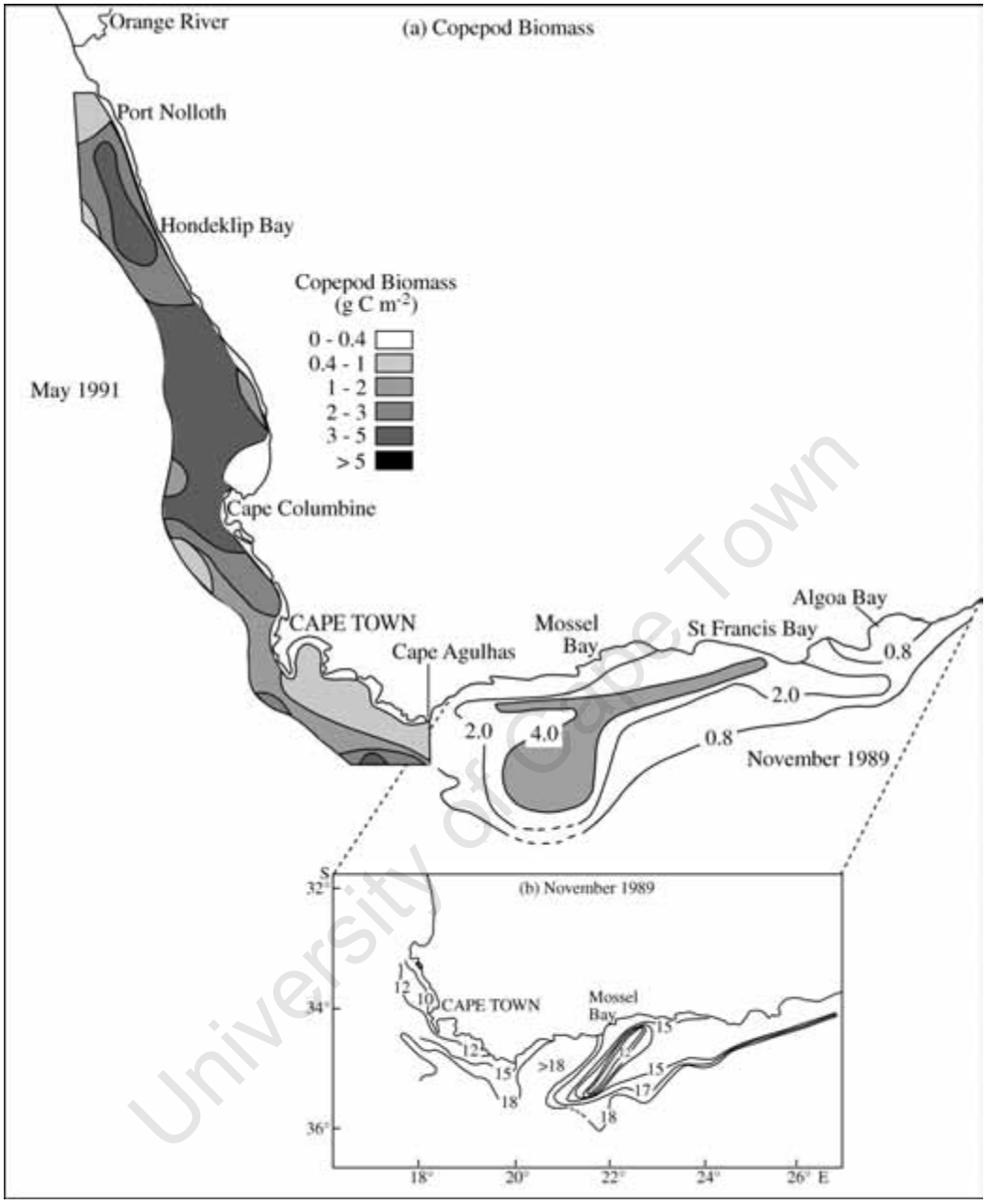

Figure 2.7: (a) Composite distribution of copepod biomass between the Orange River and Port Alfred during two surveys (denoted by different shading). (a) West coast (May 1991) and Agulhas Bank (November 1989). Data are joined at Cape Agulhas (20˚E). (b) Subsurface temperatures at a depth of 20 m show a ridge of cold upwelled water off Mossel Bay.

Tsitsikamma, as well as confirming the intermediate levels of chlorophyll over the central Bank clear in Figure 2.6a.

Copepod biomass on the Agulhas Bank appears to be ~4 gC m^{-2}, almost equivalent to that on the west coast. However, biomass is low east of St Francis Bay and over the outer shelf, possibly the result of the oligotrophic Agulhas Current and an associated advective loss. Several authors (e.g. Largier *et al.* 1992; Peterson *et al.* 1992; Verheye *et al.* 1992, 1994; Boyd and Shillington 1994; Peterson and Hutchings 1995; Hutchings *et al.* 1995) mention that high densities of copepods on the central Bank are associated with a quasi-permanent, shallow, subsurface ridge of cold upwelled water off Mossel Bay, seen in Figure 2.7b. Huggett and Richardson (2000) quantitatively demonstrate this association in their Figure 2, which used data from three cruises (1988, 1989, 1990). More recent data and analyses in Huggett (2003) support this. Boyd and Shillington (1994) suggest that cyclonic circulation around the cold ridge may enhance local retention of copepods.

Alongshore environmental gradients and spawning habitat

The alongshore gradients depicted in Figure 2.8 offer a means by which the information presented above can be simplified and viewed coherently in relation to the spawning grounds. Factors that affect the eggs and the paralarvae have been separated. Gradients were constructed using data at a distance of ~15 nautical miles from the coast, extracted from Figure 2.4a, 2.5c, 2.6b and 2.7a. This is the closest inshore measurement possible, given the spatial scales used, although it is acknowledged that such a distance offshore may not correctly portray some shallow inshore environments (e.g. embayments), so some misinterpretation is possible.

The alongshore gradient of BT in Figure 2.8a suggests that squid can hatch successfully only between Cape Point and Cape St Blaize, and between Cape Recife and just west of East London, because minimum temperatures elsewhere are outside the optimal temperature range (12–17˚C) for embryonic development (the shaded zone in Figure 2.8a). From East London eastwards, BT increases above 19˚C, too warm for successful embryonic development. This potential spawning habitat is reduced when BDO is considered; adult squid are generally not found where BDO is ≤3 ml l^{-1}. Low BDO excludes the west coast as spawning habitat, but also the region between Cape Agulhas and Ystervark Point. The strong seasonality of low BDO in the latter region could mean that it is not always unsuitable for spawning. It is questionable whether the western Bank (Cape Point–Cape Agulhas) offers suitable habitat, because the minimum BDO approaches the 3 ml l^{-1} critical threshold. Of importance in this study is the fact that the main spawning grounds between Plettenberg Bay and Port Alfred are positioned where the BDO is almost always ≥4 ml l^{-1}.

There is a declining west–east trend in chlorophyll (Figure 2.8b), and hence phytoplankton. To some extent, the copepod biomass gradient follows that of chlorophyll, with concentrations highest on the west coast. Such a region could be good for squid paralarvae

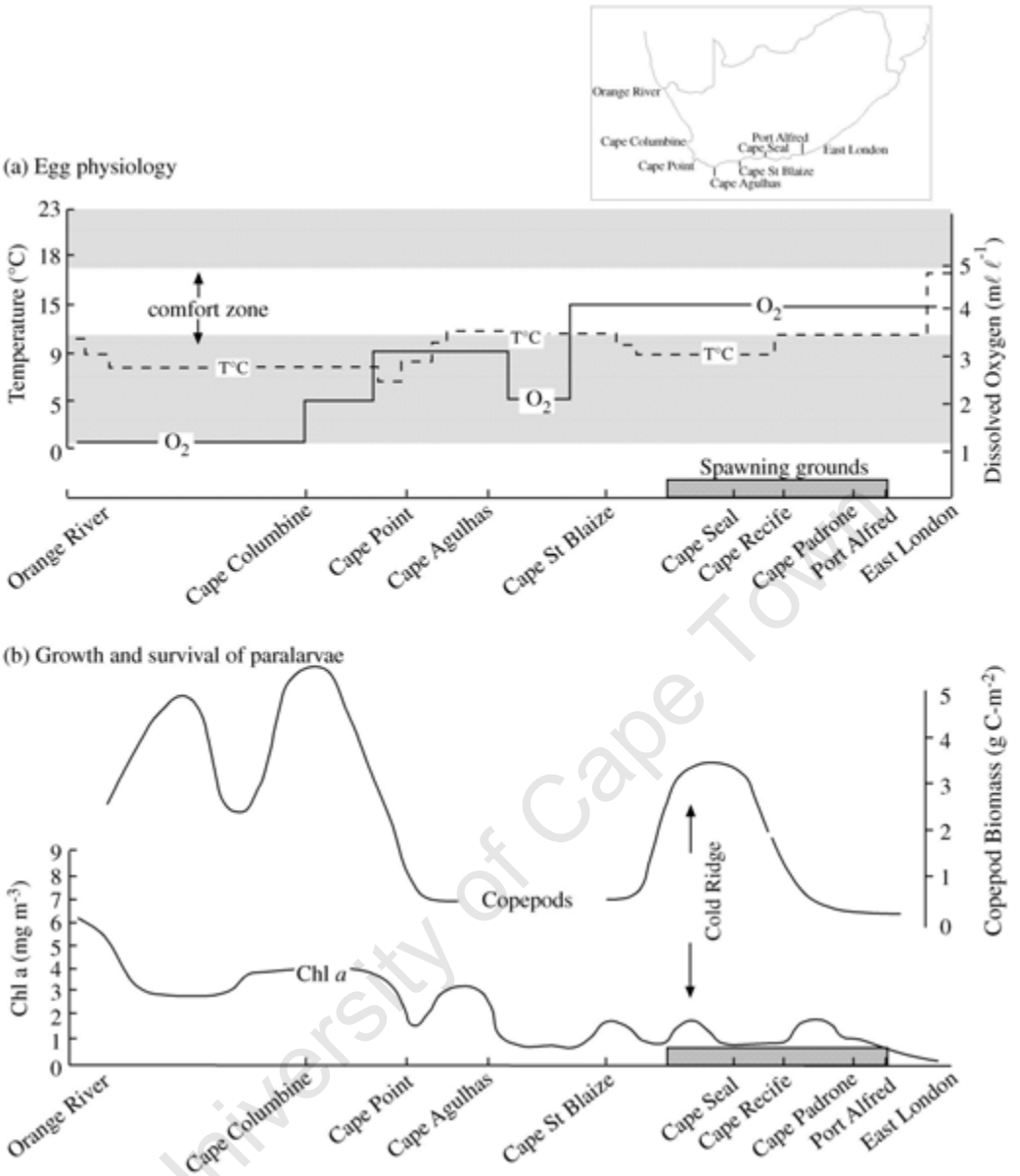

Figure 2.8: Alongshore gradients around the coast between the Orange River and East London in relation to the main chokka squid spawning grounds. (a) Minimum levels of bottom temperature and bottom dissolved oxygen. (b) Phytoplankton and copepod concentrations. Data taken from Figures 2.4a, 2.5c, 2.6b, and 2.7a, approximately 15 miles from the coast.

because food is plentiful, but Forsythe (1993) showed that low temperatures retard growth of squid paralarvae and juveniles. Over the Agulhas Bank, though, most of the copepod biomass is centred off the coast between Tsitsikamma and Mossel Bay, with biomass low to either side. The main spawning grounds of chokka squid are positioned on the eastern side of this maximum, resulting in some mismatch between place of hatching and location of abundant food. This is suboptimal compared with BT and BDO, which are well matched with the sites of egg deposition. Therefore, it would appear that the position of the spawning grounds favours egg development over survival of paralarvae.

BT, BDO, and chlorophyll are based on statistical data, so the conclusions can only be seen as generalized. In the case of copepods, specific survey data were used. In a complex, dynamic, marine system such as that surrounding southern Africa, great variability will exist in these parameters on daily, seasonal, and longer time-scales. Accordingly, the gradients shown in Figure 2.8a could vary, and suitable spawning habitat may be found sometimes outside the main region identified here. This could explain why eggs are found occasionally in False Bay and near East London, i.e. fringe spawning. Conditions within the main spawning grounds too may occasionally be adverse and discourage spawning, perhaps also promoting fringe spawning.

Perhaps the gradients shown in Figure 2.8 are used by mature adults to find the spawning grounds. It is known now that some species of fish make use of natural (magnetic, physical, and chemical) fields for navigation (Dingle 1996).

Currents and western transport

As indicated in Chapter 1 currents can play important roles in the life cycle of some squid species, e.g. *Illex illecebrosus*, *Illex argentinus*, *Todarodes pacificus*, and *Ommastrephes bartramii* (see Roberts *et al*. 1998). With all these ommastrephids, western boundary currents transport free-floating eggs and paralarvae from the spawning grounds in subtropical regions to feeding grounds in temperate climes several thousand kilometers away (O'Dor and Dawe 1998). For example, *Illex illecebrosus* spawn off the Florida coast, and their translucent gel balloons about 100 cm in diameter, containing 50 000–100 000 eggs, settle to neutrally buoyant depths of typically 200–400 m in the Gulf Stream, where temperatures are optimal for embryonic development (O'Dor and Balch 1985). By the time they hatch, the paralarvae have been transported to the food-rich Grand Banks, where they remain until maturity. In the case of loliginid squid, there are no known cases where currents play a similar role, but the life cycles of loliginids are less understood. The environmental gradient analysis in this study indicates a mismatch of a few hundred kilometers between the main spawning grounds of chokka squid and optimal feeding for paralarvae to the west. Although on a smaller scale, this is analogous to the life cycle of the ommastrephids mentioned above, and it may suggest that currents provide a critical link in the life cycle of chokka squid.

Shelf currents are usually less defined and more difficult to understand than western boundary currents. Until 1990 knowledge of the current patterns on the eastern Agulhas Bank

was limited to inferences from bathythermograph plots (Bang 1970), a synthesis of ship-drift measurements collected between 1959 and 1964 by Harris (1978), a study of drift cards by Lutjeharms *et al.* (1986), several unpublished shallow current-meter records in Algoa Bay, and the results of a cruise analysed by Goschen and Schumann (1988). Data acquisition was greatly improved when Acoustic Doppler Current Profilers (ADCPs) were installed on South Africa's research ships "Africana" and "Algoa" in 1989. The technique gave wide data coverage, but lacked temporal resolution, with only three surveys made annually. A substantial part of this data set was analysed and presented by Boyd *et al.* (1992), Boyd and Oberholster (1994), and Boyd and Shillington (1994), and it remains spatially the most comprehensive work published to date.

For this study, average (15'×15' blocks) current vectors at a depth of 30 m, presented in Boyd and Oberholster (1994), are reproduced in Figure 2.9a. Deeper currents at 50 m showed a similar pattern, indicating barotropic conditions. A number of flow domains can be observed. The fast-flowing Agulhas Current (>100 cm s^{-1}) clearly dominates the offshore oceanography over the Agulhas Bank (>200 m). Actual velocities can range between 150 and 350 cm s^{-1} (Boyd and Shillington 1994). East of Port Alfred, the current strongly influences the narrow shelf environment, but this influence decreases as the shelf widens onto the eastern Bank (Goschen and Schumann 1988).

On the eastern Bank, velocities reduce considerably, with average currents typically 20–30 cm s^{-1}. The net flow pattern is complex, particularly towards the central Bank. Average vectors on the mid-shelf indicate net westward flow in the upper layer, at times clear in ADCP survey data, e.g. cruise AA 108 depicted in Figure 2.9b. The average vectors show net westward flow on the mid-shelf moving also southwards near 23˚E (Cape Seal), and around the inner central Bank to continue northwestwards along the narrower western Bank. Boyd and Shillington (1994; Figure 2.8a) showed the same. In Figure 2.9b, westward flow dominates the entire eastern Bank, but the incoherent and zero average vectors near the eastern Bank, shown in Figure 2.9a, indicate great variability in flow direction. The same is found on the inner central Bank, i.e. <100 m between Cape Agulhas and Cape Seal. Weak circulation is expected there, because BDO is low during summer (see above). Between Mossel Bay and Cape Seal, there is a narrow coastal eastward flow, shown by average vectors.

Western transport hypothesis

In light of these data on currents and the environmental gradients, it may well be that the spawning grounds for chokka squid are positioned not only to exploit optimal bottom temperatures, but also to use the net westward current on the eastern Bank to link hatching site with food maxima located to the west, off the Knysna–Tsitsikamma coast. Such a strategy would optimize the chances of survival during early life. Passive transport of hatchlings in this net flow would be at average speeds of 18–25 km d^{-1}. Actual currents on Figure 2.9b indicate transport speeds of 35–43 km d^{-1}. This implies that paralarvae as far away as Algoa Bay

would take an average of 4–7 days to reach the site of favoured food, or 3–5 days in the case of Figure 2.9b. Such time-spans match the results of Vidal *et al.* (2002), who reported that *Loligo opalescens* hatchlings initially undergo a "no net growth phase", while dependence on the internal yolk diminishes and prey capture success increases. This they state to be a critical period in the early life history. *In vitro* prey-starved hatchlings lived between 4 and 6 days utilizing internal yolk, depending on ambient water temperature. This implies, assuming similar behaviour, that chokka squid hatchlings can survive while in transport to the richer feeding grounds.

On the western side of the copepod maximum, any fringe spawning between Mossel Bay and Cape Seal would benefit from the narrow eastward coastal current shown in Figure 2.9a. Currents may also define the eastern boundary of the chokka squid spawning grounds near Port Alfred. This limit may not necessarily be due to higher BTs, as stated earlier, but perhaps a consequence of the strong influence of the Agulhas Current there, as well as the potential removal of hatchlings from the eastern Agulhas Bank ecosystem (Lutjeharms *et al.* 1986).

The cold ridge and ecosystem changes

The copepod maximum on the Agulhas Bank shown in Figure 2.7a is commonly associated with a subsurface ridge of colder water (Figure 2.7b), i.e. an upward doming of the thermocline. This is believed to underpin the enhanced secondary production found there (Largier *et al.* 1992; Probyn *et al.* 1994; Verheye *et al.* 1994), and was first observed and noted by Largier and Swart (1987), and subsequently by Boyd and Shillington (1994), and Carter *et al.* (1987). No description of this feature is conclusive, but the doming implies movement of nutrient-rich bottom layers towards the surface, undoubtedly stimulating primary production.

Several mechanisms have been proposed for the forcing of this prominent, central, oceanographic feature. Swart and Largier (1987) suggested that either up-slope veering of the bottom boundary layer along the shelf edge of the eastern Bank (owing to side-wall friction) could cause mid-shelf upwelling, or perhaps that cross-current Ekman transport attributable to sustained wind stress by westerly winds on a laterally sheared flow could be the driving force. Such mechanisms would be time-dependent, and related to the position of the inner margin of the Agulhas Current. Boyd and Shillington (1994) also suggested, on the assumption that the outer shelf is dominated by the Agulhas Current and the inner shelf flow by wind-forcing, that the widening of the shelf between Port Elizabeth and Knysna may be responsible for the cold ridge. The divergent nature of the resulting flow could cause upwelling of the thermocline in the shelf interior, resulting in cyclonic circulation. Boyd and Shillington (1994) analysed November cruise data between 1987 and 1991, found that the cold ridge was not always present, and suggested a connection between its development and coastal upwelling. To date, however, all mechanisms remain speculative.

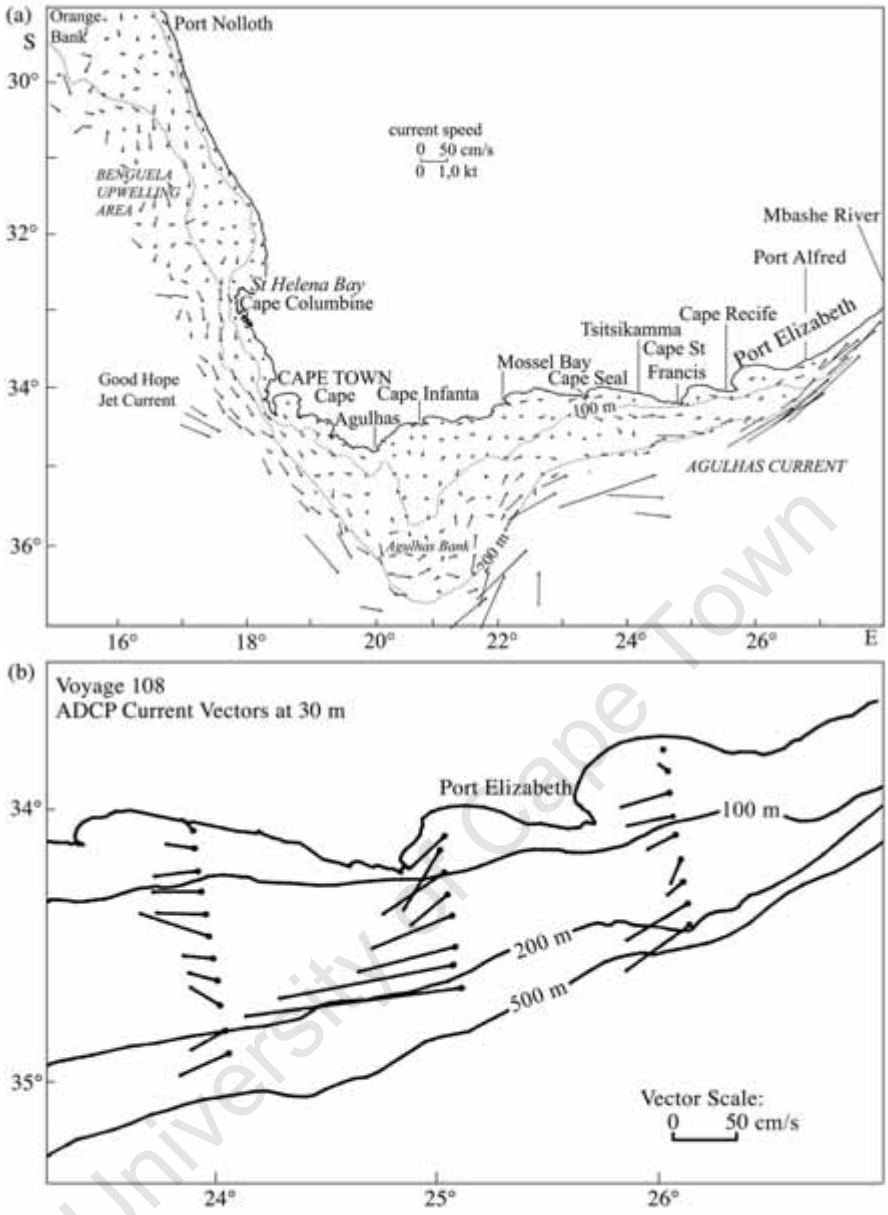

Figure 2.9: (a) Average currents at a depth of 30 m on the west coast and the Agulhas Bank. Data were collected between 1989 and 1994 using ship-borne ADCPs and averaged over 15'×15' blocks of longitude and latitude (reproduced from Boyd and Oberholster 1994). The direction of current is away from the dot. (b) ADCP data collected at 30 m during cruise 108 in November 1992.

Given the significance of the cold ridge in the Agulhas Bank ecosystem, and in particular the potential role it plays in chokka squid spawning, it is important that its driving forces and dynamics are better understood. From new evidence given below, it may be that the cold ridge is just an intermittent upwelling filament that originates at the coast as a consequence of wind-driven coastal upwelling. The typical configuration observed in Figure 2.7b may be formed by the advection of a cold-water plume in a southwest direction by the shoreward edge of the prevailing westward shelf current described in Figure 2.9.

Such a situation is depicted by the depth plot of the 14˚C isotherm (November 1987) in Figure 2.10a. This isotherm was chosen because it reflects the middle of the thermocline (see transects). The cold ridge is seen as a prominent, sloping, tongue-like, thermal structure that surfaces at the Tsitsikamma coast. A vertical temperature section (Transect 2; Figure 2.10b) taken across the cold coastal core (i.e. the upwelling plume) confirmed upwelling against the coast. The vertical sections for Transects 3 and 4 show a dome effect in the thermal structure, denoting cold coastal water moving offshore onto the shelf. Subsidence of the 14˚C isotherm to a depth of about 10 m implies some warming in the filament's surface layer, probably through a combination of insolation, sinking of dense cold water, and turbulent mixing with adjacent surface waters. Nonetheless, the surface water of the filament remained colder than the surrounding water.

The colder surface water of the filament conveniently provides a signature that is seen in thermal satellite imagery. For the above case, this is shown in Figure 2.11, which depicts a substantial filament (light grey) extending well onto the shelf. Bearing in mind that a ship's survey is not synoptic, the configuration of this filament is well matched with the subsurface thermal structure shown in Figure 2.10. Interestingly, the outer reaches of the cold ridge filament extend to, and possibly interact with a large Agulhas Current cyclonic eddy (dark grey), clearly visible in Figure 2.11. These eddies have a cold core (Lutjeharms *et al.* 1989), seen in the thermal structure in Figure 2.10a as an isolated thermocline rise immediately south of the cold ridge.

The sea surface temperature in Figure 2.11 depicts the filament emanating from the coastal upwelling zone. Coastal upwelling on the Agulhas Bank is common during summer, and is driven by seasonal easterly winds (Schumann *et al.* 1982). Upwelling is initiated on the western side of the prominent capes of Cape Padrone (just west of Port Alfred), Cape Recife, and Cape St Francis, and along the coastline between Tsitsikamma and Knysna (Figure 2.9), because the orientation is such that the easterly wind has an offshore component, which combined with Ekman transport and the steep and prominent bathymetry, readily draws cold bottom water to the surface within the inertial period of 21 h (for this latitude). Minor upwelling also occurs at the smaller capes between Mossel Bay and Cape Agulhas. Satellite imagery and in situ measurements show that coastal upwelling is most extensive and intensive, however, between Tsitsikamma and Knysna, commonly with plumes of cold surface water that extend 10–40 km offshore, with surface temperatures of 11–15˚C (see Schumann *et al.* 1982; Largier and Swart 1987; Schumann 1999).

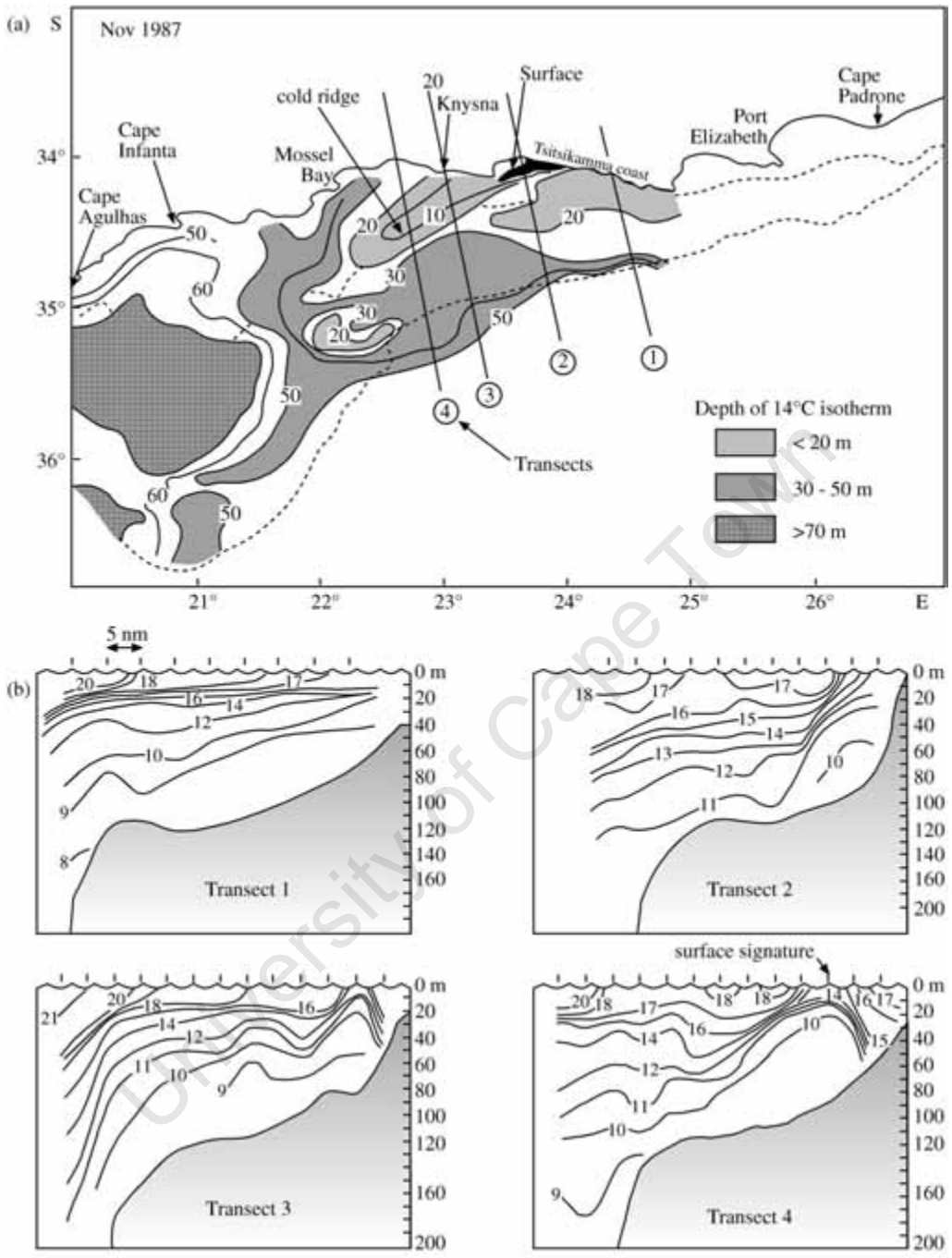

Figure 2.10: (a) Depth (m) of the 14˚C isotherm on the central and eastern Agulhas Bank highlights upward doming of the thermocline off Knysna in November 1987, a feature commonly referred to as a cold ridge. (b) Transect 2 shows upwelling at the coast. Transects 3 and 4 show a doming in the temperature structure through the cold ridge. Transect 1 is through an upwelling plume farther east.

The dependence of the cold ridge on wind-driven coastal upwelling is further demonstrated in Figure 2.12, in which an analysis of 8.5 years of cloud-free AVHRR satellite imagery is displayed. This encompasses the event surveyed in Figure 2.11 (indicated). Figure 2.12a shows the cold ridge mainly during summer upwelling, between November and April.

However, the cold ridge, or filament, is not always formed, despite intensive coastal upwelling (e.g. see October 1986). This indicates that offshore advective forces are necessary for the formation of the classical cold ridge feature.

As already stated, net surface flow on the eastern Bank is westwards, then offshore (to the southwest) near Knysna. The flow continues onto the outer central Bank. This pattern is possibly caused by the dissimilar flow of water on the inner central Bank (shown in Figure 2.9a). Under such circumstances, an upwelling plume off the Tsitsikamma–Knysna coast would similarly be advected on the inshore edge of this westward flow, giving rise to the typical cold ridge configuration seen in Figure 2.10 and Figure 2.11. The plume, more adequately described then as a filament, would exist on the boundary between the westward flow and the inner central Bank, typically overlying the 100 m contour. The physics at this interface may act to sustain the doming in the thermal structure, and maintain the cold ridge. Also, the possible impact of the small eastward coastal flow off Mossel Bay, which causes a deepening of the thermocline inside the cold ridge, needs to be borne in mind. If the interface between the westward flow and the inner central Bank did not exist on the 100 m contour, then a cold-water plume would remain closer to the coast, and have a thermal structure similar to the upwelling plume observed to the east in Figure 2.10a, i.e. Transects 1 and 2, in which no doming of the thermocline is seen.

Given the gaps in satellite imagery, it is not possible to comment with certainty on the temporal variability of the cold ridge. However, it does appear that the feature lasts for periods of several days to weeks. In some summers, it appears to be a semi-permanent feature, e.g. 1988–1989, but as seen in Figure 2.12b, that case is anomalous. Besides this anomaly, there is also an interesting declining trend in the number of observations of the cold ridge over the years 1985–1993. This, demonstrated by the dashed line in Figure 2.12b, is not altogether due to a decline in the number of cloud-free images, but could be caused by decade-scale changes in either the upper layer flow regime on the eastern Bank, or coastal upwelling intensity (and wind field).

Another means of observing temporal variability in the cold ridge is found in the monthly average times-series of sea surface temperature (1975–2001), shown in Figure 2.13. These ongoing *in situ* measurements were made at Knysna, within the upwelling region that feeds the cold ridge filament (see Figure 2.10 and Figure 2.11). However, as already stated, coastal upwelling does not necessarily imply formation of the cold ridge, so some caution needs to be exercised when using this method.

The data in Figure 2.13 show clear cyclical warming of coastal waters during summer, and cooling during winter. However, there were conspicuous anomalies in the summers of 1988–1989, 1993–1994, 1994–1995, and 1995–1996, implying intense upwelling seasons.

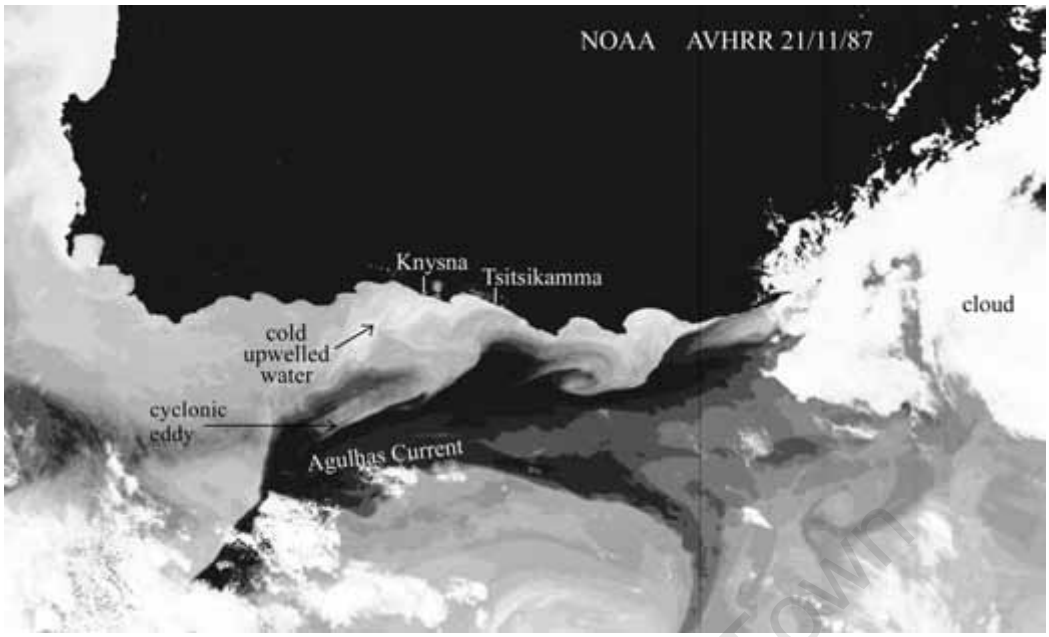

Figure 2.11: The cold ridge depicted in Figure 2.10 has a surface signature seen in this SST satellite image. Light grey indicates cold water, dark grey/black warm Agulhas Current water. Note the coincident existence of a cold core cyclonic eddy south of the cold ridge.

The first of these "anomalous" summers corresponded with a substantial La Niña event in the Pacific Ocean. The others were in a period beginning with weak El Niño conditions, becoming weak La Niña conditions. Warming and cooling of eastern Bank coastal waters have been described by Schumann *et al.* (1995) and Roberts (1998b).

The correspondingly high number of satellite observations of the cold ridge during the anomalous summer of 1988–1989 (Figure 2.12b) suggest that the Knysna surface temperature measurements can be used to infer cold ridge activity, i.e. that summer peaks in monthly average surface temperature (Figure 2.13) signify less cold ridge activity, and depressed summer peaks signify greater activity. Such activity could be linked to primary and secondary production.

A comparison of the structure and behaviour of the cold ridge with upwelling filaments studied in the southern Benguela and on the Californian shelf shows similarities. For example, Taunton-Clark (1985) described the formation, growth, and decay of wind-induced upwelling tongues that extend 50–80 km offshore during summer at three sites on the west coast of South Africa (Cape Peninsula, Cape Columbine, and Hondeklip Bay). Local bathymetry, orographic, and meteorological effects were implicated in the intense upwelling at those sites, and the elongated tongue-like configuration of surface isotherms originating at the coast were similar to those of the cold ridge. Off California, Flament *et al.* (1985) showed an upwelling filament similar in configuration to the cold ridge associated with an offshore meander (300 km) in the narrow alongshore frontal (equatorward) current on the shelf edge, which had entrained cold coastal surface water in an offshore direction. Ships' data indicated that temperature and salinity fronts defining the filament at the surface extended to the bottom of the mixed layer. Upward doming of the thermohaline structure in the filament, also seen in the Agulhas Bank cold ridge, was observed. Good illustrations of such doming can be seen in other studies of filaments in that region (e.g. Dewey and Moum 1990; Kosro *et al.* 1991; Mackas *et al.* 1991; Strub *et al.* 1991), although the depths of the filament fronts were often deeper (100–150 m).

Of importance in all these studies is that the filaments extend beyond the shelf into depths of 2 000 m, unlike South Africa's cold ridge, which remains on the shelf in depths of 100–150 m. Life spans of the filaments off California were often between 30 and 60 days, similar to the cold ridge. Subsidence of cold surface water in filaments was also observed (e.g. Brink *et al.* 1991; Washburn *et al.* 1991).

Cold ridge links to chokka squid biomass and catches

A similarity in the fluctuating trends of peak monthly average sea surface temperature for each summer in Figure 2.13 (referred to as the summer SST peak hereafter) and the following autumn squid biomass shown in Figure 2.3a, suggests some cause and effect. This is better seen in Figure 2.14b, in which linear regression has been superimposed on the data for the years 1988–1997. Two outliers (1989, 1993) deteriorate an otherwise good linear relation (dotted trend line), which has a fit of (r^2) of 0.94. While a number of factors can

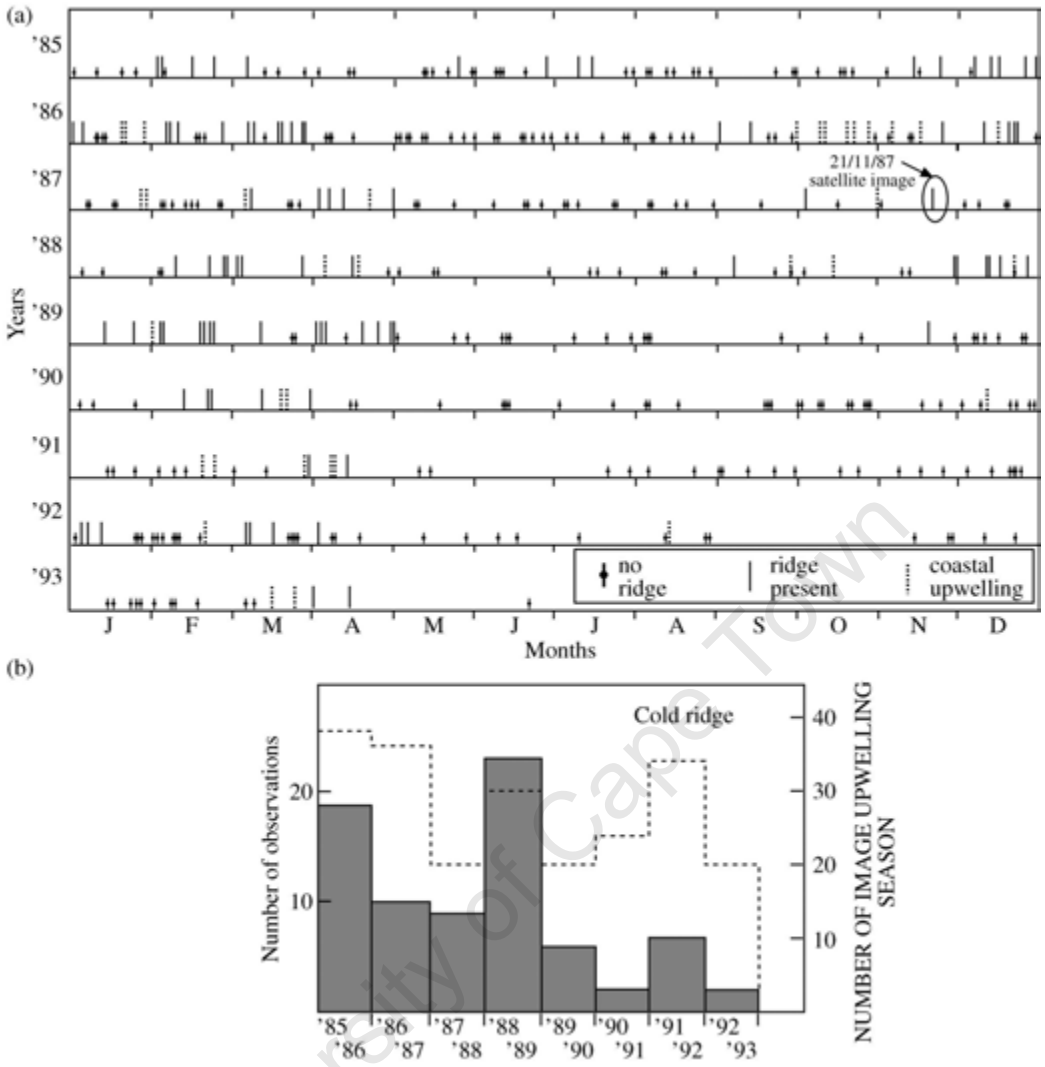

Figure 2.12: (a) Analysis of 420 cloud-free NOAA SST satellite images (AVHRR) between January 1985 and April 1993 indicates that the cold ridge is mainly found during summer (November–April). (b) Number of observations of the cold ridge per summer. With the exception of 1988–1989, there appears to be a declining trend over the period. Dotted line indicates the number of cloud-free satellite images for each summer (RHS axis).

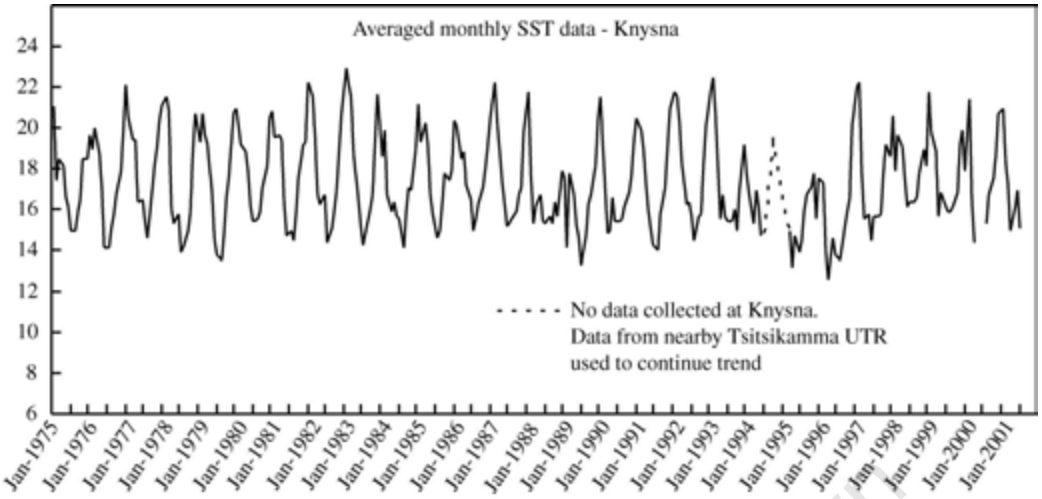

Figure 2.13: Average monthly SST data measured at Knysna (depth of sensor is 6 m). Note the strong seasonal heating and cooling, and the anomalous summers of 1988–1989, 1993–1994, 1994–1995, and 1995–1996.

influence biomass, it is plausible, as identified in this paper, that a western transport hypothesis, coupled with cold ridge activity (copepod abundance), can equally control paralarval survival and hence be responsible for the correlation. The relationship is appealing for biomass prediction, because the summer SST peak is obtained at the beginning of each year.

The inclusion of the outliers into this regression reduces the trend line fit to an r^2 of 0.37 (solid line in Figure 2.14b), which limits its use. Several factors could be responsible for the outliers. The first is the reliability of the biomass estimates (see Roel 1998), which unlike the temperature data, are not calibrated. In the case of 1989, the anomalously high catches shown in Figure 2.3b, and the corresponding relatively low biomass in Figure 2.3a, certainly raise questions about the estimate. Other factors could be environmental. In 1989, squid biomass in autumn was far below the anticipated level, given the intense upwelling in the previous (1988–1989) summer. Such intense upwelling may be self-limiting, as described by Cury and Roy (1989), who suggest an optimal environmental window in upwelling regimes, leading to good recruitment. Too much or too little upwelling either side of this window would lead to poor recruitment. Moreover, the lack of upwelling in summer 1992–1993, plus the high biomass in autumn 1993 (if correct), suggests that coastal upwelling and the cold ridge are not the only mechanisms to enhance paralarval food abundance and survival. Changes in the current regime on the eastern Bank could also potentially influence recruitment. The latter could lead to loss of paralarvae from the Agulhas Bank or, alternatively, boost entrainment of paralarvae in some manner. The summers of 1988–1989 and 1992–1993 were extreme in terms of sea surface temperature, and both correspond to El Niño–Southern Oscillation (ENSO) events. Ecosystem changes during such times could also adjust paralarval predation levels, which would influence recruitment. Finally, aside from these possibilities, the biology is not always in synchrony with the physics, and cannot always respond to physical changes, especially exceptional ones. Hence, anomalies should be expected. Ideally, these need to be anticipated to assist fisheries management.

Also of importance is the apparent positive correlation between squid autumn biomass and the corresponding annual jig catch. This has been dealt with in some detail by Roel (1998), using a GLM in anticipation of catch prediction. In that study, a linear relationship best described the data (Figure 2.14a), albeit with an r^2 of 0.45. Accordingly, a (linear) correlation was found between the summer SST peak and the annual catch, with an r^2 of 0.69 (Figure 2.14c). The latter plot uses all annual data points between 1988 and 1997. When utilized to predict catches for 1998, 1999, and 2000, the regression yielded values less than those actually reported i.e. 91.3, 67.0, and 89.5% of reported values, respectively. If the regression is repeated including the actual reported data for the years 1998–2000, then the fit is reduced to an r^2 of 0.59. In either case, use of the summer SST peak appears to be a better predictor of forthcoming catch than biomass, and may therefore hold promise for squid fishery management.

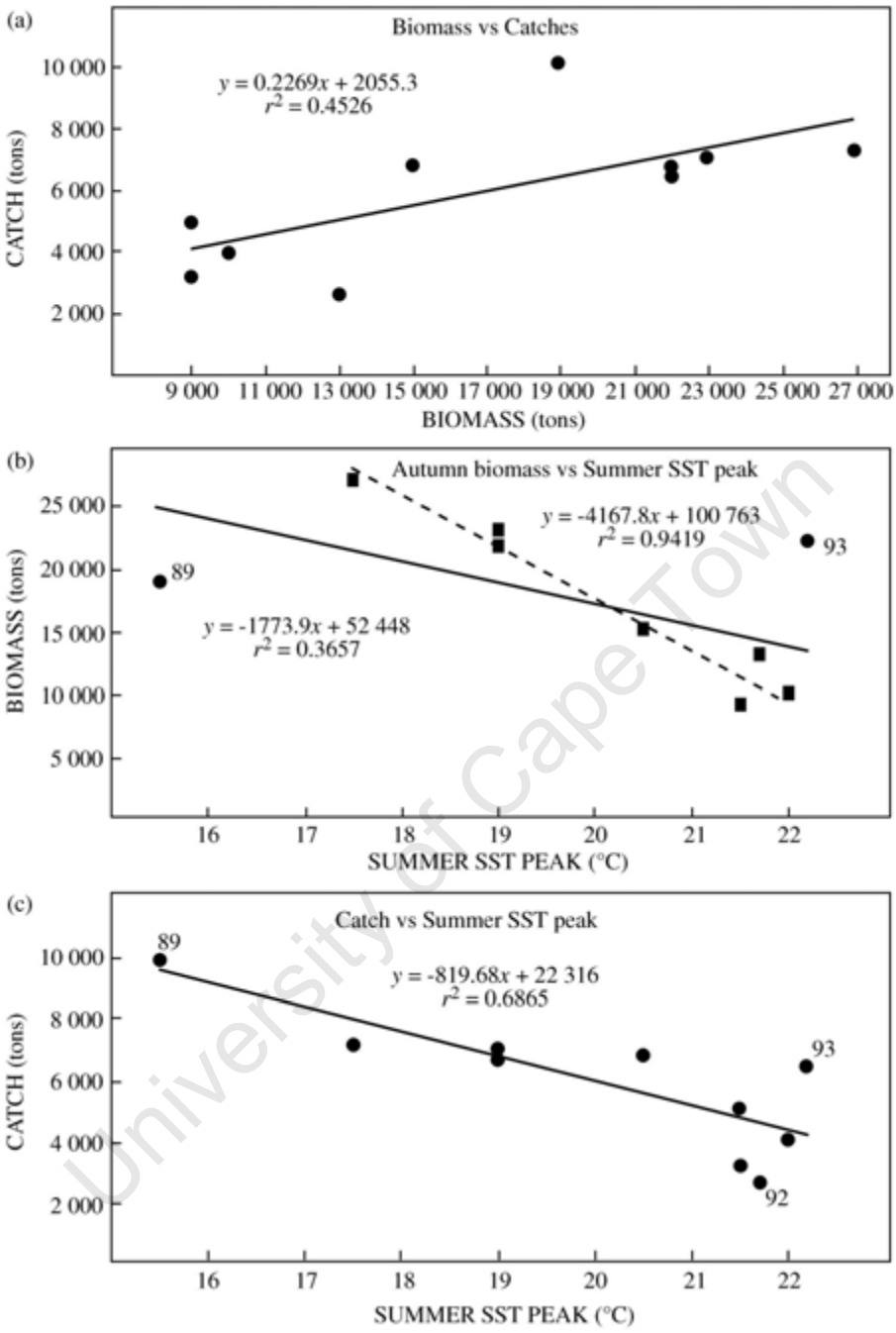

Figure 2.14: (a) Estimated chokka squid biomass vs. total annual jig catch, 1988–1997 [modified after Roel, 1998]. The trend is seemingly linear. (b) Biomass vs. maximum monthly average SST (from Figure 2.13; solid line). The linear fit is improved if the anomalous years 1989 and 1993 are excluded (dashed line). (c) Total annual jig catch vs. maximum monthly average SST, with a linear trend line.

Conclusions

This work has demonstrated that, within the complex oceanography surrounding southern Africa, chokka squid have found, or evolved to use, a niche on the eastern Agulhas Bank that optimizes spawning and survival of their early life stages. Nowhere else on the shelf are both bottom temperature and bottom dissolved oxygen simultaneously at optimal levels for egg development. However, the spawning grounds are displaced from the typical copepod maximum by some 200 km, which is near a cold ridge that is optimal for feeding of paralarvae (on copepods), and hence for survival. ADCP data indicate that this spatial shortcoming is offset by the existence of a barotropic net westward current capable of transporting paralarvae to the cold ridge before starvation.

This exploitation of currents to optimize the use of separate environments during spawning and early life has been referred to in this paper as a westward transport hypothesis. Although on a smaller scale, such a strategy is analogous to that used by the ommastrephids *Illex illecebrosus*, *Todarodes pacificus*, and *Illex argentinus*, which use fast-flowing, large-scale, western boundary currents to connect spawning grounds with feeding grounds. Such a life cycle strategy, however, has three obvious weaknesses that can impact recruitment. These involve uncharacteristic behaviour of (1) bottom environmental conditions on the spawning grounds, (2) the net westward current, and (3) the cold ridge that supports the copepod maximum.

The latter was pursued in this chapter, and the cold ridge was described as a coastal upwelling filament frequently found off the Knysna coast during summer. Its formation appears to be controlled by a combination of easterly winds and westward flow on the eastern Agulhas Bank. *In situ* sea surface temperature data indicate occasionally intense summer upwelling along the coast, which leads to greater cold ridge stability (i.e. it becomes quasi-permanent). This is expected to yield prolonged periods of copepod abundance beneficial for paralarvae survival. However, the cold ridge can be absent much of the time during summer, especially during ENSO events.

A negative linear regression (r^2 = 0.94) between the maximum summer monthly sea surface temperature (an index of cold ridge activity) and the following autumn chokka squid biomass (and catches; r^2 = 0.69) supports the spawning and early life strategy outlined above, and is potentially useful for prediction, because the maximum monthly SST is available at the beginning of the year.

Future research should focus on environmental conditions on chokka squid spawning grounds, the flow regime on the eastern Agulhas Bank, paralarvae swimming capability and transport, and cold ridge–primary production–copepod maximum coupling.

References

Augustyn CJ. 1990. Biological studies on the chokker squid *Loligo vulgaris reynaudii* (Cephalopoda: Myopsida) on spawning grounds off the south-east coast of South Africa. *South African Journal of Marine Science* 9: 11–26.

Augustyn CJ, Lipiński MR, Sauer WHH. 1992. Can the *Loligo* squid fishery be managed effectively? A synthesis of research on *Loligo vulgaris reynaudii*. *South African Journal of Marine Science* 12: 903–918.

Bang ND. 1970. Dynamic interpretations of a detailed surface temperature chart of the Agulhas Current retroflexion and fragmentation area. *South African Geographical Journal* 52: 67–76.

Barón PJ. 2002. Embryonic development of *Loligo gahi* and modelling of hatching frequency distributions in Patagonia. *Bulletin of Marine Science* 71: 165–174.

Beckley LE, van Ballegooyen RC. 1992. Oceanographic conditions during three ichthyoplankton surveys of the Agulhas Current 1990/91. *South African Journal of Marine Science* 12: 83–93.

Boletzky S, von Rowe L, Aroles L. 1973. Spawning and development of the eggs, in the laboratory, of *Illex coindetii* (Mollusca: Cephalopoda). *Veliger* 15: 257–258.

Boyd AJ. 1987. The oceanography of the Namibian shelf. Ph.D. thesis, University of Cape Town. [xv] + 190 pp.

Boyd AJ, Oberholster GPI. 1994. Currents off the west and south coasts of South Africa. *South African Shipping News and Fishing Industry Review, Sept./Oct. 1994*: 26–28.

Boyd AJ, Shillington F. 1994. Physical forcing and circulation patterns on the Agulhas Bank. *South African Journal of Science* 90: 114–122.

Boyd AJ, Taunton-Clark J, Oberholster GPI. 1992. Spatial features of the near-surface and midwater circulation patterns off western and southern South Africa and their role in the life histories of various commercially fished species. *South African Journal of Marine Science* 12: 189–206.

Brink KH, Beardsley RC, Niiler PP, Abbott M, Huyer A, Ramp S, Stanton T, Stuart D. 1991. Statistical properties of near-surface flow in the California coastal transition zone. *Journal of Geophysical Research* 96(C8): 14693–14706.

Brown PC. 1992. Spatial and seasonal variations in chlorophyll distribution in the upper 30 m of the photic zone in the southern Benguela/Agulhas ecosystem. *South African Journal of Marine Science* 12: 515–525.

Brown PC, Cochrane KL. 1991. Chlorophyll *a* distribution in the southern Benguela, possible effects of global warming on phytoplankton and its implications for pelagic fish. *South African Journal of Science* 87: 233–242.

Carter RA, McMurray HF, Largier JL. 1987. Thermocline characteristics and phytoplankton dynamics in Agulhas Bank waters. *South African Journal of Marine Science* 5: 327–336.

Chapman P, Largier JL. 1989. On the origin of Agulhas Bank bottom water. *South African Journal of Science* 89: 515–519.

Chapman P, Shannon LV. 1987. Seasonality in the oxygen minimum layers at the extremities of the Benguela system. *South African Journal of Marine Science* 5: 85–94.

Cury P, Roy C. 1989. Optimal environmental window and pelagic fish recruitment success in upwelling areas. *Canadian Journal of Fisheries and Aquatic Sciences* 46: 670–680.

De Jager B, van D. 1957. The South African pilchard (*Sardinops ocellata*) and maasbanker (*Trachurus trachurus*). Variations in the phytoplankton of the St Helena area during 1954. *Investigational Report, Division of Sea Fisheries, South Africa* 25: 78 pp.

De Mont ME, O'Dor RK. 1984. The effects of activity, temperature and mass on the respiratory metabolism of the squid *Illex illecebrosus*. *Journal of the Marine Biological Association of the UK* 64: 535–543.

De Ruijter WPM, van Leeuwen PJ, Lutjeharms JRE. 1999. Generation and evolution of Natal Pulses: solitary meanders in the Agulhas Current. *Journal of Physical Oceanography* 29: 3043–3055.

Dewey RK, Moum JN. 1990. Enhancement of fronts by vertical mixing. *Journal of Geophysical Research* 95(C6): 9433–9445.

Dingle H. 1996. Migration. The Biology of Life on the Move. Oxford University Press, Oxford: 474 pp.

Duncombe-Rae CM. 1991. Agulhas retroflection rings in the South Atlantic Ocean; an overview. *South African Journal of Marine Science* 11: 327–344.

Duncombe-Rae CM, Shillington FA, Agenbag JJ, Taunton-Clark J, Gründlingh ML. 1992. An Agulhas ring in the South Atlantic Ocean and its interaction with the Benguela upwelling frontal system. *Deep-Sea Research* 39: 2009–2027.

Eagle GA, Orren MJ. 1985. A seasonal investigation of the nutrients and dissolved oxygen in the water column along two lines of stations south and west of South Africa. *Research Report 567, Council for Scientific and Industrial Research*, Stellenbosch, South Africa: 52 pp.

Flament P, Armi L, Washburn L. 1985. The evolving structure of an upwelling filament. *Journal of Geophysical Research* 90(C6): 11765–11778.

Forsythe JW. 1993. A working hypothesis of how seasonal temperature change may impact the field growth of young cephalopods. *In* Recent Advances in Cephalopod Fisheries Biology. Okutani T, O'Dor RK, Kubodera T (eds). Tokai University Press, Tokyo. 133-143.

Goschen WS, Schumann EH. 1988. Ocean current and temperature structures in Algoa Bay and beyond in November 1986. *South African Journal of Marine Science* 7: 101–116.

Harris TFW. 1978. Review of coastal currents in southern African waters. *Research Report 30, Council for Scientific and Industrial Research*, Stellenbosch, South Africa. 103 pp.

Howell P, Simpson D. 1994. Abundance of marine resources in relation to dissolved oxygen in Long Island Sound. *Estuaries* 17: 394–402.

Huggett JA. 2003. Comparative ecology of the copepods *Calanoides carinatus* and *Calanus agulhensis* in the southern Benguela and Agulhas Bank ecosystem. Ph.D. thesis, University of Cape Town. [iii] + 296 pp.

Huggett JA, Richardson AJ. 2000. A review of the biology and ecology of *Calanus agulhensis* off South Africa. *ICES Journal of Marine Science* 57: 1834–1849.

Hutchings L, Verheye HM, Mitchell-Innes BA, Petersen WT, Huggett JA, Painting, SJ. 1995. Copepod production in the southern Benguela system. *ICES Journal of Marine Science* 52: 439–455.

Kosro MP, Huyer A, Ramp SR, Smith RL, Chavez FP, Cowles TJ, Abbott MR, Strub PT, Barber RT, Jessen P, Small LF. 1991. The structure of the transition zone between coastal waters and the open ocean off northern California, winter and spring 1987. *Journal of Geophysical Research* 96(C8): 14707–14730.

Largier JL, Chapman P, Peterson WT, Swart VP. 1992. The Western Agulhas Bank: circulation, stratification and ecology. *South African Journal of Marine Science* 12: 319–339.

Largier JL, Swart VP. 1987. East-west variation in the thermocline breakdown on the Agulhas Bank. *South African Journal of Marine Science* 5: 263–272.

Lutjeharms JRE. 2001. Agulhas Current. In *Encyclopedia of Ocean Science*. Steele JH, Thorpe SA, Turekian KK (eds). 104–113. Academic Press, New York. 104-113.

Lutjeharms JRE, Baird D, Hunter LT. 1986. Seeoppervlak drygedrag aan die Suid-Afrkaanse suidkus in 1979. *South African Journal of Science* 82: 324–326.

Lutjeharms JRE, Catzel R, Valentine HR. 1989. Eddies and other boundary phenomena of the Agulhas Current. *Continental Shelf Research* 9: 597–616.

Lutjeharms JRE, Cooper J. 1996. Interbasin leakage through Agulhas Current filaments. *Deep-Sea Research* 43: 213–238.

Lutjeharms JRE, Cooper J, Roberts MJ. 1999. Upwelling at the inshore edge of the Agulhas Current. *Continental Shelf Research* 20: 737–761.

Lutjeharms JRE, Matthysen CP. 1995. A recurrent eddy in the upwelling front off Cape Town. *South African Journal of Science* 91: 355–357.

Lutjeharms JRE, Monteiro PMS, Tyson PD, Obura D. 2001. The oceans around southern Africa and regional effects of global change. *South African Journal of Science* 97: 119–130.

Mackas DL, Washburn L, Smith SL. 1991. Zooplankton community pattern associated with a California Current cold filament. *Journal of Geophysical Research* 96(C8): 14781–14797.

McMurray HF, Carter RA, Lucas MI. 1993. Size-fractionated phytoplankton production in western Agulhas Bank continental shelf waters. *Continental Shelf Research* 13: 307–329.

Mitchell-Innes BA. 1988. Changes in phytoplankton populations after an incursion of cold water along the coast at Tsitsikamma Coastal National Park. *South African Journal of Marine Science* 6: 217–226.

Nelson G. 1989. Poleward motion in the Benguela area. *In* Poleward Flows along Eastern Ocean Boundaries (Coastal and Estuarine Studies, 34). Neshyba SJ, Mooers CNK, Smith RL, Barber RT (eds). Springer, New York.110-130.

Nelson G, Boyd AJ, Agenbag JJ, Duncombe-Rae CM. 1998. An upwelling filament north-west of Cape Town, South Africa. *South African Journal of Marine Science* 19: 75–88.

O'Dor RK, Balch N. 1985. Properties of *Illex illecebrosus* egg masses potentially influencing larval oceanographic distribution. *NAFO Scientific Council Studies* 9: 69–76.

O'Dor RK, Balch N, Foy EA, Hirtle RWM, Johnson DA, Amaratunga T. 1982. Embryonic development of the squid *Illex illecebrosus* and effect of temperature on development rates. *Journal of Northwest Atlantic Fisheries Science* 3: 41–45.

O'Dor RK, Dawe EG. 1998. *Illex illecebrosus*. *In* Squid Recruitment Dynamics. Rodhouse PG, Dawe EG, O'Dor RK (eds). *FAO Fisheries Technical Paper* 376: 77-104.

O'Dor RK, Hoar JA, Webber DM, Carey FG, Tanaka S, Martins HR, Porteiro FM. 1994. Squid (*Loligo forbes*i) performance and metabolic rates in nature. *In* Physiology of Cephalopod Molluscs – Lifestyle and Performance Adaptations. Pörtner HO, O'Dor RK, Macmillan DL (eds). Gordon and Breach Publishers, Switzerland: 163-177.

Oosthuizen A, Roberts MJ, Sauer WHH. 2002. Temperature effects on embryonic development and hatching success of the squid *Loligo vulgaris reynaudii*. *Bulletin of Marine Science* 71: 619–632.

Peterson WT, Hutchings L. 1995. Distribution, abundance and production of the copepod *Calanus agulhensis* on the Agulhas Bank in relation to spatial variations in the hydrography and the chlorophyll concentration. *Journal of Plankton Research* 17: 2275–2294.

Peterson WT, Hutchings L, Huggett JA, Largier JL. 1992. Anchovy spawning in relation to the biomass and replenishment rate of their copepod prey on the western Agulhas Bank. *South African Journal of Marine Science* 12: 487–500.

Pörtner H–O, Zeilinski S. 1998. Environmental constraints and the physiology of performance of squid. *South African Journal of Marine Science* 20: 207–221.

Probyn TA, Mitchell-Innes BA, Brown PC, Hutchings L, Carter RA. 1994. A review of primary production and related processes on the Agulhas Bank. *South African Journal of Science* 90: 166–173.

Roberts MJ. 1998a–The influence of the environment on chokka squid *Loligo vulgaris reynaudi*i spawning aggregations: steps toward a quantified model. *South African Journal of Marine Science* 20: 267–284.

Roberts MJ. 1998b. What happened to the South Coast El Niño 1997-98, squid catches? *In*: Fishing Handbook: South Africa, Namibia, Moçambique 1998. 26th Edition. Stutterford M (ed): 233-238.

Roberts MJ, Engelbrecht N, Johnson A, Spolander B, Blanke B. Unpublished. A semi-permanent bottom cyclonic circulation found on the edge of the Eastern Agulhas Bank (South Africa).

Roberts MJ, Rodhouse P, O'Dor R, Sakurai Y. 1998. A global perspective of environmental research on squid. *ICES Document* CM1998/M: 27.

Roberts MJ, Sauer WHH. 1994. Environment: the key to understanding the South African chokka squid (*Loligo vulgaris reynaudii*) life cycle and fishery? *Antarctic Science* 6: 249–258.

Roel BA. 1998. Stock assessment of the chokka squid *Loligo vulgaris reynaudii*. Ph.D. thesis, University of Cape Town, South Africa. 217 pp.

Sauer WHH. 1995a. South Africa's Tsitsikamma National Park as a protected breeding area for the commercially exploited chokka squid *Loligo vulgaris reynaudii*. *South African Journal of Marine Science* 16: 365–371.

Sauer WHH. 1995b. The impact of fishing on chokka squid *Loligo vulgaris reynaudii* concentrations on inshore spawning grounds in the South-Eastern Cape, South Africa. *South African Journal of Marine Science* 16: 185–193.

Sauer WHH, Smale MJ. 1993. Spawning behaviour of *Loligo vulgaris reynaudii* in shallow coastal waters of the south-eastern Cape, South Africa. *In* Recent Advances in Cephalopod Fisheries Biology. Okutani T, O'Dor RK, Kubodera T (eds). Tokai University Press, Tokyo: 489-498.

Sauer WHH, Smale MJ, Lipiński, MR. 1992. The location of spawning grounds, spawning and schooling behaviour of the squid *Loligo vulgaris reynaudii* (Cephalopoda: Myopsida) off the Eastern Cape coast, South Africa. *Marine Biology* 114: 97–107.

Schön P–J. 2000. An investigation into the influence of the environment on spawning aggregations and jig catches of chokka squid (*Loligo vulgaris reynaudii*) off the south coast of South Africa. M.Sc. thesis, Rhodes University, South Africa. 108 pp.

Schumann EH. 1999. Wind-driven mixed layer and coastal upwelling processes off the south coast of South Africa. *Journal of Marine Research* 57: 671–691.

Schumann EH, Cohen AL, Jury MR. 1995. Coastal sea temperature variability along the south coast of South Africa and the relationship to regional and global climate. *Journal of Marine Research* 53: 231–248.

Schumann EH, Perrins LA, Hunter IT. 1982. Upwelling along the south of the Cape Province, South Africa. *South African Journal of Science* 78: 238–242.

Shannon LV. 1985. The Benguela ecosystem. 1. Evolution of the Benguela, physical features and processes. Oceanography and Marine Biology. *An Annual Review* 23: 105–182.

Shannon LV, Field JG. 1985. Are fish stocks food-limited in the southern Benguela pelagic ecosystem? *Marine Ecology Progress Series* 22: 7–19.

Shannon LV, Hutchings L, Bailey GW, Shelton PA. 1984. Spatial and temporal distribution of chlorophyll in southern African waters as deduced from ship and satellite measurements and their implications for pelagic fisheries. *South African Journal of Marine Science* 2: 109–130.

Shannon LV, Nelson G. 1996. The Benguela: large scale features and processes and system variability. *In* The South Atlantic: Present and Past Circulation. Wefer G, Berger WH, Siedler G, Webb D (eds). Springer, Berlin. 163-210.

Strickland JDH, Parsons TR. 1972. A practical handbook of seawater analysis. *Bulletin of the Fisheries Research Board of Canada* 167, 2nd edn: 310 pp.

Strub PT, Kosro PM, Huyer A. 1991. The nature of the filaments in the California Current system. *Journal of Geophysical Research* 96(C8): 14743–14768.

Swart VP, Largier JL. 1987. Thermal structure of Agulhas Bank water. *South African Journal of Marine Science* 5: 243–253.

Taunton-Clark J. 1985. The formation, growth and decay of upwelling tongues in response to the mesoscale wind field during summer. *In* South African Ocean Colour and Upwelling Experiment. Shannon LV (ed). Sea Fisheries Research Institute, Cape Town: 47-61.

Tyson PD, Preston-White RA. 2000. The Weather and Climate of Southern Africa. Oxford University Press, Cape Town. 408 pp.

Van Leeuwen PJ, de Ruijter WMP, Lutjeharms JRE. 2000. Natal Pulse and the formation of Agulhas rings. *Journal of Geophysical Research* 105: 6425–6436.

Venter JD, van Wyngaardt S, Verschoor JA, Lipiński MR, Verheye HM. 1999. Detection of zooplankton prey in squid paralarvae with immunoassay. *Journal of Immunoassay* 20(3): 127–149.

Verheye HM, Hutchings L, Huggett JA, Carter RA, Peterson WT, Painting SJ. 1994. Community structure, distribution and trophic ecology of zooplankton on the Agulhas Bank with special reference to copepods. *South African Journal of Science* 90: 154–165.

Verheye HM, Hutchings L, Huggett JA, Painting SJ. 1992. Mesozooplankton dynamics in the Benguela ecosystem, with emphasis on the herbivorous copepods. *South African Journal of Marine Science* 12: 561–584.

Vidal EAG, DiMarco FP, Wormuth JH, Lee PG. 2002. Influence of temperature and food availability on survival, growth and yolk utilization in hatchling squid. *Bulletin of Marine Science* 71: 915–931.

Washburn L, Kadko DC, Jones BH, Hayward T, Kosro PM, Stanton TP, Ramp S, Cowles T. 1991. Water mass subduction and the transport of phytoplankton in a coastal upwelling system. *Journal of Geophysical Research* 96(C8): 14927–14945.

CHAPTER 3

Currents along the Tsitsikamma Coast and potential transport of squid paralarvae

A bottom-mounted Acoustic Doppler Current Profiler was deployed at 36 m depth on the Tsitsikamma coast on the eastern Agulhas Bank. The purpose was to investigate transport of chokka squid *Loligo reynaudii* paralarvae on the inshore spawning grounds (<60 m). Analysis of the first 12 months of data showed that surface flow was mainly eastward (alongshore), with a maximum velocity (u-component) of +115 cm s^{-1} and an average of +24 cm s^{-1}. Generally, velocity decreased with depth, with a maximum bottom velocity (u-component) of +65 cm s^{-1} and an average of +10 cm s^{-1}. Data from a nearby thermistor array showed that the water column was usually isothermal during winter (July–September), with bottom flow in the same direction as the surface layer. In summer (December–March), vertical stratification was most intense and surface and bottom flows differed in velocity and direction. Potential net monthly displacement calculated for three depths (5 m, 23 m and 31 m) indicated that passive, neutrally buoyant biological material (e.g. squid paralarvae, fish eggs and larvae) would likely be transported eastwards in the surface layer for 8 of the 12 months, and generally exceed 220 km $month^{-1}$. Displacement in the bottom layer was more evenly distributed between east and west, with net monthly (potential) transport typically 70–100 km, but reaching a maximum of 200 km. Wind-driven coastal upwelling, prevalent during the summer, cause the surface layer of the coastal counter current to flow offshore for several days, resulting in potential displacement distances of 40 km from the coast. This mitigates eastward transport and potentially moves squid paralarvae in the Tsitsikamma current offshore and into the westward mid shelf current which flows towards the cold ridge.

Keywords: Agulhas Bank, currents, South Africa, squid spawning grounds, paralarvae

Introduction

In South African waters, chokka squid *Loligo reynaudii* spawn mainly on the eastern Agulhas Bank in depths <60 m between Plettenberg Bay and Cape Padrone (Augustyn *et al.* 1994). This region is east of a prominent, semi-permanent oceanographic feature, referred to as the cold ridge (Chapter 2; Figure 3.1; Largier and Swart 1987, Boyd and Shillington 1994). This elongated, tongue-like, feature is formed when the shelf thermocline is locally lifted towards the sea surface (doming), resulting in cold, nutrient-rich, bottom layer water entering the photic zone. Primary and secondary production is generally elevated above this layer (Probyn *et al.* 1994). Ship-bourne Acoustic Doppler Current Profiler (ADCP) measurements presented by Boyd *et al.* (1992) and Boyd and Oberholster (1994) indicated a net barotropic westward flow of water over the mid-shelf region of the eastern Agulhas Bank, with more variable currents inshore. Based on these data and the distribution of sampled squid paralarvae shown in Figure 3.1, Chapter 2 speculated that the eastern position of the chokka squid spawning grounds may be allied to a spawning strategy that relies on the westward transport

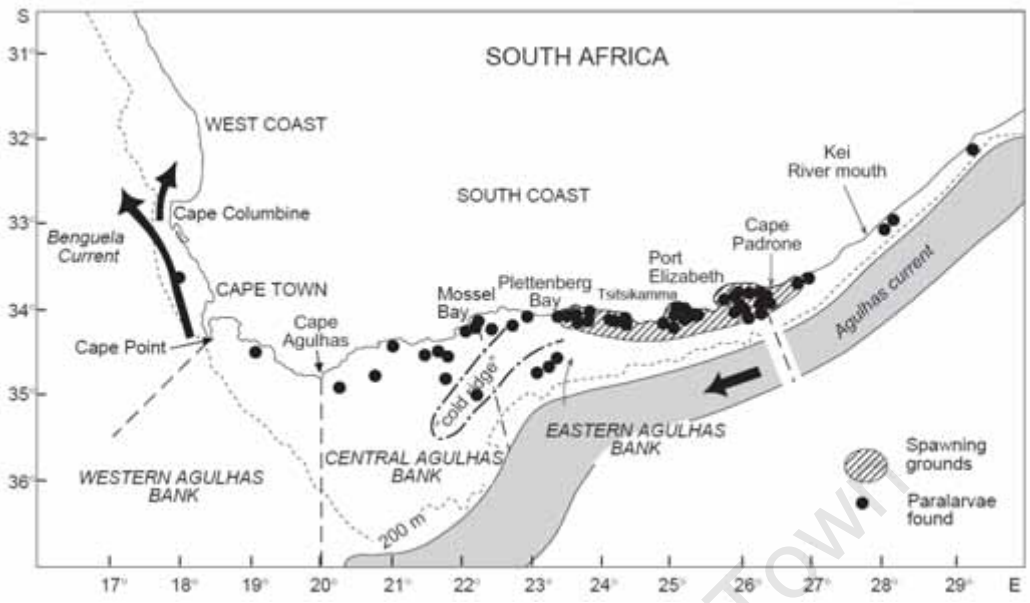

Figure 3.1: Map showing the main spawning grounds of chokka squid on the eastern Agulhas Bank, east of the 'cold ridge'. Positions where paralarvae have been found are indicated (data from Augustyn *et al.* 1994).

of squid paralarvae towards the abundant food source near the cold ridge. Chapter 2 suggested that anomalies in the physical and biological processes of such a system could influence successful recruitment, and explain at least in part the observed high variability in squid biomass and catches. More specifically, it showed that the cold ridge was an upwelling filament that originates in the intense coastal upwelling zone along the Tsitsikamma coast, which displayed unusual behaviour during ENSO events. Anomalies in the westward current regime might also explain why paralarvae are found east of the Kei River mouth (Figure 3.1).

Larval transport has also been of interest in the Tsitsikamma National Park (TNP), a marine protected area located within the squid spawning grounds just east of Plettenberg Bay (Figure 3.2b). Tilney *et al.* (1996) attempted to evaluate the export potential of sparid fish larvae from the TNP using a bottom-moored (ACM2) current meter deployed at a depth of 51 m over 6 months period (Figure 3.2a). Together with SST satellite imagery depicting coastal upwelling events on the South Coast, Tilney *et al.* (1996) proposed that larvae were transported beyond the boundaries of the park via three mechanisms, which they referred to as 'current-closure scenarios', (see Figure 6 in Tilney *et al.* 1996): (1) coastal, barotropic, alongshore flow oscillations (east-west), mainly during winter, (2) surface layer, offshore-onshore, closure circulation associated with minor coastal upwelling during spring/summer, and (3) surface layer, offshore-onshore, closure circulation associated with major coastal upwelling, also during spring/summer. The 'closure' implied that the particle trajectory was offshore and westwards during upwelling, which returned inshore during relaxation, after the cessation of easterly wind (i.e. producing a closed trajectory).

Such mechanisms, however, complicate the 'westward transport hypothesis' for squid paralarvae that was proposed in Chapter 2 and, given the short time of 6 days before starvation (Vidal *et al.* 2005), appears to render the cold ridge out of reach for many newly hatched paralarvae. Attwood *et al.* (2002) followed up on the work of Tilney *et al.* (1996) using surface drogues and showed the potential for larval export from the TNP. They also found that the coastal current was more westward than eastward, which did not support the 'current-closure scenarios' hypothesis.

To advance the understanding of factors influencing squid recruitment on the Agulhas Bank, both the 'westward transport hypothesis' and the 'current-closure scenarios' needed to be further investigated and reconciled. Part of the problem is that different data and analyses were used to derive each hypothesis. The ship-borne ADCP results presented by Boyd *et al.* (1992) and Boyd and Oberholster (1994) were based on 40 cruises, but only 10 covered the study area referred to here, and at best were made three times a year. These sparse data may not necessarily reflect the general flow regime on the mid-shelf or inshore, and certainly ignore seasonal trends. On the other hand, Tilney *et al.* (1996), measured bottom currents only, which are slower than surface flow, and therefore the potential for larval transport in the surface layer was underestimated in that study. Even including the drogue work by Attwood *et al.* (2002), there is insufficient time-series data to cover the flow dynamics and seasonal trends of currents along the Tsitsikamma coast. Moreover, none of these studies took into

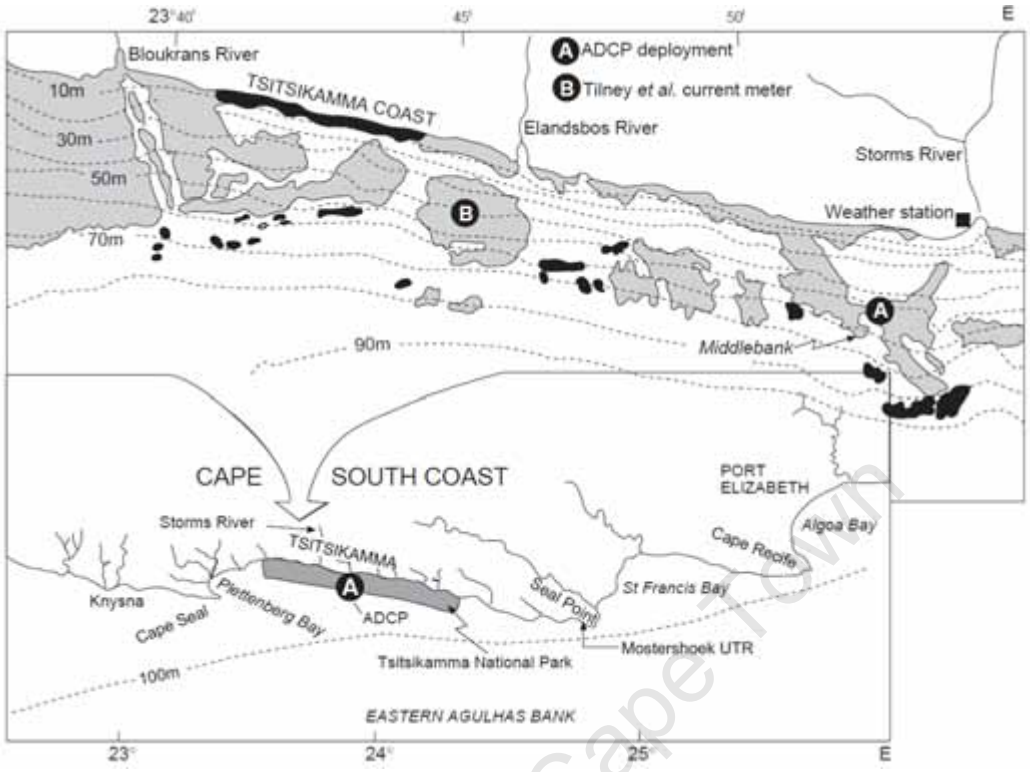

Figure 3.2: The locality of the Tsitsikamma coast on the South Coast, showing its bathymetry and the position of the ADCP (A: this study) and the bottom-moored current meter (B: Tilney 1996). The grey shaded areas in the top expanded map represent reef.

consideration the intense thermal stratification that occurs on the eastern Agulhas Bank (Schumann and Beekman 1984, Swart and Largier 1987, Schumann 1999), and the possibility of opposing surface and bottom flows complicating larval transport.

Mindful of these shortcomings, and the fact that measurements at a single site do not necessarily present a complete understanding of the flow pattern in an area, the aim of this chapter was to augment previous studies with a continuous 12-month, multi-layered, description of the coastal current along the Tsitsikamma coast. These data were then used to assess the potential transport of squid paralarvae on the inshore spawning grounds, including ichthyplankton from the TNP.

Material and Methods

The TNP extends 72 km along the coast of the eastern Agulhas Bank east of Plettenberg Bay, and up to 5.5 km offshore to a depth of around 100 m. In July 1998, a 300kHz ADCP was deployed at the centre of the TNP (2.5 km from the shore) on a prominent reef known as Middlebank at 34º02.72' S, 23º52.51' E (Figure 3.2a). The reef has a steep offshore slope of about 45˚, which rises from the seabed at 60 m to the shallowest point at 23 m. Inshore of this high point, the reef drops less steeply (~15˚) to 45 m. The ADCP was deployed on the inshore slope of the reef at a depth of 36 m. This position was chosen as a compromise between minimising flow changes on account of reef topography and to remain within a safe working depth for SCUBA diving during deployment and recovery of the instruments. An array of Hugrún mini underwater temperature recorders, positioned at depths of 12, 19, 27 and 31 m in the water column, was deployed 20 m away from the ADCP mooring. Service and data download was every four months.

The ADCP was configured to record every 30 minutes using an ensemble size of 120 pings (one ping per second). The water column was sampled using 15 bins, each of 2-m depth, between 3 and 31 m. Prior to processing, the data for each bin were checked for quality on a monthly basis. For this analysis, only bins in which >75% of the readings computed to be 'good' were used (see Lee Gordon 1996 for details defining 'good' data.) This criterion eliminated the 3 m bin. The first 12 months of data presented here did not require filters to remove noise, but were averaged to hourly values. It is noteworthy that a decline in the percentage of 'good' data was observed between depths 17–27 m during the summer (November–March), which may be related to stratification of the water column. Directional data were converted to true north (i.e. –25º) internally at the time of measurement.

Wind data, measured 15 m above sea level, were obtained at hourly intervals from a dial-in automatic weather station located at Storms River (see Figure 3.2). This location is not ideal, because the coastline topography is exceptionally steep and rises to a coastal plain at an altitude of 180–220 m. In addition, the small embayment at Storms River mouth introduces an inflection in the otherwise linear coastal topography (Figure 3.2). This may have influenced measurements made at this site, so these data were not necessarily representative of the

wind field farther offshore. A New Hampshire Lanczos filter, with 71 weights and a power point of 36 h was used to remove land breeze effects in the analysis.

NOAA AVHRR images were used to highlight SST on the South Coast during an upwelling event between 13 and 20 January 2000. Images on 16, 17, 18 and 20 January were chosen to best represent the evolution of the upwelling plume. Cloud cover was removed from the images using composites of data from several satellite passes.

Results

Polar histograms of the surface (5 m) and bottom (31 m) currents from July 1998 to June 1999 (not shown) illustrated that currents flowed predominately in an east-west direction at both depths, with the principal axis being between 78° and 259°. Interestingly, this was not parallel to the coastline, but aligned with a deeper bathymetry, the 100-m isobath (Figure 3.2), and the principal wind axis (not shown).

The characteristics of velocity for this dataset are depicted in Figures 3.3 and 3.4, which show the east-west (u–) and north-south (v–) velocity components. These components were resolved using true north-east co-ordinates, which closely match the observed principal flow axis. Positive values in the u–component plots represent eastward flow. Similarly, positive values in the v–component plots represent northward (onshore) flow. The surface (5 m) u–component velocities (Figure 3.3a) reached maximum peak values of +115 cm s^{-1} in December/January and –101 cm s^{-1} in October. Velocities of this magnitude did not appear to be sustained for periods of more than three days. The average eastward and westward velocity components were +24 cm s^{-1} and –21 cm s^{-1} respectively (Figure 3.3a). Velocities above these averages generally did not persist for periods of more than five days, although in August 1998 an eastward current with above average velocity flowed for 15 days. Periods of sustained high velocity appeared to be more common in the eastward current than in the westward current, and lacked seasonality. To validate this, however, a longer time-series is required. Slack water (i.e. u–component <5 cm s^{-1}) was seldom measured, and when found did not last longer than five days.

East-west component velocities at 31 m (Figure 3.3b) were considerably smaller than those at the surface. The maximum peak velocity in the eastward bottom current was +65 cm s^{-1} and coincided with the maximum peak eastward surface current on Day 186, in December. The maximum peak westward velocity was –40 cm s^{-1}, observed on three occasions in October. All three events were of short duration, lasting between 24 h and 72 h, and coincided with maximum westward surface velocities. The average bottom eastward and westward velocity components were +10 cm s^{-1} and –11 cm s^{-1} respectively (Figure 3.3b). Most sustained high-velocity events in the bottom layer coincided with those in the surface layer, resulting in similar overall velocity trends. However, during summer there were instances when the bottom velocity was low and the surface flow high (e.g. surface velocity on Day 168 was 63 cm s^{-1}), or the surface current was slack and the bottom current was relatively fast (e.g. bottom velocity on Day 209 was 28 cm s^{-1}). On some occasions, surface

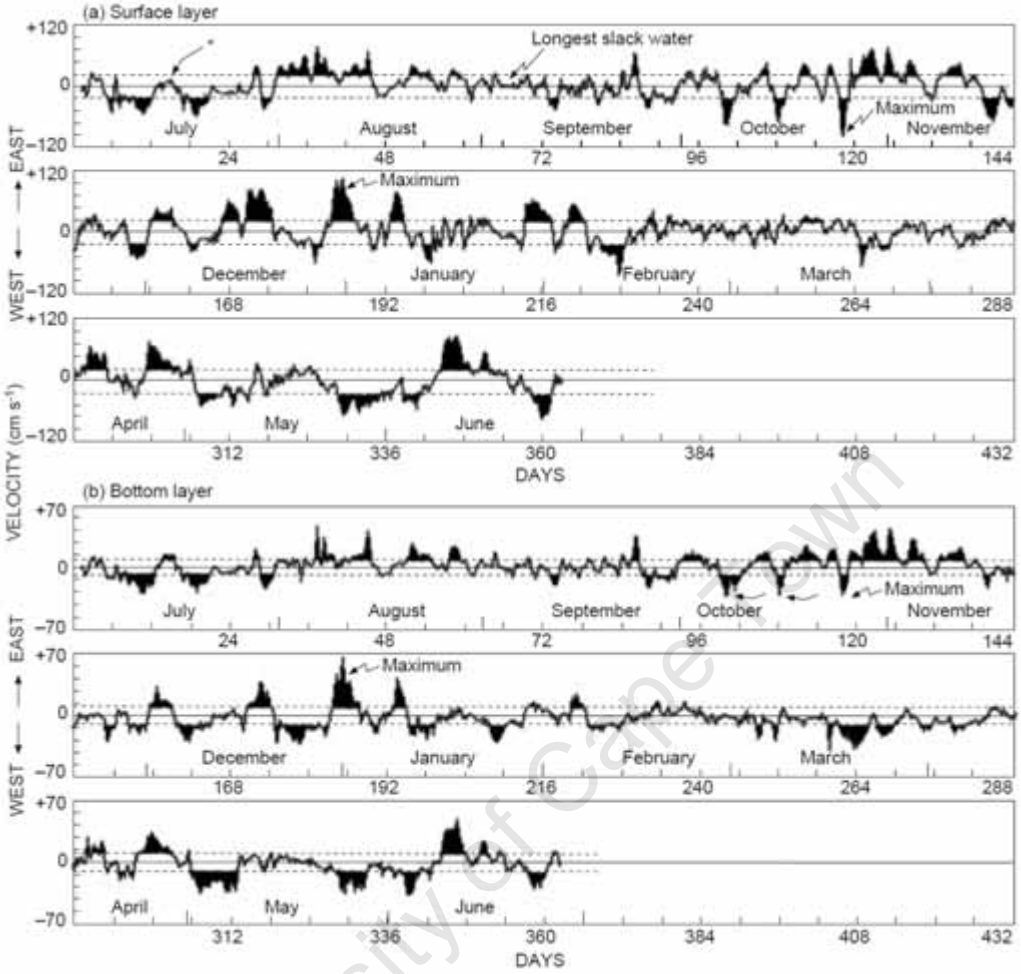

Figure 3.3: ADCP measurements of the 12-monthly time-series of the east–west (u–) velocity component of the Tsitsikamma inshore current for (a) surface layer (5 m) and (b) bottom layer (31 m). Positive y-axis values indicate eastward flow, negative values denote westward flow. Note the different y-axis scales. Average eastward and westward velocities are represented by the dotted line and shaded regions highlight above-average velocities.

and bottom currents flowed in opposite directions. For example, on Day 262 surface velocity was +25 cm s^{-1} for about 12 h while bottom velocity was –30 cm s^{-1}).

The maximum peak v–component velocities in the surface layer (Figure 3.4a) were +39 cm s^{-1} in December and –36 cm s^{-1} in June. Relative to the u-component, these velocities were short in duration, seldom lasting for more than a few hours. Average values indicate that the offshore and onshore velocity components in the surface layer were similar in magnitude, i.e. –7 cm s^{-1} and +6 cm s^{-1} respectively. In the bottom layer (Figure 3.4b), the maximum peak v–component velocities of +20 cm s^{-1} and –15 cm s^{-1} were about half those observed in the surface layer (averaging +3 cm s^{-1} and –2 cm s^{-1} respectively). Compared to the u-component, the frequency of variability in the v–component, in both the surface and bottom, was much higher. Semidiurnal tides and inertial currents could be attributable in part to this variability in velocity (Welsh 1964, Schumann and Perrins 1982, Largier 1987, Schumann 1999). Towards the end of the study, during April, May and June, there was an underlying low-frequency oscillation (of a period of a few days to weeks) in the v–component velocity. This was most pronounced in the surface layer, but also noticeable in the u–component.

The flow regime can further be examined using 12-month progressive (cumulative) u– and v–component displacement plots for the surface and bottom layers (Figure 3.5). In both layers, the u–component was dominant. In the surface layer, the theoretical 12-month net alongshore displacement was estimated to be 1 306 km eastward. It is important to note that this displacement cannot be interpreted literally, because this distance would extend far beyond the eastern boundary of the Agulhas Bank and onto the narrow Eastern Cape shelf domain, which is dominated by the strong south-westward-flowing Agulhas Current. However, such displacement could explain the appearance of squid paralarvae far east of the main spawning grounds, at Kei River mouth (Figure 3.1). The alongshore displacement depicted in Figure 3.5a is characterised by seven periods (indicated) when substantial easterly flow was concomitant with lengthy periods of sustained high velocities (Figure 3.3a). For instance, the persistent easterly flow in August (Event 1) lasted four weeks. Substantial displacement events in the westerly direction, similar in magnitude to the large easterly displacements, were found in July 1998 and May 1999, also on account of lengthy periods of sustained high current velocity. But overall, westward flow in the surface layer does not appear to be a major feature of the currents off the Tsitsikamma coast, as is any form of seasonal behaviour in displacement. On this scale, the relative contribution of the onshore-offshore flow (v-component) to total displacement in the surface layer is clearly seen in Figure 3.5a to be of minor importance. However, as shown later, it should not be ignored.

In contrast, the u-component of the bottom layer appeared to have a seasonal trend in displacement (Figure 3.5b). There was similarity between the bottom and surface u-component during July–November 1998 and May–June 1999, but the effect of dissimilar flows (at times opposite) is clear between December and March, where little net displacement took place relative to the upper layer. Factors such as wind, vertical stratification, coastal-trapped waves and upwelling frontal jets could be responsible for this dissimilarity. However, the

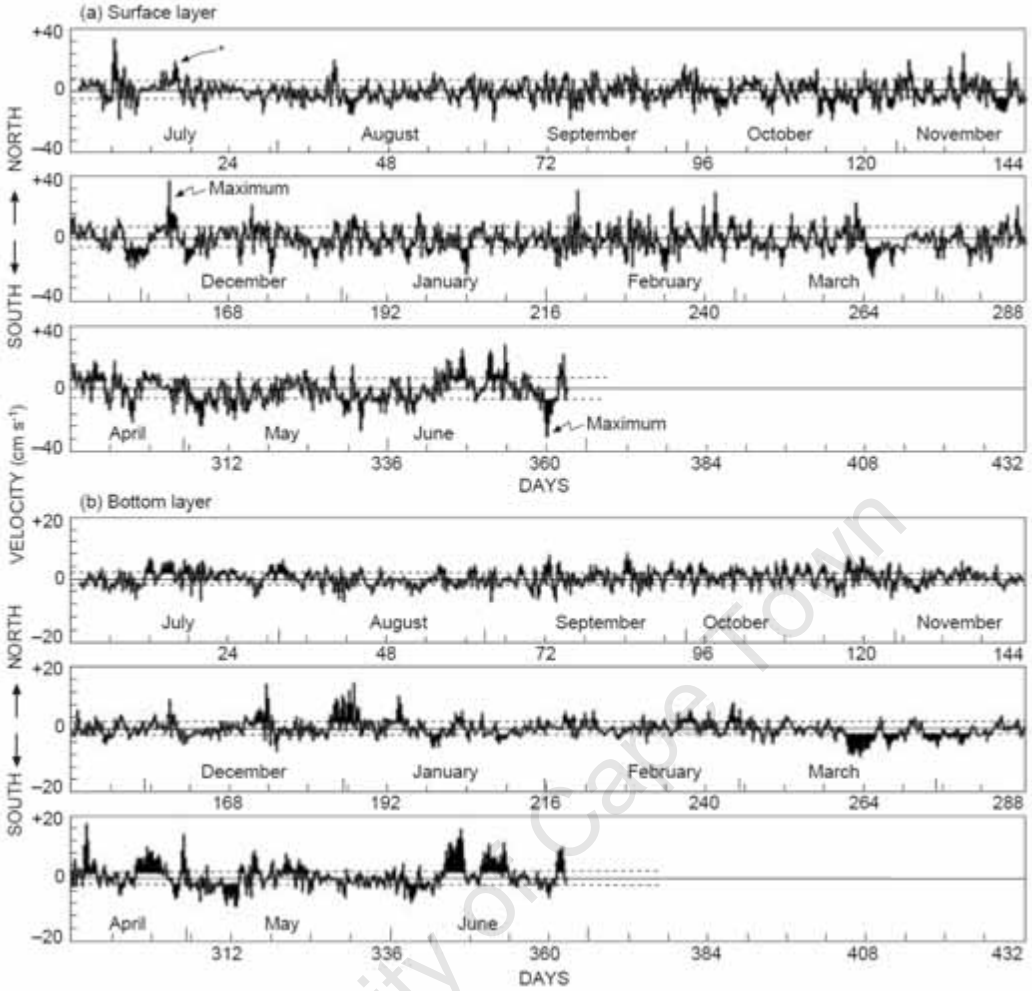

Figure 3.4: ADCP measurements of the 12-month time-series of the north–south (v–) velocity component of the Tsitsikamma inshore current for (a) surface layer (5 m) and (b) bottom layer (31 m). Positive y-axis values indicate northward flow, negative values denote southward flow. Note the different y-axis scales. Average northward and southward velocities are represented by the dotted line and shaded regions highlight above-average velocities.

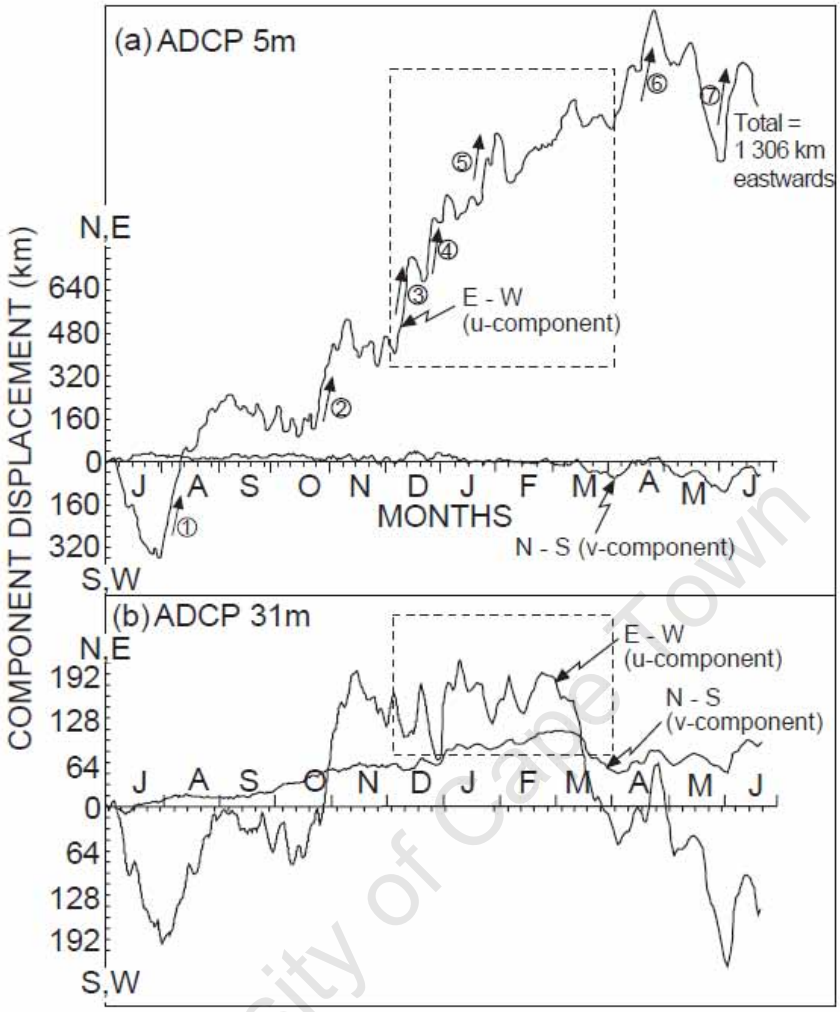

Figure 3.5: 12-month component displacement (progressive vectors) in (a) the surface layer (5 m) and (b) bottom layer (31 m) flows off the Tsitsikamma coast. Flow in the surface layer was characterised by seven periods of sustained easterly (+u–) displacement (denoted 1–7), with no seasonal trend. Contribution of the north–south (v–) component to the surface current is small. Much of the surface trend is also seen in the bottom current (b), except during December–March (dotted box).

former maybe more pertinent, because temperature data from a nearby thermistor array (Figure 3.6) showed that the period December–March is when vertical stratification in the water column is most intense (i.e. difference of >4°C between surface and bottom temperature), and Schumann (1999) demonstrated that easterly winds are more prominent during that time. Compared to the surface layer (Figure 3.5a), northward (onshore) displacement in the bottom layer was more obvious, particularly during October–February. Both layers showed a change in this trend between March and May, when there was more offshore displacement. Displacements such as these could be in response to Ekman transport in the upper water column, i.e. offshore displacement in the surface layer as a result of wind-induced coastal upwelling and onshore displacement in the bottom layer (Schumann 1999).

An indication of the potential transport of non-swimming larvae (assumed here to be passive, neutrally buoyant particles) can be gained by combining the u– and v–component displacements, providing total progressive displacement. In this fashion data for July and August 1998 (winter) and December, January, February 1999 (summer) were plotted in Figure 3.7. During winter, displacement in the surface and bottom layers was similar in direction, but differences in velocity caused disparate net transport distances (Figure 3.7a). In this case, surface and bottom particles released simultaneously from the origin would be hypothetically separated by 340 km in the alongshore direction after 62 days, with net surface and bottom displacement of the individual particles being 200 km east and 140 km west of the origin respectively.

During summer (Figure 3.7b), when there is stratification and on occasions surface and bottom flows differed greatly, the net alongshore displacement in the surface layer after 89 days would potentially be 705 km east of the origin. In marked contrast, a passive particle released from the origin in the bottom layer would have oscillated between eastward and westward displacement, with a net displacement of only 45 km east of the origin.

In both examples, the contribution of the v–component to the net total displacement on these time and distance scales is relatively small (see Figure 3.5a). On smaller scales, however, the v–component cannot be ignored, particularly in the surface layer (see three similar events marked by asterisks in Figure 3.7), and given the width of the shelf, can have a potentially significant role in larval dispersion. It is important to note that the north–south axis scale has been enlarged in the figure to 2 km per tick to highlight the onshore/offshore transport. This alters the true trajectory direction of these events. The onshore event in Figure 3.7a was caused by a slackening of the westward, alongshore surface current for about 4 days in mid July (see Figure 3.3a). During that time, the northward velocity component (Figure 3.4a) increased to 20cm s^{-1}, implying a potential displacement of 22 km. Of course,

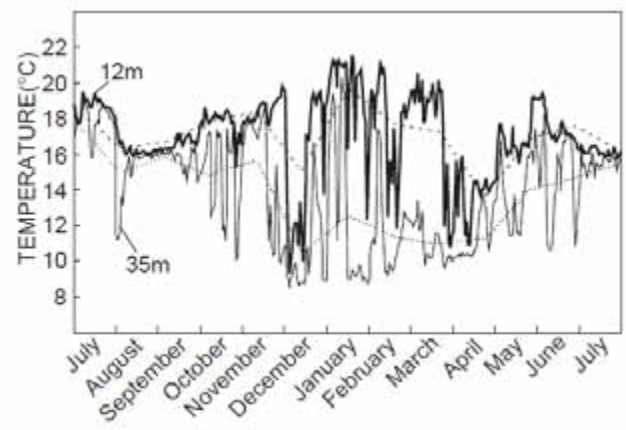

Figure 3.6: Daily (solid lines) and monthly (hashed lines) averaged temperatures for 12 m and 35 m depths on Middlebank. Thermal stratification is most intense during summer.

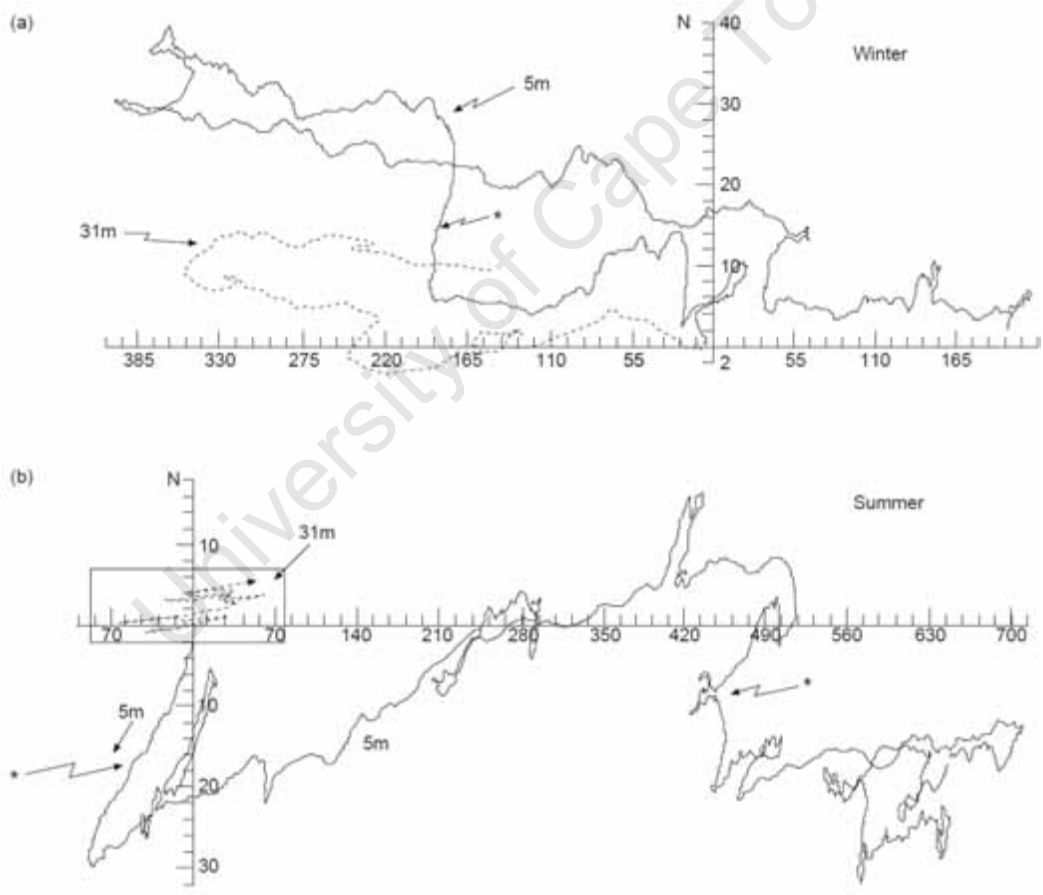

Figure 3.7: Potential transport (trajectories) of passive, neutrally buoyant biological material during (a) winter (July, August) and (b) summer (December, January, February) are presented by combining u–component and v–component displacements. Note the y-axis scale differs. The asterisks mark significant onshore and offshore displacement. Note the y-axis scale has been expanded for clarity. This distorts true direction (see Figure 3.8).

given that the coast is only 2.5 km to the north of the ADCP site, a literal displacement of this magnitude is impossible, so there must have been either downwelling or alongshore flow closer to the coast to maintain the continuity of flow (mass transport). The two offshore events in the net eastward flow shown in Figure 3.7b indicate potential displacement of about 30 km.

The cause of such events can be explored by considering data collected in January 2000 (Figure 3.8). Here, an offshore event interrupted eastward flow along the Tsitsikamma coast between 13 and 19 January. Offshore potential displacement was 40 km. The event coincided with a strong easterly wind (>6 m s^{-1}), which began in the early hours of 13 January (Figure 3.9b). Data collected (not shown) by a UTR located near Mostertshoek at a depth of 5 m, 100 km east of Middlebank (see Figure 3.2b for location) indicated a drop in temperature a few hours later, i.e. coastal upwelling began soon after the wind changed from west to east. The thermistor array on Middlebank (Figure 3.9c) also showed the surface layer cooling, but it took 48 h for the water column to become well mixed at 9°C. The progressive vector plot shown in Figure 3.8a indicated that, concomitant with this cooling, the surface layer had turned to offshore flow, which continued steadily until 19 January. Note that the axis scales differ in Figure 3.8a and the true direction of offshore advection relative to the coast is shown in the insert. Of interest is that this direction matches well the orientation of the 'cold ridge' (see Figure 3.1) and supports the belief that this feature is an upwelling filament with origins in the coastal upwelling zone (Chapter 2).

As evident by the rise in surface temperature at Middlebank (Figure 3.9c), the upwelling process had ceased by 20 January. There was an immediate return of the eastward surface current, albeit initially with an onshore component that possibly compensated the lower sea surface height adjacent to the shore. The response of the bottom layer (31 m) during this event was not immediate and differed in flow direction. The change from eastward flow (Figure 3.8b) lagged the upper layer by several hours, with the reversal only lasting until (mid) 18 January. Offshore flow was near absent in the bottom layer, unlike the surface (i.e. current reversal occurred). This however, could be on account of obstruction by the shallower offshore reef topography adjacent to the ADCP mooring (see Material and Methods).

It is significant that the easterly wind (driving force) stopped on 16 January and was followed by a south-westerly wind on 17 January (Figure 3.9b), and that upwelling was still active as evident in the sea surface temperature (SST) satellite imagery shown in Figure 3.9a. The upwelling plume off the Tsitsikamma coast continued to expand offshore between 17 and 18 January. Wind on 18 and 19 January was light and variable. The SST image for 20 January shows relaxation in the intensity of upwelling, with little evidence of cool water in the region by 23 January. The area influenced by this upwelling event on 20 January extended some 75 km from the coast. Also, the surface layer on the mid-shelf over this period was westwards, as evident by the advection of the cold-water plumes.

To assess larval transport along the Tsitsikamma coast, the net potential east–west displacement for each month between July 1998 and June 1999 was calculated using progressive vectors for depth 5, 23 and 31 m (Figure 3.10). This method was deemed

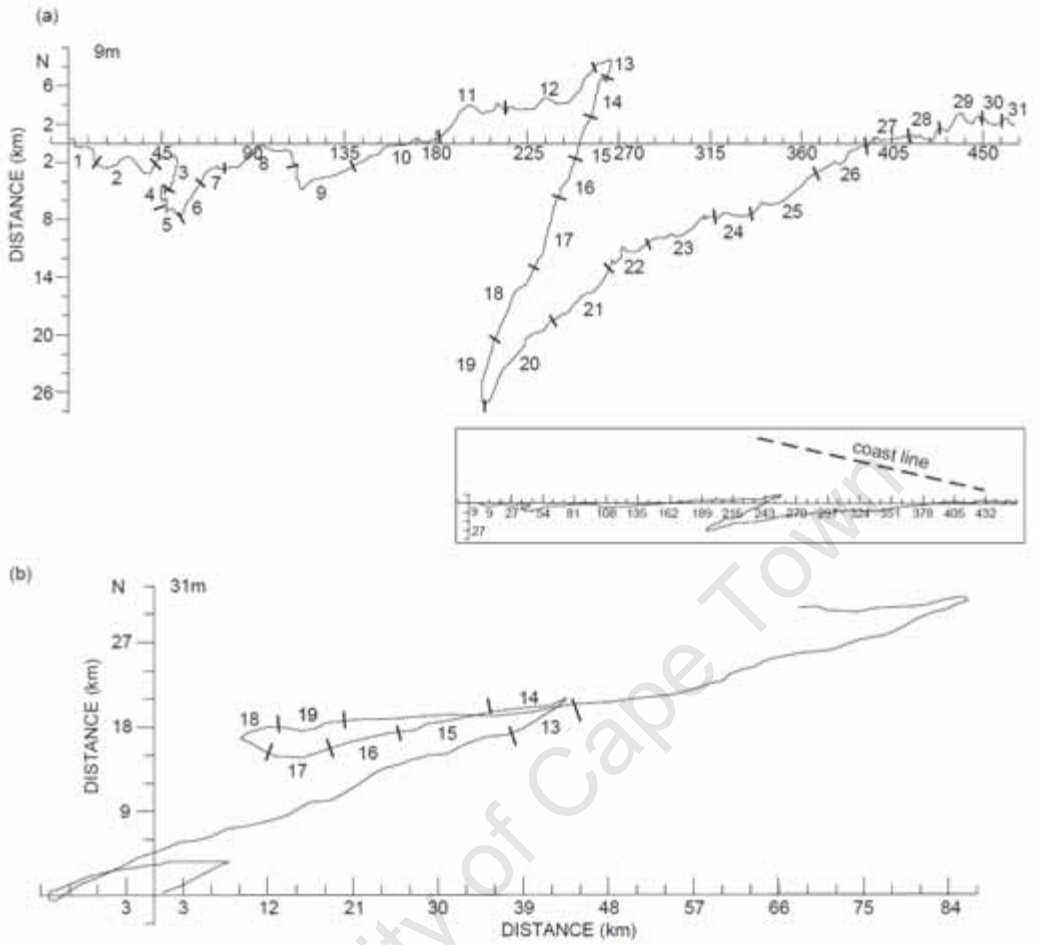

Figure 3.8: Progressive vector diagrams for January 2000 using ADCP data collected at Middlebank for (a) surface layer 5 m and (b) bottom 31 m. Days of the month are indicated. The eastward current was interrupted by an upwelling event between 13 and 19 January, causing an offshore flow. Note the y-axis scale in (a) has been expanded for clarity. This distorts true direction as seen in the insert.

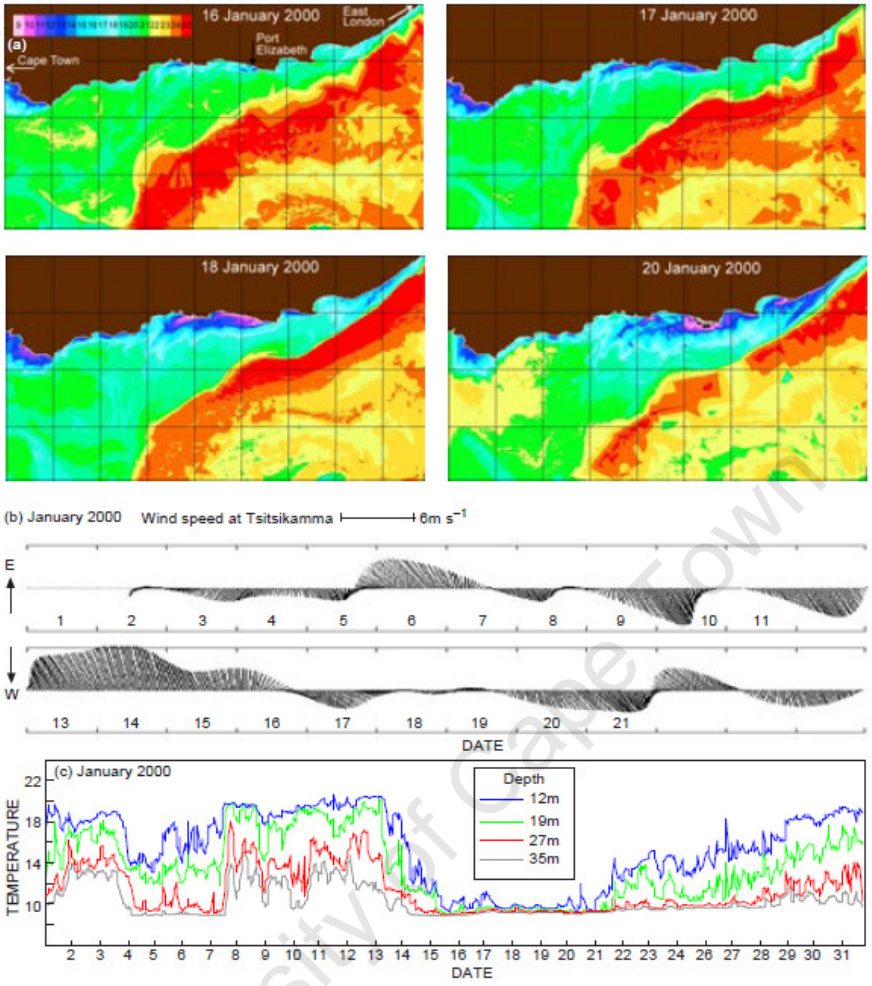

Figure 3.9: The upwelling event in mid January 2000; (a) SST images depicting the evolution of the upwelling plume along the Tsitsikamma coast; (b) filtered winds measured at Storms River; (c) temperature data collected by a thermistor array on Middlebank.

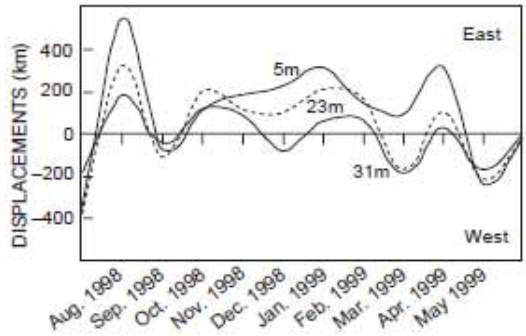

Figure 3.10: Monthly east–west (alongshore) transport of passive, neutrally buoyant biological material at (a) 9 m and (b) 31 m off the Tsitsikamma coast. Monthly displacements are based on ADCP data collected for the period July 1998–June 1999. The midwater displacement is approximately at the depth of the thermocline during the summer month.

appropriate to view potential displacement on a comparative spatial and temporal scale. The mid-depth was chosen as a compromise between work by Schumann (1999), who calculated the average depth of the upper mixed layer to be 6.9 m (based on six CTD sections between January and May) and data from Figure 3.6, which shows the mixed lay reaches 35 m. Figure 3.10 shows that net egg and (para)larval transport in the surface layer was overwhelmingly eastwards, with the greatest distance of 550 km in August. The average monthly transport in the surface layer was about 200 km. In only three months was net displacement westwards (July, September and May). There was a general decline in net displacement with depth, with exceptions in October in midwater (23 m) where displacement was greater than in the surface layer (possibly retarded by wind), and in March when displacement at 23 m and 31 m was opposite. Overall, net displacement in the bottom layer lacked the dominant eastward trend found near the surface, with maximum distances of 220 km.

Discussion

Coastal currents off Tsitsikamma

ADCP data collected during research ship surveys showed a net westward flow at a depth of 30 m over most of the eastern Agulhas Bank (Boyd *et al.* 1992, Boyd and Oberholster 1994). Exceptions to this current pattern were found on the outer- and inner-shelf regions (i.e. <15 km from the coast), where averaged vectors indicate a distinct lack of net spatial and temporal trends. In the vicinity of Storms River, the limited data presented by Boyd *et al.* (1992) and AJ Boyd (Marine and Coastal Management, unpublished data) show a mix of flow directions (including onshore). Eastward coastal flow seems to oppose the greater westward shelf flow at times, suggesting the existence of a narrow coastal counter current off the Tsitsikamma coast.

The 6-month bottom dataset collected by Tilney *et al.* (1996), using a moored ACM2 acoustic phase-shift current meter, showed that eastward flow is common near the seabed (51 m) off the Tsitsikamma coast. Those data also indicated a strong onshore component in this flow and that transient peaks (current reversals over a day) are integrated into the ambient flow. Spectral analysis indicated that these were caused by coastal trapped waves generated by synoptic weather patterns (Schumann 1983, Schumann and Brink 1990).

The drogue study by Attwood *et al.* (2002) demonstrated that the surface current off Storms River is mainly alongshore. In contrast to Tilney *et al.* (1996), Attwood *et al.* (2002) found that the current was more westwards than eastwards and showed minor onshore and offshore components, thought to be indicative of Ekman drift. The scale of the drogue tracks, however, was too small to test the coastal upwelling-related 'current-closure scenarios'. Averaged velocities for individual drogues ranged between 2 cm s^{-1} and 58 cm s^{-1} with a modal average of 23 cm s^{-1}. Surface current and wind were poorly correlated, often in opposite directions, suggesting that wind is not a primary driving force of the current along the Tsitsikamma coast. Attwood *et al.* (2002) found that most drogue tracks remained parallel to

one another. Successive drogue releases demonstrated that the direction of the surface current can remain consistent for periods of at least four days. Between 1.5 km and 4.5 km from the coast (distribution of drogues), the surface current commonly exhibited a horizontal velocity gradient, with either a reduction in velocity towards the shore (as might be expected on account of coastal interference) or the opposite, where the inshore surface current was faster.

The 12-month, hourly time series of vertical current profiles collected in this study overcomes some of the limitations of previous work. The most important findings are (1) the quantification of the eastward surface flow (5 m), which dominated over westward flow by 68% vs 32%, (2) there are differences between surface and bottom flow (e.g. eastward flow in the bottom layer was less dominant), and (3) seasonal trends in the flow pattern. Moreover, there is good agreement between the bottom layer data collected by the ADCP and that of Tilney *et al.* (1996), despite the difference in depth between the two deployments (i.e. 51 m vs 36 m respectively). For instance, there are similar periods of sustained eastward flow (~4 weeks), which result in net eastward displacement, and the westward flow exhibited in both studies is of shorter duration than eastward flow. Transient current reversal peaks (caused by coastal trapped waves) are evident in both datasets, as is northward displacement.

However, there are important differences between the deeper (ACM2) current mooring used by Tilney *et al.* (1996) and shallower (ADCP) deployment in this study. The north-south displacement at the deeper site dominated over the east-west component, whereas the ADCP data showed the opposite to be the case. More specifically, the deeper mooring showed a net northward displacement of 187 km in 198 days, compared with a displacement of 80 km for the same time period using ADCP data. The dominance of onshore flow over alongshore at the deep mooring is an unexpected result, but it may be caused by a channel or nearby high profile reef. Another difference is that greater maximum peak velocities were recorded by the ADCP compared with the ACM2 mooring, i.e. 65 cm s^{-1} vs 17 cm s^{-1}. A number of factors could be responsible for this difference, including bottom topography, tidal and inertial currents as well as long-term shifts in the oceanographic regime on the Agulhas Bank. It is therefore likely that transport rates higher in the water column were underestimated by Tilney *et al.* (1996).

In the absence of data on surface currents, Tilney *et al.* (1996) used results from drift card studies undertaken on the South and South-West coasts to assess surface transport of ichthyoplankton (Duncan and Nell 1969, Shelton and Kriel 1980). These studies indicated (track-averaged) maximum surface speeds of about 30 cm s^{-1}. The drogue study by Attwood *et al.* (2002) showed a track-averaged maximum velocity of 58 cm s^{-1}. The present ADCP surface data (5 m) indicated a near-instantaneous maximum velocity of 115 cm s^{-1}, suggesting that previous studies underestimated maximum surface currents along the Tsitsikamma coast by a factor of between two and four. Apart from being near instantaneous, the higher velocity obtained using the ADCP is likely a result of the greater number of observations over the year, through all conditions, and the small vertical bin size of 2 m

compared with 8 m for the drogues. However, when averaged, the ADCP surface layer data agrees well with the others studies (i.e. 23 cm s^{-1} vs +24/–21 cm s^{-1} respectively). The ADCP data show that currents can persist for periods in excess of four days, as observed by Attwood *et al.* (2002).

The present data clearly showed the effect of an easterly wind on the eastward flow, and the resultant change in direction to offshore flow in the surface layer concomitant with coastal upwelling (Figure 3.9). The data indicated a potential offshore displacement of 40 km. Given that the shelf is 80–100 km wide in the study region, pelagic material in the surface layer would likely be transported to the mid shelf. However, as noted in the satellite imagery (Figure 3.9), upwelling plumes indicated a westward mid-shelf flow, which would transport particles in that direction. Moreover, in theory, there should be a westward-flowing jet current along the upwelling front. The ADCP data shows a return of the eastward current after cessation of upwelling, with a clear onshore component. It is therefore possible for a particle on the mid shelf to be transported back to the coast, which supports the 'current-closure hypothesis'.

The dynamics and extent of the coastal countercurrent are not known. As demonstrated in this study, wind can influence the flow throughout the water column, at least to depths of 40 m, but it appears not to be the main driving force, as suggested by Attwood *et al.* (2002).

Larval transport and reconciliation of hypotheses

Little is known about the behaviour of chokka squid paralarvae. The few hatchlings that have been collected (depicted in Figure 3.1) were found near the surface (M. Lipiński, Marine and Coastal Management, pers. comm.), suggesting that they vertically migrate despite them being negatively buoyant (Vidal *et al.* 2005). In the absence of information on time of spawning and hatching, egg density and swimming speeds, it was assumed, for the purposes of this study, that squid paralarvae are influenced by advection (i.e. passive drifters) for one month, and remain at similar depths in the water column during that period. This time span could be an oversimplification, but it is a convenient time-scale for analysis and provides an interim means to quantitatively assess their potential transport. For squid paralarvae, a one-month pelagic period could be realistic (Yang *et al.* 1986).

Also, it must be emphasised that displacement obtained using current measurements made at a single site are theoretical and do not consider surrounding constraints such as bathymetry, coastline, differential horizontal flows and turbulence, factors that can result in large deviations from the theoretical 'trajectories' presented here. Progressive displacement plots, however, can highlight seasonal and depth differences. Given the dominant alongshore flow in the Tsitsikamma coastal system, this simplistic approach was considered adequate for a first attempt to calculate net potential east-west displacement for each month of the study, instead of more elaborate sequential displacements for daily releases throughout the year. The results showed that the net potential egg and (para)larval transport in the surface layer was overwhelmingly eastward, with theoretical distances of up to 550 km. However, the diminishing dominance of the eastward current with depth would result in decreased

displacement towards the bottom, with distances up to 220 km being achieved. Taking vertical migration into account, the dispersion pattern will become complex, especially if bottom and surface layers flow in opposite directions. Also, displacement would depend on the time spent by larvae at different depths.

The ADCP data collected in this study demonstrated that the inshore current along the Tsitsikamma coast flows westwards at times, which supports the westward transport hypothesis proposed in Chapter 2. However, this pattern is not as common as the eastward flow, which would transport larvae away from the cold ridge and the enhanced food source there. This hypothesis, in its simple state, is therefore relevant only under certain conditions.

Coastal upwelling can cause displacement in the surface layer, particularly during eastward flow along the coast. Neutrally buoyant larvae (and eggs) being transported eastwards would move offshore onto the mid-shelf and simultaneously westwards, and return to the coast downstream in the Tsitsikamma coastal current. Such trajectories would retard net eastward displacement, supporting the 'current-closure scenarios' suggested by Tilney *et al.* (1996). Westward advection on the mid shelf, although commonly observed in SST and ship-borne ADCP data, still needs to be investigated to determine its prevalence and implications for larval transport. Only moored current-meter measurements can establish this. If westward flow is common, eggs and larvae could be carried into the area of the cold ridge and benefit from the enhance food supply there. In this respect, westward flow on the mid shelf would seem to benefit larvae hatched on the deep chokka squid spawning grounds.

Coastal upwelling occurs mainly during summer, which is the main spawning period for chokka squid. Upwelling, and its apparent retentive nature, could therefore be advantageous when the eastward current flows, by limiting eastward displacement of paralarvae and the possible detrimental effects of moving into a poorer food environment. The fate of larvae in the eastward coastal current remains unknown, but loss from the Agulhas Bank is a possibility. Such displacement offers an explanation for the presence of squid paralarvae east of the Kei River mouth (Figure 3.1).

The method used in this study to assess larval displacement is somewhat simplistic, and upwelling and the associated 'closure' mechanisms have not been taken into account. Nonetheless, the results demonstrate the potential for larval transport in the Tsitsikamma coast region and, in the absence of knowledge on vertical migration behaviour, that both squid paralarvae and ichthyoplankton are likely to be transported beyond the boundaries of the TNP.

Conclusion

The results presented indicate the presence of an alongshore current on the Tsitsikamma coast, which is predominantly eastwards. The current can flow in the same direction for periods of four weeks, and attain high surface velocities of 115 m s^{-1} (average 23 cm s^{-1}). Velocity generally decreases with depth, from up to 65 m s^{-1} near the bottom (average 11 cm s^{-1}). Although not a common phenomenon, bottom and surface layers can flow in opposite

directions when the water column is thermally stratified. Potential displacement trajectories indicated an average monthly transport distance from Middlebank of up to 550 km to the east in the surface layer. Near-bottom transport was less dominated towards the east, reaching a maximum of 200 km. During periods of easterly winds and eastward coastal currents, the surface flow veered offshore, highlighting Ekman transport and concomitantly coastal upwelling. Potential displacement of at least 40 km from the coast was attained during upwelling events during the study.

The existence of a dominant eastward surface flow, however, requires modification to the 'westward transport hypothesis' proposed in Chapter 2. Whereas it is probable that squid paralarvae on the mid shelf are transported westward (as indicated by the ship-borne ADCP data), the data here indicate that squid paralarvae on the inshore spawning grounds, between Cape Seal and Seal Point (Figure 3.2b), are mainly transported eastwards in the surface layer and away from the cold ridge. The onshore-offshore cyclonic advection would imply that some inshore paralarvae are advected offshore into the westward mid-shelf current, and possibly swept towards the cold ridge. Alternatively, the paralarvae could be returned inshore, thereby retarding eastward displacement and maintaining them at the base of the 'cold ridge'. The fate of the paralarvae transported eastward remains unknown.

References

Attwood CG, Allen J, Claasen PJ. 2002. Nearshore surface current patterns in the Tsitsikamma National Park, South Africa. *South African Journal of Marine Science* 24: 151–160.

Augustyn CJ, Lipinski MR, Sauer WHH, Roberts MJ, Mitchell-Innes BA. 1994. Chokka squid on the Agulhas Bank: life history and ecology. *South African Journal of Science* 90(3): 143–154.

Boyd AJ, Oberholster GPJ. 1994. Currents off the west and south coasts of South Africa. *South African Shipping News and Fishing Industry Review* 49(5): 26–28.

Boyd AJ, Shillington FA. 1994. Physical forcing and circulation patterns on the Agulhas Bank. *South African Journal of Science* 90(3): 114–122.

Boyd AJ, Taunton-Clark J, Oberholster GPJ. 1992. Spatial features of the near-surface and midwater circulation patterns off western and southern South Africa and their role in the life histories of various commercially fished species. *In* Benguela Trophic Functioning. Payne AIL, Brink KH, Mann KH, Hilborn R (eds). *South African Journal of Marine Science* 12: 189–206.

Duncan CP, Nell JH. 1969. Surface currents off the Cape coast. *Investigational Report of Division of Sea Fisheries, South Africa* 76: 19 pp.

Largier JL. 1987. Internal shelf tides and wind-driven motions in deepening the surface mixed layer. Ph.D. thesis, University of Cape Town, South Africa: 192 pp.

Largier JL, Swart VP. 1987. East-west variation in thermocline breakdown on the Agulhas Bank. *In* The Benguela and Comparable Ecosystems. Payne AIL, Gulland JA, Brink KH (eds). *South African Journal of Marine Science* 5: 263–272.

Lee Gordon R. 1996. *Principals of Operation for Acoustic Doppler Current Profilers*. 2nd ed., San Diego, California; RD Instruments: 54 pp.

Probyn TA, Mitchell-Innes BA, Brown PC, Hutchings L, Carter RA. 1994. A review of primary production and related processes on the Agulhas Bank. *South African Journal of Science* 90(3): 166–173.

Schumann EH. 1983. Long-period coastal trapped waves off the southeast coast of southern Africa. *Continental Shelf Research* 2: 97–107.

Schumann EH. 1999. Wind-driven mixed layer and coastal upwelling processes off the south coast of South Africa. *Journal of Marine Research* 57: 671–691.

Schumann EH, Beekman LJ. 1984. Ocean temperature structures on the Agulhas Bank. *Transactions of the Royal Society of South Africa* 45(2): 191–203.

Schumann EH, Brink KH. 1990. Coastal-trapped waves off the coast of South Africa: generation, propagation and current structures. *Journal of Physical Oceanography* 20: 1206–1218.

Schumann EH, Perrins L-A. 1982. Tidal and inertial currents around South Africa. In *Proceedings of the Eighteenth International Conference on Coastal Engineering, Cape Town, November 1982.* New York; American Society of Civil Engineers: 2562–2580.

Shelton PA, Kriel F. 1980. Surface drift and the distribution of pelagic-fish eggs and larvae off the south-east coast of South Africa, November and December 1976. *Fisheries Bulletin, South Africa* 13: 107–109.

Swart VP, Largier JL. 1987. Thermal structure of Agulhas Bank water. *South African Journal of Marine Science* 5: 243–253.

Tilney RL, Nelson G, Radloff SE, Buxton CD. 1996. Ichthyoplankton distribution and dispersal in the Tsitsikamma National Park marine reserve, South Africa. *South African Journal of Marine Science* 17: 1–14.

Vidal E, Martins, R, Roberts M. 2005. Yolk utilization, metabolism and growth in reared *Loligo vulgaris reynaudii* paralarvae. *Aquatic Living Resources* 18: 385–393.

Welsh JG. 1964. Measurements of currents on the Agulhas Bank with an Ekman current meter. *Deep-Sea Research* 11(1): 43–52.

Yang WT, Hixon RF, Turk PE, Krejci ME, Hullet WH, Hanlon RT. 1986. Growth, behavior, and sexual reproduction of the market squid, *Loligo opalescens*, cultured through the life cycle. *Fishery Bulletin* 84: 771–798.

CHAPTER 4

Re-examination of the dependence of chokka squid paralarvae on the cold ridge and the role of currents

Annual variability in chokka squid biomass and catches may be linked to recruitment success. For the oceanic *Illex* species, recruitment variability has been shown to be strongly related to changes in Western Boundary Currents (WBCs) as these play a major role in their life cycle. This chapter examines the role of currents in the early life cycle of chokka squid and the dependency of paralarvae on the cold ridge. A synthesis of currents on the Agulhas Bank is undertaken within the context of paralarvae food distribution and availability. Flow patterns are shown to be less defined and more complex than WBCs. Copepods are widely available for the paralarvae on the shelf, which suggests that starvation is not a limiting factor in chokka squid recruitment success. Although currents can play a positive role in the early life history of the chokka squid, currents also appear to at times present a threat to the survival of paralarvae by removal from the shelf ecosystem.

Keywords: chokka squid, paralarvae, food abundance, cold ridge, ocean currents

Introduction

Recruitment variability in oceanic squids such as the Ommastrephid species has been shown to be closely linked to changes in Western Boundary Currents (WBCs) (Dawe *et al.* 2000). As indicated in Chapter 1, these large scale, well defined currents play a major role in the early life cycle of these squid (Hatanaka *et al.* 1985; Coelho 1985; O'Dor 1992; O'Dor and Coelho 1993). Egg masses and paralarvae of *Illex illecebrosus* and *Todarodes pacificus,* two of the best studied species, are transported in the Gulf Stream and Kuroshio Current respectively, from the spawning grounds upstream to the feeding grounds down stream. Much of the food for the paralarvae is generated along the frontal zone by the physical interaction of the WBC with the shelf waters (Bakun and Csirke 1998). With such strong dependence, anomalies in these WBCs have the potential to impact squid recruitment (Trites 1983; O'Dor *et al.* 1997; Dawe *et al.* 2000).

In contrast, the life cycle of the loliginid squids is superimposed on shelf dynamics where currents are usually slower, complex, and not always well defined like WBCs. Primary production is not only driven by physical processes related to the dynamics of currents, but is more reliant on others such as wind-driven coastal upwelling. Very different early life history strategies for loliginid squid have consequently evolved, which tend to be localised and include multiple mating over large fixed benthic egg beds.

In South Africa the squid fishery targets the species *Loligo reynaudii,* found on the Agulhas Bank to depths of 200 m (Figure 4.1). The Agulhas Bank is the most extensive shelf region on the African continent. Locally it is known as chokka squid. The fishery experiences erratic fluctuations in catch on both a monthly and an annual basis. Monthly

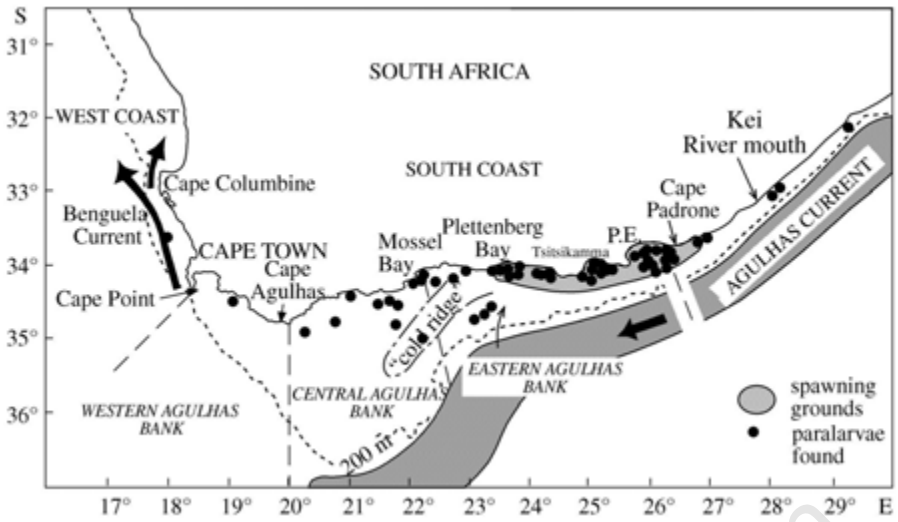

Figure 4.1:. Adult chokka squid (*Loligo reynaudii*) are found on both the west and south coasts of South Africa. They spawn mainly inshore between Plettenberg Bay and Algoa Bay. Paralarvae have been found near Cape Point in the west and East London (29°E) in the east, with the majority found in the vicinity of the main spawning grounds.

variability is thought to be strongly linked to changes in spawning behaviour on the inshore spawning grounds in response to short-term oceanographic conditions (Roberts, Unpublished). Catch variability on an annual basis is thought to be influenced by recruitment strength, which as shown in Chapter 2, is linked to changes in the Agulhas Bank ecosystem and includes currents.

The aim of this chapter is to further examine the role of currents in the early life history strategy of chokka squid and, in a similar manner to that accomplished for some of the oceanic squids, to find potential links that may explain recruitment strength and ultimately annual catch variability. This is done within the context of food (copepods) production and distribution on the Agulhas Bank as paralarvae starvation is an important factor that can greatly impact recruitment strength. Currents can play an important role in transporting paralarvae to places of high food abundance (Chapter 2), but the converse may also hold (Chapter 3). The review of food sources also serves to highlight differences between the WBC and Agulhas Bank systems.

Egg and paralarvae distribution

Adult chokka squid migrate from the west and south coast shelf-region of southern Africa to the eastern Agulhas Bank to spawn. Most of the spawning occurs between Algoa Bay and Plettenberg Bay (Figure 4.1). Here they form large aggregations of mature male and female squid. Eggs are attached to the seabed to form large beds (Roberts 1998). The depth of spawning ranges between 10-120 m (Sauer *et al.* 1993; Augustyn *et al.* 1994). From an environmental point of view, the spawning grounds have been divided into shallow (<60 m) and deep (>60 m) regions due to the distinct vertical structure of the water column here, and consequently, different benthic conditions. Water temperatures shallower than 60 m are highly variable and range between 9-24°C (Roberts and Downey, Unpublished). Temperatures at greater depths are more stable and range between 9-13°C. Laboratory trials have shown the hatching rate to be temperature dependent, varying between 21 and 87 d (Oosthuizen *et al.* 2002).

Data on paralarvae are scarce. The little available (Figure 4.1) depicts most paralarvae to be found in the vicinity of the main spawning grounds, both on the inshore and deeper regions (Augustyn *et al.* 1994). Few appear to be found north of Cape Point or east of Algoa Bay. Some were found on the outer shelf of the eastern Agulhas Bank.

Food (copepod) distribution and abundance

Copepods are believed to form an important component of the chokka squid paralarvae diet (Venter *et al.*, 1999), as is the case with many other squids, e.g., *Loligo opalescens* (Hanlon *et al.* 1979; Chen *et al.* 1996), *Loligo vulgaris* (Turk *et al.* 1986) and *Loligo pealei* (Hanlon *et al.* 1987). The distribution and abundance of copepods relative to that of paralarvae would presumably then be an important factor influencing paralarval survival and hence recruitment. As shown in Chapter 2, if spatial separation exists, currents may play a vital role in connecting

food and paralarvae. To gain further insight into this possibility, a more detailed examination of food production on the Agulhas Bank is undertaken.

Upwelling

The Benguela region on the west coast of southern Africa is regarded as one of the largest upwelling systems in the world, and accordingly, is highly productive (Parrish *et al.* 1983). By comparison, upwelling on the south coast is considerably more modest, as well as intermittent. Most of the upwelling here occurs on the eastern Agulhas Bank adjacent to prominent coastal capes (Figure 4.1), the Tsitsikamma coast, and on the narrow shelf between Cape Padrone (26°E) and the Kei River mouth (28°E). Coastal upwelling west of Cape Padrone is wind driven and mainly occurs during the summer months (Schumann *et al*. 1982). Upwelling east of Cape Padrone does not exhibit a seasonal trend, and appears to be linked to the hydrodynamics associated with the divergence of the Agulhas Current from the coast (Lutjeharms *et al.* 2000). Several times each year, AVHRR satellite imagery shows cold surface water originating from this divergence zone, which extends over much of the eastern Agulhas Bank. Minor sporadic upwelling is also found along the inshore boundary of the Agulhas Current as a result of boundary phenomena (Lutjeharms *et al.* 1989). During summer, a quasi-permanent submerged cold ridge is found near Mossel Bay (Figure 4.1) (Largier and Swart 1987; Chapter 2). This feature is the result of local doming of the shelf thermocline which brings deeper nutrient-rich water into the photic zone. The cause of this doming is unknown, but Chapter 2 has shown it to be linked to coastal upwelling.

Phytoplankton Biomass

SeaWIFS satellite images (Figure 4.2a-d) show elevated levels of chlorophyll in the vicinity of the upwelling cells on the eastern Agulhas Bank and cold ridge. High temporal variability of chlorophyll levels exists between cells as a result of differing physical upwelling mechanisms. Overall, however, the coastal region appears to be the most important contributor to primary production, as indicated in the composite image (Figure 4.2e) produced using 8 yrs of CZCS satellite data. It is perhaps noteworthy that this significant zone coincides with the spawning grounds of chokka squid. The composite image is also useful for regional comparison purposes, and clearly shows primary production on the Agulhas Bank to be less extensive and intensive as that found on the west coast.

A limitation of ocean colour satellite imagery, however, is that upwelled ocean irradiance measured by satellite sensors, only indicates chlorophyll levels in the upper layers of the water column, depending on conditions (1-20 m). This can give an incorrect impression of primary production, as may be the case on the Agulhas Bank. Figure 4.3a shows that a subsurface chlorophyll maximum, found between 10-20 m, is commonly observed in this

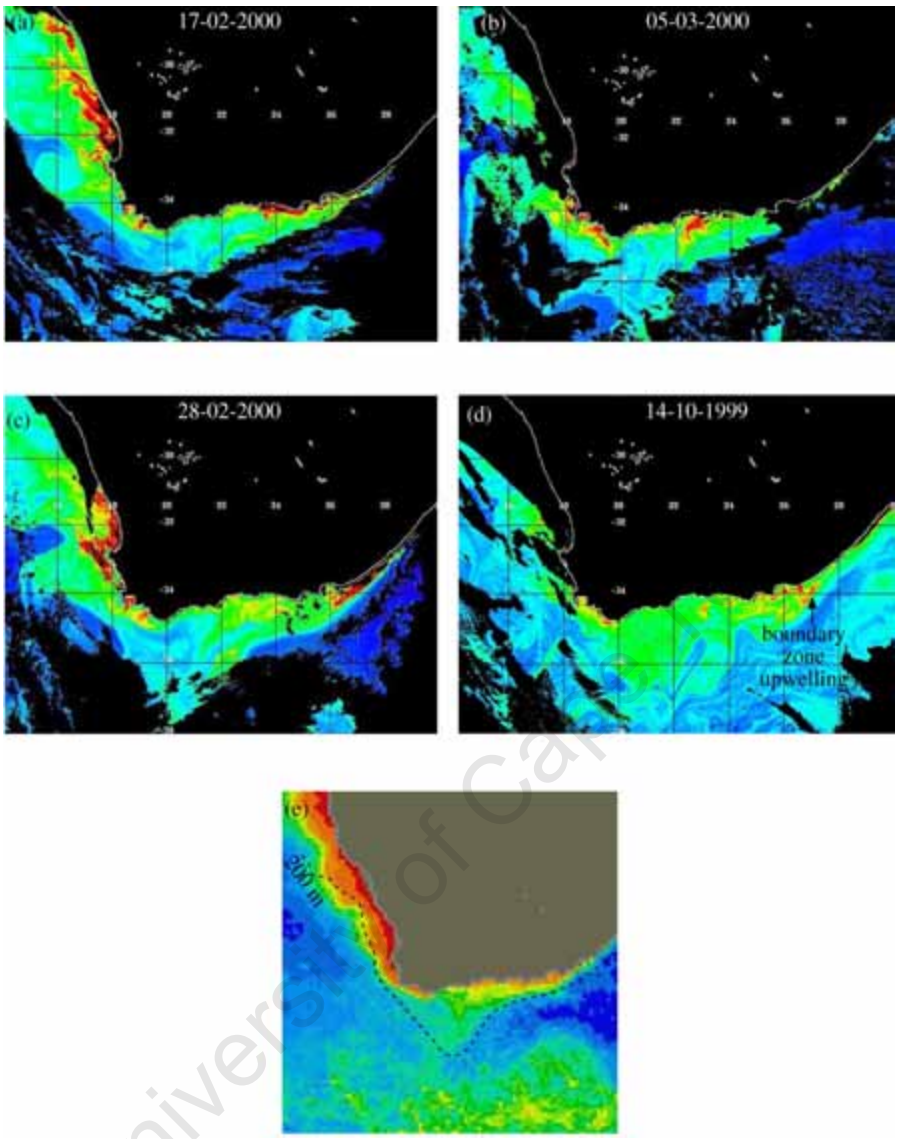

Figure 4.2: SeaWIFS satellite imagery (not calibrated) shows surface chlorophyll levels to be highest (red and yellow) in upwelling zones: (a) Tsitsikamma coast, (b) cold ridge, (c) divergence zone of the Agulhas Current, (d) a combination of these, including the Agulhas Current boundary zone. (e) An 8 year composite of CZCS satellite data. High chlorophyll levels indicate primary production to be most prominent adjacent to the coast.

region. The formation and persistence of this maximum is primarily the manifestation of light- and nutrient-limited growth, accumulation at the density interface, and stability effects (Cullen 1982). It is particularly prominent on the outer shelf of the eastern Agulhas Bank, cold ridge and inshore regions (Figure 4.3b).

To determine the most productive zones on the Agulhas Bank, it is clear that the subsurface chlorophyll maxima must be taken into account. Ideally, chlorophyll concentrations need to be integrated over the water column and spatially presented, however, work of this nature has only recently begun on the west coast (e.g., Longhurst *et al.* 1995; Mitchell-Innes *et al.* 2001) and has yet to be extended onto the south coast. Meanwhile, the only information available that takes subsurface levels into account is that published by Brown (1992). In this, mean *in situ* measurements of chlorophyll, collected over the upper 30 m of the water column, between 1971-1989, show most of the central and eastern Agulhas Bank to range between 1-2 mg m^{-1}. The highest mean chlorophyll concentrations ranged between 2-3 mg m^{-3}, found in two small areas off the Tsitsikamma coast and Mossel Bay, respectively. Low mean concentrations of <1 mg m^{-3} were found east of Cape Padrone, beyond the shelf edge (>200 m), and on the outer western Agulhas Bank. By comparison, the lowest mean chlorophyll concentration on the west coast was 3 mg m^{-1}, with values exceeding 4 mg m^{-3} for 50% of the region. Brown's (1992) mean chlorophyll values suggest that the chlorophyll levels generated by the subsurface maxima match those generated by the coastal upwelling cells, and that both mechanisms are equally important in terms of primary production on the central and eastern Agulhas Bank. Moreover, together they provide a good horizontal distribution of chlorophyll in the region.

Zooplankton Biomass

There are two species of large copepods found on the shelf of southern African that are important food items for pelagic fish - C*alanoides carinatus* and *Calanus agulhensis.* Copepods are also believed to form an important dietary component of the chokka squid paralarvae (Augustyn *et al.* 1994; Venter *et al.* 1999). As depicted in the composite maps in Figure 4.4, *C. carinatus* (a) is the dominant species on the west coast but is also found to a lesser extent on the outer Agulhas Bank. *C. agulhensis* (b) is the dominant copepod on the Agulhas Bank, and to a much lesser extent, is found on the west coast, particularly in the offshore region (Huggett and Richardson 2000). The northern distribution of this species on the west coast is thought to be the result of advection from the Agulhas Bank. Statistically, the highest biomass of *C. agulhensis is* found on the central Agulhas Bank in the vicinity of the cold ridge, a feature believed to enhance local retention (Verheye *et al.* 1994; Chapter 2).

The distribution and abundance of *C. agulhensis* usually exhibits spatial and temporal variability, as is depicted in the November 1991 survey in Figure 4.5. In this case, the greatest abundance of *C. agulhensis* was found offshore, certainly on the eastern and western Agulhas Bank. There were few stations at which copepods were absent and those that did

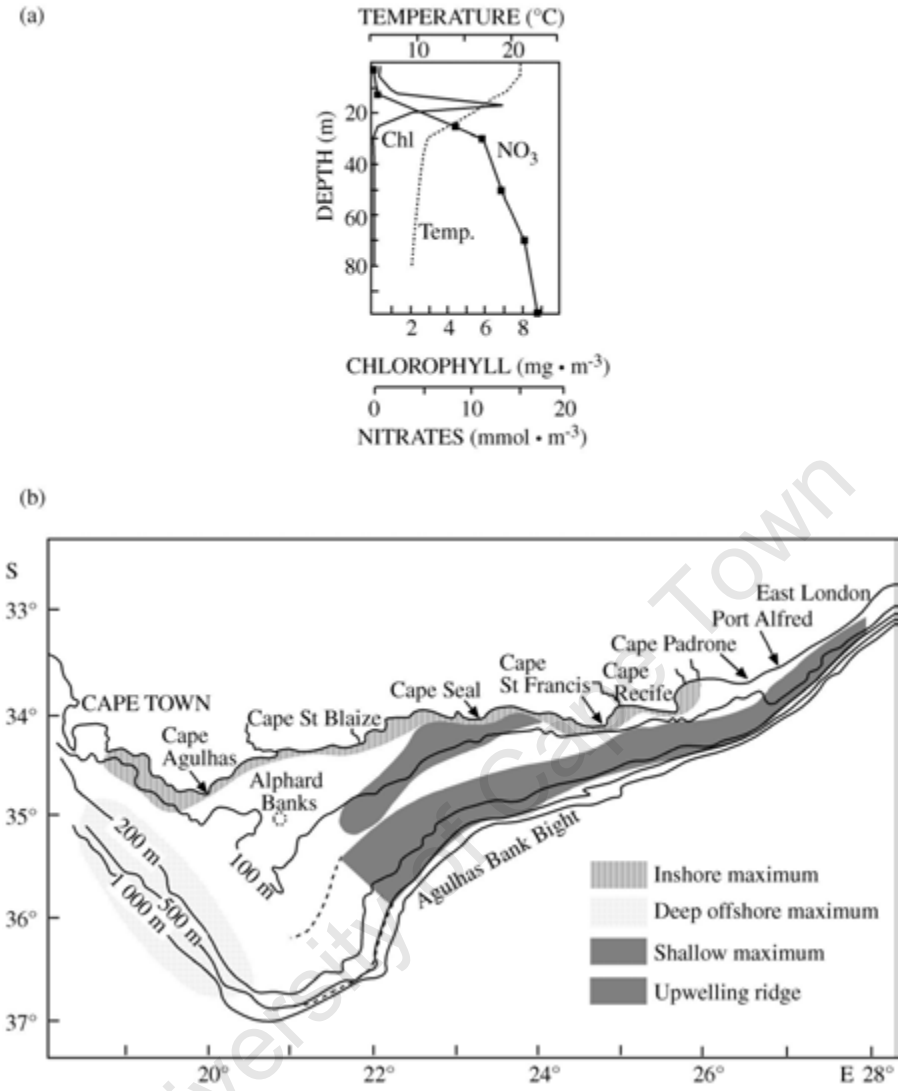

Figure 4.3: (a) A subsurface chlorophyll maxima exists on the Agulhas Bank which is particularly prominent on the (b) outer-shelf and cold ridge (after Probyn *et al.* 1994)

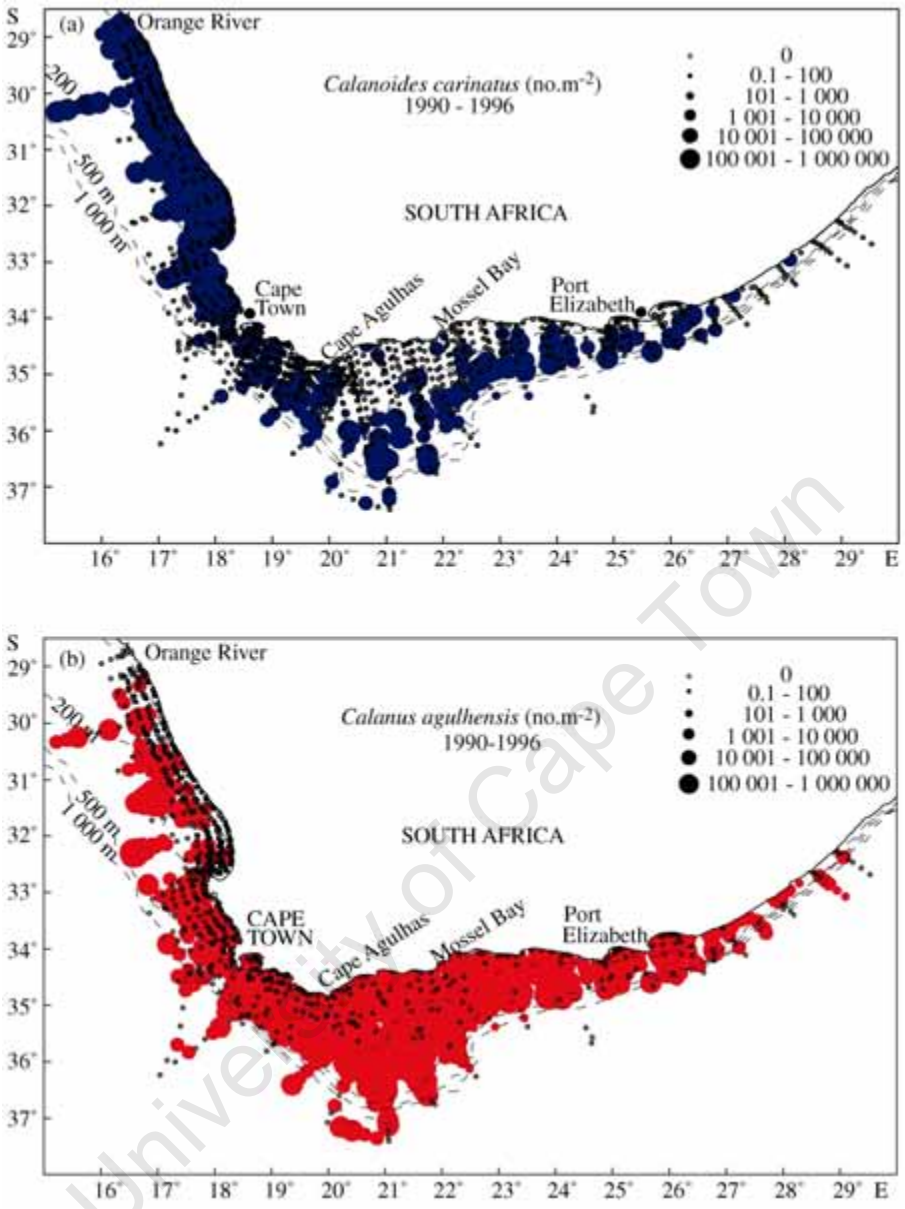

Figure 4.4: Distribution of two copepod species important for the diet of chokka squid paralarvae - *Calanoides carinatus* and *Calanus agulhensis,* shown in the composites maps (a) and (b) respectively. (after Huggett and Richardson 2000)

exist were in the vicinity of the cold ridge, which was poorly formed during this survey (Boyd and Shillington 1994; Chapter 2). No correlation analysis has yet been undertaken between horizontal distributions of phytoplankton abundance and copepod abundance, but a strong positive correlation has been demonstrated between the daily vertical migration of large copepod stages and food abundance in the chlorophyll rich layer (maxima). This behaviour coupled to the existence of an extensive, relatively shallow, subsurface maximum on much of the Agulhas Bank is probably the reason why copepods are able to flourish in regions other than the upwelling cells.

It is clear from this synthesis that food (copepods) for chokka squid paralarvae is generated and supported by several physical and primary production processes on the Agulhas Bank, of which currents *per se* only play a limited role, i.e., boundary phenomena along the Agulhas Current. This is unlike the *Illex illecebrosus* situation on the east coast of the USA and Canada where the dynamics of the Gulf Stream are the main driving force for food generation. In general, it has been shown that copepods are found in abundance over most of the Agulhas Bank, which implies that starvation is not a major factor influencing the recruitment success of chokka squid. However, copepod distributions are not homogeneous, and patches of low abundance do exist. It is therefore conceivable that paralarvae within such an area may starve if other food items cannot be found. In this case, it is questionable whether currents will make a difference to survival as the paralarvae will be advected within the low abundance patch, leaving either vertical migration (if this is possible) or hydrodynamic turbulence as the only mechanisms able to change this association.

Currents on the Agulhas Bank

We argue that if currents are not important in food generation for paralarvae, maintaining the association between food and paralarvae, or transporting paralarvae to rich food sources, then we need to ask what other role (or influence) could they have in the chokka squid life cycle? To begin addressing this, a review of the currents on the Agulhas Bank is first required.

Currents on the Agulhas Bank are more complex and less distinct than the peripheral ocean currents. Obtaining a clear understanding of the overall flow pattern has been made difficult by the scattered and limited number of current meter measurements undertaken since the mid 1980s (see Figure 4.6). The introduction of ship-borne ADCPs in 1990 greatly improved the spatial coverage and the number of current measurements, which soon after prompted a review by Boyd and Shillington (1994) and a regional (averaged) current vector map (Boyd and Oberholster 1994). These were instrumental in highlighting prominent large-scale spatial features in the near- surface flow in this region (Figure 4.6). However, as is shown later, the ADCP data lacks comprehensive temporal coverage, and can be misleading. To overcome this, a synthesis was undertaken which integrated all available data, including the ship-borne ADCP, current meter deployments, satellite imagery and the results of a

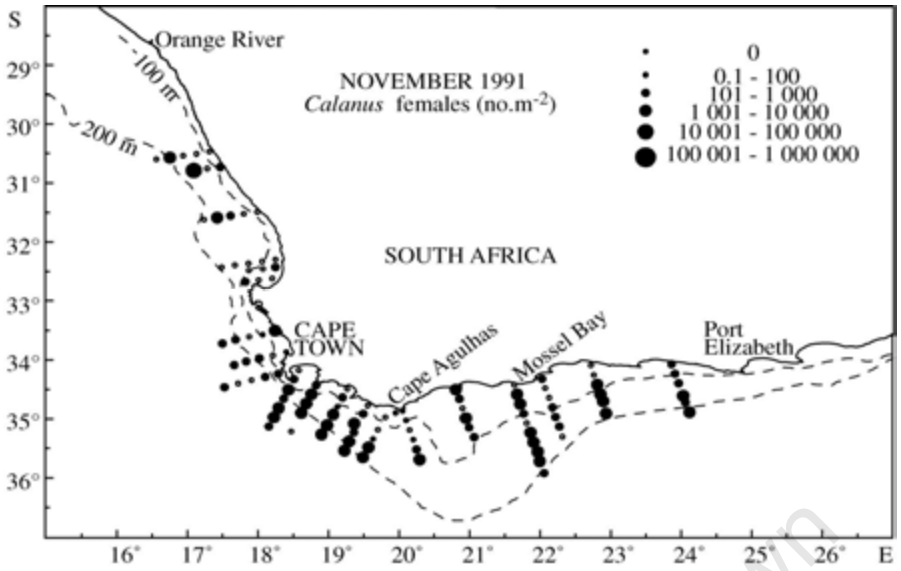

Figure 4.5: Although in general *Calanus agulhensis is* found over the entire Agulhas Bank, its abundance exhibits high spatial and temporal variability, as seen in this November 1991 survey (data from Huggett (2003)).

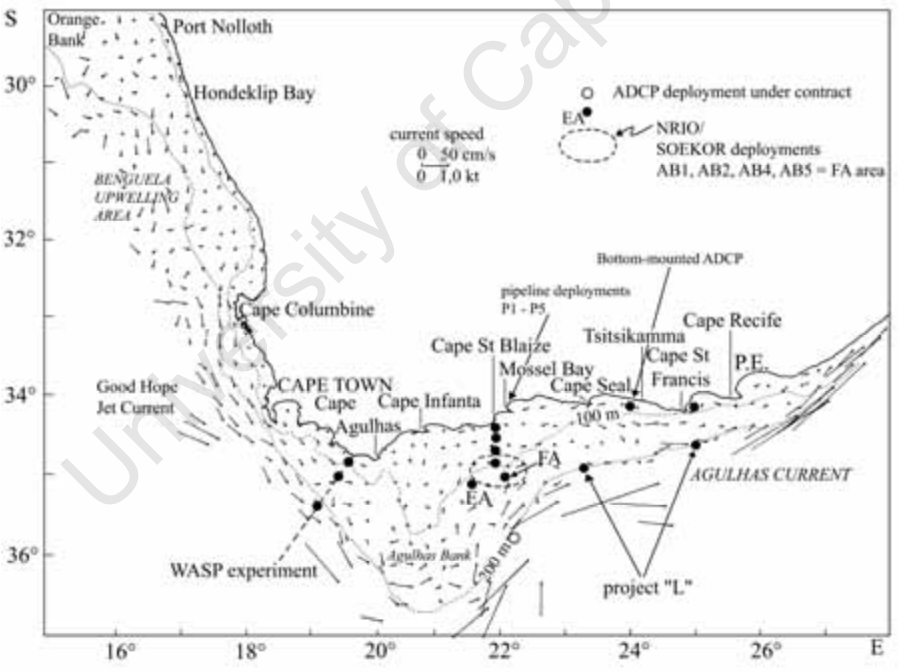

Figure 4.6: Current meter deployments undertaken on the Agulhas Bank since the 1980s, superimposed on averaged near-surface (depth 30 m) current vectors collected using ship-borne ADCPs (vector map after Boyd and Oberholster 1994)

recently applied hydrodynamic model. It was found that currents on the Agulhas Bank could be conveniently discussed under three sub-regions — the inshore, mid shelf and outer shelf.

Inshore Region

The averaged ship-borne ADCP data depicted in Figure 4.6 shows no dominant surface current pattern close to the coast between Cape Padrone and Plettenberg Bay (i.e., inshore spawning grounds) or on the inner central Agulhas Bank. Measurements between these two areas, however, indicate the presence of a low velocity (15-20 m s^{-1}) eastward coastal flow.

Current meter deployments on the inshore spawning grounds show otherwise. Data collected by a bottom-mounted ADCP, deployed for 12 months off the exposed Tsitsikamma coast at a depth of 36 m between July 1998 and June 1999 (Figure 4.6 for position), indicate that a distinct and dynamic inshore current exists at times along the Tsitsikamma coast (Chapter 3). Judging from average current vectors in Figure 4.6, it seems that the offshore extent of this flow is about 10-20 km. The flow in the surface layer (5 m) was found to oscillate longshore, lacking any seasonal trend, but overall was eastward (68%). The highest longshore surface velocity on record was 115 cm. s^{-1}, but on average was 23 cm s^{-1}. In contrast, the bottom flow did follow a seasonal trend. Temperature data showed that during winter, the water column was mainly isothermal and the bottom flow was in the same direction as the surface layer. Opposite flows in the surface and bottom layers, however, occurred between December and March when vertical stratification was most intense. A maximum bottom longshore velocity of 65 cm s^{-1} was measured with an average of 11 cm s^{-1}.

The potential influence of the current off the Tsitsikamma coast on larval transport is shown in Figure 4.7 using progressive vector plots. These emphasize the differences between the surface and bottom flows. For instance during winter (July and August) passive neutrally buoyant particles released simultaneously in both the surface and bottom layers from the ADCP site, would be displaced eastward and westward respectively. The final distance between the total displacements after 62 d was 340 km. Similarly, during summer (December, January and February), a passive particle released in the bottom layer would oscillate between eastward and westward displacement, but finally after 89 d, be only 45 km east of the origin. In contrast, displacement in the surface layer over this period was 705 km east of the release site. Net monthly displacement calculated for three depths (5, 23 and 31 m) for the period July 1998-June 1999 are presented in Figure 4.7c. It is clear that eastward advection dominated in the upper mixed layer over this period.

Near-surface (13 m) and bottom Anderaa (RCM7) current meters have also been deployed in St Francis Bay (Kromme Bay) between July 1991-March 1995 in a depth of 24 m amidst several well known squid spawning sites (Roberts *et al.* Unpublished). Surface data for the summer months November to March depicted in Figure 4.8a, showed a persistent southwest flow parallel with the bathymetry of the bay (see map). The average current velocity in this direction was 19 cm s^{-1} which is similar to that observed for the Tsitsikamma coast (23 cm s^{-1}). The surface flow during the winter months July to September (Figure 4.8c)

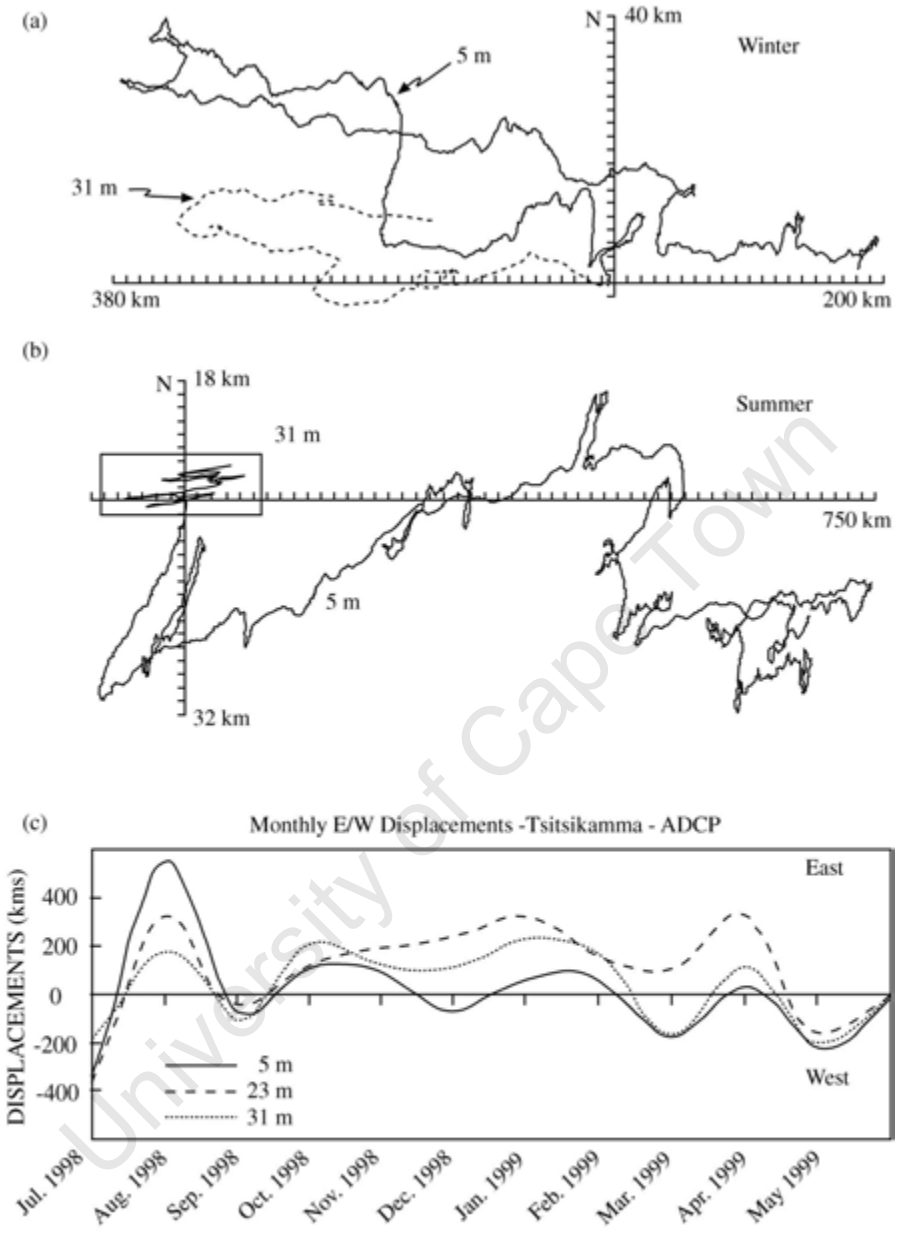

Figure 4.7: ADCP measured coastal currents on the chokka squid spawning grounds off the Tsitsikamma coast. (a) progressive vector plot showing the difference in transport rates for the surface (5 m) and bottom (31 m) layer during winter (July and August), (b) similarly for the summer months (December, January, February), (c) calculated monthly cast/west displacement for 5, 23, and 31 m. Note that this diagram is a composite from Figures 3.7a, b and Figure 3.10.

was also strongly westward but lacked a prominent southward component. These trends can not be matched against the Tsitsikamma data as the deployment times do not overlap. However, given the extent of the dominance, it would appear that the principle flows in the surface layer are in opposite directions between these two areas. This implies one of two circulation patterns: The first is that the Tsitsikamma flow does not extend as far east as Cape St. Francis. The other is that the common eastward coastal current along this coast spins up an anticyclonic eddy in Kromme Bay. During the winter months (Figure 4.8d) when stratification in the water column was weak (also seen in Tsitsikamma), the bottom flow was commonly observed to be in the same direction as the surface. Periods were noted when the bottom flow was in the opposite direction to the surface. Net bottom flow during the summer months (Figure 4.8b) was southeast out of Kromme Bay, possibly the result of hydrodynamic set-up in the sea level due to the dominant easterly winds. Therefore in all seasons, it is evident that squid paralarvae would be exported from Kromme Bay (St Francis Bay) to the mid-shelf.

Mid-shelf Region

The averaged ship-borne ADCP data in Figure 4.6 shows a general westward flow (15-30 cm s^{-1}) in the upper mixed layer over the mid eastern Agulhas Bank, which continues southwest onto the outer shelf of the central Agulhas Bank.

A number of Anderaa current meter (RCM4) deployments made in the vicinity of the FA gas production platform (see Figure 4.6) between 1978 and 1985 confirm this velocity (CSIR report, 1986). These data indicate that the surface (29 m) and bottom currents (94 m) here are strongly dominated throughout the year by a southwest to southerly flow. The greatest velocities observed were consistently in this direction with surface and bottom averages of 33 cm s^{-1} and 21 cm s^{-1}, respectively. Mean surface and bottom velocities in the three remaining directional quadrants ranged from 18-20 cm s^{-1} and 12-15 cm s^{-1}, respectively. A maximum surface velocity of 140 cm s^{-1} was observed indicating strong influence by the Agulhas Current at times, but velocities of this magnitude made up only a small fraction of the data. Surface velocities of about 80 cm s^{-1} were observed at a frequency of 0.6%. The maximum bottom velocity was about 80 cm s^{-1}. About 0.5% of the data comprised velocities above 55 cm s^{-1}. The northern most mooring (station AB5 not shown) however, lacked a dominant flow and demonstrated lower current velocities. This is consistent with the averaged ADCP data shown in Figure 4.6 and indicates that a different physical regime exists on the inshore region of the central Agulhas Bank. A later deployment of two bottom mounted ADCPs, one at the FA site, the other at the EA well site (see Figure 4.6) in July to December 1990, confirmed the Anderaa rotor data, but in addition, showed that the currents on the outer shelf are strongly barotropic (CSIR Report, 1993). That is the speed and direction throughout the water column is often very similar. In some instances, the bottom flow was observed to be stronger than the surface.

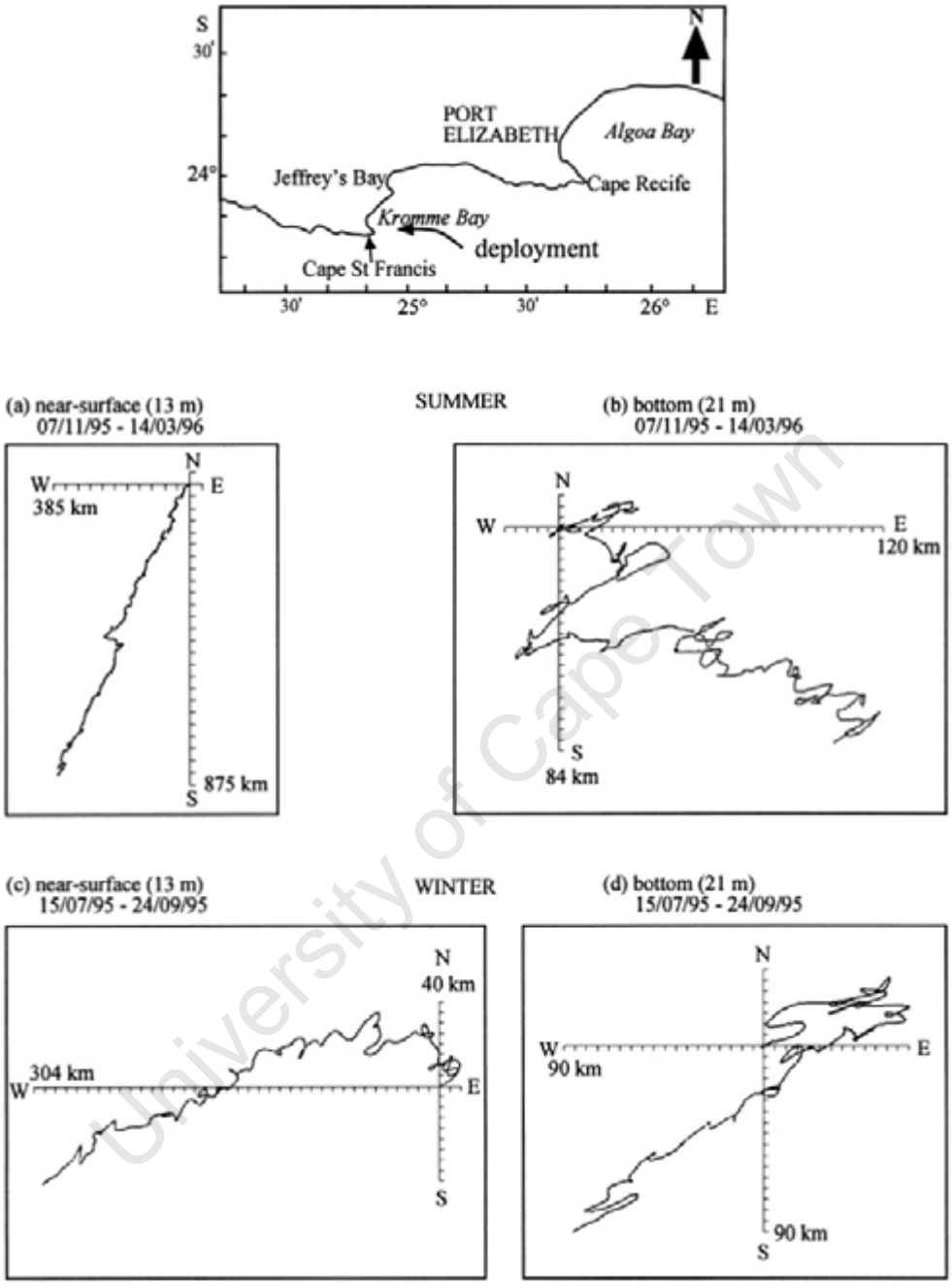

Figure 4.8: Rotor measured (RCM7) currents in Kromme Bay. Progressive vector plots for (a) surface (13 m) and (b) bottom (21 m) layers during the summer months (November-March). Similarly, plots (c) and (d) during winter (July-September). Note scales differ between plots.

The average ship-borne ADCP measurements show that the westward mid shelf current on the central Agulhas Bank continues over most of the western Agulhas Bank and feeds into the Benguela jet (50-100 cm s^{-1}). Current meter moorings deployed in depths of 75, 150 and 270 m on the western Agulhas Bank (see Figure 4.6 - WASP) between December 1986 and January 1987 (Largier *et al.* 1992), support the averaged ship-borne ADCP data. Mean current velocity vectors indicated westward flow at nearly all depths, with the exception of the mid shelf where the average current near the bottom was onshore. The data also indicated that the inshore region can at times be distinct from the mid and outershelf as a result of coastal upwelling. Currents near the coast can therefore be in an opposite direction to those offshore.

Shelf Edge Region

Surface currents on the outer shelf of the eastern Agulhas Bank (i.e., in the vicinity of the 200 m isobath) generally reflect localised, transient, current reversal in places as a result of Agulhas Current boundary phenomena such as large meanders, plumes, filaments and eddies (Lutjeharms *et al.* 1989). These current reversals are seen in the averaged ship-borne ADCP measurements (Figure 4.6) where mean velocities of 5-15 cm s^{-1} are denoted and adjacent vectors intermittently show eastward and westward flow. Actual velocity measurements here indicate reversal currents as large as 60 cm s^{-1} (see Boyd and Oberholster 1994).

The impact of boundary phenomena on the shelf waters can be considerable, as seen in the SST and ocean colour satellite images depicted in Figure 4.9. The SST image in Figure 4.9b shows an unusual situation where the Agulhas Current has abruptly turned southwards off Algoa Bay (Port Elizabeth), instead of turning at Cape Agulhas (20°E) or continuing along the shelf of the western Agulhas Bank. The matching ocean colour image depicted in Figure 4.9a indicates, that this meso-scale feature drew outer shelf surface water containing biological material, away from the shelf and transported this several hundred kilometers southwards. This material undoubtedly was lost from the Agulhas Bank ecosystem. In Figure 4.9d a large plume of Agulhas Current water (green) is seen sweeping over the Eastern Agulhas Bank, impinging on the inshore chokka squid spawning grounds. This feature entrained, isolated and removed from the Agulhas Bank upper layer shelf water containing biological material (Figure 4.9c).

Two current meters deployed between April and December 1996 along the 200 m contour of the eastern Agulhas Bank (Figure 4.6 - project 'L'), one 100 km south of Cape Seal, the other 60 km south of Cape St. Francis, revealed a strong current near the bottom moving eastwards and opposite to the Agulhas Current (Smook and Roberts 1999). This eastward flow was found to vary with a period of 6 d, approaching zero or reversing weakly at times. The peak current speed observed in the eastward direction was 54 cm s^{-1} for the Cape Seal mooring and 74 cm s^{-1} for that off Cape St. Francis. Nothing is yet known about the

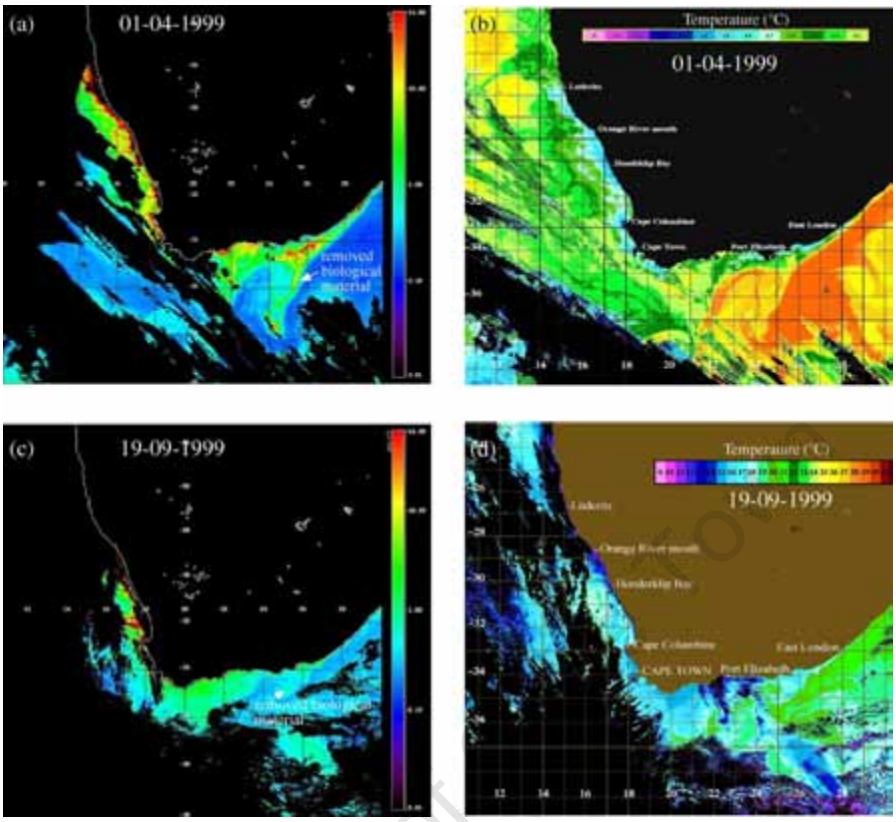

Figure 4.9: The impact of the Agulhas Current on shelf waters. (a) SeaWIFS imagery shows shelf water with biological material drawn south off the shelf by (b) the dynamics of an abrupt southwards turn in the Agulhas Current (NOAA AVHRR SST imagery). (c) Plankton laden surface water displaced by a filament of warm, oligotrophic Agulhas Current water (d) that sweeps onto the Eastern Agulhas Bank.

width, depth or eastward extent of this current. It is possible that this flow is an extension of the poleward undercurrent (Nelson 1989) found on the west coast shelf, but the current data collected off the western Agulhas Bank at 270 m (Largier *et al.* 1992) indicated a northwest flow at a similar depth, and suggests otherwise. Recently Beal and Bryen (1997) found an eastward bottom current on the continental slope off Port Alfred, which supports the data collected off Cape St. Francis and Cape Seal.

Ocean Modelling

The first work on currents in the Agulhas Bank region was based on ship's drift and drifter studies, e.g., Harris (1978), Shelton and Kriel (1980). As demonstrated in this synthesis, mooring data and ship-borne ADCP measurements have greatly expanded this knowledge base. Despite this progress however, a comprehensive knowledge of the current patterns on the Agulhas Bank is far from complete, especially for the purpose of understanding larval dispersion as intended in this paper. Limitations with the existing data set are: (1) neglected areas (e.g. Cape Padrone to Port Alfred, inner central Agulhas Bank, bottom layer on the eastern Agulhas Bank), (2) poor spatial and temporal resolution, and (3) the lack of synoptic integrity. These make it difficult to obtain an accurate, overall understanding of the circulation on the Agulhas Bank.

To overcome these limitations, a Regional Ocean Modelling System (ROMS) (Song and Haidvogel, 1994; Shcheptkin and McWilliams 2001) was recently adapted and applied to the west coast and the Agulhas Bank (Penven 2000). This is a numerical, hydrodynamic computer model which uses the basic equations of fluid motion in a rotating framework to calculate current, temperature, salinity and density fields. A pie-shaped spatial grid was used, which currently extends eastwards to 24°E on the Agulhas Bank (see Figure 4.10). Horizontal resolution ranges from 9 km adjacent to the coast to 16 km offshore. Vertical resolution ranges from 2 m at the surface to 100 m in deep water off the shelf (for more detail see Chapter 5).

Results from the first series of runs (Penven 2000) in the form of monthly averaged vectors, e.g., Figure 4.10, indicate many of the surface circulation features highlighted by the ship-borne ADCP measurements. For instance, the westward outer-shelf surface flow on the Agulhas Bank dominates year round. Surface currents on the inner central and coastal region on the eastern Agulhas Bank show low velocities and highly temporal trends. The Benguela jet exists between Cape Point and Cape Columbine and upwelling is observed on the west coast. More detail on model performance are given in Chapter 5. Not observed in the averaged ship-borne ADCP data, however, is the leakage into the south Atlantic of westward flowing outer-shelf surface water (see Figure 4.10). The simulated data confirms that the remainder of this flow is channelled into the Benguela jet, where after offshore flow also occurs northwest of Cape Columbine. Moreover, the coastal current on the eastern Agulhas Bank, i.e., between Mossel Bay and Algoa Bay, appears to be part of a meso-scale,

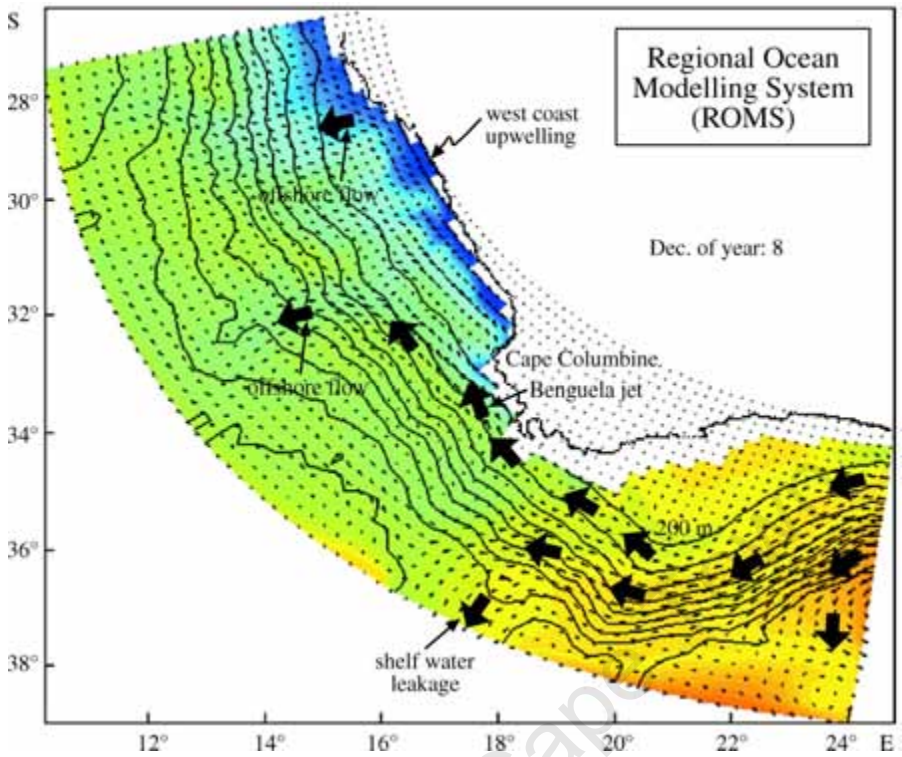

Figure 4.10: A Regional Ocean Modelling System (ROMS) (Song and Haidvogel 1994; Shcheptkin and McWilliams 2001) has recently been adapted and applied to the west coast and the Agulhas Bank (Penven 2000). Here monthly averaged surface velocity vectors are shown for December from the first series of runs.

quasi–permanent cyclonic gyre centred around a depressed sea surface height (not shown in Figure 4.10). This gyre is formed as a result of offshore flow into the Agulhas Current boundary zone near Algoa Bay and onshore flow from this zone south of Mossel Bay. The existence of this gyre conforms to the ADCP current meter data collected on the Tsitsikamma coast and suggests that the prominent southwest flow observed in the Kromme Bay data is caused by a small anticyclonic eddy in this bay.

What role do currents play in the early life cycle of chokka squid and recruitment?

Chapter 2 demonstrated that the main spawning grounds for chokka squid occupy an environmental niche on the south coast, which appears to favour embryonic development rather than hatchling survival. Moreover it was hypothesised (i.e. hypothesis 1) that currents play an important role in the early life cycle of chokka squid: Laboratory trials indicated that the inshore water temperatures on the south coast are optimal for embryonic development (Oosthuizen *et al.* 2002). However, spawning mainly occurs in the east between Plettenberg Bay and Algoa Bay. These authors suggested two reasons to explain low levels of spawning on the remainder of the south coast, i.e., west of Plettenberg Bay. The first was that low bottom dissolved oxygen levels develop on the inner central Agulhas Bank during the summer months, which squid (and possibly eggs) are not able to tolerate (Pörtner and Zeilinski 1998). Secondly, ship-borne ADCP data indicated that a westward flow was dominant on the eastern Agulhas Bank, and that squid might take advantage of this to transport and concentrate paralarvae toward the cold ridge where copepods were most abundant.

However, as detailed in this chapter, more biological and physical information is now available. Certainly, abundant food for paralarvae (copepods) is not limited to the cold ridge, but can be found in all regions of the Agulhas Bank, albeit with spatial and temporal variability. A better understanding of the currents on the Agulhas Bank now indicates that while a westward flow does occur on the inshore spawning grounds, this is not common and in fact an eastward coastal flow is more dominant. This calls for a revision, or perhaps expansion, of the hypothesized role of currents in the early life history of chokka squid.

Rather than westward advection, it is possible that passive, neutrally buoyant, biological material (i.e. paralarvae) will be transported eastward along the coast into the narrower shelf region near Algoa Bay. Here, according to the presently applied Regional Ocean Modelling System (ROMS), this material will then be advected offshore into the boundary shear zone of the Agulhas Current, and possibly be returned to the shelf in the quasi-permanent 'gyre'. In this scenario, food does not seem to be a limiting factor for survival since both *Calanus* and *Calanoides* appear to be potentially plentiful on the shelf edge. However, paralarvae in the boundary zone are at risk of being removed from the Agulhas Bank ecosystem through shelf water leakage.

The location of a few paralarvae on the east coast, however, suggests that some paralarvae transported eastwards from the main spawning grounds, may miss offshore advection near Algoa Bay, perhaps when the 'gyre' is weak, and end up on the narrow shelf east of Port Alfred where food abundance is very low. Here, paralarval starvation, or entrainment into the Agulhas Current and removal from the shelf ecosystem, may be real possibilities. Certainly the transport rates determined from the Tsitsikamma ADCP data indicate that at times such displacements would be accomplished in less than 26 d, a period that could be realistically relevant to the passive nature of chokka squid paralarvae. Paralarvae on the deep spawning grounds, whether in the upper mixed layer or the bottom layer, would appear to be transported in the mid shelf westward flow towards the central and western Agulhas Bank possibly by passing the outer periphery of the cold ridge centred on the 100 m contour. Potentially two fates can occur for the squid larvae. Either they continue up the west coast along with anchovy and pilchard eggs and larvae (Roel *et al.* 1994), or they are removed from the shelf ecosystem through offshore leakage on the outer western Agulhas Bank. Transport onto the highly productive west coast may not be as beneficial as it seems as the low temperatures, low dissolved oxygen levels, considerable offshore transport and high predation levels, could further reduce the chances of survival. A calculation based on the mean westward surface velocity of 30 cm s^{-1} (from RCM4 data near the FA platform) indicates that a passive, neutrally buoyant particle on the mid shelf would travel the distance between 25°E and 19°E in 26 d. At 50 cm s^{-1} this time is reduced to 16 d. In view of this, it is highly possible then that the paralarvae shown on the mid shelf south of Mossel Bay in Figure 4.1 will not be recruited. It is plausible that this scenario may account for recruitment variability in the fishery, since it is believed that at times unfavourable oceanographic conditions on the preferred inshore spawning grounds force spawning into deeper mid shelf waters (Augustyn *et al*. 1994). Amongst other factors, varying frequency of unfavourable inshore conditions would give rise to annual variability in recruitment success.

It is interesting that most paralarvae sampled (Figure 4.1) were found on the main spawning grounds despite the existence of a well-defined coastal current. Of course, these could be new hatchlings. However, the possibility also exists that, in view of the high potential loss in other regions, it is desirable for paralarvae to remain inshore and midway along the south coast. Apart from active horizontal swimming by paralarvae to counter currents (it is presumed this is only possible for hatchlings a few weeks old), the only means to avoid advection is to practice vertical migration. It is shown in Figure 4.8 that bottom currents are not only weaker than the surface, but can be at times opposite in direction especially during the summer months when spawning on the inshore spawning grounds is most intense. Paralarvae positioned here would be retained on the spawning grounds. As indicated elsewhere, unfortunately nothing is known about chokka squid paralarvae movement in the water column.

Conclusions

In the case of oceanic squids such as *Illex illecebrosus* and *Todarodes pacificus,* WBCs are an essential part of the early life history strategy. They connect, over thousands of kilometers, warm regions of the ocean (subtropical latitudes) which favour egg development, to colder parts in higher latitudes where productivity is high and feeding is best. Chokka squid do not appear to have evolved a mechanism to use the Agulhas Current in the same way that the ommastrephids use WBC.

By comparison, there appears to be both positive and negative roles for currents in the early life history of the neritic chokka squid. While it is possible for passive biological material to be transported from the warmer Agulhas Bank to the cold but highly productive west coast, it would appear that this mechanism is not useful to chokka squid paralarvae. Moreover, as copepod abundance appears to be more distributed on the Agulhas Bank, and flow patterns are complex, there is perhaps less need for currents to connect paralarvae to the rich food sources. This however, does not disqualify the WTH. As demonstrated in Chapter 2, Figures 4.2 and 4.3, the cold ridge remains a highly dominant source of enrichment on the Agulhas Bank, and the net westward mid shelf current will at times transport paralarvae to this region. It is therefore possible that chokka squid have evolved to cope with a disconnect between the preferred spawning grounds and (putative) optimal feeding ground. Nonetheless, the high potential for loss of paralarvae from the shelf ecosystem, suggests that currents may at times be a threat to the early life history strategy of chokka squid, and in this way, influence recruitment (i.e. hypothesis 2 — **currents may remove squid paralarvae from the Agulhas Bank ecosystem**). This may be particularly applicable when there is an increase in mid shelf (deep) spawning activity. To overcome advection into high risk areas, it is possible that paralarvae use vertical migration, particularly when currents in the surface layer are strong.

Future Research

To progress beyond the concepts presented in this chapter, research must now focus on two main areas: First, the nature of vertical migration of paralarvae squid must be examined as this may greatly influence the concepts presented here. Secondly, greater use of the ROMS must be made. The model needs to be fine tuned and its performance verified. This must be done using better flow pattern data, and hence multi-layered *in situ* current measurements are required, especially in the neglected areas of the eastern Agulhas Bank. ROMS can then be linked to Individual–Based Models (IBMs) and used to explore paralarval advection scenarios.

References

Augustyn CJ, Lipinski MR, Sauer WHH, Roberts MJ, Mitchell-Innes BA. 1994. Chokka squid on the Agulhas Bank: life history and ecology. *South African Journal of Science* 90: 143-154.

Bakun A, Csirke J. 1998. Environmental processes and recruitment variability. *In* Squid recruitment dynamics. Rodhouse PG, Dawe EG, O'Dor RK (eds). FAO Fisheries Technical Paper 376, Rome: 105-124.

Beal LM, Bryen HL. 1997. Observations of an Agulhas Undercurrent. *Deep-Sea Research* 44: 1715-1724.

Boyd AJ, Oberholster GPJ. 1994. Currents off the West and South Coasts of South Africa. *South African Shipping News and Fishing Industry Review*, Sept/Oct: 26-28.

Boyd AJ, Shillington FA. 1994. Physical forcing and circulation patterns on the Agulhas Bank. *South African Journal of Science* 90(3): 114–122.

Brown PC. 1992. Spatial and seasonal variation in chlorophyll distribution in the upper 30 in of the photic zone in the southern Benguela/Agulhas ecosystem. In *Benguela trophic functioning.* Payne AIL, Brink KH, KH Mann, Hilbourne R (eds). *South African Journal of Marine Science* 12: 515-525

Chen DS, van Dykhuizen G, Hodge J, Gilly WF. 1996. Ontogeny of copepod predation in juvenile squid (*Loligo opalescens*). *Biology Bulletin* 190: 69-81.

Coelho ML. 1985. Review of the influence of oceanographic factors on Cephalopod distribution and life cycles. *NAFO Scientific Council Studies* 9: 47-57.

CSIR report. 1986. Mossel Bay off-shore development project environmental data for design, vol. 3, current data. *CSIR Report* C/SEA 8643/3. December 1986. Stellenbosch, South Africa. 343 pp.

CSIR report. 1993. Agulhas Bank metocean data summary 1993 update of environmental design parameters: ocean current. *CSIR Report* EMAS-C 93044. November 1993. Stellenbosch, South Africa. 187 p.

Cullen JJ. 1982. The deep chlorophyll maximum: Comparing vertical profiles of chlorophyll *a. Canadian Journal of Fisheries and Aquatic Science* 39: 791-803.

Dawe EG, Colbourne EB Drinkwater KF. 2000. Environmental effects on recruitment of short-finned squid *(Illex illecebrosus). ICES Journal of Marine Science* 57(4): 1002-1013.

Hanlon RT, Hixon RF, Hulet WH, Yang WT. 1979. Rearing experiments on the California market squid. *Verliger* 21(4): 428-431.

Hanlon RT, Turk PE, Lee PG, Yank WT. 1987. Laboratory rearing of the squid *Loligo pealei* to the juvenile stage: growth comparisons with fishery data. *Fishery Bulletin* 85(l): 163-167.

Harris TFW. 1978. Review of coastal currents southern African waters. *South African National Scientific Programmes Report* 30. 103 p.

Hatanaka H, Kawahara S, Uozumi Y, Kasahara S. 1985. Comparison of life cycles of five ommastrephid squids fished by Japan. *Todarodes pacificus, Illex illecebrosus, Illex*

argentinus, Notodarus sloani sloani, Notodarus sloani gouldi. NAFO Scientific Council Studies 9: 59-68.

Huggett JA. 2003. Comparative ecology of the copepods *Calanoides carinatus* and *Calanus agulhensis* in the southern Benguela and Agulhas Bank ecosystem. Ph.D. thesis, University of Cape Town. [iii] + 296 pp.

Hugget JA. Richardson AJ. 2000. A review of the biology and ecology of *Calanus agulhensis* off South Africa. *ICES Journal of Marine Science* 57: 1834-1849.

Largier JL, Swart VP. 1987. East-west variation in thermocline breakdown on the Agulhas Bank. In *Benguela Comparable Ecosystems.* Payne AIL, Brink KH, KH Mann, Hilbourne R (eds). *South African Journal of Marine Science* 5: 263-272.

Largier JL, Chapman P, Peterson WT, Swart VP. 1992. The Western Agulhas Bank: circulation, stratification and ecology. In *Benguela trophic functioning*. Payne AIL, Brink KH, KH Mann, Hilbourne R (eds). *South African Journal of Marine Science* 12: 319-339.

Longhurst AR, Sathyendranath S, Platt T, Caverhill, CM. 1995. An estimate of global primary production in the ocean from satellite radiometer data. *Journal of Plankton Research* 17: 1245-1271.

Lutjeharms JRE, Catzel R, Valentine HR. 1989. Eddies and other boundary phenomena of the Agulhas Current. *Continental Shelf Research* 9(7): 597-616.

Lutjeharms JRE, Cooper J, Roberts MJ. 2000. Upwelling at the inshore edge of the Agulhas Current. *Continental Shelf Research* 20(2000): 737-761.

Mitchell-Innes BA, Silulwane NF, Lucas MI. 2001. Variability of chlorophyll profiles on the west coast of southern Africa in June/July 1999. *South African Journal of Science* 97: 246-250.

Nelson, G. 1989. Poleward motion in the Benguela Area. In *Poleward flows along eastern ocean boundaries*. Neshyba SJ, Mooers CNK, Smith RL, Barber RT (eds). Springer-Verlag, New York. 110-130.

O'Dor RK. 1992. Big squid in big currents. *South African Journal of Marine Science* 12: 225–235.

O'Dor RK, Coelho ML. 1993. Big squid, currents and big fisheries. In. *Recent advances in fisheries biology*. Okutani T, O'Dor RK, Kubodera T (eds). Tokai University Press, Tokyo: 385-396.

O'Dor RK, Rodhouse P, Dawe EG. 1997. Squid recruitment in the genus *Illex*. *In Developing and sustaining world fisheries resources*. Hancock DA, Smith DC, Grant A, Beumer JP (eds).CSIRO Publishing, Collingwood, Australia: 116-121.

Oosthuizen A, Roberts MJ, Sauer WHH. 2002. Temperature effects on embryonic development and hatching success of the squid *Loligo vulgaris reynaudii*. *Bulletin of Marine Science* 71(2): 619-632.

Parrish RH, Bakun A, Husby DM, Nelson CS. 1983. Comparative climatology of selected environmental processes in relation to eastern boundary current pelagic fish reproduction. In. *Proceedings of the Expert Consultation to Examine Changes in Abundance and*

Species Composition of Neritic Fish Resources. Sharp GD, Csirke J (eds). FAO Fisheries Report 291: 731-778.

Penven P. 2000. A numerical study of the Southern Benguela circulation with an application to fish recruitment. Ph.D. thesis, University de Bretagne Occidentale, Brest, France. 190 pp.

Pörtner H–O, Zeilinski S. 1998. Environmental constraints and the physiology of performance of squid. *South African Journal of Marine Science* 20: 207–221.

Roberts MJ. 1998. The influence of the environment on chokka squid *Loligo vulgaris reynaudii* spawning aggregations: steps towards a quantified model. *South African Journal of Marine Science* 20: 134–149.

Roberts MJ. Unpublished. Synthesis and formulation of a model to predict chokka squid jig catches.

Roberts MJ, Downey NJ. Unpublished. Influence of benthic turbidity and temperature on the spawning behaviour of chokka squid *(Loligo reynaudii).*

Roberts MJ, N. Engelbrecht and M. van den Berg. Unpublished. Currents in Kromme Bay (St. Francis Bay) and potential transport of squid paralarvae.

Roel BA, Hewitson J, Kerstan S, Hampton I. 1994. The role of the Agulhas Bank in the life cycle of pelagic fish. *South African Journal of Science* 90: 185-196.

Sauer WHH, McCarthy C, Smale MJ, Koorts AS. 1993. An investigation of the egg distribution of the chokka squid, *Loligo vulgaris reynaudii,* in Kromme Bay, South Africa. *Bulletin of Marine Science* 53(3): 1066-1077.

Schumann EH, Perrins L-A, Hunter IT. 1982. Upwelling along the south coast of the Cape Province, South Africa. *South African Journal of Science* 78(6): 23 8-242.

Shcheptkin AF, McWilliams JC. 2001. The regional ocean modelling system: A split-explicit, free-surface, topography- following coordinates ocean model. *UCLA* 31pp.

Shelton PA, Kriel F. 1980. Surface drift and the distribution of pelagic-fish eggs and larvae off the south-west coast of South Africa, November and December 1976. *Fishery Bulletin, South Africa* 13: 107-109.

Smook A, Roberts MJ. 1999. Eastern Agulhas Bank shelf edge upwelling (project 'L:). Marine and Coastal Management, Cape Town, Report. 78 pp.

Song Y, Haidvogel DB. 1994. A semi-implicit ocean circulation model using a generalized topography-following coordinate system. *Journal of Comparative Physiology* 115(1): 228-244.

Trites RW. 1983. Physical oceanographic features and processes relevant to *Illex illecebrosus* spawning in the western North Atlantic and subsequent larval distribution. *NAFO Scientific Council Studies* 6: 39-55.

Turk PE, Hanlon RT, Bradford LA, Yang WT. 1986. Aspects of feeding, growth and survival of the European squid *Loligo vulgaris* Lamarck (1799) reared through the early growth stages. *Vie et Milieu* 36(1): 9-13.

Venter JD, van Wyngaardt S, Verschoor JR, Lipinski MR, Verheye HM. 1999. Detection of zooplankton prey in squid paralarvae with immunoassay. *Journal of Immunoassay* 20(3): 127149.

Verheye HM, Hutchings L, Huggett JA, Carter RA, Peterson WT, Painting SJ. 1994. Community structure, distribution and trophic ecology of zooplankton on the Agulhas Bank with special reference to copepods. *South African Journal of Science*. 90: 154-165.

CHAPTER 5

First Lagrangian ROMS–IBM simulations indicate large losses of chokka squid (*Loligo reynaudii*) paralarvae from the Agulhas Bank

Present knowledge of ocean currents based on *in situ* observations and models suggests that passive biological material such as eggs and larvae can be advected offshore away from the Agulhas Bank and hence removed from the ecosystem on which their survival and recruitment depends. Such losses have been cited as the root cause of the sudden drop in annual squid catches experienced in 2001. In this study, a Lagrangian IBM (Individually-Based Model) coupled to a ROMS (Regional Ocean Model System) model was used to investigate this hypothesis. Three simulations were performed for 12 model months using neutrally buoyant particles released from the seabed every second day on the mid shelf of the eastern, central and western parts of the Agulhas Bank. Particles were given life spans of 40 days. Results demonstrated large particle losses from the eastern Agulhas Bank (76%) and the western Agulhas Bank (64%), with the latter perhaps having a seasonal trend. In contrast few particles were lost from the central Agulhas Bank (2%) making this, in terms of the model, the most suitable place on the Agulhas Bank for spawning. Visualization of the ROMS outputs revealed that leakage on the eastern Agulhas Bank was caused by a cyclonic eddy resident in the Agulhas Bight. Similarly leakage from the western Agulhas Bank was caused by deep water cyclonic eddies in the adjacent Atlantic Ocean.

Keywords: South Africa, chokka squid, *Loligo reynaudii*, IBM, ocean modelling, Agulhas Bank, paralarvae, recruitment

Introduction

The ecosystem of the Agulhas Bank is bound by the swift (2.0–2.5 m s^{-1}), warm Agulhas Current on the eastern flank (east of 20°E) and a mixed system of northward flowing (0.75–1.20 m s^{-1}) slope current, mesoscale Atlantic eddies and offshore flowing filaments (Boebel *et al.* 2003) on the western side (Figure 5.1). The slope current on the western Agulhas Bank (Largier *et al.* 1992) converges into the narrow Benguela coastal jet which flows past the Cape Peninsula towards the west coast (Shannon 1985). Both cold (Boebel *et al.* 2003) and warm (Olson and Evans 1986) core eddies are found adjacent to the western Agulhas Bank with the latter being Agulhas rings shed from the retroflexion of the Agulhas Current. Instability in the Agulhas Current results in boundary shelf edge phenomena such meanders in the trajectory, attendant plumes that sweep the shelf and cyclonic eddies along the shelf edge (Lutjeharms *et al.* 1989).

Chokka squid mainly spawn on the eastern Agulhas Bank both inshore (Figure 5.1b) and on the mid shelf region (Figure 5.1c) and seldom deeper than 130 m (Roberts *et al.* Unpublished). But spawning is not limited to the eastern Agulhas Bank and does extend onto the mid shelf region of the central Agulhas Bank. In some years the hand-jig fishing fleet is

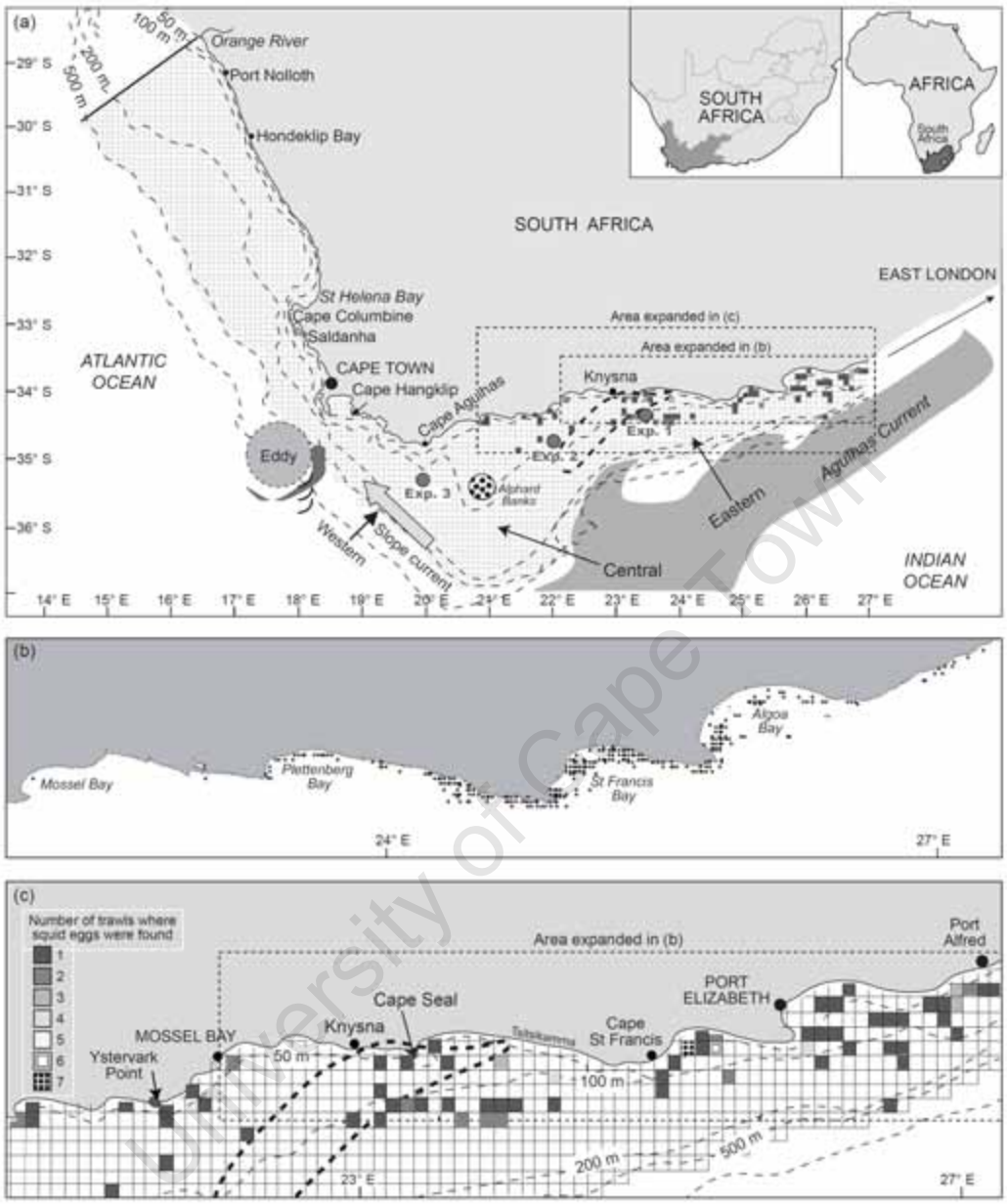

Figure 5.1: (a) Map of the west and south coasts of South Africa, showing the division of the Agulhas Bank into three regions; larger grey dots indicate release positions for particles in the IBM simulations (Experiments 1–3) and the bold dashed black line off Knysna represents the cold ridge. The Agulhas Bank is flanked on the eastern side by the swift Agulhas Current and by a mixed system of slope currents, eddies and filaments on the western side. Present knowledge of chokka squid spawning on the Agulhas Bank is based on (b) positions of commercial hand-line catches that target inshore (<60 m) spawning aggregations (small dots) and (c) trawl positions where eggs have been found (>60 m) (shaded squares).

known to catch spawning squid near the Alphard Banks (see Figure 5.1a). Chapter 2 proposed that shelf currents play an important role in connecting newly hatched squid paralarvae to high production commonly found in the vicinity of the cold ridge — a significant sub surface feature on the central Agulhas Bank where upward doming of the thermocline brings nutrients into the upper layer of the water column. A quantitative relationship was demonstrated between water temperature measured at the base of the cold ridge and subsequent year's squid biomass and catches indicating the importance of this feature in the life cycle of chokka squid and successful recruitment.

Chapter 4 indicated that currents may also potentially play an adverse role in the life cycle of chokka squid in that shelf water containing paralarvae can leak into the surrounding Indian and Atlantic Oceans and be removed from their ecosystem (hypothesis 2). A number of leakage areas and mechanisms were identified which include the Algoa Bay region where the shelf narrows and offshore flow into the Agulhas Current as measured by Goschen and Schumann (1988). Losses here may also be augmented with paralarvae from the inshore spawning grounds via transport in the eastward flowing Tsitsikamma coastal current which at times may reach Algoa Bay (Chapter 3). Entrainment and removal of shelf water is also possible by meander plumes in the shoreward edge of the Agulhas Current. These have been observed to sweep over the eastern Agulhas Bank (e.g. see Figures 10 and 11 in Lutjeharms *et al.* 1989) and Figure 4.9 in Chapter 4 and surely must have a displacement impact. In a similar vain cyclonic eddies located inside of passing Natal Pulses (e.g. Figure 4.25 in Lutjeharms 2006) also appear to be capable of removing water from the eastern Agulhas Bank. Satellite imagery indicates that Natal Pulses are found in the Agulhas Current about 20% of the time (Lutjeharms and Roberts 1988). A mechanism of great interest is the situation of an early retroflection in the Agulhas Current an example of which is highlighted by SST satellite images in Figure 5.2a. Early retroflection is commonly found after northward penetration and merging of the Agulhas Return Current with the Agulhas Current and the consequent shedding of a warm core ring (Lutjeharms and van Ballegooyen 1988). As seen in Figure 5.2b, early retroflection of the Agulhas Current seemingly causes substantial southerly leakage of shelf water laden with production from the eastern Agulhas Bank. The frequency of early retroflection is not known.

Chapter 4 also identified the potential for leakage of shelf water from the western Agulhas Bank through offshore mechanisms such as eddies and filaments. While spawning is not significant here, it was proposed that squid paralarvae can be transported to this region by westward mid shelf currents on the central and eastern Agulhas Bank. It was thus concluded that the removal of paralarvae from the Agulhas Bank via leakage of shelf water into the surrounding oceans may lead to recruitment failure and consequently poor annual catches such as experienced in 2001 with a near all time low of 3200 t.

The aim of this study therefore was to investigate the possibility of shelf water leakage and with it the removal of squid paralarvae from the Agulhas Bank ecosystem (i.e. test

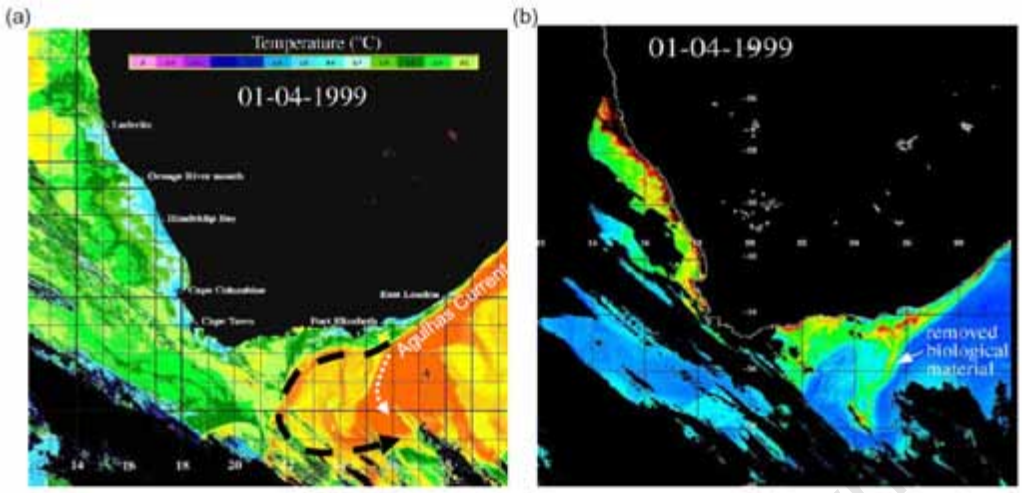

Figure 5.2: (a) SST imagery showing an early retroflection in the Agulhas Current. Early retroflection commonly occurs after northward penetration and merging of the Agulhas Return Current with the Agulhas Current and the consequent shedding of a warm core ring. The thick black dotted line highlights the normal trajectory of the retroflection. (b) Substantial southerly leakage of shelf water, laden with production, is observed on the eastern Agulhas Bank.

hypothesis 2). Two methods can be used for this purpose — drifter floats and computer models. This study used the latter.

Methods

The investigation used an Individually-Based Model (IBM) coupled to the output of a 3-D regional hydrodynamic model (ROMS).

Regional Hydrodynamic Model (ROMS)

Description

Penven (2000, 2001) adapted and applied a Regional Ocean Model System (ROMS) to the southern Benguela region of southern Africa. The numerical code for this 3-D hydrodynamic model was developed at Rutgers University and the University of California (Los Angeles) (Haidvogel *et al.* 2000). This had the advantage over other models at the time of offering an advanced tool for efficiently and robustly simulating the circulation at high resolutions in the coastal domain.

The model solves the free surface, primitive and hydrostatic equations for fluid dynamics over variable topography using stretched terrain-following coordinates in the vertical and orthogonal dimensions, with curvilinear coordinates in the horizontal dimension (Song and Haidvogel 1994). This allows enhanced resolution at the coast and is more accurate in dealing with the hydrodynamics of a coastal system. Active open boundaries connect the regional model with the open ocean. A pie-shaped grid that follows the south-western corner of the African continent from 40°S to 28°S and from 10°to 24°E was used. The topography was derived from the ETOPO2 dataset. Both a low (18 km at the coast) and a high-resolution (9 km at the coast) grid were configured (Figure 5.3). Twenty levels along the vertically stretched terrain-following coordinates provide enhanced resolution at the surface while preserving an adequate resolution in the deeper layers (Figure 5.3). The third order upstream-biased advection scheme implemented in ROMS allowed the generation of steep gradients, enhancing the effective resolution for a given grid size. The model was forced with winds, heat and salinity fluxes from COADS ocean surface monthly climatology (Da Silva *et al.* 1994). At the three lateral boundaries facing the open ocean, an implicit radiative boundary scheme forced by a seasonal climatology computed from the AGAPE basin-scale ocean model (Biastoch and Krauß 1999) connects the model to the surroundings. The set of open boundaries were completed by introducing a condition for the depth-integrated transport originally proposed by Flather (1976) for tidal models which proved to handle more robustly the highly energetic and meandering Agulhas Current that flows westward in the south east corner of the domain.

Summer values of the climatology were used for the initial conditions. The model started from rest and reached a statistical equilibrium after 1–2 model years. Details of the configuration implemented in the southern Benguela and an in-depth analysis of the spin-up

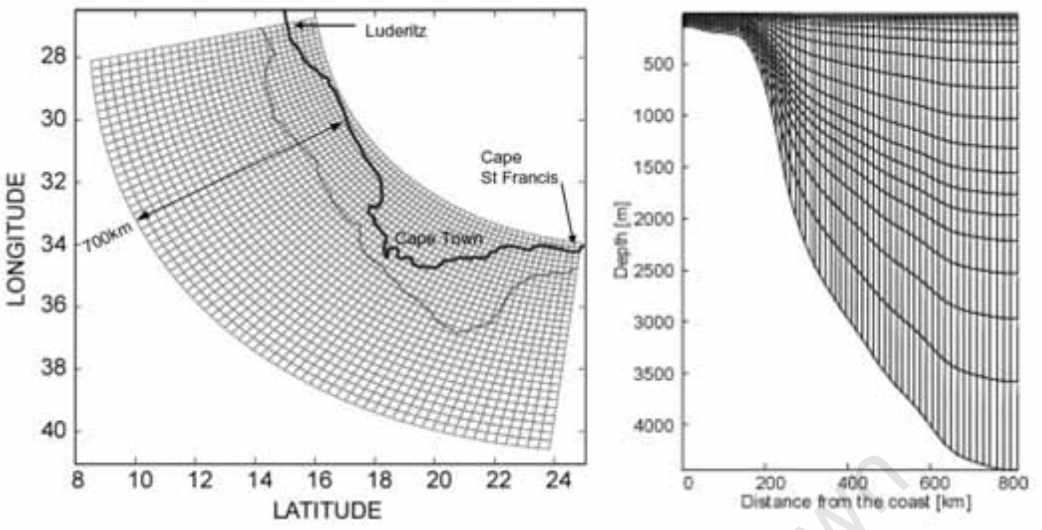

Figure 5.3: Spatial grid used in the regional configuration of ROMS in the southern Benguela — (a) orthogonal, curvilinear, coordinates in the horizontal (b) stretched, terrain-following coordinates in the vertical. This allows the model to solve free surface hydrostatic primitive equations of fluid dynamics over variable topography.

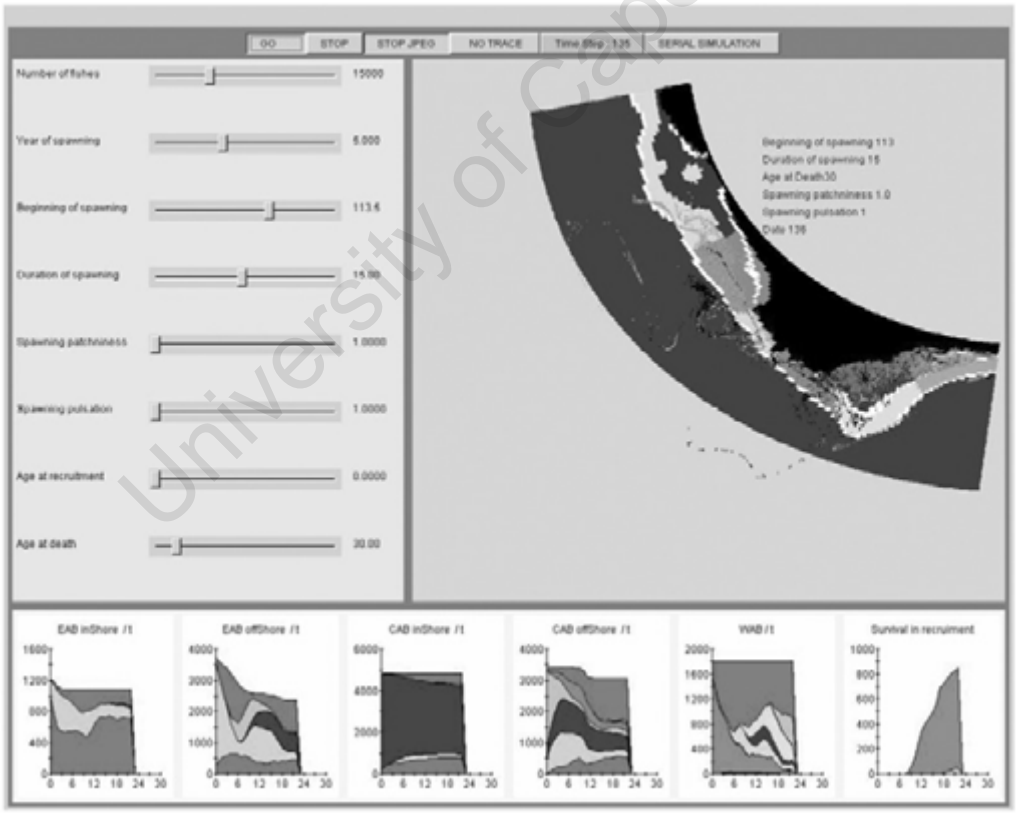

Figure 5.4: Screen of the simulator during a single trial showing on the left controllers of the variable coefficients of the model, on the right view of the domain of the model and the process at the individual level, on the bottom of the screen represent the output of the model at real time.

are given in Penven (2000). This configuration of the ROMS was referred to as "PLUME". Several simulations were then performed using the low and high resolution configurations. Only the latter was used in this experiment.

The high resolution horizontal grid with a spatial step varying from 9 km at the coast to 18 km offshore allowed a more realistic bathymetry compared to the low resolution configuration. This produced most of the mesoscale dynamics of the Benguela Upwelling system. Using the same forcing conditions as in the low resolution experiment, a 10 yr simulation was conducted. The data output were stored every two model days to provide inputs for biological models.

Model Validation

A review of the PLUME model outputs showed a high level of mesoscale activity during the 10-year simulation with the generation of Agulhas rings and the shedding of cyclonic eddies near the southern tip of the Agulhas Bank, the Cape Peninsula and Cape Columbine. On the west coast, the upwelling front showed variability which developed into meanders, plumes and filaments in a realistic manner to that observed in remote sensing (Agenbag and Anderson 1985). Reasonable agreement between simulated and observed circulation structures, both at the surface and at deeper levels was also observed, i.e. the Benguela Jet, bifurcation of flow off Cape Columbine and the poleward undercurrent (Shannon 1985). In the southern part of the model domain, a comparison with surface and subsurface data showed that the model reproduced cyclonic eddies in the lee of the Agulhas Bank in good agreement with observed features (Penven *et al.* 2001). Although the model is forced by a repeated climatology (i.e. no inter-annual variability in the forcing fields) there were pronounced differences in the simulated outputs between individual years. For example the thermal structure and the current fields of model year 4 are significantly different from those of year 3 for the same time of the year. Intrinsic mesoscale activity is the main contribution to this inter-annual variability (Penven 2000), and results from oceanic instability processes in the absence of added forced variability by synoptic and inter-annual atmospheric fluctuations. This is in agreement with previous studies of the dynamics of the California Current upwelling ecosystem (Marchesiello *et al.* 2003).

Penven *et al*. (2001), however, cautioned when coupling the PLUME model to biological models in that the response of the thermal structure and current fields to inter-annual atmospheric fluctuations had not been resolved in the simulations i.e. inter-annual variability in the model outputs vs. atmospheric forcing such as a relaxed or intensified south-easterly wind or remote oceanic forcing such as Rossby or Kelvin waves generated outside of the model. They noted that the main discrepancy between the model outputs and observed data occurs on the west coast during summer when simulated SSTs are lower than those observed from satellites.

Also the use of data from a monthly atmospheric climatology has smoothed out the high-frequency variability in the wind i.e. daily to weekly. This results in persistent upwelling-

favourable wind during the entire summer season in the model. In reality the pulsing pattern of the summer south-easterly wind in this region results in concomitant alternating reduced–enhanced upwelling off the west coast. Such variations in wind forcing will cause warming closer to the shore and probably reversals in the along shore currents (McCreary *et al*., 1987).

Summer wind-driven upwelling on the south coast is less extensive compared to the west coast and occurs off prominent capes (Schumann *et al.* 1982). It is most intense along the Knysna–Tsitsikamma coast where deep bathymetry is closest to the coast, and similarly varies on time scales of days (Schumann 1999). Chapter 2 has strongly advocated that the cold ridge, an important physical feature promoting biological production in the region, is a consequence of enhanced coastal upwelling in this area. The effect in the model of monthly wind climatology on coastal upwelling along the south coast has not been investigated, but there is presently a study examining the drivers of the cold ridge using a child model embedded in a new regional model called SAfE (Chang 2009).

Individually-Based Model (IBM)

The IBM tool used in this study was developed by the second author (C. Mullon) using Java language and run on a J-Builder platform professional 3.0 (Borland, 1999). The model uses the output time-series fields of current velocity, temperature and salinity archived from oceanic simulations by ROMS — in this case PLUME. Interfaces allowed visual analysis of the performance of the IBM by means of on-screen animations with a synthetic view of the whole modelling procedure i.e. the processes, hypotheses, control parameters, animations and the real simulation results (Figure 5.4). Control parameters included the number of particles (fishes), ROMS model year (year of spawning), day of release (beginning of spawning), duration of particle release (duration of spawning), patchiness of particle release (spawning patchiness), pulsation of released particles (spawning pulsation), age at recruitment and age at death. These use sub-model routines. The IBM has been applied to two other ecological studies in the southern Benguela — anchovy (Parada *et al.* 2003) and sardine (Miller *et al*. 2006). A more improved version of this IBM called *Ichthyop* has recently been released by Lett *et al.* 2008).

A review of the literature indicated very little is known about squid paralarvae — particularly regarding their density, buoyancy, early swimming capabilities, how long they can last without food, and feeding. Clearly, with such knowledge missing it is difficult to accurately portray paralarvae in the IBM. Hence as a first step, the IBM was set up as a Lagrangian tool with the main focus on investigating the potential for loss of squid paralarvae from the Agulhas Bank system rather than recruitment.

The IBM was run for a period of 12 months using year 3 from the PLUME archived output data. Year 3 was considered the first year where the ROMS was in a state of equilibrium. Three simulations (referred to as experiments) were performed, each releasing 5000 particles every second day (time step in the model) from one of the locations depicted in Figure 5.1 — position 1 on the eastern Agulhas Bank at 34.3°S; 23.5°E, position 2 on the

central Agulhas Bank at 22°S, 34.5°E, and position 3 on the western Agulhas Bank at 35°S; 20°E. All particles were released in the bottom level of the model which equated to a depth of 70–100 m. Position 1 is important because it represents advection on the main mid shelf spawning ground immediately east of the cold ridge. Its position also takes cognisance of the proximity of the model's eastern boundary at 23°E (St Francis Bay). Position 2 represents deep spawning off Mossel Bay and is fartherest from the shelf edge and potentially has the best retention. Position 3 is designed to test the retentive characteristics of the western Agulhas Bank. Spawning and hand-line catches are known to occur on the inner central Bank. Positions closer to the coast representing the shallow (<60 m) spawning grounds should also be investigated but boundary artefacts were a concern as was the model resolution.

Particles were assigned a life span of 40 days and neutral density. In each simulation, all "alive" particles were plotted for each time step according to position and depth in the model domain. Sequential time step outputs (a total of 180) were then made into animations to produce particle trajectories. Particles in the graphics were colour coded according their depth in the model (see Figures 5.5, 5.6 and 5.7) and ranged in the colour palette from dark blue for the deepest level to red in the surface layer. For each simulation the number of particles that crossed the 200 m depth contour was recorded. These were considered lost from the Agulhas Bank ecosystem.

Results

Selected model time steps that characterise the 180 time-step simulations for all three release sites (blue boxes) are shown in Figures 5.5, 5.6 and 5.7. The relevant area in the model domain has been enlarged for clarity (inserts).

Experiment 1 (eastern Agulhas Bank)

In this simulation all particles released in the "spawning" box were advected towards the east taking 6 days to reach the model periphery (Figure 5.5a). A calculation indicated the eastward bottom current here to have a velocity of 29 cm s^{-1} which is realistic for shelf currents in this region. Particles near the boundary moved offshore into the northern periphery of the fast flowing Agulhas Current where they travelled westwards reaching 20°E before vanishing from the simulation at the end of their 40 day life span (Figure 5.5b). The plume length varied at times retreating to 23°E. On two occasions particles in the Agulhas Current plume were partly reticulated in the cyclonic eddy, a feature commonly found in the Agulhas Bight (discussed later), but failed to survive long enough to complete a revolution. Particles mainly remained in the bottom layer. During this configuration the plume bend (see Figure 5.5b) moved very close to the coast near Cape St Francis resulting in some particles moving into the upper part of the water column and others transported westward along the Tsitsikamma coast toward Plettenberg Bay. (These are difficult to see in Figure 5.5b and require a magnification (i.e.

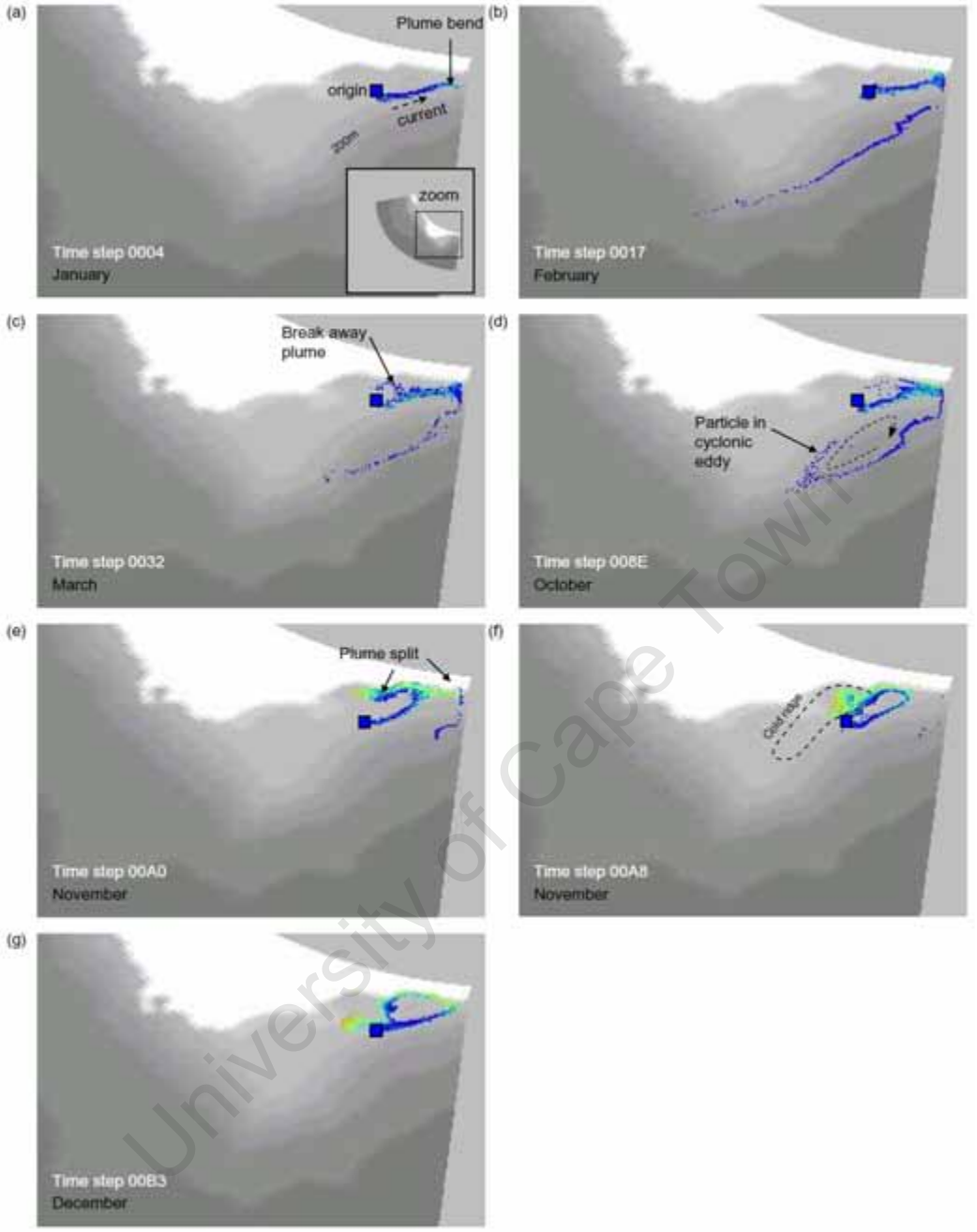

Figure 5.5: Eastern Agulhas Bank — selected time steps in the 12-month simulation highlighting (a) the particle plume after 3 days, (b) onshore encroachment of the plume bend, (c) a small break away plume, (d) entrapment of particles in the cyclonic eddy, (e) onshore movement of plume and split along Tsitsikamma coast, (f) westward split takes particles to cold ridge area, (g) particles move offshore and eastward to original release position which is marked by the blue square. Refer to Figure 5.1 for regional orientation i.e. latitude and longitude, and place names

zoom). Although this may appear an arbitrary observation, it does signify westward flow on the innershelf. A further characteristic of the configuration is that at all times the particle plume was dense and well defined i.e. long and thin. Small numbers of particles occasionally could be seen breaking away (dispersing) into the adjacent mid shelf waters. The most significant event of this is shown in Figure 5.5c.

The strongly dominant offshore configuration depicted in Figure 5.5a–d lasted 10 months in the simulation. Indications of change began in the month of October when the particle plume moved towards the coast (Cape St Francis) concomitant with particles spreading in a narrow trail westwards along the Tsitsikamma coast. In 16 model days the coastal contact of the plume trajectory moved from Cape St Francis to mid way on the Tsitsikamma coast (Figure 5.5e) resulting in bifurcation and coastal transport of particles both towards the west and east reaching an equal particle distribution. For the first time in the simulation, large numbers of particles could be seen to move from the bottom layer to higher parts of the water column. The eastern split, while initially restrained against the coast, eventually turned offshore at Cape St Francis, and continued to leak particles beyond the shelf edge. The westward split grew quickly in the number of particles, transporting them directly to the base of the cold ridge. Here the plume broadened for the first time as mature particles became dispersed, and importantly, mainly occupied the upper part of the water column (orange–red).

Near the end of the simulation (i.e. December), the particle plume against the Tsitsikamma coast became narrow, closely imitating the Tsitsikamma coastal current identified in Chapter 3 and redirected particles away from the cold ridge to join the plume near the spawning site — highlighting the existence of a mesoscale anticyclonic eddy on the eastern Agulhas Bank.

Figure 5.8a shows the percentage of particles on a monthly basis which flowed offshore across the 200 m depth contour. The almost complete loss of particles from the Agulhas Bank for 10 of the 12 months (January to October) implies that retention on the eastern Agulhas Bank is very poor when the cyclonic eddy exists. However 100% of particle retention is possible at times.

Experiment 2 (central Agulhas Bank)

This simulation essentially showed three transport configurations — (a) multi directional dispersions on the central bank, (b) strong eastward displacement with tail-end loss at the eastern model boundary (observed in Experiment 1), and (c) a particle plume split against the Tsitsikamma coast (also observed in Experiment 1).

Initially (January), particles dispersed towards the west onto the inner region of the central Agulhas Bank reaching the vicinity of Cape Infanta (plume 1 in Figure 5.6a). In early February transport was redirected offshore (Figure 5.6b) taking particles to the Alphard Banks (plume 2), leaving particle plume 1 near Cape Infanta to mature and disappear after 40 days. The Alphard Banks dispersion trajectory was short lived, and in mid February, was

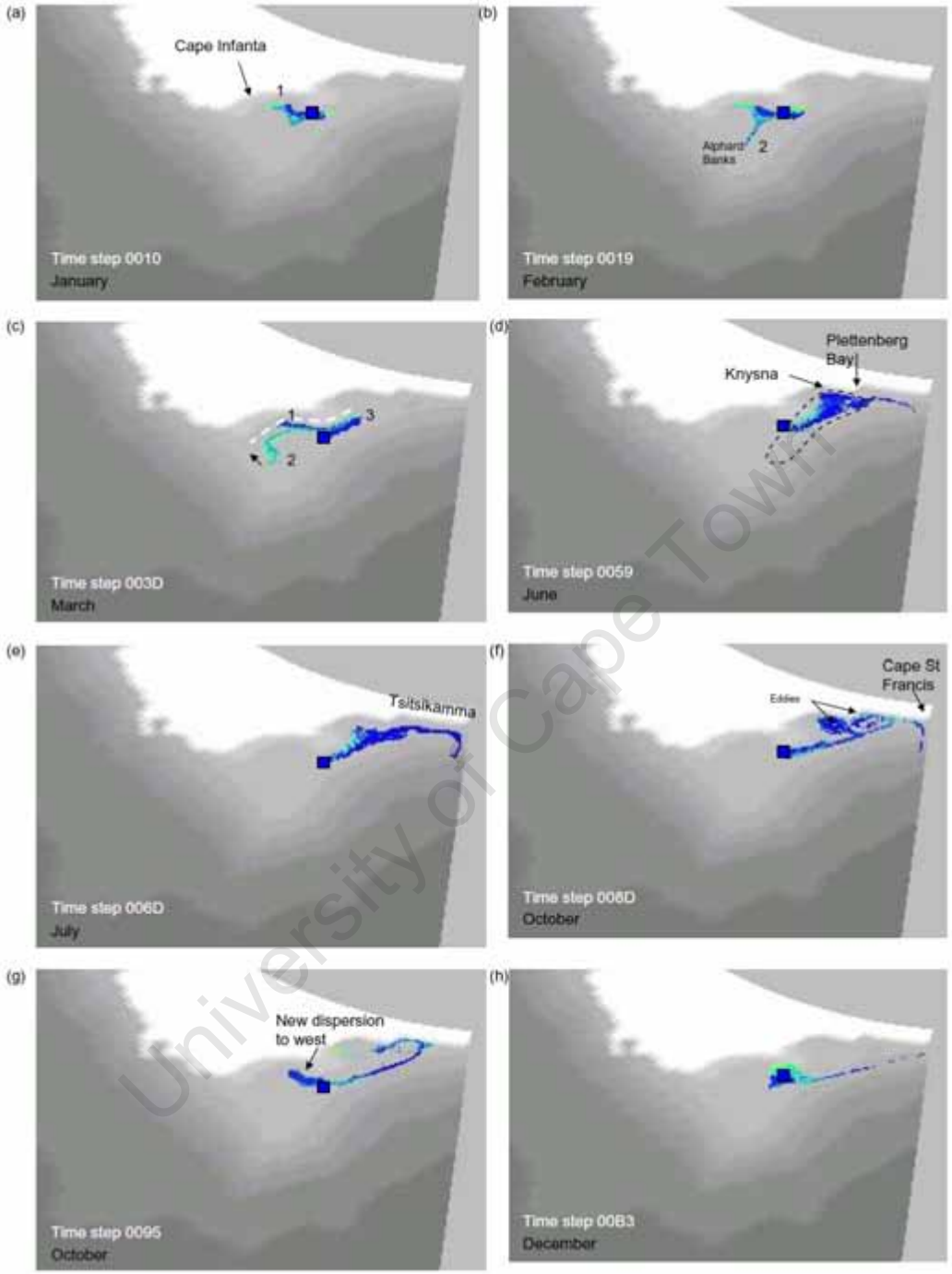

Figure 5.6: Central Agulhas Bank — selected time steps in the 12-month simulation highlighting (a) initial dispersion onto the inner bank, (b) re-directed transport to Alphard Banks, (c) emergence plume 3 towards the east, (d) particles flooding Knysna-Plettenberg Bay area, (e) continued dispersion to Cape St Francis, (f) onshore movement of plume and split against the Tsitsikamma coast caused by small cyclonic eddies, (g) retroflexion of plume to cold ridge area and emergence of new westward dispersion from the release site (h). Refer to Figure 5.1 for regional orientation i.e. latitude and longitude, and place names.

superseded by eastward dispersion from the release position (plume 3). Dispersion continued simultaneously along trajectories 1 and 3 with a new plume 2 eventually being formed as an end of plume 1. By the end of March (Figure 5.6c) all three plumes had formed one long east–west elongated multidirectional dispersion plume (dotted line in Figure 5.6c).

At the end of April, eastward transport (plume 3) had become dominant as particles moved towards the base of the cold ridge (dotted line) located between Knysna and Plettenberg Bay and was broadly dispersed. In late June (Figure 5.6d,e) the tail-end particles were swiftly swept away eastward along the mid shelf forming a long thin plume which terminated in offshore advection at Cape St Francis — also observed in simulation 1. Several eastward propagating "waves" (not captured in the depicted portraits) were observed to move along this trajectory which caused a broadening of the plume near St Francis and particles encroaching against the coast.

In early October two small cyclonic eddies (swirls) emerged to the west and east of Plettenberg Bay (Figure 5.6f) and entrained particles to flood the base of the cold ridge and the Tsitsikamma coast. At this time, opposite flowing particle trajectories existed on the Tsitsikamma coast — referred to in simulation 1 as a plume split and possibly validate the existence of Tsitsikamma current. At the emergence of the two eddies, dispersion from the source began to move westwards as was observed at the beginning of the simulation except this time with a dense, much broader, plume (Figure 5.6g). A possible merging of the two eddies led to a thin plume flowing along the western end of Tsitsikamma coast, terminating west of Plettenberg Bay (Figure 5.6g). But at the same time profound north-westward dispersion onto the central Agulhas Bank also occurred. This eventually retracted and the eastward plume straightened out to reach the eastern boundary of the model.

An important aspect of this simulation was the tendency for particles on the central Agulhas Bank to move into the upper part of the water column (green-yellow) while particles remained deep on the eastern Agulhas Bank.

Figure 5.8b shows the monthly percentage of particles lost from the Agulhas Bank ecosystem — defined by those which move offshore of the 200 m depth contour. The losses are small compared to simulation 1 with a maximum of 9% in the model month of September. The loses occurred when the particle plume was configured between Figure 5.6e–f which lasted a little over two months (late July to early October).

Experiment 3 (western Agulhas Bank)

The dispersion patterns in this simulation were complex with northward transport along the western Agulhas Bank and offshore advection caused by eddy activity being principle features.

In January (Figure 5.7a) particles were initially advected in a northwest direction along the outer shelf towards Cape Point as would be expected given that the Benguela jet is commonly found here. The Benguela jet has been an important characteristic of transport in two other IBMs set up for the southern Benguela for anchovy (Parada 2003) and sardine

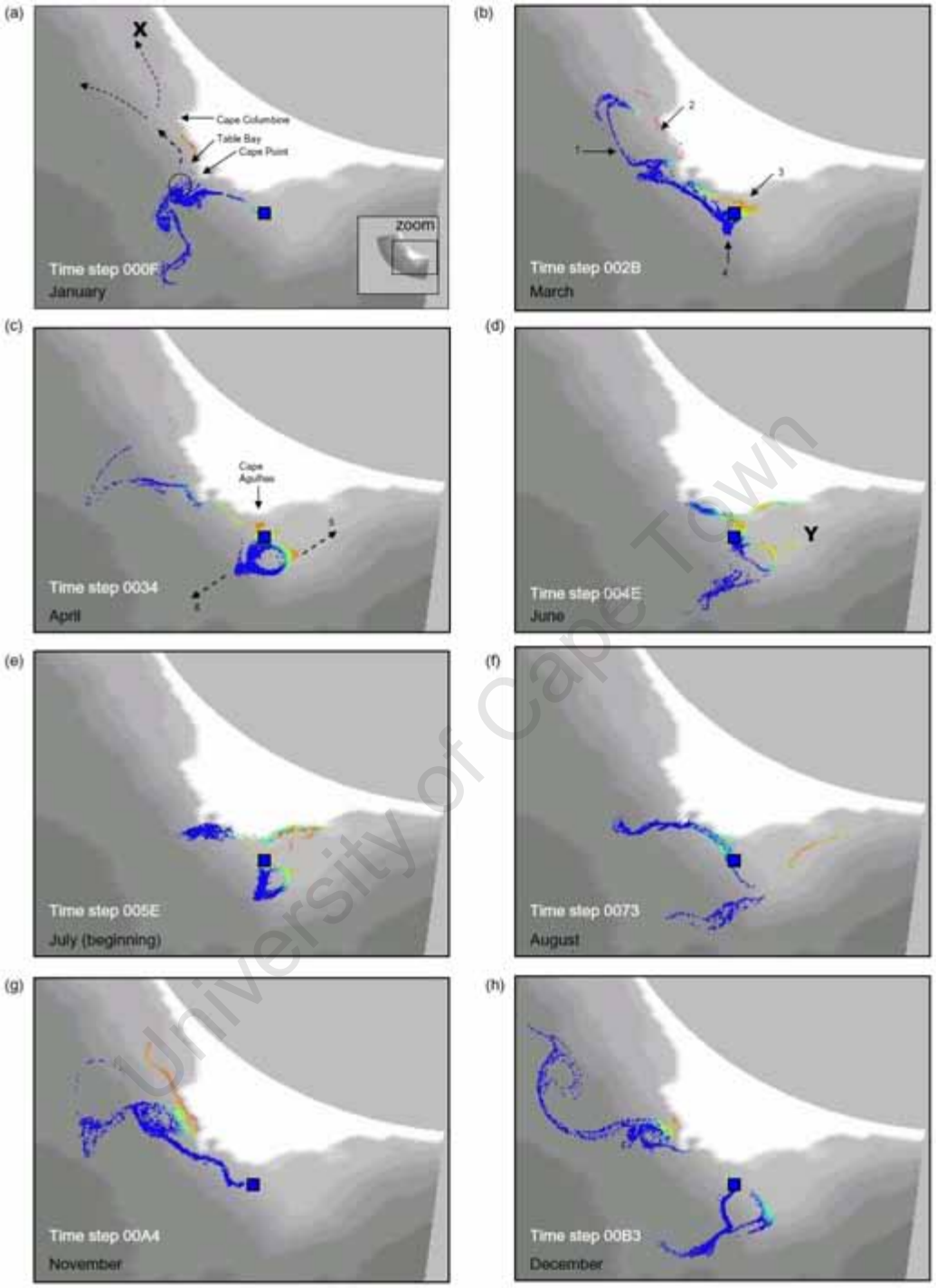

Figure 5.7: Western Agulhas Bank — selected time steps in the 12-month simulation highlighting (a) particles initially advected towards Cape Point and offshore due to anticyclonic activity. Some particles reached position X on the west the coast. (b) Four dispersion routes (1–4) existed in February to March (c) a small anticyclonic eddy emerged dispersing particles in directions 5 and 6, (d–e) the plume towards Cape Agulhas splits at the coast with eastward and westward coastal flows, (f) small anticyclonic eddy disappears leaving three dispersion plumes, (g–h) similar dispersion patterns as observed in initial stages of simulation. Refer to Figure 5.1 for regional orientation i.e. latitude and longitude, and place names.

(Miller *et al.* 2006). But south of Cape Point the particle plume was pulled offshore by anticyclonic activity reaching distances of some 250 km from the 200 m contour. This was anticipated in Chapter 4 in Figure 4.10. Interestingly, a small cluster of particles was caught in a micro subsidiary cyclone (circle) which transported them to coastal waters near Table Bay. These then moved northwards past Cape Columbine (orange) and well onto the west coast shelf as far as position 'X'.

In the period February to early March four dispersion routes were observed (Figure 5.7b) — (1) Northward transport producing a large particle plume along the outer shelf past Cape Point. Influence of offshore eddies was clearly evident in the plume trajectory as was the (2) continuation of transport (albeit minor) along the coast past Cape Columbine. Also (3) particles from the spawning site moved inshore towards Cape Agulhas and into the surface layers of the water column. These particles were swept towards Cape Point in the shelf waters. Lastly (4) particles began moving offshore in a south-westerly direction.

This dispersion pattern changed in April (Figure 5.7c) with the emergence of a small anticyclonic feature on the shelf edge which transported particles in a loop back to the spawning site and terminated transport towards Cape Point. Although most particles remained trapped in the anticyclone, some were transported in a new eastward plume (5) along the outer shelf of the central Agulhas Bank to position 'Y' south of Mossel Bay. This mode was short lived and disappeared by July with the re-emergence of the Cape Agulhas dispersion route and a new intermittent offshore plume (6). The plume towards Cape Agulhas split eastward and westward (Figure 5.7d,e) with the latter showing movement of particles to deeper layers (blue). By early July the anticyclone had stopped advection towards the coast and re-established transport around itself leaving maturing isolated and disparate trails of particles flowing along the coast east and west of Cape Agulhas (Figure 5.7e).

By August the anticyclonic feature had abated and particles were advected away from the hatching site in three directions simultaneously (Figure 5.7f) — two of which led to off shelf leakage in the south-west and at Cape Point while those moving eastward were retained on the central Agulhas Bank. This pattern gave way to similar ones observed in the initial stages of the simulation, i.e. Figures 5.7a,b, which lasted the remainder of the model year (Figures 5.7g,h). This similarity might be construed as seasonal. It is also interesting that the anticyclonic transport highlight in Figure 5.7c adjacent to the hatching site is semi-permanent in the simulation.

Monthly leakage in terms of percentage of particles removed from the Agulhas Bank ecosystem is shown in Figure 5.8c. Leakage varied between 10 and 96% with perhaps a seasonal trend if the months of May and November are considered anomalous.

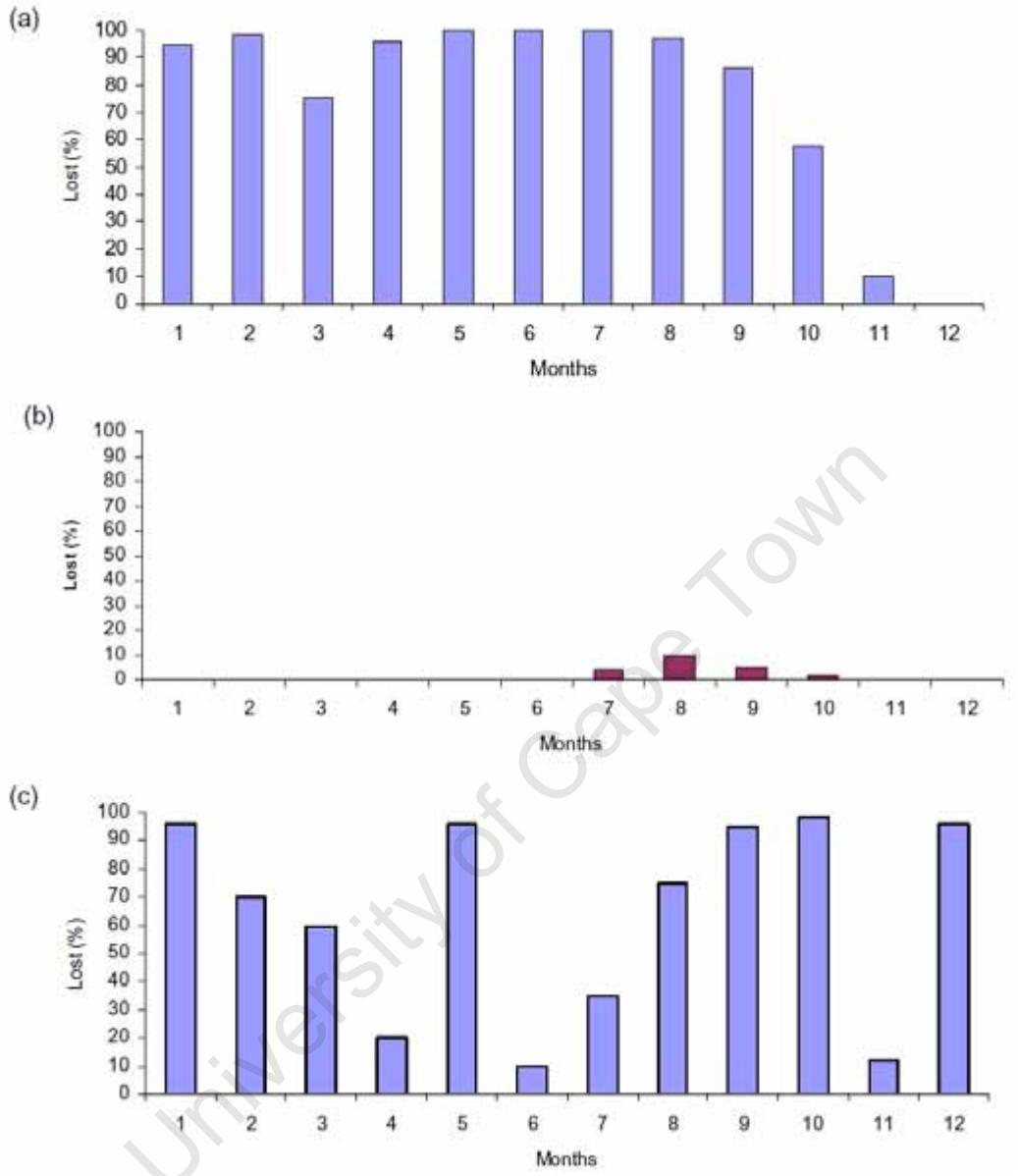

Figure 5.8: Monthly percentages of particles that crossed over the 200m depth contour and considered lost from the Agulhas Bank ecosystem. (a) Eastern Agulhas Bank, (b) Central Agulhas Bank, (c) Western Agulhas Bank. The time scale is model months for year 3 in the 10-year PLUME (ROMS) archived data set.

Discussion

Is paralarvae leakage possible?

The aim of this study was to test the hypothesis that chokka squid paralarvae can be removed from the Agulhas Bank ecosystem through leakage over the shelf edge into the Indian and Atlantic Oceans. Given magnitude and duration, this scenario would lead to recruitment failures and hence be responsible for poor squid catch such as in 2001.

The test was performed using a Lagrangian IBM coupled to the output of a ROMS model already set up. The simulations clearly demonstrated that large losses of neutrally buoyant paralarvae, represented as neutrally buoyant passive particles, are possible from the eastern Agulhas Bank (76%) and the western Agulhas Bank (64%) — with the latter showing a tendency of a seasonal trend if the months of May and November are considered spurious. This is despite being "hatched" (i.e. released) in the bottom layer. Losses on the eastern Agulhas Bank were consistently high throughout 10 of the 12 month modelling period but for the last two months of November and December, a shoreward anticyclonic circulation resulted in complete retention of particles and transport to the base of the cold ridge. In contrast, almost complete retention of particles was experienced on the central Agulhas Bank with loses to the Indian Ocean of only 2%. The results therefore indicate that the central Agulhas Bank is the most suitable place for spawning in this region if dispersion and retention alone are considered. However, in reality we know that most spawning takes place on the eastern Agulhas Bank, and if these results are taken literally, then paralarvae loss certainly from the mid shelf is possible.

An observation from these results is that most particles released on the central Agulhas Bank remained in the bottom layers i.e. vertical mixing was limited. In contrast, a much greater number of particles were observed to move towards the surface on both the eastern and western Agulhas Banks. From an ecological perspective, the central Agulhas Bank is important for the early squid life cycle because it is here that the cold ridge is found — a feature which is responsible for enhance production (biomass) (Chapter 2). In fact Chapter 2 quantitatively demonstrated that the strength of this feature i.e. degree of upwelling is linked to squid recruitment and catches. However, the resultant production from the cold ridge (and hence food) is in the upper part of the water column and may not be accessible to those paralarvae in the bottom layers.

But of course, the question of how realistic these simulations are — given the large number of simplifications and assumptions made in the ROMS model and the coupled IBM with its ascribed Lagrangian particle characteristics — still needs to be addressed. The degree of confidence in the PLUME model and its ability to replicate certain oceanographic features has already been introduced in the methods section.

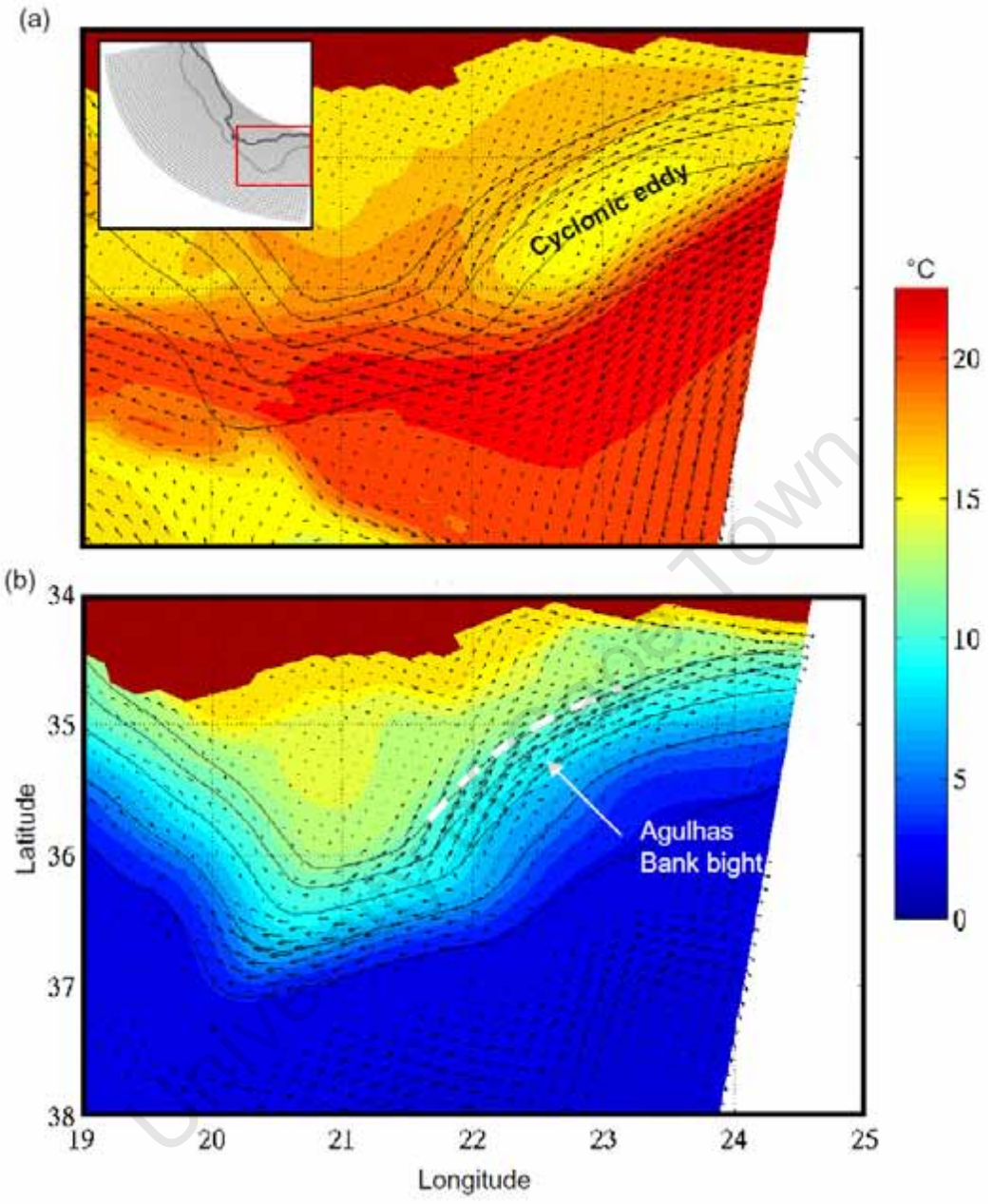

Figure 5.9: Currents for the (a) surface level 20 and (b) bottom level 2 during the model month of July in year 3. Trajectories of particles released on the eastern Agulhas Bank were strongly influenced by barotropic, mesoscale cyclonic eddy (indicated) which is commonly found in the Agulhas Bank bight.

Mechanisms responsible for shelf leakage

It is important to identify the mechanisms in the model responsible for the particle losses and to ascertain whether they are real.

In the case of the eastern Agulhas Bank experiment, particle trajectories indicated a clear and dominant pattern of swift transport eastward with subsequent offshore flow into the boundary of the westward flowing Agulhas Current. At times eastward reticulation in the boundary was observed, i.e. Figure 5.5d, suggesting the presence of a cyclonic eddy. Eastward transport along the mid shelf is also evident at times in the central Agulhas Bank experiment (Figure 5.6e). This eastward transport on the mid shelf is also in stark contrast to observations in Chapter 4 which reported net westward flow on the mid shelf of the eastern Agulhas Bank.

Visualisation of the forcing ROMS (PLUME year 3) data used as inputs to the IBM experiment (Figure 5.9) shows a large cyclonic eddy resident in the Agulhas Bight which stretches along the entire eastern Agulhas Bank shelf edge as far east as 24°E. The eddy is evident in the bottom layer on the shelf slope. This feature was also recognised in the PLUME model by Lutjeharms *et al.* (2003) who described it as being semi permanent in nature, and noted that it escapes the bight on occasion and moves westward around the southern tip of the Agulhas Bank. The cyclonic eddy has also been observed in cruise survey data and AVHRR satellite imagery (Lutjeharms *et al.* 1989). Chapter 2 suggests its presence may influence the cold ridge. Comparison with the *in situ* observations indicates that the eddy in the model is over sized which may account for its strong dominance on the mid shelf region and possibly exaggerated particle losses.

It is well documented that water on the mid and outer western Agulhas Bank is thought to generally flow northwards into the Benguela jet which then closely bypasses the Cape Peninsula culminating in bifurcation north of Cape Columbine (Shannon and Nelson 1996). This, however, was not observed very commonly in the results of the IBM experiment. Instead, as depicted in Figure 5.7, large particle losses from the western Agulhas Bank were experienced usually in the form of long filamentous trajectories stretching well into the Atlantic Ocean. Again visualization of the forcing ROMS (PLUME year 3) data used as inputs to the IBM experiment (Figure 5.10) indicate several well established cyclonic eddies on west coast which clearly have strong influence on the mid and outer shelf waters on the western Agulhas Bank. In reality such features are well known and have been documented by Lutjeharms and Matthysen (1995).

Limitations of the simulations

There are several limitations in the ROMS–IBM used in this study that must be recognised and considered when interpreting and applying the simulation results.

The first of these concerns the PLUME model domain and forcing. As depicted in Figure 5.1, chokka squid spawning occurs on the eastern Agulhas Bank as far east as Algoa Bay and even Port Alfred at times. This represents some 50% of the spawning area which has not

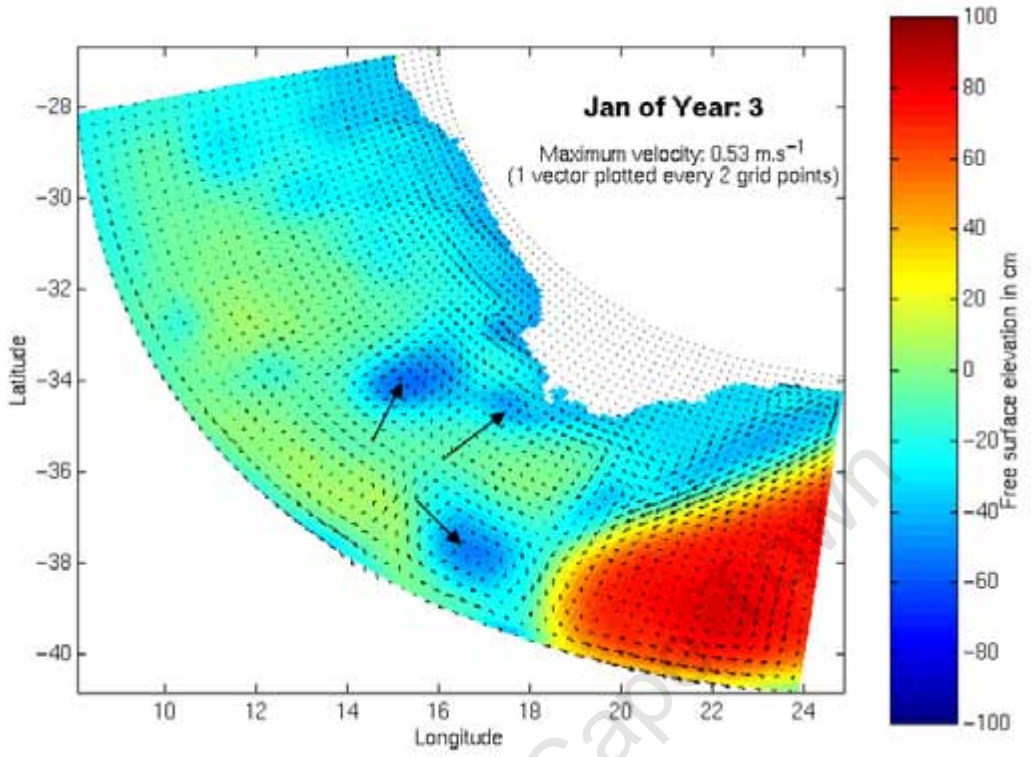

Figure 5.10: Surface elevation and barotropic currents for the model month January of year 3. One vector has been plotted every 2 grid points. Cyclonic eddies commonly found west of the Cape Peninsula (highlighted by arrows) are instrumental in pulling Agulhas Bank shelf water into the Atlantic Ocean.

been considered here in the PLUME model. To include this area the model domain needs to be extended eastward. Also, despite the ROMS boundaries being permeable, the distinct offshore deflection of particles near the existing model boundary at 24°E limits confidence in the reality of the ROMS-IBM simulations. Moreover, Lutjeharms *et al.* (2003) have noted and described a significant semi permanent upwelling cell which exists east of Algoa Bay. Remote sensing data indicate that this feature can extend at times to East London and influence shelf waters near Algoa Bay. The increased model domain should therefore be extended to at least 28°E.

Furthermore the model is forced using a monthly climatology. To be more realistic, i.e. to include forcing on shorter time scales, this needs to be changed to atmospheric forcing on a higher temporal resolution i.e. daily.

A second limitation of this study is the use of particles with neutral buoyancy and zero swimming capacity (i.e. passive) for a period of 40 days to represent real squid paralarvae. This was necessary because of the absence of any actual data or information. Buoyancy and swimming influence the position of paralarvae in the water column. The effect of neutral buoyancy can add error if real squid paralarvae are more dense than sea water, then they would continually remain in the bottom layer where currents are usually slower than those in the surface layer. Neutrally buoyant particles in the model on the other hand may be moved towards the surface and hence the simulation would provide greater dispersion. The converse also holds. Swimming can add the effect of diel vertical migration.

In reality the passive period ascribed here of 40 days maybe too long, however, given that the main aim of this study was to investigate the possibility of paralarvae loss over the shelf edge, it is instructive. On the other hand, a 40 day passive period may not be too far from reality given that squid paralarvae begin displaying schooling behaviour at about 40 days (Yang *et al.* 1986) and this clearly requires skilful swimming abilities for which fins are essential.

A third limitation concerns the chosen release positions in the model. As indicated in Figure 5.1a, spawning also occurs inshore. In fact Roberts *et al.* (Unpublished) have calculated that only 25% of trawled egg mass is found in depth >60m. While this figure still needs further verification, it does emphasise the need to also consider the inshore spawning grounds in the model despite the strong possibility that they are less susceptible to shelf edge physical processes. Uncertainty of boundary effects and model resolution finally eliminated release sites on the inshore spawning grounds.

Nonetheless, despite there being uncertainty as to the characteristics of squid paralarvae which no doubt influence the Lagrangian results, this investigation has clearly demonstrated that the potential exists for passive, neutrally buoyant material such as squid paralarvae, to be drawn off the shelf and removed from the Agulhas Bank ecosystem.

Future efforts should focus on expanding the model domain, along with laboratory experiments to determine the density and swimming characteristics of chokka squid paralarvae to more accurately portray their vertical movement (DVM) in the IBM. Such

experiments need to be related to temperature, as density will be dependent on yolk consumption, which in turn will affect buoyancy. Additionally, swimming capability will be related to paralarval age. A drifter experiment should also be undertaken to validate these results.

References

Agenbag JJ, Anderson FP. 1985. The role of satellite remote sensing in South African marine research: The present and the future. Shannon LV (ed.), South African Ocean Colour and Upwelling Experiment, Cape Town; Sea Fisheries Research Institute: 251-255.

Biastoch A, Krauβ W. 1999. The role of mesoscale eddies in the source regions of the Agulhas Current. *Journal of Physical Oceanography* 29: 2303–2317.

Boebel O, Lutjeharms J, Schmid C, Zenk W, Rossby T, Barron C. 2003. The Cape Cauldron: a regime of turbulent inter-ocean exchange. *Deep Sea Research II* 50(1): 57–86.

Borland 1999. Developer's guide, Borland Jbuilder for Windows 95, Window 98 and Windows NT. Version 3. A division of inprise corporation, USA.

Chang N. 2009. Cold Ridge dynamics on the Agulhas Bank: A numerical model study. PhD Thesis, University of Cape Town, South Africa.

Da Silva AM, Young CC, Levitus S. 1994. Atlas of surface marine data 1994. Vol 1, Algorithms and Procedures, NOAA Atlas NESDIS 6, US Department of Commerce, NOAA, NESDIS, Washington, DC.

Flather RA. 1976. A tidal model of the northwest European continental shelf. *Mémoires de la Société Royale des Sciences de Liège* 10: 141–164.

Goschen WS, Schumann EH. 1988. Ocean current and temperature structures in Algoa Bay and beyond in November 1986. *South African Journal of Marine Science* 7: 101–116.

Haidvogel DB, Blanton J, Kindle j, Lynch DR. 2000. Coastal ocean modelling: processes and real-time systems. *Oceanography* 13: 35–46.

Largier JL, Chapman P, Peterson WT, Swart VP. 1992. The western Agulhas Bank: circulation, stratification and ecology. *South African Journal of Marine Science*12: 319–339.

Lett C, Verley P, Mullon C, Parada C, Brochier T, Penven P, Blanke B. 2008. A Lagrangian tool for modelling ichthyoplankton dynamics. *Environmental Modelling & Software* 23: 1210–1214.

Lutjeharms 2006. *The Agulhas Current*. Springer, Berlin: 329 pp.

Lutjeharms JRE, Catzel R, Valentine HR. 1989. Eddies and other border phenomena of the Agulhas Current. *Continental Shelf Research* 9(7): 597–616.

Lutjeharms JRE, Matthysen CP. 1995. A recurrent eddy in the upwelling front off Cape Town. *South African Journal of Science* 91: 355–357.

Lutjeharms JRE, Penven P, Roy C. 2003. Modelling the shear-edge eddies of the southern Agulhas Current. *Continental Shelf Research* 23(11–13): 1099–1115.

Lutjeharms JRE, Roberts HR. 1988. The Natal Pulse: an extreme transient on the Agulhas Current. J*ournal of Geophysical Research* 93(C1): 631–645.

Lutjeharms JRE, van Ballegooyen RC. 1988. The retroflection of the Agulhas Current. *Journal of Physical Oceanography* 18(11): 1570–1583.

Marchesiello P, McWilliams JC, Shchepetkin AF. 2003. Equilibrium structure and dynamics of the California Current system. *Journal Physical Oceanography* 33: 753-783.

McCreary JP, Kundu PK, Chao S-Y. 1987. on the dynamics of the California current system. *Journal Marine Research* 45: 1–32.

Miller DCM, Moloney CL, van der Lingen C, Lett C, Mullon C, Field J. 2006. Modelling the effects of physical–biological interactions and spatial variability in spawning and nursery areas on transport and retention of sardine *Sardinops sagax* eggs and larvae in the southern Benguela ecosystem. *Journal of Marine Systems*, 61: 212–229.

Olson DB, Evans RH. 1986. Rings of the Agulhas Current. Deep Sea Research 33(1): 27–42.

Parada C. 2003. Modelling the effects of environmental and ecological processes on the mortality, growth and distribution of early stages of anchovy (*Engraulis capensis*) in the Benguela system. PhD Thesis, University of Cape Town, South Africa.

Penven P. 2000. A numerical study of the Southern Benguela circulation with an application to fish recruitment. PhD thesis, University de Bretagne Occidentale, France.

Penven P, Roy C, Brundrit G, Colin de Verdière A, Fréon P, Johnson A, Lutjeharms JRE, Shillington FA. 2001. A regional hydrodynamic model of upwelling in the Southern Benguela. *South African Journal of Science* **97**: 472–475.

Roberts M, Downey N, Sauer W. Unpublished. Existence of deeper spawning grounds for the South African chokka squid *Loligo reynaudii*.

Schumann EH. 1999. Wind-driven mixed layer and coastal upwelling processes off the south coast of South Africa. *Journal of Marine Research* 57: 671–691.

Schumann EH, Perrins L-A, Hunter IT. 1982. Upwelling along the south coast of the Cape Provence, South Africa. *South African Journal of Science* 78: 238–242.

Shannon LV. 1985. The Benguela Ecosystem. 1. Evolution of the Benguela, physical features and processes. *Oceanography and Marine Biology, An Annual overview* 23: 105–182.

Shannon LV, Nelson G. 1996. The Benguela: large scale features and processes and system variability. In, *The south Atlantic: present and past circulation*. Wefer G, Berger WH, Siedler G, Webb DJ (eds). Springer, Berlin: 163–210.

Song Y, Haidvogel D. 1994. A semi-implicit ocean circulation model using a generalized topography-following coordinate system. *Journal of Computational Physics* 115: 228-244.

Yang WT, Hixon RF, Turk PE, Krejci ME, Hullet WH, Hanlon RT. 1986. Growth, behaviour, and sexual reproduction of the market squid, *Loligo opalescens*, cultured through the life cycle. *Fishery Bulletin* 84: 771–798.

CHAPTER 6

Satellite tracked drifter observations on the Agulhas Bank and their relevance to the dispersion of chokka squid (*Loligo reynaudii*) paralarvae — summer 2002/3

Four satellite tracked drifters were released on the eastern Agulhas Bank to investigate the transport of chokka squid paralarvae. Two drifters with drogues to 8 m (near-surface) were released on the inshore spawning grounds off the Tsitsikamma coast directly above a bottom-mounted ADCP in 36 m of water. The other two drifters were released on the mid shelf where squid eggs had previously been found in 120 m. This position had also previously been used to release "virtual paralarvae" in an IBM experiment which showed substantial loss of particles from the shelf ecosystem. One of the drifters was tethered to a drogue at a depth of 70 m to monitor flow in the bottom layer. Comparison between the ADCP and drifter data showed the latter to accurately reflect current velocity and direction in the near-surface layer when wind was < 4 m s^{-1}. Inshore transport projections based on the ADCP data (progressive vector plots) were found to be reliably accurate for distances of ~ 50 km on this straight coastline. Both inshore drifters were transported 70 km eastwards in the Tsitsikamma counter current to Tsitsikamma Point. Here one beached while the other went southwards to leave the shelf 20 days after release. The surface drifter on the mid shelf was transported westward across the central and western Agulhas Bank (550 km) to leave the shelf after 58 days just south of the Cape Peninsula. The deeper drifter also travelled westward, but remained on the shelf and was recovered after 40 days inshore (100 km) of the release position. Satellite SST and ocean colour imagery indicated frequent offshore flows of shelf water near the southern tip of the Agulhas Bank, as well as an intrusion of oceanic water onto the western Bank during this experiment. The latter caused an anti-cyclonic circulation which led to further leakage of shelf water from the inner central Agulhas Bank. The combination of drifters and satellite imagery in this experiment has demonstrated that retention of chokka squid paralarvae in the Agulhas Bank ecosystem is not certain, even for the inshore spawning grounds, and that the risk would be less if paralarvae were found near the bottom. So far *in situ* sampling indicates they occupy the surface layer.

Key words: satellite drifters, currents, chokka squid, *Loligo reynaudii*, paralarvae, transport, cold ridge, shelf water leakage, Agulhas Bank

---

Introduction

The Agulhas Bank at the southern tip of Africa is the largest expanse of shelf on the continent spanning 800 km from east to west and 300 km from north to south at its widest point (see Figure 6.1a). The continental shelf break is at 200 m giving the shelf an average depth of ~ 100 m. The Bank is bordered in the east by the fast (~ 200 cm s^{-1}) and warm (24–25ºC) Agulhas Current which flows poleward along the continental slope, diverging from the coast as the shelf widens between 27º and 21º E. This powerful western boundary current typically

forms an 80 km wide barrier between the shelf water and the Indian Ocean. South of the Bank, the Agulhas Current undergoes a number of final fates which range between continuing north-west along the slope of the western Agulhas Bank, generating anticyclonic eddies which move into the Atlantic Ocean, and retroflexion to the south with final flow eastwards along the Subtropical Convergence. Numerous configurations exist between these extremes some of which can be seen in Figure 6.9.

The Benguela Current on the western side is less defined, mainly because it is the eastern component of the South Atlantic gyre, and has lower velocities (~ 40 cm s^{-1}). A strong but small jet (Benguela Jet) is often formed along the Cape Peninsula. This leaves the western Bank less confined than the central and eastern regions. More detailed regional overviews of the oceanography are given in Boyd and Shillington (1994), Lutjeharms (2001) and Chapters 2 and 4 of this thesis.

The Agulhas Bank plays a major role in the early life histories of many species including but not least, clupeids, sciaenids, sparids, merluccids, carangids, and squid (Augustyn *et al.* 1994; Hutchings 1994; Japp *et al.* 1994; Roel *et al.* 1994; Tilney *et al.* 1996; Barrange *et al.* 1998; Hutchings *et al.* 2002). In particular, the western and central Banks are the main spawning ground for sardine (*Sardinops sagax*) and anchovy (*Engraulis capensis*) with the latter often spawning between the cold ridge and the Agulhas Current (see Figure 6.1a and Roel *et al.* 1994). Several modelling studies based on ADCP ship-borne data (Shannon *et al.* 1996), averaged winds and geostrophy (Skogen 1999), and more recently a Regional Ocean Modelling System (ROMS) coupled to an Individual-Based Model (IBM) (Mullon *et al.* 2003; Parada 2003), have demonstrated that sardine and anchovy eggs and larvae are largely transported westwards towards the Cape Peninsula where they are typically moved by the Benguela Jet onto the west coast feeding grounds. Hutchings *et al.* (2002) identified the outer shelf of the central Agulhas Bank as playing a critical role in the retention of eggs and larvae.

Chokka squid (*Loligo reynaudii*), another commercially important species, also spawn on the eastern Agulhas Bank depositing their egg capsules on the seabed both inshore and on the mid shelf regions (Augustyn *et al.* 1994). In contrast to the more defined transport of sardine and anchovy, Chapter 4 suggested that the paralarvae are at risk by currents on the Agulhas Bank and at times could be removed from the ecosystem through the leakage of shelf water into the greater ocean (see their Figures. 9, 10). Even on the inshore Tsitsikamma spawning grounds, paralarvae may be at risk as Chapter 3 demonstrated a predominately eastward coastal current which potentially can transport paralarvae to Algoa Bay. These squid paralarvae reach Algoa Bay where *in situ* data collected by Goschen and Schumann (1988), and ROMS model results by Penven (2000), have demonstrated offshore advection.

To test for offshore transportation of squid paralarvae, a first version of an IBM was developed in which hatchlings were treated as Lagrangian particles with an assumed 40 day pelagic phase i.e. no swimming ability. Dispersion simulations were performed for paralarvae in the bottom layer at a depth of 120 m (Chapter 5). This was considered a worst case scenario relative to higher in the water column where currents are stronger (CSIR report

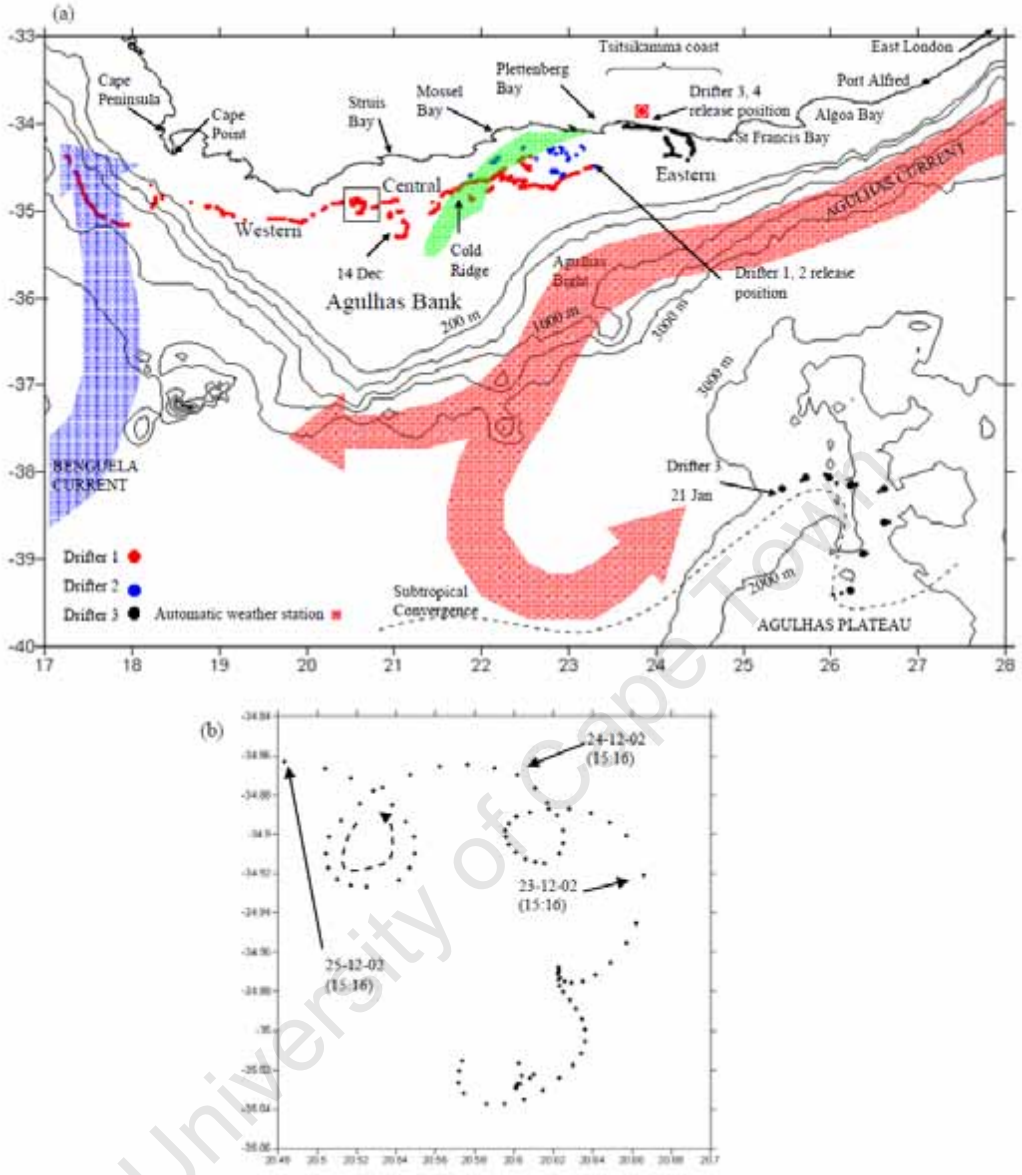

Figure 6.1: (a) Overview of tracks for all four satellite drifters (see legend). Drifters 1 and 2 were released on the mid shelf on 10 November 2002. Drifter 3 was released 1.5 km from the coast at Middlebank (Storms River) on 11 November and Drifter 4 on the 19 November. Drifter 4's track is masked by that of Drifter 3 (Expanded view given in Figure 6.5). The last recorded position of Drifter 1 is 132 km west of the Cape Peninsula, and that of Drifter 3 about 450 km south of the continent near the Agulhas Plateau. Drifter 4's last position on the shelf was 26 November 2002. (b) Expanded view of the box shows anticyclonic inertial motions in the track of Drifter 1.

1986). The IBM was driven by the output from a hydrodynamic ocean model based on the Regional Ocean Modelling System (ROMS) numerical code (see Haidvogel *et al.* 2000) which has been adapted to the Agulhas Bank and west coast (Penven 2000; Penven *et al.* 2001). This was used in the sardine and anchovy IBM studies cited above (Mullon *et al.* 2003; Parada 2003). Results from the squid ROMS–IBM showed the majority of hatchlings to be transported eastwards on the shelf and then swept offshore in the vicinity of St Francis Bay where they were then displaced westwards in the Agulhas Current and finally lost to the greater ocean. This result was surprising because flow on the mid shelf is thought to be mainly westward (Chapter 4). In its present form the ROMS–IBM is not reliable in the shallower coastal region and hence can not be used to validate the results of Chapter 3, already mentioned.

Understanding egg and larval transport in the ocean is not trivial and no one method is definitive. In this chapter satellite tracked drifters were employed as a complementary method to those already used. The aims were two fold: (1) to validate the results of the squid ROMS–IBM simulations for the mid shelf spawning grounds, and (2) determine the potential fate of squid paralarvae in the Tsitsikamma coastal current where the ROMS–IBM could not be employed. Lagrangian measurements have been used in numerous experiments to study surface currents and larvae dispersion e.g. Pepin and Helbig (1997) and Kasai *et al.* (2002). In the case of (2) above, drifters were also used to validate the use of progressive vector plots, in Chapter 3, as a means of estimating potential egg and larvae transport.

Methods

Four satellite tracked surface drifter buoys were used in this experiment, each tethered to a standard 6.4 m long “holey sock” drogue. This is a well used design and has been deployed extensively in the Surface Velocity Program (SVP) of the World Ocean Circulation Experiment (WOCE) (Sybrandy and Niiler, 1991).

Two drifters (referred to as 1 and 2) were simultaneously released on the mid shelf of the eastern Agulhas Bank on the 10 November 2002 (16:45) at the same position used in the ROMS–IBM experiment to release virtual particles (34˚ 29.53 S; 23˚ 20.06 E; Figure 6.1a). Drifter 1 monitored movement of the upper mixed layer with the drogue hanging 2 m below the float. Drifter 2 monitored the bottom mixed layer with the drogue hanging 70 m below the float. The depth here is 120 m and the thermocline in summer is typically at 30 m (Largier and Swart 1987). All drifters transmitted their positions (GPS) hourly. The remaining drifters (Drifters 3 and 4) were released at different times on the inshore squid spawning grounds off the Tsitsikamma coast directly above a permanently bottom-mounted ADCP on Middlebank in 36 m (34˚ 02.64' S; 23˚ 52.58' E; Figure 6.1a). Drifter 3 was released on 11 November at 10:50 and Drifter 4 a week later on the 19 November at 11:26. Drogues on both drifters hung 2 m below the float. The intention was to monitor all drifters for 40 days, the same period used to track virtual particles in the IBM experiment.

Other data required were wind, current velocity and direction at Tsitsikamma, and satellite imagery. Wind data shown in Figure 6.3, measured 15 m above sea level and hourly, were obtained from a dial-in automatic weather station (AWS) located on the Tsitsikamma coast opposite to the drifter release position (see Figure 6.1a). This location is not ideal because the coastline topography is exceptionally steep and rises to a coastal plain at an altitude of 180–220 m. In addition, the small embayment at Storms River mouth introduces an inflection in the otherwise linear coastal topography. This may influence measurements made at this site so that these data do not accurately reflect the wind field farther offshore i.e. velocities offshore are probably greater. However, for this study these data are adequate because the main wind directions are parallel to the coast i.e. east–west. A New Hampshire Lanczos filter (UNH), with 71 weights and a power point of 36 h was used to remove land breeze effects in the analysis.

The current meter data used to compare inshore drifter trajectories were collected at Middlebank (coordinates give above) using an *RDI Sentinal Worhorse* 300 kHz ADCP configured to measure every 30 minutes with 2 m bins (see Chapter 3 for details). The data did not require filtering to remove noise. Currents shown in Figure 6.2 were made prior to Drifter 1 and 2 deployments using a hull mounted *RDI Ocean Surveyor I* 150 kHz ADCP aboard the "FRS Algoa" with four meter sample bins. SeaWIFS ocean colour satellite imagery (chlorophyll *a*) was used to distinguish Agulhas Bank water from that of the surrounding ocean. SST AVHRR imagery was obtained from NOAA.

Results

Drifter release conditions

An ADCP survey undertaken by the research ship "FRS Algoa" immediately prior to drifter deployment showed both the upper and bottom mixed layers of the water column to be flowing westward on the mid shelf between Plettenberg Bay (23ºE) and St. Francis Bay (25ºE), including the inshore region along the Tsitsikamma coast. The Plettenberg Bay transect data are shown in Figure 6.2. Near-surface velocities ranged between 20–30 cm s^{-1}. The westward inshore current was confirmed by ADCP data collected at Middlebank (see Figure 6.6). Wind at the time (10 November) was light to moderate (3–4 m s^{-1}) easterly (Figure 6.3). Clearly the strong south-westerly wind on 8 and 9 November had little lasting effect on the westward shelf current.

Drifter tracks

An overview of all four drifter tracks is shown in Figure 6.1a with selected time frames in Figure 6.4. Drifter 2 (deep mid shelf) had fewer positional data than the other drifters seemingly caused by the inability of the float with its long tether to ride on the surface of large wind waves and successfully transmit. This can be seen on 19–20 November in Figure 6.4 when a strong south-westerly wind of > 6 m s^{-1} blew (Figure 6.3) and no data were received

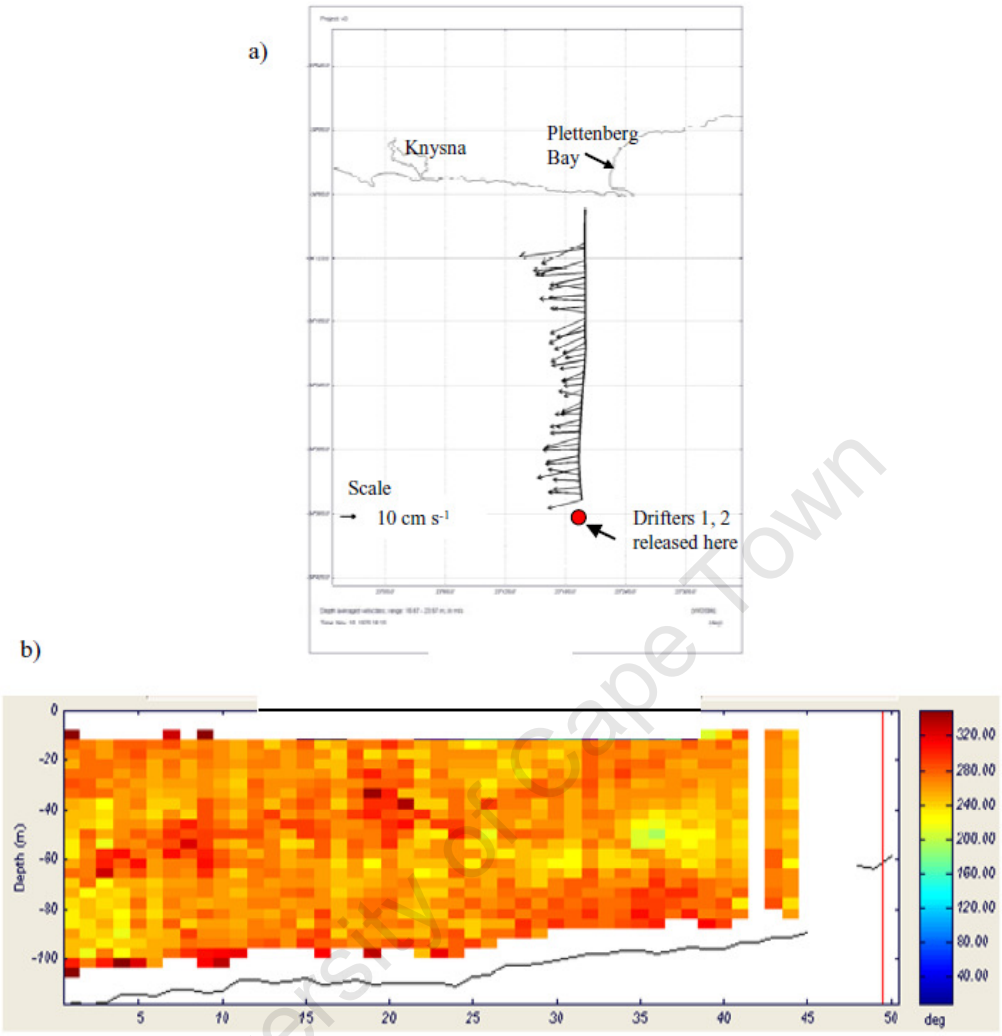

Figure 6.2: ADCP measured currents across the eastern Agulhas Bank between the coast (Plettenberg Bay) and the release position of Drifters 1 and 2. (a) Near-surface (10 m) vector field depicting westward flow. (b) Vertical profile (4 m depth bins) showing westward flow throughout the water column.

for this period. Notice in Figure 6.4 that linear interpolations have been used to fill data gaps for clarity. Drifter 3 lost communication with the satellite for a period of 57 days between 26 November 2002 and 21 January 2003. It is interesting that drifters in other experiments have experienced similar data loss in the Agulhas Current retroflection region.

Drifter 3

Initially Drifter 3 was observed to move westwards with the rest of the shelf water under the 3–4 m s^{-1} north-easterly wind reported above (Figure 6.5a), but then reversed course to eastwards late on 12 November (Day 2) coincident with a wind change to strong south-westerly (6 m s^{-1}). The drifter continued eastwards to Tsitsikamma Point (see Figures 6.4, 5.5a) with a velocity of ~ 43 cm s^{-1} despite a further change in wind to light north-easterly (2–3 m s^{-1}) on 14 and 15 November (Days 4 and 5). On 15 November Drifter 3 turned offshore onto the mid shelf and completed two clockwise gyrations in the same place with the drifter revisiting the inshore counter current before disappearing altogether on 26 November (Day 16). When communication was re-established on 21 January (Day 71), Drifter 3 was observed directly south of Algoa Bay some 400 km from the shelf edge in the vicinity of the Agulhas Plateau and the Subtropical Convergence (26º E; 38º S; see Figure 6.1a). From here it travelled further south to reach 41º S before turning eastwards. Communication finally failed on 26 March 2003 (Day 137) at 42ºE.

The inshore data also show that wind and sea state had an influence on drifter communication. This can be seen for example on 14 November (see Figure 6.5a) when Drifter 3 was travelling swiftly (48 cm s^{-1}) eastwards along the Tsitsikamma coast against a moderate easterly wind which had started in the morning. Communication failed (presumably caused by float submergence) for 13 h until the wind decreased in strength.

Drifter 4

On the first day of release Drifter 4 moved offshore for 10 km (Figure 6.5b). This was opposite in direction to Drifter 3 which was 30 km away, also 10 km from the coast, and was moving inshore during a clockwise gyration (see Figures 6.5a,b). By Day 2 Drifter 4 had moved back towards the coast under a strong south-westerly wind and continued to move steadily eastwards with a similar velocity as had been experienced by Drifter 3. On 23 November (Day 5) under a strong north-easterly wind (6 m s^{-1}) it floundered at Tsitsikamma Point (see Figure 6.5a). The cause of the initial temporary offshore excursion is not obvious. The ADCP data collected at Middlebank (Figure 6.6) also measured an offshore flow with similar displacement. Chapter 3 demonstrated that coastal upwelling events cause offshore flow on the Tsitsikamma coast, but in this case, no coastal upwelling was evident from data collected by a thermistor array on Middlebank (data not shown), nor in SST imagery. Another possible cause could be an offshore land breeze, but then a similar event was not caused by the much stronger offshore breeze on 21 November which temporally stalled the drifter

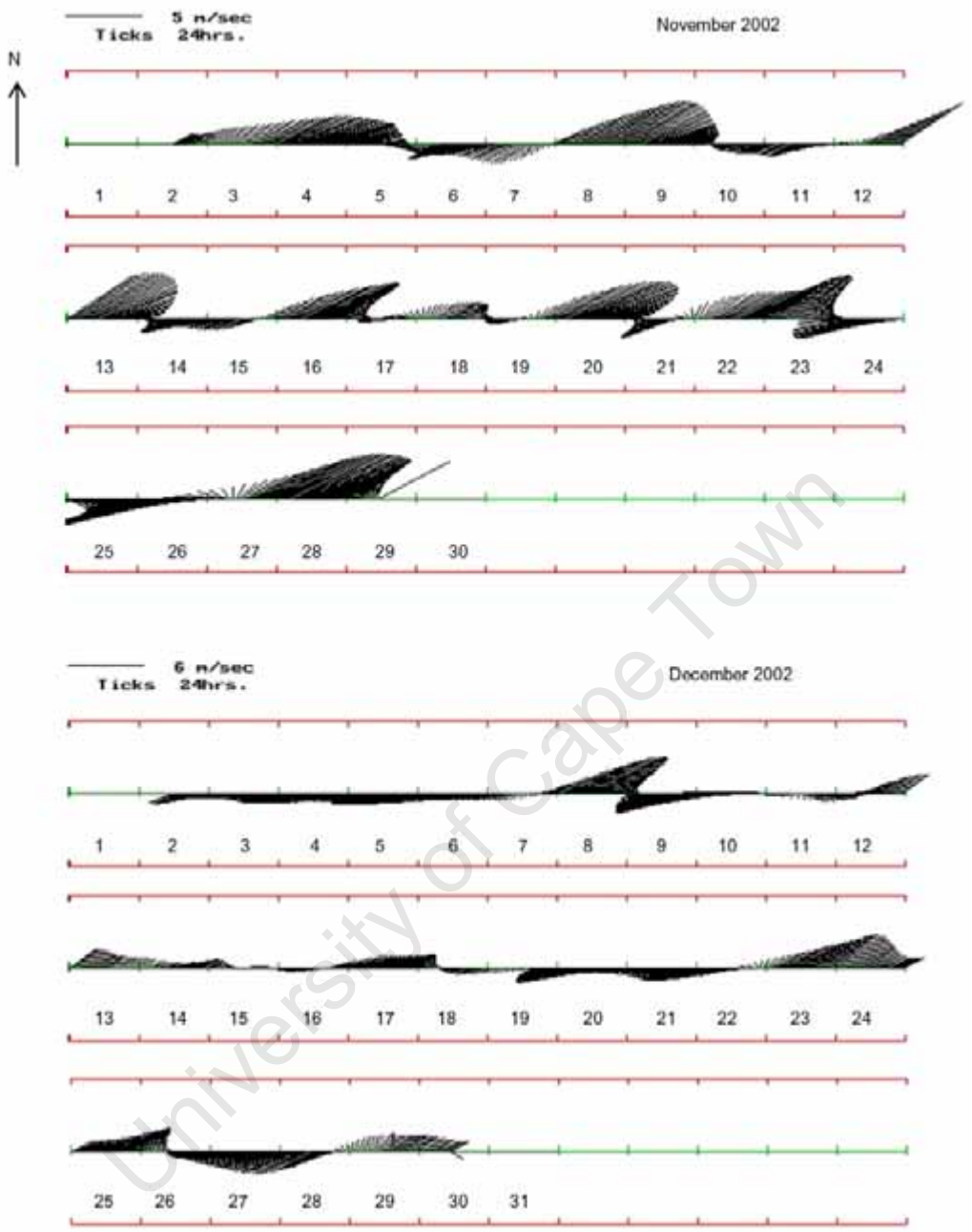

Figure 6.3: Winds measured at Storms River on the Tsitsikamma coast for November and December 2002 (see Figure 6.1a for location). Middlebank is 1.5 km offshore from here. The filter (see methods) used on the data eliminates vectors for the first and last days of the month and has a tendency to decrease wind velocity.

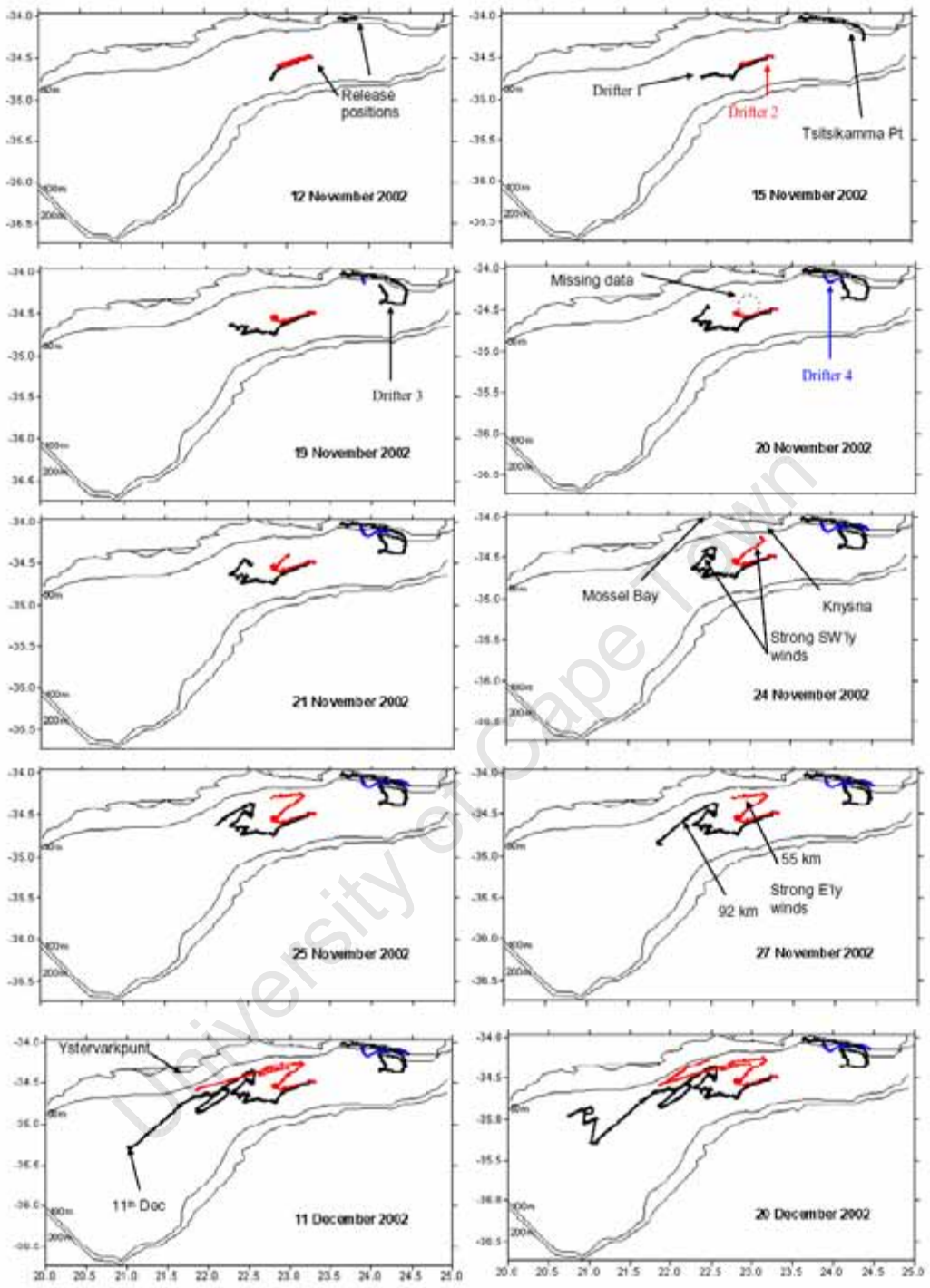

Figure 6.4: Selected time frames for all four satellite drifter tracks. Note that data gaps in the tracks have been filled using linear interpolations.

(see Figure 6.5b). A connection with an onshore event a few days previous could imply Coastal Trapped Wave (CTW) forcing.

Drifters 1 and 2

The tracks of the surface (Drifter 1) and deep (Drifter 2) drifters on the mid shelf initially showed westward movement under the moderate north-easterly wind on 11 November and followed the southward curvature of the shelf edge with velocities of about 31 cm s^{-1} and 30 cm s^{-1} respectively (Figures 6.1a, 6.4), strongly suggesting barotropic conditions. This initial trajectory supports the general westward flow observed in the ship-borne ADCP data (Figure 6.2). The drifters then underwent a number of reversals of varying distances (i.e. in a north-east direction), the longest being 43 km between 19 and 23 November (Days 9 and 13).

Closer examination shows that these track reversals corresponded with strong south-westerly wind events measured by the AWS on the Tsitsikamma coast (see Figure 6.3). For instance on 19 November (Day 9) the wind was light and variable. Drifter 1 was travelling directly westward across the shelf and no longer followed the south-westward curved bathymetry of the shelf edge. Drifter 2 at the time was semi stationary. Late on 19 and then 20 November the wind changed to a strong (~6 m s^{-1}) south-westerly. Both the surface and deep drifters responded by moving eastwards for some 20 km. Wind on 21 November returned to light conditions with the drifters then semi stationary. Similar eastward movement of the drifters was again observed when the next strong south-westerly wind followed on 22 and 23 November. This time the bottom drifter moved the furthest by some 20 km. Such response is understandable for the near-surface layer but not for the deeper layers of the water column and raises concern about the influence of wind on the floats. Of course it is possible that this is evidence of the bottom layer responding to an atmospheric pressure change at sea level (i.e. a cold front approaching), which could change the water pressure gradient and hence background current.

The effect of these track reversals was a net northward encroachment towards the coast (see Figure 6.4, 24 November). Overall the deep and surface drifters tended to move in tandem but the latter track was usually more exaggerated than the bottom as a result of the greater velocities. By 24 November (Day 14) both drifters were close to the 100 m isobath between Knysna and Mossel Bay and about 80 km apart, well away from the shelf edge. This is the usual position of the cold ridge (see Chapter 2; Figure 6.1a; Largier and Swart 1987; Shillington and Boyd 1994). Between 24 and 26 November a strong easterly wind blew (~6 m s^{-1}; the strongest in November) which moved the drifters westwards until the wind changed on 27 November yielding a distance of 92 km for the surface drifter and a velocity of about 30 cm s^{-1}. The bottom drifter moved 55 km with a lower velocity of about 20 cm s^{-1}. These trajectories are of interest because the south-west flow of water here is what Chapter 2 suggested was required for the formation of the cold ridge described as an upwelling filament.

Between 28 November and 11 December (Days 18 and 31) both drifters continued to edge their way westwards. The deep drifter reached a position 22 km off Ystervarkpunt

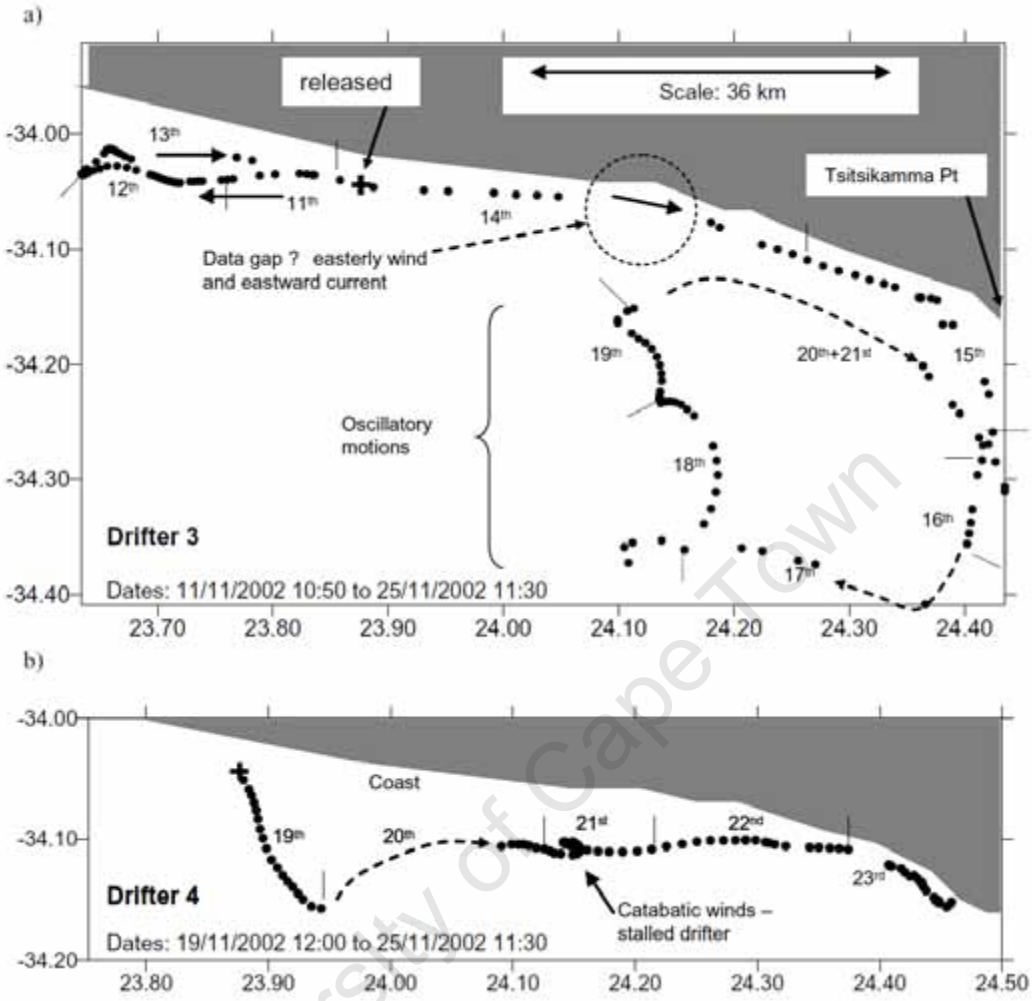

Figure 6.5: Expanded view of the inshore drifter tracks on the Tsitsikamma coast. The "**+**" indicates the release position for both drifters which is directly above a bottom-mounted ADCP in 36 m. Dates in November 2002 are indicated. (a) Drifter 3 first travelled westwards to return directly over the ADCP mooring and then parallel along the Tsitsikamma coast. It turned offshore on 15 November at Tsitsikamma Point and completed two clockwise gyrations before leaving the shelf. Inertial motions were observed on 19 and 20 November. The data gap (dashed circle) was caused by opposed wind and current. (b) Drifter 4 also moved eastwards along the coast but ran aground at Tsitsikamma Point on 23 November. The small direction reversal on 21 November was coincident with a strong breeze. Interestingly, this was not observed in the ADCP data i.e. stick vectors (Figure 6.6b) suggesting it was localised.

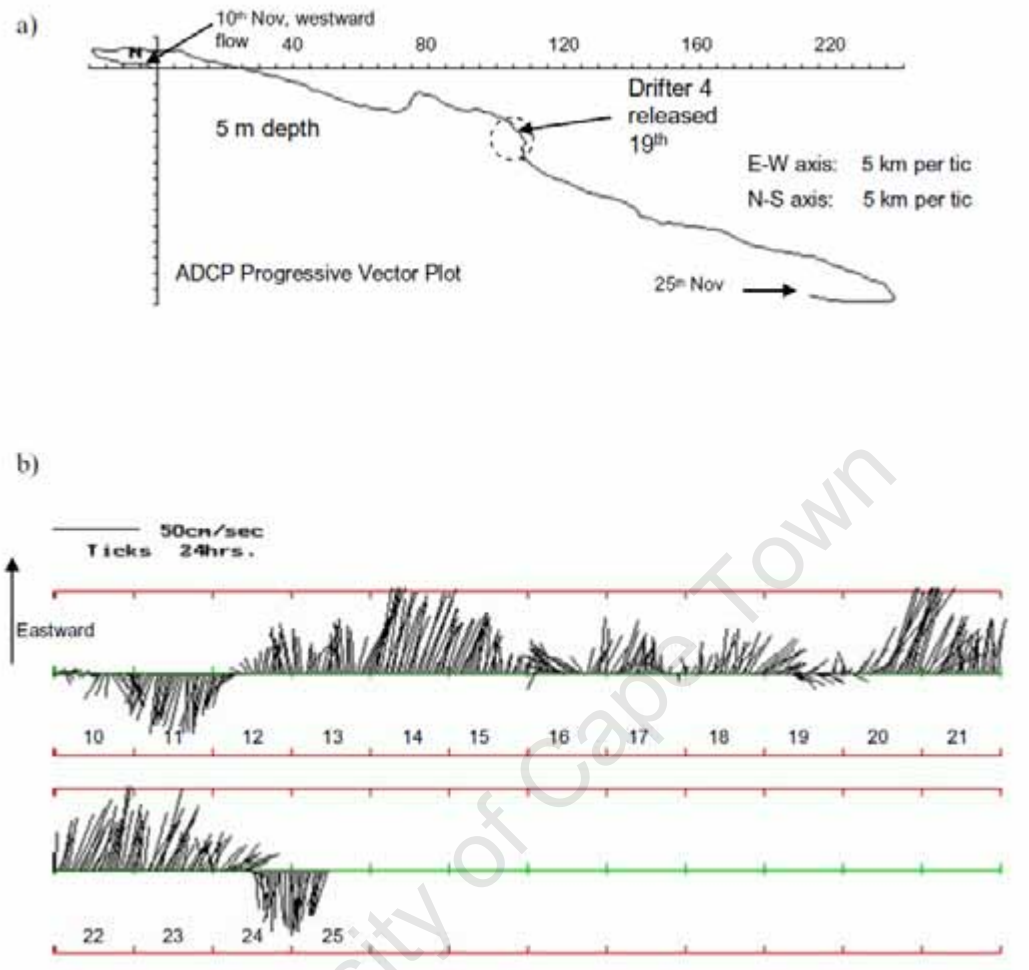

Figure 6.6: ADCP data collected at Middlebank (see Figure 6.5a for position). (a) ADCP data between 10 and 25 November presented as a progressive vector plot. Note true north is towards the top of the page and the origin of the plot coincides with the position of the ADCP mooring. Initial flow was westward but became eastward on 12 November and parallel with the coast. Drifter 3 was released at the beginning of this data set with the release of Drifter 4 midway. (b) The same ADCP time-series as above but presented as stick vectors. Note the orientation of the plot is such that eastward flow is to the top of the page.

(21.7 ºE; see Figure 6.4, 11 December for location) after which it turned eastward and headed back towards Mossel Bay and was picked up by a fishing vessel on 20 December (Day 40) having moved a linear distance of 100 km from the place of release. It is noteworthy that Drifter 2 moved eastwards between Ystervarkpunt and Mossel Bay. This is where averaged ADCP ship data collected by Boyd and Oberholster (1994) showed a short eastward current, which Chapter 2 speculated would move squid paralarvae hatched in this area towards the cold ridge where food abundance is generally highest on the Agulhas Bank. The change in direction of the deep drifter to eastward travel was initially coincident with a 3–4 m s^{-1} south-westerly wind but the remainder of the eastward track occurred under light and variable winds (see Figure 6.3). Wind during this period was clearly not a factor in this drifter track reversal.

On 11 December (Day 31; Figure 6.4), the surface drifter (Drifter 1) had reached a position in the middle of the central Bank having followed approximately the southward curved 100 m isobath. Here it became thwarted in its steady westward progression and instead moved directly inshore for 55 km between 14 and 18 December (Days 34 and 38). On Day 40 the drifter was still in this vicinity and remained here until 25 December (Day 45) where after it followed a direct route westwards across the inshore region of the western Bank to leave the shelf edge at 35º S. The drifter continued into the Atlantic Ocean on a curved northward course to reach a position 132 km directly west of Cape Point on 15 January 2003 (Day 67). Later communication showed the drifter to have moved up the west coast following similar trajectories as those observed by Largier and Boyd (2001).

High frequency drifter motions

Although not obvious in Figure 6.1a, a closer look at the data reveals at times small anticlockwise circular trajectories in both mid shelf drifter tracks (Drifters 1 and 2). The best example of these is found in the track of Drifter 1 whilst on the inner central Bank (indicated by the box in Figure 6.1a). Figure 6.1b shows an enlargement of this area. The oscillations became obvious late on the 21 December and lasted until the 25 December. This period corresponded with a 5 m s^{-1} south-westerly wind which peaked in wind velocity on the 23 December (Figure 6.3). (Note that this peak occurred on 24 December in the AWS record but the wind takes a day to reach Tsitsikamma from the central Bank). The emergence of the two distinct anticlockwise oscillations later on the 23 December (Figure 6.1b) after the peak wind speed suggests that these motions were inertial. Certainly their period, i.e. ~23 h, corresponds with the inertial period for this latitude ≈ 21 h.

Largier and Boyd (2001) found similar high frequency motions in a comparable drifter study on the west coast during the winter of 1999. These were observed sporadically along the entire shelf and also lasted for 3–5 days. The authors undertook an analysis of drifter velocity and found near-diurnal cycles characteristic of inertial motions in the southern hemisphere at these latitudes. They suggested that these followed distinct increases or decreases in wind force, advocated in text books such as Dietrich *et al.* (1980).

Alternatively, the motions in Figure 6.1b could be turbulence induced created by the intrusion of oceanic water onto the western Bank (see Figure 6.8), although similar oscillatory motions observed on the 18 November on the eastern Bank in the tracks of Drifter 1, 2 and 3 (see Drifter 3 in Figure 6.5a) suggest otherwise.

Discussion

Drifter Performance

Of fundamental importance in this experiment is whether the satellite drifters reliably depicted the currents to which they were "anchored" and hence provide Lagrangian measurements of transport. Equally, the reliability of using progressive vector projections for displacement (transport) based on moored current meter measurements in Chapter 3 also needs to be examined.

Inshore drifters

On several occasions the performance of the inshore drifters could be assessed by making comparisons with the ADCP deployed at Middlebank.

For instance on 11 November Drifter 3 was released directly above the ADCP mooring under a light to moderate 3 m s^{-1} easterly wind. The first hourly measurement made by the ADCP indicated a westward current of 37 cm s^{-1} at a depth of 5 m. Five meters was mid depth of the holey-sock drogue of Drifter 3 which had moved at an average velocity of 35 cm s^{-1} over the first 2 h. Three days later on 14 November, under a 2–3 m s^{-1} easterly wind, Drifter 3 back-tracked over the ADCP mooring travelling in an eastward direction with an average 24 h velocity of 48 cm s^{-1}. The average velocity for the same period measured by the ADCP at 5 m was 49 cm s^{-1}. The progressive vector plot based on the ADCP measurements for this 24 h period yielded a displacement of 37 km. The distance travelled by Drifter 3 was 36 km with the difference in direction being about 6° over this distance.

Drifter 4 was released on 19 November similarly under light (1–2 m s^{-1}) easterly wind conditions which became strong south-westerly after mid day. At deployment, a two hour average velocity of 14 cm s^{-1} was measured by the ADCP at 5 m. Drifter 4 for the same period showed an average of 13 cm s^{-1}. On the fourth day after release (22 November) Drifter 4 was some 30 km east of the ADCP. Wind at the time was 4 m s^{-1} south-westerly. The 24 h ADCP average velocity was 38 cm s^{-1} compared to the drogue average of 32 cm s^{-1}.

These comparative results provide assurance that under light to moderate wind conditions, both with the current in sympathy with wind and opposed, drifters of the holey-sock design provide reliable measurements of the near-surface current. Also progressive vector plots used to project displacement from a single current meter can be used to simulate transport but clearly are limited to straight coast lines and understandable become inaccurate with greater projection time span.

Mid shelf drifters

The surface drifter on the mid shelf indicated unquestionably that the net flow during November 2002 was westward despite the wind regime for this month being dominated by opposing south-westerly winds. But the size of both the surface and deep drifter track reversals suggests substantial current reversals which include at least the upper portion of the bottom layer on the eastern Agulhas Bank, assuming a thermocline at a depth of ~ 30 m. Interestingly, similar reversals were not seen in the inshore drifter tracks off Tsitsikamma but this could be because strong opposing winds (> 6 m s^{-1}) were not experienced during their release and occupation of the coastal zone. Without current meter measurements beneath the mid shelf drifters, it is impossible to verify that these reversals were indicative of actual currents. Instead, we have to use theory.

There are a number of theoretical mechanisms through which wind can impact flow in the surface layer of the ocean. Two of the more important are Ekman drift (Ekman 1905) and Stokes drift (1847). Stokes drift is caused by wind induced waves and the associated incomplete closure of the vertical orbital paths of water particles in the surface layer. This results in a near-surface current moving in the direction of wave propagation. Application of Coriolis wave stress theory on the other hand eliminates Stokes drift as a mechanism to explain the track reversals because it drives a current that oscillates at the inertial period but has a mean flow that exactly mirrors the Stokes drift (Ursell 1950; Pollard 1970; Hasselmann 1970). Therefore, the total wave-averaged current regime, after including the Stokes drift, is one that oscillates at the inertial period but with no net transport i.e. Stokes drift is exactly cancelled by its mirror image generated by the Coriolis wave stress.

In the case of Ekman drift, wind in the southern hemisphere sets up in the upper layer a left rotating current spiral which exponentially decreases in velocity with depth to the bottom of the Ekman layer (DE). The direction of the current at the surface is given to be 45° to the left of the down wind direction (southern hemisphere) and its velocity by:

$$V_0 = \frac{0.0127}{\sqrt{\sin|\varphi|}} U_{10}$$

Where φ is the latitude and U_{10} the velocity of the wind measured 10 m above sea level. The depth of the Ekman layer (D_E) is found using:

$$D_E = \frac{7.6}{\sqrt{\sin|\varphi|}} U_{10}$$

Substituting a wind speed of 6 m s^{-1}, V_0 = 0.10 m s^{-1} and D_E = 60 m for the latitude of 35° S (approximate latitude of drifters). At an increased wind speed of 10 m s^{-1}, V_0 = 0.17 m s^{-1} and D_E = 100 m.

A number of *in situ* experiments have attempted to verify Ekman theory. Examples include Davis *et al.* (1981) who measured currents between 2–175 m using 19 vector-measuring current meters deployed from a mooring for 19 days in 1977 in the northeast

Pacific. Weller and Plueddmann (1996) measured currents between 2–132 m using 14 vector-measuring current meters deployed from the Floating Instrument Platform FLIP in 1990 some 500 km off California. Ralph and Niiler (2000) tracked 1503 drifters with drogues at 15 m in the Pacific between 1987 and 1994. Results indicated that inertial currents are the largest component of the flow and that the flow is nearly independent of depth within the mixed layer for periods near the inertial period, i.e. the mixed layer moves like a slab at the inertial period. Current shear is concentrated at the top of the thermocline. The flow averaged over many inertial periods is almost exactly that calculated from Ekman's theory. The shear of the Ekman current extends through the averaged mixed layer and into the thermocline. In particular, Ralph and Niiler (2000) adjusted the above equations to fit their observations by decreasing the numerators to 0.0068 and 7.12, respectively. This meant that the Ekman layer depth D_E is almost exactly that proposed by Ekman (above equation) but the surface current V_0 is half his value. Moreover, they calculated transport is 90° to the right of the wind in the northern hemisphere, which agrees well with Ekman's theory.

Application of the modified equations to the Agulhas Bank finds that V_0 = 0.09 m s^{-1} and D_E = 94 m for a strong 10 m s^{-1} wind. This means that we should still observe a westward going current in the presence of an unchanged pressure gradient (background current). In other words, a near-surface velocity of ~ 31 cm s^{-1} would be reduced to ~ 21 cm s^{-1}, but Ekman mass transport would induce a north-westerly drifter track (acts at 90° to the down wind direction). For the deeper drifter the reduction in westward current would be less, especially considering that a component of the Ekman current theoretically would reinforce the pressure gradient current near D_E. This is not observed in the surface and bottom drifter tracks in this study and must mean that either the pressure gradient reversed causing the track reversals or that the drifters where dragged in a breaking sea. This argument can be strengthened considering the large track reversals are not seen in December when south-westerly winds were less frequent and their wind speeds much lower.

In conclusion, it is likely that strong winds (*c.* > 6 m s^{-1}) on the mid shelf with large breaking seas tended to drag the drifters downwind, particularly obvious between 19 and 24 November, resulting in the observed surface and deep drifter track reversals. Conversely in the case of the strong north-easterly wind between 24 and 26 November (i.e. cold ridge area), drifter track velocities were probably exaggerated by the wind drag given that the pressure gradient remained to the west. The similar behaviour of the surface and deeper drifters in November suggests that the drogue of the latter was pulled higher into the water column during these times and therefore was not indicative of the bottom current. Nonetheless, the obvious separation of the two drifters means that at other times the deeper drifter was definitively influence by subsurface flow.

Larval transport in coastal waters

Chapter 3 attempted to estimate squid larval transport along the Tsitsikamma coast using measurements from the bottom-mounted ADCP deployed on Middlebank. The data was

portrayed as progressive vector plots as a means of estimating displacement, and assumed squid paralarvae to be passive, neutrally, buoyant for 30 days and to mainly occupy the upper layer of the water column. The data suggested transport to be mainly eastward with potential distances ranging up to 550 km from Middlebank. Literally interpreted this meant squid paralarvae could be transported as far east as Port Alfred and East London (Figure 6.1a) where indeed a few paralarvae have been sampled in a survey (see Chapter 4, Figure 4.1 and Augustyn *et al*., 1994). Coastal upwelling was also shown to temporally influence the eastward Tsitsikamma counter current causing offshore flow with potential displacement of 40 km. Eastward flow was found to return to the coastal current with relaxation of the upwelling process (and onset of westerly winds), suggesting that squid paralarvae may well be transported offshore onto the mid shelf and returned into the eastward coastal counter current upstream i.e. they are carried in a clockwise circle. This supported earlier work by Tilney *et al.* (1996) who postulated that such "current-closure scenarios" existed on this coast. Unfortunately, it was not possible to use the squid paralarvae ROMS–IBM (Chapter 5) to verify these results because of inadequate resolution at the coast and model boundaries conditions.

The use of drifters however, has made it possible to test the transport scenarios near the coast. The results confirmed the existence of a coastal counter current off the Tsitsikamma coast, and for short distances of up to 50–60 km, the use of progressive vector projections to gauge transport can be appropriate but become unrealistic beyond these dimensions. Certainly, as demonstrated by Drifter 3, the progressive vector displacements in Chapter 3 were unable to contend with the realities of bathymetry such as Tsitsikamma Point and the offshore movement of water there. The complexity of this offshore flow is seen in Figure 6.7b where a cyclonic swirl is evidently responsible for the circular track of Drifter 3. (Satellite altimetry data also indicated a localised lower SSH here at the same time.) Whether this is a common phenomenon, and hence, the usual end of the Tsitsikamma counter current has yet to be established. The swirl, it would appear from Figure 6.7c, existed for more than 10 days and remained stationary suggesting it could be a lee eddy created by the westward shelf flow moving past Seal Point (Figure 6.7c).

Alternatively, as noted above, coastal upwelling could have caused the offshore movement of Drifter 3. For example Chapter 3 showed in Figure 3.9a (SST imagery) the emergence of a westward curved plume of cold water extending 10–15 km offshore from Tsitsikamma Point. A drifter in this is expected to have a similar trajectory as seen in Figure 6.5a, although the upwelling event would need to be much larger to account for the dimension of this track. Upwelling as the mechanism for offshore movement of the drifter was plausible because a light north-easterly wind was blowing at the time. But examination of temperature records from an Underwater Temperature Recorder (UTR) at Middlebank (data not shown) and SST imagery in Figure 6.7b, showed no signs of coastal upwelling on 14 and 15 November leaving the swirl as the accountable mechanism.

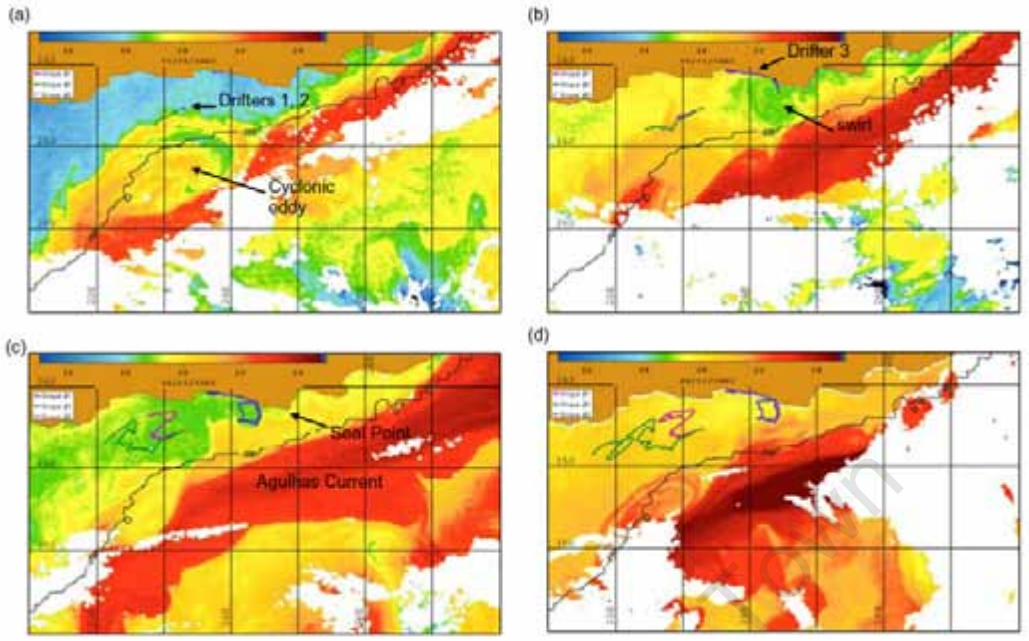

Figure 6.7: Selected daily AVHRR SST images of the eastern Agulhas Bank. The Agulhas Current (> 23°C) is clearly seen flowing along the shelf break with the shelf water ranging between 18–20°C. (a) On 11 November the Agulhas Bight cyclonic eddy was seen sweeping onto the shelf with Drifters 1 and 2 only a few kilometers north of the thermal front. Drifter 3 was travelling westwards close to the Tsitsikamma coast. (b) On 15 November Drifters 1 and 2 were moving westwards on the mid shelf while Drifter 3 left the coast at Tsitsikamma Point under the influence of a meso-scale cyclonic swirl. (c) The cyclonic swirl still existed 11 days later (26 November) with Drifter 3 having completed 1½ gyrations shortly before communications failed. Drifters 1 and 2 had moved well inshore. (d) By Day 25 (4 December) the mid shelf drifters were separated by 170 km and well away from the Agulhas Bight eddy.

The fact that Drifter 3 left the inshore squid spawning grounds near Tsitsikamma Point and went so far south is perhaps the most significant but also surprising result from this experiment. Spawning on the inshore shelf of the Agulhas Bank has been seen by many researchers as being retentive for fish eggs and larvae (Tilney *et al.* 1996). The possibility of paralarvae being lost from the inshore chokka squid spawning grounds has been suggested in Chapter 4 but this was thought to happen further east in the vicinity of Algoa Bay and beyond where the Agulhas Current is closer to the coast (Goshen and Schumann 1988). Mechanisms responsible for loss of shelf water and squid paralarvae are discussed later.

Larval transport on the mid shelf (ROMS–IBM model validation)

In the absence of behavioural information on chokka squid paralarvae, the first ROMS–IBM dispersion experiment treated hatchlings as virtual particles of neutral buoyancy lasting 40 days (Chapter 5). Five thousand individuals were released every second day for 12 "model" months in the bottom layer (~120 m) at three single point locations on the mid shelf. Results overall indicated the potential for considerable loss of paralarvae from the Agulhas Bank ecosystem through three routes: (1) mid way on the western Agulhas Bank shelf edge between the southern tip of the Agulhas Bank and Cape Point, (2) immediately south of Cape Point, and (3) off the eastern Agulhas Bank via the Agulhas Bight cyclonic eddy (Lutjeharms *et al.* 2003). The central Agulhas Bank was observed to have better larval retention since most of the virtual particles moved onshore and entered the coastal region of the central and eastern Banks.

Absent in the ROMS-IBM was north-westward advection of particles along the narrowing outer western Agulhas Bank, as suggested by Chapter 4, where assessment was based on current meter data collected by Largier *et al.* (1992). Together with similar supportive data collected by the CSIR[2] on the outer central Agulhas Bank (CSIR report 1986), Robert and van den Berg (2002) anticipated that shelf water on the eastern Agulhas Bank flows westward around the central Agulhas Bank then continues as a north-westward flow on the western Agulhas Bank towards Cape Point. Squid paralarvae on the mid shelf of the eastern Bank (i.e. deep spawning grounds) are expected to follow this route if not retained near the cold ridge (Boyd and Shillington 1994; Chapter 2).

This flow pattern is also thought to exist by others e.g. Shannon *et al.* (1996), Boyd and Oberholster (1994), and Hutchings *et al.* (2002). But Chapter 4 did note that larval loss was occasionally possible on the eastern Agulhas Bank through offshore directed filaments of shelf water observed in satellite imagery (see Chapter 4, Figures 4.9, 4.10). Nonetheless, it still came as a surprise to observe the majority of ROMS–IBM virtual particles released on the eastern Agulhas Bank being advected eastwards to the model perimeter at 25˚E, and then offshore into the boundary zone of the Agulhas Current, and ultimately lost from the ecosystem.

2 Council for Scientific and Industrial Research.

At first glance the results from this drifter study seemed to contradict those of the ROMS–IBM, and instead strengthen the claim of westward transport on the eastern Bank mid shelf. The ADCP ship data collected during drifter deployment add support for this contradiction in that the flow on the eastern Agulhas Bank is seen to be barotropic (Figure 6.2). (This is similarly seen to some degree by the deep drifter despite the influence of strong south-westerly winds on drifter performance). In terms of the "40 day drifter—IBM comparison" the mid shelf drifters did not leave the shelf and instead moved inshore. By Day 40 the deep drifter was off Mossel Bay in less than 100 m and its surface counterpart was in the middle of the central Agulhas Bank similarly in 100 m. While it is acknowledged that a drifter of such proportions is far from an impersonation of a squid paralarvae 2.5–3 mm in length, these devices have demonstrated that paralarvae in the upper water column, hatched in the vicinity of the release position, could have been retained on the Agulhas Bank during November/December 2002. This verdict is strengthened when considering that the chosen time span of 40 days for paralarval passive dispersion is possibly too long and could in reality be as short as 20–30 days.

The drifters also demonstrated that squid paralarvae hatched near the 10 November would have been transported to the position of the cold ridge. This supports the "westward transport hypothesis" proposed in Chapter 2, which states that chokka squid spawning relies on the westward drift on the eastern Agulhas Bank to transport new hatchlings to the cold ridge region where food is more abundant (Huggett and Richardson 2000). Although in this case (November and December 2002), neither SST imagery nor *in situ* SST data showed any hint of cooler surface water here, which usually is indicative of the cold ridge. This is understandable since wind data in Figure 6.3 shows very little easterly winds which are required to drive coastal upwelling and the cold ridge (Chapter 2).

The apparent conflict of results from the drifter experiment and the IBM i.e. westward transport with retention vs. eastward transport with shelf loss, however, can be resolved to a large extent by closer examination. Inspection of the ROMS output indicated the presence of a large cyclonic eddy in the Agulhas Bight which also occupied most of the shelf edge of the eastern Bank in the model domain i.e. up to ~24˚E. Lutjeharms *et al.* (2003) had also noted this feature in the model and showed that it escaped down stream from time to time. Superimposing the release positions of Drifters 1 and 2 on the same day SST image (Figure 6.7a) revealed that they were deployed only 1–2 km from the edge of a large Agulhas Current cyclonic eddy located in the Agulhas Bight, as simulated in ROMS. The SST imagery showed the eddy influencing a considerable portion of the outer shelf including some of the mid shelf. Should the drifters have been deployed a little further south, then it is highly probable that they would have been advected eastwards in this cyclonic eddy and yielded very similar results as the ROMS–IBM. This implies that the cyclonic eddy in ROMS is exaggerated and encroaches too far onto the mid shelf compared with reality.

Beyond 40 days (offshore leakage of shelf water)

Drifter 3

A large data gap exists for inshore Drifter 3 between the last mid shelf position on Day 16 (26 November) and the next reported position some 400 km south of the continent on Day 71 (21 December) near the Subtropical Convergence. This is unfortunate because the route off the shelf and the time of exit are unknown, and hence important information leading to an understanding of shelf water leakage has been lost. Nonetheless, some insight into the mechanisms responsible for the drifter's removal from the Agulhas Bank can be provided by satellite imagery, and it appears there are two.

The first involves leakage of shelf water from the Agulhas Bank via filaments which extend southwards off the shelf edge mainly in the vicinity of 21° E (i.e. tip of the Agulhas Bank). Daily SeaWIFS ocean colour images for January 2003, examples of which are depicted in Figure 6.8, showed the existence of chlorophyll filaments which extended from the typical cold ridge position on the mid shelf, distances of 100–300 km south of the shelf edge (see Chapter 2 for details of the cold ridge). These filaments were stretched along the north-western boundary of the Agulhas Current. In all four images depicted in Figure 6.8, elevated chlorophyll streaks can be seen on the shelf indicating the existence of the cold ridge. From their south-westward, at times curved orientation, it is clear that biologically active shelf water was at the time being drawn off the shelf to form these filaments.

It is appropriate here to recall the work in Chapter 2 in which it was demonstrated that the cold ridge was a cold water filament that originated at the coast as a result of wind driven coastal upwelling. It was suggested that this water was transported onto the mid shelf by the westward bound flow coming from the eastern Bank. This explained the "classic" diagonally aligned (SW–NE), at times curved, shape of the cold ridge. It was noted in the data (Figures. 2.10a, 2.11), however, the existence of the Agulhas Bight cyclonic eddy at the time, and its possible interplay with the cold ridge. In this satellite imagery analysis we similarly note the eddy's presence, suggesting its movement of water onto the shelf, seen clearly in Figure 6.8d, plays a role in the formation of the classic cold ridge filament shape i.e. this eddy could be facilitating the offshore movement of shelf water on the eastern Bank.

The offshore chlorophyll filaments at the time of this drifter experiment appeared in the imagery around the 30 November (Day 21) and lasted in various forms such as those depicted in Figure 6.8 until about the 21 January. Given the last known position of Drifter 3 on the 26 November, and the appearance of these features, it is possible that Drifter 3 was swept westwards in the eastern Bank flow along with the chlorophyll enriched shelf water and then southwards off the shelf into one of these filaments. Once in the boundary zone of the Agulhas Current, it could be carried around the retroflexion, if it existed at that time, and then eastwards along the Subtropical Convergence. Some caution needs to be exercised with this argument because upwelling is known to occur in filaments and therefore not all the chlorophyll maybe from the Agulhas Bank.

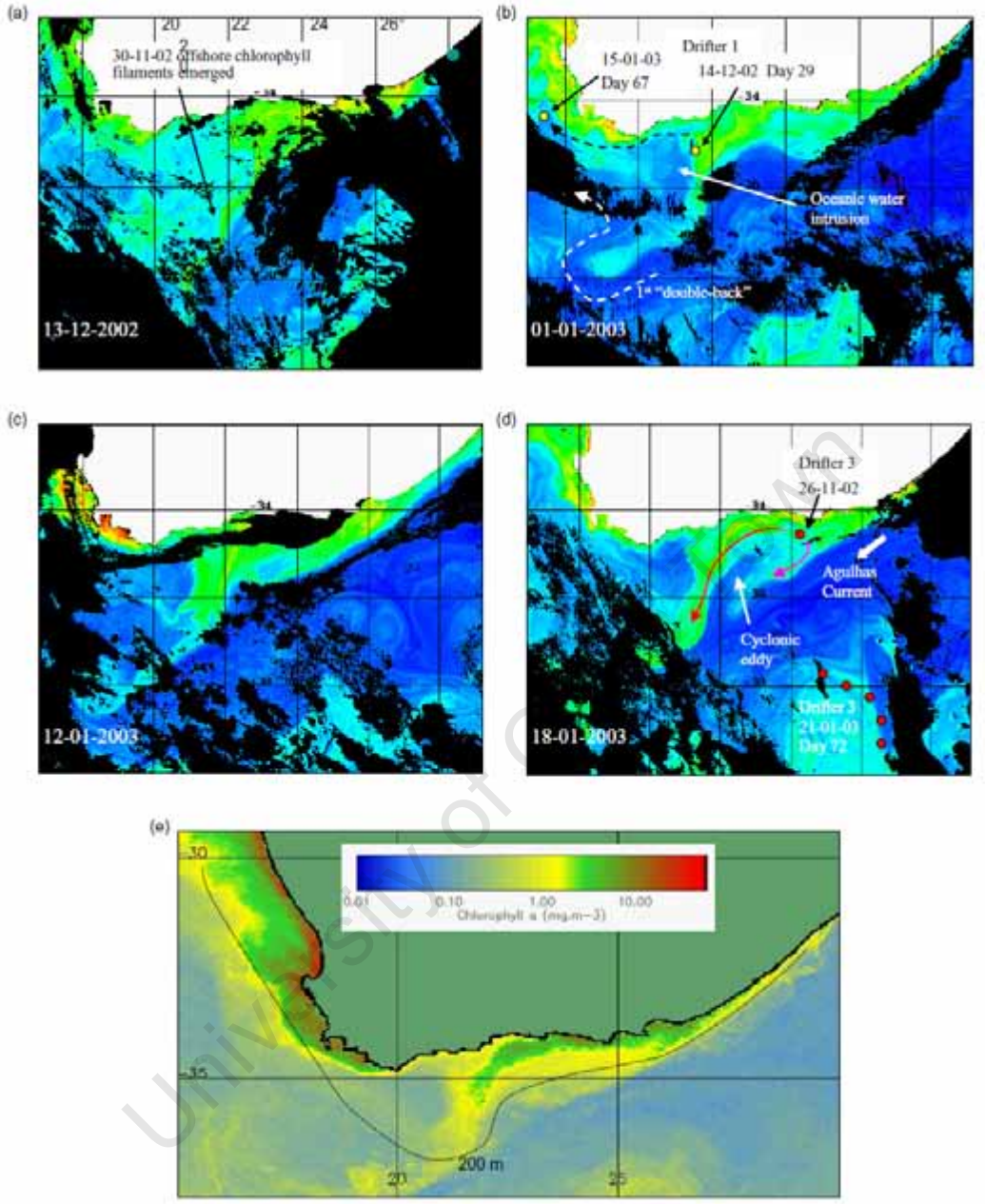

Figure 6.8: SeaWIFS ocean colour images. (a) Long filaments of chlorophyll (of shelf water origin) were observed to lead southwards off the shelf from 30 November. These stretched along the westward boundary of the Agulhas Current (deep blue). (b) A chlorophyll filament being drawn off the southern tip of the Agulhas Bank by the first "double back" current trajectory (see Figure 6.9b). (c) The Agulhas Bight cyclonic eddy drawing in shelf water (high in chlorophyll) and the closure and disappearance of the first "double back" filament. (d) Another chlorophyll filament being drawn off the south tip of the Agulhas Bank into the second "double back". Routes by which Drifter 3 could have left the shelf are illustrated by the red arrows. (e) A composite of low resolution SeaWIFS GAC data for January 2003 highlights the semi-presence of chlorophyll filaments trailing southwards off the shelf (yellow in Figure).

Analysis of SST imagery showed that the Agulhas Current began to turn due south around the same time the chlorophyll filaments appeared in the SeaWIFs data. By the 5 December (Day 26) the current was in full reflection mode (see Figure 6.9a) and stayed in this configuration until about the 21st December (Day 40), where after, the retroflexion began to retreat and the core flow (warmest water) instead moved westward towards the Atlantic. In the process, the end trajectory of the current "doubled backed" eastwards on its northern side creating cyclonic flow (see Figure 6.9b). This configuration corresponded with the chlorophyll filament leading off the shelf depicted in Figure 6.8b, and existed between the 29 December and 4 January 2003. The "double-back" then moved away in a north-west direction expanding the configuration but also unfolding itself. On the 11 January, the Agulhas Bight semi-permanent cyclonic eddy was well formed with another "double back" cyclonic feature further down stream just west of the tip of the Agulhas Bank (Figure 6.9c,d). This similarly appeared to be the cause of the offshore chlorophyll filament seen in Figure 6.8c recorded on the 12 January. In contrast to the previous occasion, this "double back" formed a cyclonic eddy a few days later on the 24 January, which corresponded to the cessation of chlorophyll filaments off the Agulhas Bank.

This is not the first mention of shelf water leakage on the eastern Agulhas Bank. Chapter 4, also using SeaWIFS ocean colour imagery, noted that an unusual eastward position of the Agulhas Current retroflexion off Algoa Bay in April 1999 caused a spectacular chlorophyll filament to stretch southwards along the current's western boundary for some 200 km (see Figures 5.9a, b). A second offshore chlorophyll extension in the vicinity of the ones cited in this paper was also evident.

In the case of Drifter 3, it is unlikely that it was pulled off the shelf by the "double back" features, as these would have transported it into the Atlantic Ocean. Rather, it must have happened during the retroflexion mode in the first three weeks of December (Days 25–40). A simple trajectory calculation around the retroflexion to the Subtropical Convergence at an average speed of 80 cm s^{-1} (which maybe too slow) suggests the drifter left the shelf about the 11 January which is not possible given there was no retroflexion then and the existence of the "double back" features. It is also unlikely that the drifter would have crossed the main core of the Agulhas Current. This means that the drifter must have spent at least 30 days caught up in eddies and boundary like phenomena whilst being transported south.

Of course, given that offshore leakage occurs, the question is how often does this happen? Here SeaWIFS GAC (4 x 4 km) ocean colour data is useful. A monthly composite for the month of January 2003 which includes images discussed above (i.e. Figure 6.8b–d) produced a distinct plume of chlorophyll extending off the Agulhas Bank due to the persistence of these filaments during this period (Figure 6.8e). Although not a rigorous analysis, a search for similar patterns in a monthly GAC composite time-series between September 1997 and October 2004 (not depicted here) showed that this pattern is common, suggesting that shelf water leakage is frequent near the tip of the Agulhas Bank.

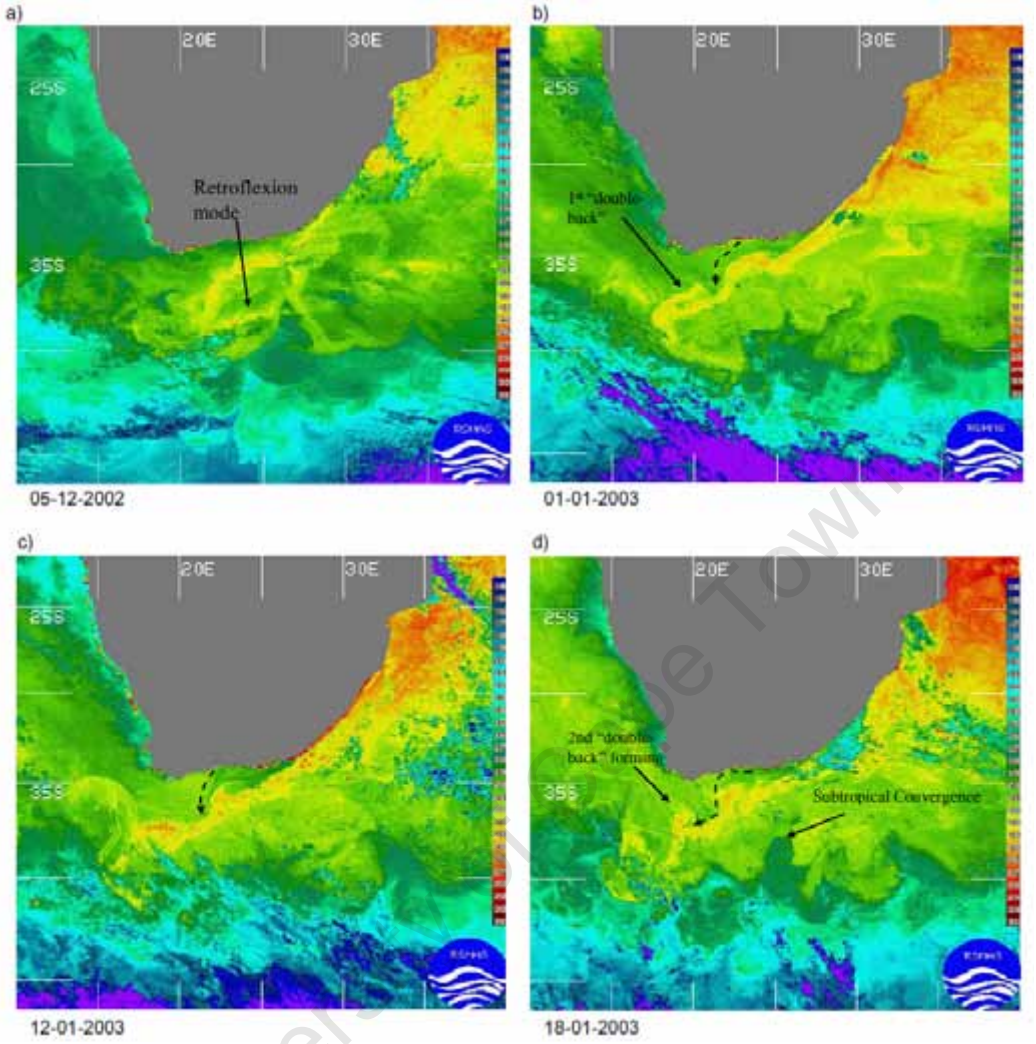

Figure 6.9: Selected daily AVHRR SST images from NOAA showing the Agulhas Current with a number of final flow configurations south of the Agulhas Bank. (a) Full retroflexion mode with warm water flowing along the northern boundary of the subtropical convergence. (b) Retroflexion has retreated and the core flow (warmest water) instead has moved westward towards the Atlantic, in the process creating a "doubled back" in the current trajectory on its northern side. This feature is seen to correspond with the chlorophyll filament leading off the shelf depicted in Figure 6.8b and black arrow. (c) and (d) A second "double-back" trajectory forming and drawing in a chlorophyll filament shown in Figure 6.8d.

While the offshore filament mechanism is a probable contender to explain the removal of Drifter 3 from the eastern Bank, there is another mechanism equally likely. This involves the drifter being drawn from the mid shelf into either the semi-permanent cyclonic eddy observed spinning in the Agulhas Bight (Figures 5.8c, 5.9a) or another cyclonic border eddy moving eastwards along the shoreward boundary of the Agulhas Current. Lutjeharms *et al.* (1989) has provided a good description of these phenomena and has shown that these features exist almost all the time when the current is against the shelf. At times, as many as three eddies can be observed between the Agulhas Bight and Algoa Bay. As seen in the example in Figure 6.8d, shelf water (chlorophyll) is entrained into these features. While this route might mean that the drifter would move around the eddy for a while, ultimately it would be carried away when the eddy escapes the bight, as demonstrated by Lutjeharms *et al.* (2003) using the ROMS adapted for this region. Given that the Agulhas Current in this case was in a retroflexion mode, the result would be transportation of the drifter to the Subtropical Convergence.

Given the above, it is a wonder that Drifters 1 and 2 were not pulled off the shelf by these filaments. Inspection of the tracks, however, shows that these two drifters by 30 November had moved westwards and well inshore away from the south-westward arching offshore flow of shelf water.

Drifter 1

Another unexpected result in this experiment was the westward traverse of Drifter 1 across the central and western Agulhas Bank and its exit on 6 January 2003 (Day 58) from the shelf south of Cape Point. Its last reported position shown in Figure 6.1a was 132 km west of Cape Point on 15 January 2003 (Day 67). The exit position is of interest because this is a shelf leakage point identified in the ROMS (Chapter 4, Figure 4.10; Penven 2000) and the coupled IBM (Chapter 5), and verifies the model's performance in this regard. The traverse is unexpected because it crosses the distinct inner central Bank where water flow is thought to be subdued as indicated by the low bottom dissolved oxygen levels experienced during the summer months and the net low current velocities (Chapter 2; Eagle and Orren 1985; Chapman and Shannon 1987). As already mentioned, typically it is thought that eastern Bank water flows around the inner central Bank (outside of the 100 m contour) and onto the western Bank (Chapter 2; Largier *et al.* 1992; Boyd *et al.* 1992; Boyd and Oberholster 1994). So why did Drifter 1's track not follow this conventional flow model?

Again SeaWIFS ocean colour satellite imagery is useful here and in this case is more informative than SST. The imagery showed that around mid December a distinct body of water with low chlorophyll levels occupied the entire western Bank as far east as ~ 22° E (see Figure 6.8b). This body was easily distinguished from the water on the eastern Bank and was likely of oceanic origin. At the time the Agulhas Current was in retroflexion mode (noted above) with chlorophyll filaments leaking (streaming) southwards off the shelf (see Figure 6.8a). Around 29 December, new oceanic water identified by extremely low chlorophyll levels,

was observed moving into this same area from the west leaving a narrow band of coastal water (higher chlorophyll levels) along the coast between Cape Point and Struiss Bay (see Figure 6.8b,c,d). This was especially evident around 11 January when the second Agulhas Current "double back" was forming (see Figure 6.9c,d). The oceanic body of water appeared to reinforce the southward funnelling of eastern Bank water into the leakage filaments described earlier, and resided on the western Bank until about 27 January. This is also observed in the monthly GAC ocean colour composite (Figure 6.8e).

On 14 December (Day 29), Drifter 1 located at 21.5° E was seen to move abruptly northwards, no doubt pushed by the first intrusion of oceanic water (low chlorophyll levels) onto the western Bank. By 20 December the drifter was well on its way westwards across the western Bank moving along the interface between the oceanic and shelf waters, indicating anticyclonic circulation in this region (this is confirmed by a deepening of the thermocline on the western Bank, not shown here). The departure of Drifter 1 from the shelf just south of Cape Point clearly demonstrated the return of this water to the Atlantic Ocean.

Conclusions

Satellite tracked drifters are clearly poor imitations of squid paralarvae, and as experienced in this study, can be prone to surface drag during very rough tumbling seas. During calmer seas, however, they proved to represent horizontal water movement quite accurately, and therefore, can provide useful insight into the Lagrangian behaviour of passively drifting material such as early larvae in the upper layers of the water column.

In this study, tracks of both the surface and deep mid shelf drifters have convincingly demonstrated the potential for paralarvae hatched on the mid shelf of the eastern Agulhas Bank — but shoreward of the Agulhas Bight semi-permanent shelf edge cyclonic eddy — to be transported westwards and retained in the ecosystem near the cold ridge during their first 40 days. After this, it is believed that they become capable swimmers and no longer are dispersed by currents. This evidence supports the "western transport hypothesis" proposed in Chapter 2. Had the drifters been deployed a few kilometers further offshore, then it is highly likely that they would have been entrained into the Agulhas Bight cyclonic eddy and removed from the shelf as was so clearly revealed in the ROMS-IBM experiment in Chapter 5.

In contrast, squid hatchlings in the surface layer on the inner central Bank, at times used by squid as a peripheral spawning ground and thought to be a good retention area, would have been advected off the shelf in this instance caused by an intrusion of oceanic water onto the western Bank. This expulsion occurred in ~ 30 days and within the assumed "passive period" for loliginid squid paralarvae.

Paradoxically, the drifter representing near-surface paralarvae on the inshore spawning grounds off the Tsitsikamma coast left the shelf and headed into the southern ocean due to a propitious coupling of a small cyclonic swirl observed off Tsitsikamma Point at the end of the eastward coastal counter-current and deeper shelf edge boundary physical processes operating at the time. These involved an off-shelf directed filament which appears to be

common or entrainment into the Agulhas Bight cyclonic eddy. How often this set of circumstances occurs is unknown but clearly has the potential to negative impact recruitment.

In closing it is notable that large off-shelf chlorophyll filaments were observed in SeaWIFS imagery in 2000 during a time when the Agulhas Current retroflected east of its usual position (this usually occurs south of the Agulhas Bight), and that in 2001 the squid fishery almost collapsed with an annual catch around 3 200 t. The average catch is ~ 7 000 t with an all time high of 10 000 t in 2004.

References

Augustyn CJ, Lipinski MR, Sauer WHH, Roberts MJ, Mitchell-Innes BA. 1994. Chokka squid on the Agulhas Bank: life history and ecology. *South African Journal of Science* 90(3): 143–154.

Barrange M., Pillar SC, Hampton I. 1998. Distribution patterns, stock size and life history strategies of Cape horse mackerel *Trachurus trachurus capensis*, based on bottom trawl and acoustic surveys. *South African Journal of Marine Science* 19: 433–447.

Boyd AJ, Taunton-Clark J., Oberholster GPJ. 1992. Spatial features of the near-surface and mid water circulation patterns off western and southern South Africa and their role in the life histories of various commercially fished species. *South African Journal of Marine Science* 12: 189–206.

Boyd AJ, Oberholster GPJ. 1994. Currents off the West and South Coasts of South Africa. *South African Shipping News and Fishing Industry Review*, Sept/Oct: 26–28.

Boyd AJ, Shillington F. 1994. Physical forcing and circulation patterns on the Agulhas Bank. *South African Journal of Science* 90: 114–122.

Chapman P, Shannon LV. 1987. Seasonality in the oxygen minimum layers at the extremities of the Benguela system. *South African Journal of Marine Science* 5: 85–94.

CSIR report. 1986. Mossel Bay off-shore development project environmental data for design, vol. 3, current data. *CSIR Report* C/SEA 8643/3. December 1986. Stellenbosch, South Africa. 343 pp.

Davis RE, DeSzoeke R, Niiler P. 1981. Variability in the upper ocean during MILE. Part II: Modeling the mixed layer response. *Deep-Sea Research* 28 (12A): 1453–1475.

Dietrich G, Kalle K, Krauss W, Siedler G. 1980. Oceanography 2nd edn. John Wiley & Sons, Inc., New York. 626 pp.

Eagle GA, Orren MJ. 1985. A seasonal investigation of the nutrients and dissolved oxygen in the water column along two lines of stations south and west of South Africa. Research Report 567, *Council for Scientific and Industrial Research*, Stellenbosch, South Africa. 52 pp. + figs.

Ekman VW. 1905. On the influence of the Earth's rotation on ocean currents. *Arkiv for Matematik, Astronomi, och Fysik*: 2 (11).

Goschen WS, Schumann EH. 1988. Ocean current and temperature structures in Algoa Bay and beyond in November 1986. *South African Journal of Marine Science* 7: 101–116.

Haidvogel DB, Arango HG, Hedström KS, Beckmann A, Malanotte-Rizzoli P, Shcheptkin AF. 2000. Model evaluation experiments in the North Atlantic Basin: simulations in nonlinear terrain-following coordinates. *Dynamics of the Atmosphere and Oceans* 32: 239–281.

Hasselmann K. 1970. Wind–driven inertial oscillations. *Geophysical Fluid Dynamics* 1: 463–502.

Hugget JA, Richardson AJ. 2000. A review of the biology and ecology of *Calanus agulhensis* off South Africa. *ICES Journal of Marine Science* 57: 1834–1849.

Hutchings L. 1994. The Agulhas Bank: a synthesis of available information and a brief comparison with other east-coast shelf regions. *South Africa Journal Science* 90: 179-185.

Hutchings L, Beckley LE, Griffiths MH, Roberts MJ, Sundby S, van der Lingen C. 2002. Spawning on the edge: spawning grounds and nursery areas around the southern African coastline. *Marine and Freshwater Research* 53: 307–318.

Japp DW, Sims P, Smale MJ. 1994. A review of fish resources of the Agulhas Bank. *South African Journal of Science* 90: 123–134.

Kasai A, Kimura S, Nakata H, Okazaki Y, Kasai Y. 2002. Entrainment of coastal water into a frontal eddy of the Kuroshio and its biological significance. *Journal of Marine Systems* 37(1-2): 185–198.

Largier JL, Swart VP. 1987. East-west variation in the thermocline breakdown on the Agulhas Bank. *South African Journal of Marine Science* 5: 263–272.

Largier J, Chapman P, Peterson WT, Swart VP. 1992. The Western Agulhas Bank: circulation, stratification and ecology. *South African Journal of Marine Science* 12: 319–339.

Largier J, Boyd AJ. 2001. Drifter observations of surface water transport in the Benguela Current during winter 1999. *South African Journal of Science* 97: 223–229.

Lutjeharms JRE. 2001. Agulhas Current. In *Encyclopaedia of Ocean Science*. Steele JH, Thorpe SA, Turekian KK. Academic Press, San Diego. 104-113.

Lutjeharms JRE, Catzel R, Valentine HR. 1989. Eddies and other boundary phenomena of the Agulhas Current. *Continental Shelf Research* 9(7): 597–616.

Lutjeharms JRE, Penven P, Roy C. 2003. Modelling the shear edge eddies of the southern Agulhas Current. *Continental Shelf Research* 23(11-13): 1099–1115.

Mullon C, Fréon P, Parada P, van der Lingen C, Huggett J. 2003. From particles to individuals: modelling the early stages of anchovy in the Southern Benguela. *Fisheries Oceanography* 12(4/5): 396–406.

Parada CE. 2003. Modelling the effects of environmental and ecological processes on the transport, mortality, growth and distribution of early stages of Cape anchovy (*Engraulis encrasicolus*) in the Benguela system. Ph D thesis, University of Cape Town. [iii] + 123 pp.

Penven P. 2000. A numerical study of the southern Benguela circulation with an application to fish recruitment. Ph D thesis, University of Bretagne Occidentale, France. 189 pp.

Penven P, Roy C, Colin de Verdière A, Fréon P, Johnson A, Lutjeharms JRE, Shillington F. 2001. A regional hydrodynamic model of upwelling in the southern Benguela. *South African Journal of Science* 97: 472–475.

Pepin P, Helbig JA. 1997. Distribution and drift of Atlantic cod (*Gadus morhua*) eggs and larvae on the Northeast Newfoundland Shelf. *Canadian Journal of Fisheries and Aquatic Sciences* 54(3): 670–685.

Pollard RT. 1970. On the generation by wind of inertial waves in the ocean. *Deep-sea Research* 17(4): 795–812.

Ralph EA, Niiler PP. 2000. Wind-driven currents in the tropical Pacific. *Journal of Physical Oceanography* 29 (9): 2121–2129.

Roel BA, Hewitson J, Kerstan S., Hampton I. 1994. The role of the Agulhas Bank in the life cycle of pelagic fish. *South African Journal of Science* 90: 185–196.

Shannon LV, Nelson G, Crawford RJM, Boyd AJ. 1996. Possible impacts of environmental change on pelagic fish recruitment: Modelling anchovy transport by advective processes in the southern Benguela. *Global Change Biology* 2: 407–420.

Skogen MD. 1999. A biophysical model applied to the Benguela upwelling system. *South African Journal of Marine Science* 21: 235–249.

Stokes GG. 1847. On the theory of oscillatory waves. *Transactions of the Cambridge Philosophical Society* 8: 441–473.

Sybrandy AS, Niiler PP. 1991. WOCE/TOGA Lagrangian Drifter Construction Manual, Report 91/6. *Scripps Institute of Oceanography*, La Jolla, California. Xx pp.

Tilney RL, Nelson G, Radloff SE, Buxton CD. 1996. Ichthyoplankton distribution and dispersal in the Tsitsikamma National Park marine reserve, South Africa. *South African Journal of Marine Science* 17: 1–14.

Ursell F. 1950. On the theoretical form of ocean swell on a rotating earth. *Monthly Notices of the Royal Astronomical Society, Geophysical Supplement* 6 (1): G1–G8.

Weller RA, Plueddmann AJ. 1996. Observations of the vertical structure of the oceanic boundary layer. *Journal of Geophysical Research* 101 (C4): 8789–8806.

CHAPTER 7

Synthesis: Recruitment variability of chokka squid — the role of the cold ridge, currents and retention on the Agulhas Bank

This thesis provides the first investigation into the factors responsible for the fluctuations observed in the biomass (and catches) of the South African commercially important, neritic chokka squid *Loligo reynaudii*. The ramifications of these fluctuations are significant and create uncertainty for resource managers and the fishing industry with the net result of increased risk levels of stock collapse, economic instability and long term investment. The socio-economic importance in terms of hardship experienced by the 3070 fishers, boat owners and families was similarly highlighted. The crash of the fishery in 2001 and the consequences reinforced the value of this knowledge.

The research approach used here was based on Bakun's (1996) triad of requirements for successful recruitment — enrichment, concentration and retention in the ecosystem. For chokka squid, recruitment depends on the survival of paralarvae which in turn is largely controlled by food production (nutrients, phytoplankton, zooplankton), feeding success (copepod biomass, density, patchiness and paralarvae–copepod coupling) and retention in the Agulhas Bank ecosystem. Consequently, a series of studies were undertaken to identify and understand principal components of the Agulhas Bank ecosystem linked to these parameters which are likely to play a role in the early life history of chokka squid. These studies demanded a multidisciplinary approach comprising physical oceanography and biology, as well as a variety of scientific techniques. Two main hypotheses were formulated using Bakun's (1996) principles — the "western transport hypothesis" based on enrichment and concentration (Chapters 2 and 3), and the "possibility of leakage of shelf water (and squid paralarvae) from the Agulhas Bank ecosystem" based on retention (Chapters 4, 5 and 6).

The Western Transport Hypothesis (WTH)

The first study presented in Chapter 2 demonstrated that, within the complex oceanography surrounding southern Africa, chokka squid have evolved using a niche on the eastern Agulhas Bank that optimizes spawning and their early life stages. Nowhere else on the shelf are both bottom temperature and bottom dissolved oxygen simultaneously at optimal levels for egg development. However, the spawning grounds are displaced from the typical copepod maximum by some 200 km, which is near a cold ridge that is optimal for feeding of paralarvae (on copepods), and hence for survival. ADCP data indicated that this spatial shortcoming is offset by the existence of a barotropic net westward current capable of transporting paralarvae to the cold ridge before starvation.

This exploitation of currents to optimize the use of separate environments during spawning and early life was referred to as the **westward transport hypothesis** or **WTH**. Although on a smaller scale, such a strategy is analogous to that used by the ommastrephids

Illex illecebrosus, *Todarodes pacificus*, and *Illex argentinus*, which use fast-flowing, large-scale, western boundary currents to connect spawning grounds with feeding grounds. This strongly supports the principles of enrichment, concentration and retention proposed by Bakun (1996). Such a life cycle strategy, however, has three obvious weaknesses that can impact recruitment. These involve uncharacteristic behaviour of (1) bottom environmental conditions on the spawning grounds (egg incubation), (2) the net westward mid shelf current, and (3) the cold ridge that supports the copepod maximum.

The latter was further pursued in Chapter 2, and the cold ridge was described as a coastal upwelling filament frequently found off the Knysna coast during summer. Its formation appears to be controlled by a combination of easterly winds and westward flow on the eastern Agulhas Bank. *In situ* sea surface temperature data indicate occasionally intense summer upwelling along the coast, which leads to greater cold ridge stability (i.e. it becomes quasi-permanent). This is expected to yield prolonged periods of copepod abundance beneficial for paralarvae survival. However, the cold ridge can also be absent much of the time during summer, especially during ENSO events.

A negative linear regression (r^2 = 0.94) between the maximum summer monthly sea surface temperature (an index of cold ridge activity) and the following autumn chokka squid biomass (and catches; r^2 = 0.69) supports the spawning and early life strategy outlined above, i.e. the **WTH**, and is potentially useful for prediction, because the maximum monthly SST is available at the beginning of the year.

Inshore currents and modification of the WTH

The **WTH**, however, is based on mid shelf current data and therefore mainly relevant to the deep spawning grounds, i.e., >60 m. Chapter 3 therefore examined the circulation on the inshore spawning grounds along the Tsitsikamma coast which is east and closest to the cold ridge (see Chapter 2, Figure 2.10a). This coast line represents about 40% of the total inshore spawning ground and is straight. The remainder of the spawning grounds comprise the large embayments of St Francis Bay and Algoa Bay where circulation will be complex and more difficult to resolve. This should be addressed in future studies. Results from an ADCP current meter deployed for 12 months midway on the Tsitsikamma coast at a depth of 36 m, surprisingly indicated the presence of an alongshore current which is predominantly eastwards away from the cold ridge. The current can flow in the same direction for periods of four weeks and attain high surface velocities of 115 cm s^{-1} with an average 23 cm s^{-1}. Velocity generally decreased with depth and reached a maximum of 65 cm s^{-1} near the bottom with an average 11 cm s^{-1}. It was also found, that although uncommon, bottom and surface layers can flow in opposite directions when the water column is thermally stratified. The influence of this current on squid paralarvae transport was considered using the ADCP data in the form of displacement plots. Potential displacement trajectories indicated a theoretical average monthly transport distance of up to 550 km to the east in the surface layer with eastward transport seven of the 12 months. However, near-bottom transport was less

dominant towards the east and reached a maximum of 200 km. Also during periods of easterly winds and eastward coastal currents, the surface flow was observed to veer offshore, highlighting Ekman transport and concomitantly coastal upwelling. The data indicated potential displacement of 40 km from the coast during these upwelling events. This onshore-offshore displacement observed in the surface layer, especially during eastward flow along the Tsitsikamma coast supports the cyclonic advection theory i.e. "current-closure scenarios" and larval dispersion proposed by Tilney *et al.* (1996) and Attwood (2002).

Although transport along the Tsitsikamma coast was westward towards the cold ridge for five of the 12 months, the existence of a dominant eastward surface flow required modification of the **WTH** proposed in Chapter 2. Whereas it is probable that squid paralarvae on the mid shelf are transported westward (as indicated by ship-borne ADCP data), the ADCP data collected on the Tsitsikamma coast indicated that squid paralarvae on the inshore spawning grounds between Cape Seal and Seal Point (see Figure 3.2b) are commonly transported eastwards in the surface layer and away from the cold ridge. The onshore-offshore cyclonic advection would imply that some inshore paralarvae are advected offshore into the westward mid-shelf current, and possibly swept towards the cold ridge — maintaining the relevance of the WTH. Alternatively, the paralarvae could be returned inshore, thereby retarding eastward displacement and maintaining them at the base of the cold ridge which extends between Knysna and the western side of the Tsitsikamma coast (see Figure 2.11). This too supports the WTH. However, the fate of the paralarvae transported eastward remains unknown, and infers that the WTH is not always relavent

Of course, of critical importance here is the key assumption that squid paralarvae mainly occupy the upper part of the water column, as this will affect their dispersion by currents. The assumption is based on the small number of *in situ* samples presented in Figure 3.1, which were found in the upper layer. Other than this, no information exists on the vertical movement of chokka squid, which clearly this needs to be addressed in future work.

Is the WTH an oversimplification and what of Bakun's hypothesis?

While the **WTH** remained useful to highlight key processes in the ecosystem, and importantly has already been used to focus recruitment related studies, e.g. Vidal *et al.* (2005), — the dependency of squid paralarvae on the cold ridge as the only rich feeding area on the Agulhas Bank, as well as the role of currents in the early squid life history, needed to be re-examined (Chapter 4).

Existing data and materials on the Agulhas Bank, including satellite imagery, were used for the re-examination and synthesis. These provided a more detailed account of primary and secondary production than given in Chapter 2, and consequently, it was found that chlorophyll and copepods (mainly *C. agulhensis*) are also found at elevated levels on the thermocline in areas other than the cold ridge (see Figure 4.3). This finding questioned the critical importance for currents to link hatching position with enriched food areas, and that perhaps vertical migration was more important?

A review and synthesis was then undertaken of data scattered in reports and publications from ships surveys, moorings, and more recently a Regional Ocean Model System (ROMS) set up for the southern Benguela. Together this showed that flow patterns on the Agulhas Bank comprised a mix of inshore, mid shelf and outer shelf flow regimes, with the latter having the potential for the leakage of shelf water from the Agulhas Bank into the Atlantic and Indian Oceans. Leakage points were anticipated near the Cape Peninsula, the southern region of the western Agulhas Bank, the tip of the Agulhas Bank, and Algoa Bay.

The synthesis suggested that the WTH is a special case within the context of the Agulhas Bank ecosystem, inclusive of the eastern, central and western regions, and that Bakun's principles need to be seen within this total region. That is, there are other mechanisms responsible for enrichment (i.e., coastal upwelling, thermocline erosion-diffusion, and shelf edge upwelling) that can account for the observed greater distribution of copepods (food). These are complimentary to the cold ridge system and will not necessarily be active simulataneously. Also, that retention needs to be seen as maintaining squid paralarvae within the Agulhas Bank ecosystem, not just in the vicinity of the cold ridge.

Retention of squid paralarvae on the Agulhas Bank

Chapter 5 tested the concept (hypothesis 2) of squid paralarvae retention within the Agulhas Bank ecosystem and moreover, the possibility that advective losses could be responsible for the sudden drop in annual squid catches experienced in 2001 — i.e. recruitment failure. A Lagrangian IBM (Individually-Based Model) coupled to a ROMS (Regional Ocean Model System) model was used to investigate this hypothesis. Given some limitations of the models and the lack of knowledge regarding squid paralarvae characteristics, results indeed demonstrate that squid paralarvae can be removed from the Agulhas Bank ecosystem. Three simulations were performed for 12 model months using neutrally buoyant particles released from the seabed every second day on the mid shelf of the eastern, central and western parts of the Agulhas Bank. Particles were given life spans of 40 days. The results showed large particle losses from the eastern Agulhas Bank (76%) and the western Agulhas Bank (64%), with the latter possibly having a seasonal trend. Dispersion on the western Agulhas Bank was complex and mainly occurred northwards into the Benguela jet but with substantial influence of adjacent ocean eddies commonly pulling shelf water and particles offshore into the Atlantic Ocean. Surprisingly, dispersion also occurred towards the coast near Cape Agulhas and onto the central Agulhas Bank. A semi-permanent cyclonic eddy in the Agulhas bight was seen to be the primary mechanism for particle loss on the eastern Agulhas Bank. Few particles were lost from the central Agulhas Bank (2%) making this, in terms of the model, the most suitable place on the Agulhas Bank for spawning.

While the Lagrangian ROMS–IBM demonstrated particle leakage from the Agulhas Bank ecosystem and that this may well be one of the causes for recruitment failure and hence low biomass and catches in certain years, the study also cautioned on the application of these results due to several limitations. These included the incomplete coverage of the known

chokka squid spawning grounds by the PLUME model domain, as well as the model being forced by monthly climatic winds and hence the exclusion of shorter time scales. Also, in the absence of any actual data or information, the model used particles with neutral buoyancy and zero swimming capacity (i.e. passive) for a period of 40 days to represent real squid paralarvae. While this may be reasonable, greater or less density and shorter passive times will lead to different leakage results. Furthermore the hatching release positions in the model were mid shelf. But, as indicated in Figure 2.1a and reported in Roberts *et al.* (Unpublished), some 88% of spawning occurs inshore i.e. <60% (based trawled egg masses). While this figure still needs verification, it emphasises the need to also consider the inshore spawning grounds in the model. The inshore spawning grounds were excluded in the model experiments because of the uncertainty of boundary effects.

Validation of the ROMS–IBM and inshore current transport

Chapter 6 presented an alternative means of investigation for paralarvae dispersion and testing the hypothesis that leakage of paralarvae from the Agulhas Bank is possible. Four satellite tracked drifters were released on the eastern Agulhas Bank during the summer spawning season. Two drifters tethered to drogues at 8 m (i.e. near-surface) were released on the inshore spawning grounds off the Tsitsikamma coast directly above the bottom-mounted ADCP in a depth of 36 m (see Chapter 3). This deployment was important because virtual paralarvae particles could not be released here in the IBM experiment due to the close proximity of the coast (1.5 km) and model resolution (9 km).

The other two drifters were released on the mid shelf where squid eggs had previously been found in 120 m and virtual paralarvae particles had been released in the IBM experiment. To be comparable with the IBM, i.e. particles were released in the bottom layer, one of the drifters was tethered to a drogue at a depth of 70 m to track the bottom layer. The remaining drifter tracked the near-surface layer using a drogue at 8 m.

Both inshore drifters were transported 70 km eastwards in the Tsitsikamma coastal current to Tsitsikamma Point (see Figure 6.4) where one beached while the other went southwards to leave the shelf 20 days after release. The latter drifter, complimented with SST satellite images, highlighted a cyclonic eddy (swirl) off Tsitsikamma Point which clearly terminated the coastal current. This advection supports the **WTH** as paralarvae swept eastwards in the coastal current are moved offshore into the westward flowing mid shelf current. However, the fact that the drifter went beyond the mid shelf and finally into the Indian Ocean within the time span of 40 days demonstrated that squid paralarvae on the inshore spawning grounds are not necessarily retained in the Agulhas Bank ecosystem. Satellite SST and ocean colour imagery showed frequent leakage of shelf water near the southern tip of the Agulhas Bank (see Figure 6.8) and a cyclonic eddy in the Agulhas bight at this time, either of which could have been responsible for removal of the drifter from the shelf.

Also of significance were the trajectories of the mid shelf drifters. Both travelled westwards and were retained on the Agulhas Bank within the 40 day period — strongly

supporting the **WTH** but in sharp contrast to the IBM results. The deeper drifter spent most of this time in the position of the cold ridge and was recovered only 100 km from the release position. The surface drifter on the other hand continued across the central bank to reach the inner western Agulhas Bank (a distance of 550 km) and then left the shelf after 58 days just south of the Cape Peninsula. This leakage point was observed several times in the IBM simulations (Figure 6.7). Satellite SST and ocean colour images showed an intrusion of oceanic water onto the western Agulhas Bank during this experiment (Figure 6.8) which from the drifter track induced an anti-cyclonic circulation and leakage of shelf water from the inner central Agulhas Bank — similarly seen in the IBM simulation (Figure 6.7c–f).

At first glance it appears that the westward advection of the mid shelf drifters (which agrees with *in situ* data presented in Chapters 2 and 4) is in sharp contrast with the results of the IBM which indicated dominant eastward transport here. However, as mentioned SST images (Figure 6.7) showed a cyclonic eddy to be resident in the Agulhas Bight at the time of the drifter deployment. This was a major feature in the ROMS–IBM and was responsible for most of the particle leakage on the eastern Agulhas Bank. As shown in Figure 6.7 the drifters were deployed only a few kilometers to the north of the periphery of this eddy. Had deployment been a little farther south, then the advection would no doubt have been eastwards and the results been very similar to those of the ROMS–IBM.

Conclusion

In summary, the studies undertaken here have established likely reasons for chokka squid to use the eastern Agulhas Bank for spawning and highlighted the potential positive role that the cold ridge and its associated food enrichment may play in the early life history of this species. They demonstrated that variability in the driving forces of the cold ridge and hence food availability would be one factor controlling recruitment success. Another in this scenario (i.e. the **WTH**) would be deviation in the westward transport of the paralarvae from the main spawning grounds towards the cold ridge. This is analogous to the delivery of squid egg balloons in a WBC to the nursery grounds in higher latitudes. But these studies have also emphasized the possibility that leakage of shelf water over the shelf edge may at times result in squid paralarvae being removed from the Agulhas Bank ecosystem, which itself would be a factor impacting recruitment success and hence biomass and catch.

However, while good progress has been made here a lot of information is still missing which needs to be obtained to further interpret these results or to modify this understanding of key processes important to the early life history. Key assumptions in the various chapters have had to be made! For example, key questions which need answers include: (1) where in the water column do the paralarvae live and is this density or age dependent? The importance of this information can not be over stated as all five chapters (2–6) have had to make the assumption that chokka squid paralarvae are neutrally buoyant and passive in the absence of this information. As noted in parts of this thesis, this has ramifications for dispersion and the linking of paralarvae to areas of food enrichment. Other are, (2) what do paralarvae eat? Only copepods or can they feed on other zooplankton, and where is this food

found? (3) How long can the paralarvae survive without feeding, and how is successful feeding accomplished? And (4), how does temperature impact survival of the paralarvae? This list is not exhaustive, and other key information has been cited at the end of chapters such as the need to refine the ocean models and IBM to be more realistic.

The studies undertaken here should therefore be seen as a first step in understanding the reasons for fluctuations in the biomass and catches of the commercially important chokka squid (*Loligo reynaudii*). Through a more complete understanding, it may be possible in the future to select quantifiable indices representing critical ecosystem components upon which the early life history of the paralarvae depends, and to correlate these with recruitment success. This would move our understanding towards a predictive capability. Such a capability might be done through either coupled 3D ocean–nutrient–production and IBM models or perhaps numerical correlation. Such an understanding would also enable the fishery and resource managers to address the impending impact of climate change!

References

Attwood CG, Allen J, Claasen PJ. 2002. Nearshore surface current patterns in the Tsitsikamma National Park, South Africa. *South African Journal of Marine Science*, 24: 151–160.

Bakun A. 1996. Patterns in the Ocean. Ocean processes and marine population dynamics. California Sea Grant, *National Oceanic and Atmospheric Administration and Centro de Investigaciones biológicas del Noroeste*, La Paz, BCS México, 323 pp.

Roberts M, Downey N, Sauer W. Unpublished. Existence of deeper spawning grounds for the South African chokka squid *Loligo reynaudii*.

Tilney RL, Nelson G, Radloff SE, Buxton CD. 1996. Ichthyoplankton distribution and dispersal in the Tsitsikamma National Park marine reserve, *South African Journal of Marine Science*, 17: 1–14.

Vidal E, Hackbart V, Roberts M. 2005. Rearing yolk absorption and growth in *Loligo vulgaris reynaudii* paralarvae. *Aquatic Living Resources*, 18: 385–39.